2009

INTERMOLECULAR COMPLEXES OF GERMANIUM(II

Paul A. Rupar

INTERMOLECULAR COMPLEXES OF GERMANIUM(II)

(Spine title: Intermolecular Complexes of Germanium(II))

(Thesis format: Integrated-Article)

by

Paul A. Rupar

Graduate Program in Chemistry

A thesis submitted in partial fulfillment
of the requirements for the degree of
Doctor of Philosophy

The School of Graduate and Postdoctoral Studies
The University of Western Ontario
London, Ontario, Canada

Abstract

This thesis examines the synthesis, structural characterization, and reactivity of neutral and charged intermolecular donor complexes of germanium(II).

Base stabilized complexes of dimesitylgermylene (Mes_2Ge) (mes = mesityl = 2,4,6-trimethylphenyl) with either an anionic diisopropylphenyl-substituted N-heterocyclic gallium(I) ($NHGa^-$) ligand or a diisopropyl substituted N-heterocyclic carbene (NHC) ligand were synthesized by the addition of two equivalents of either $NHGa^-$ or NHC to tetramesityldigermene ($Mes_2Ge{=}GeMes_2$). The complexes $[NHGa\text{-}GeMes_2]^-$ and NHC-$GeMes_2$ are the first two examples of a transient germylene (Mes_2Ge) being stabilized by intermolecular donors.

A series of NHC complexes of GeR_2 (R = F, Cl, Br, I, Cl/O_3SCF_3, O^tBu, NCS, Mes) were synthesized. The ^1H NMR spectra of the NHC-GeR_2 complexes show broad signals at room temperature which was rationalized by either conformational interchanges or intermolecular exchanges. The NHC-GeR_2 complexes were also examined computationally. The energy of complexation was found to decrease if π donor atoms are located adjacent to the germanium centre.

The reactivity of selected NHC-GeR_2 (R = Cl, O^tBu, or Mes) complexes towards 2,3-dimethylbutadiene, 3,5-di-^{t}butyl-orthoquinone, methyl iodide, pivalic acid and benzophenone was examined. In comparison with uncomplexed GeR_2 species, the NHC-GeR_2 complexes are less reactive. The prospect of using the NHC-GeR_2 complexes as a synthon for GeR_2 appears to be reaction specific.

Finally, a series of cationic germanium(II) complexes were synthesized and characterized, including examples of germanium(II) centred dications. A germanium

centred dication supported by three NHC ligands $[NHC_3Ge][I]_2$ was characterized and examined computationally. The structure of $(cryptand[2.2.2]Ge)^{2+}$, as the triflate salt, was reported and is the first example of a non-metal cation situated within a cryptand. A number cationic germanium crown ether complexes were are also synthesized including $[[12]crown\text{-}4)_2{\bullet}Ge]^{2+}$, [[15]crown-5•GeOTf]+ and $[benzo[15]crown\text{-}5{\bullet}GeCl]^{+}$ and [benzo[15]crown-5•GeOTf. The geometries of the crown ether-germanium complexes were found to be highly dependent on the size of the crown ether and the substituent located on the germanium.

Keywords: germylene, germanium(II), N-heterocyclic carbene, base stabilized, crystal structure, crown ether, cryptand, gallium(I)

Co-Authorship

Chapter 2 is an amalgamation of two manuscripts which were authored by Paul Rupar, Michael Jennings, Paul Ragogna and Kim Baines. Paul Rupar was responsible for writing the manuscript. All of the experimental work was performed by Paul Rupar with the exception of the X-ray crystallographic analyses which were performed by Michael Jennings.

Chapter 3 was based on a manuscript authored by Paul Rupar, Michael Jennings and Kim Baines. Paul Rupar was responsible for writing the manuscript and all of the experimental work, except for the X-ray crystallographic analyses of two compounds, which were performed by Michael Jennings.

Chapter 5 is a combination of three separate manuscripts. Paul Rupar was responsible for the majority of the writing and experimental work in Chapter 5. The work on crown ethers (Section 5.2.3) was coauthored by Rajoshree Bandyopadhyay and Prof. Charles Macdonald of the University of Windsor. DFT calculations in Section 5.2.1 were performed by Prof. Viktor Staroverov.

The acquisition of mass spectra was performed by Doug Hairsine (Manager, Mass Spectrometry). EDX data was acquired by the staff at the Nanofabrication Lab in the Department of Physics and Astronomy at The University of Western Ontario by Dr. Todd Simpson. X-ray diffraction data for compound **85**$[OTf]_2$ (Section 5.2.2) was collected by R. McDonald at the X-Ray Crystallography Laboratory of the Department of Chemistry, University of Alberta.

Acknowledgements

First, I must thank my supervisor, Kim Baines, for allowing me to continue my studies with her in graduate school. I appreciate all of the time, dedication, and guidance. It has been pleasure to work for her. I also thank my Baines group lab mates as well. They have made time spent both in and outside of the lab enjoyable and I am thankful for the many friendships I have gained during my time here.

During the course of my graduate studies here at Western I have had the pleasure of working with a number of faculty members and staff. I am indebted to Prof. Paul Ragogna for countless conversations, suggestions, encouragement, and for allowing me to attend his group meetings. I thank Prof. Viktor Staroverov for his guidance with the computational work and for stimulating discussions on the nuances of chemical bonding. I thank Doug Hairsine for acquiring mass spectra, including a couple of last minute data collections. I would like to thank both Prof. Nicholas Payne and Dr. Michael Jennings for teaching me the ins and outs of single crystal X-ray diffraction.

I thank my family, my Dad, my Mom, Rita, Carolyn, Ian and Emily for encouraging me to achieve my goals and for helping me to succeed in my endeavours. I am especially grateful to my father for instilling within me a sense of curiousity, skepticism, and an appreciation for science.

Finally, I must thank Krysten; my best friend and the love of my life. Her constant encouragement, love and support makes all the difference. I could not have done this without her.

Table of Contents

Chapter 2
The Stabilization of Dimesitylgermylene by an N-Heterocyclic Gallium(I) Anion and an N-Heterocyclic Carbene

Chapter 3
The Synthesis and Characterization of N-Heterocyclic Carbene Complexes of Germanium(II)

Chapter 4
Reactivity Studies of N-Heterocyclic Carbene Complexes of Germanium(II)

List of Tables

List of Figures

List of Abbreviations

3c2e = 3-centered-2-electron

Å = Angstrom

br = broad

bs = broad singlet

Bu = butyl

^{t}Bu = *tertiary*-butyl

calcd = calculated

CI = chemical ionization

CP = cyclopentadienyl

CP* = pentamethyl cyclopentadienyl

d = doublet (NMR); day (time)

DCM = dichloromethane

Dep = 2,6-diethylphenyl

DFT = density functional theory

Dipp = 2,6-diisopropylphenyl

DMB = 2,3-dimethylbutadiene

Dmp = 2,6-dimethylphenyl

EDX = energy dispersive X-ray analysis

EI = electron impact

ESI = electrospray ionization

Et = ethyl

FT = fourier transform

gCOSY = gradient correlation spectroscopy

gHMBC = gradient heteronuclear multiple bond correlation

gHMQC = gradient heteronuclear multiple quantum coherence

gHSQC = gradient homonuclear spin quantum coherence

HOMO = highest occupied molecular orbital

hr = hour

Hz = hertz

^{i}Pr = isopropyl

IR = infrared

J = coupling constant

LUMO = lowest unoccupied molecular orbital

m = multiplet (NMR); medium (IR)

Me = methyl

Mes = mesityl = 2,4,6-trimethylphenyl

MHz = megahertz

min = minute

MO = molecular orbital

MS = mass spectrometry

m/z = mass-to-charge units

NBO = Natural Bond Orbital

NHC = N-heterocyclic carbene

NMR = nuclear magnetic resonance

NPA = Natural Population Analysis

OTf = triflate = O_3SCF_3

PES = potential energy scan

Ph = phenyl

ppm = parts per million

RT = room temperature

s = singlet (NMR); strong (IR)

SALC = symmetry-adapted linear combination

SCF = self consistent field

t = triplet

Tbt = 2,4,6-[$(Me_3Si)_2CH$]C_6H_2

THF = tetrahydrofuran

TMS = trimethylsilyl

Tripp = 2,4,6-triisopropylphenyl

Tsi = tris(trimethylsilyl)methyl

UV = ultraviolet

Vis = visible

w = weak

WBI = Wiberg bond index

Cast of Characters

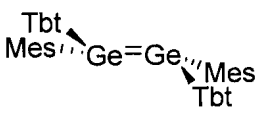

Tbt = 2,4,6-[$(Me_3Si)_2CH$]C_6H_2

1

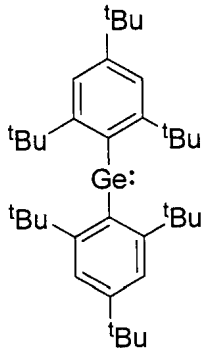

2

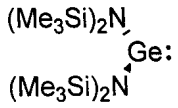

3

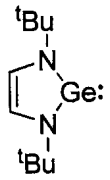

4

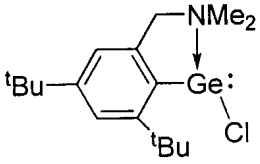

5

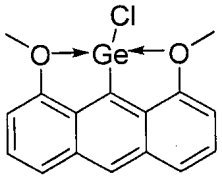

6

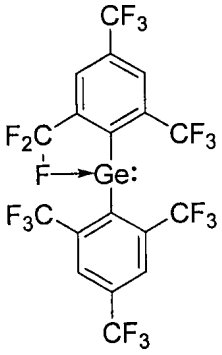

7

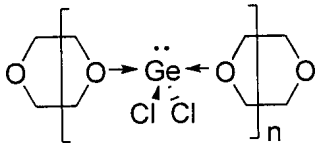

8

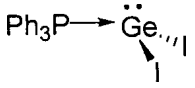

9

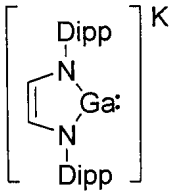

10

$R'_2Ge=GeR'_2$

R' = $CH(SiMe_3)_2$

11

$Tripp_2Ge=GeTripp_2$

12

Tripp = 2,4,6-triisopropylphenyl

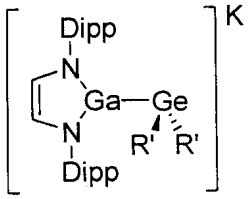

13

Dipp = 2,6-diisopropylphenyl

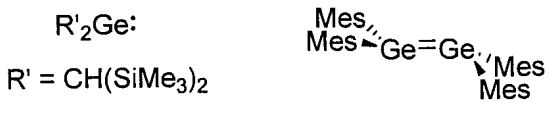

14

15

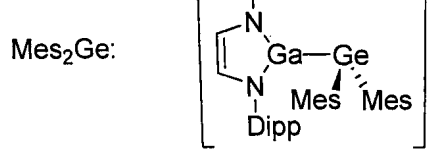

16

17

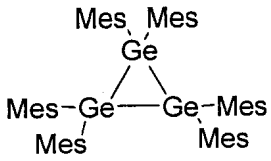

18

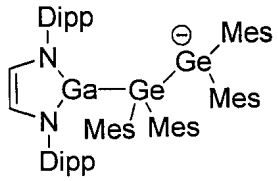

19

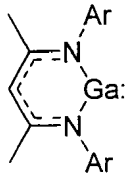

20

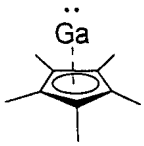

21

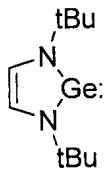

22

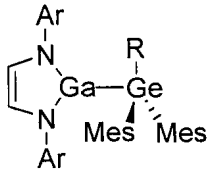

23 R = Me
24 R = Me_3Si

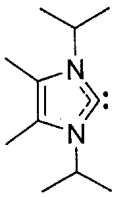

25

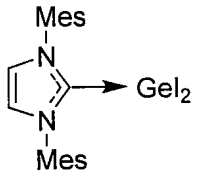

26

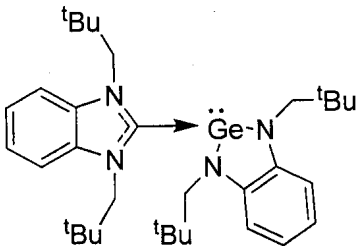

27

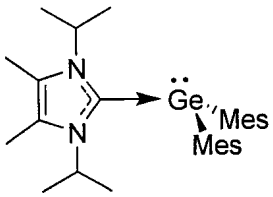

28

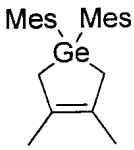

29

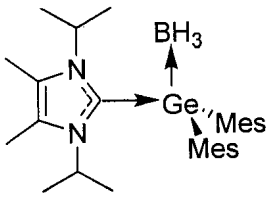

30

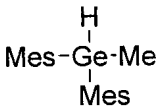

31

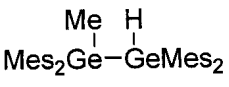

32

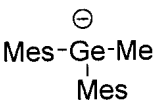

33

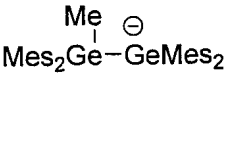

34

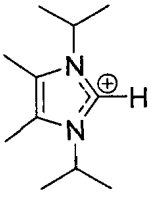

35

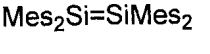

36

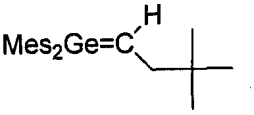

37

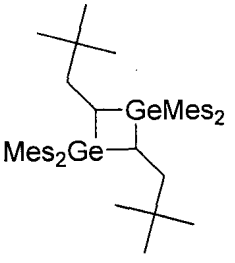

38

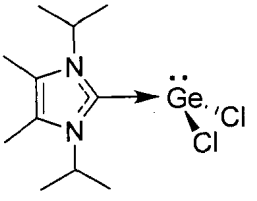

39

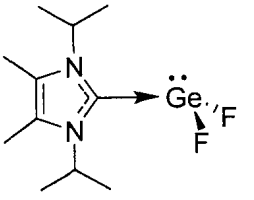

40

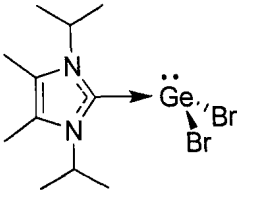

41

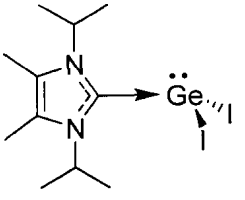

42

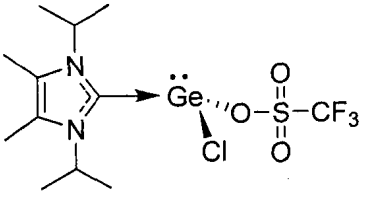

43

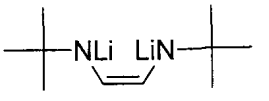

44

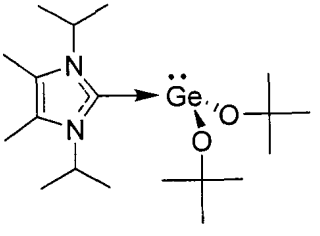

45

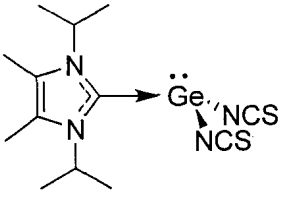

46

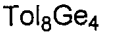

47

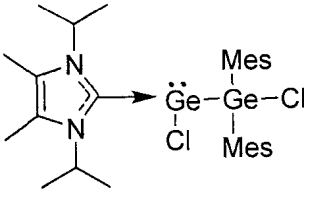

48

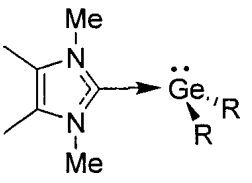

49 R = O^{t}Bu
50 R = Cl
51 R = Br
52 R = I
53 R = Mes

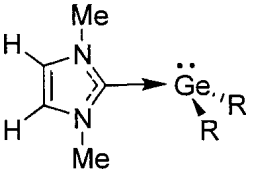

54 R = H
55 R = OH
56 R = NH_2
57 R = CH_3
58 R = F
59 R = Cl

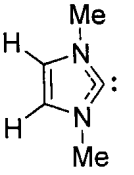

60

61

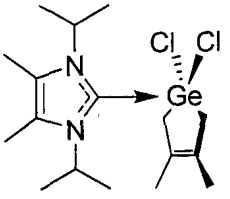

62

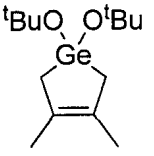

63

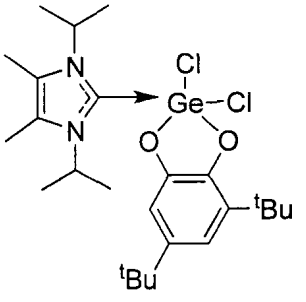

64

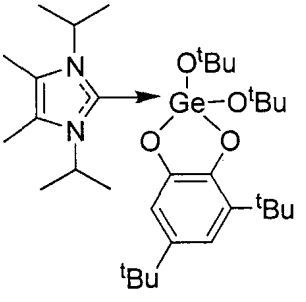

65

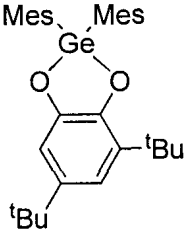

66

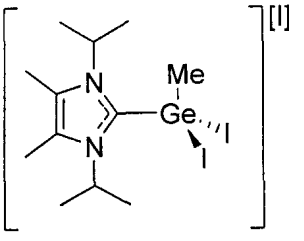

67[I]

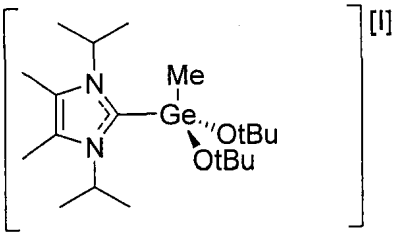

68[I]

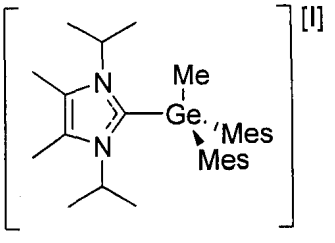

69[I]

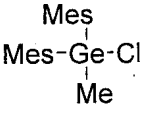

70

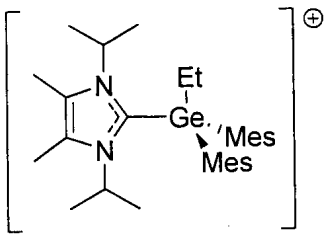

71^{+}

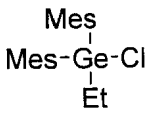

72

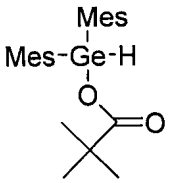

73

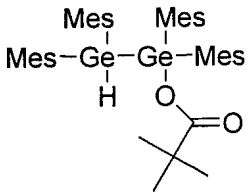

74

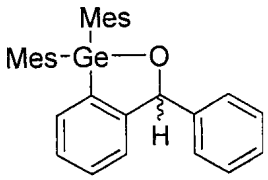

75

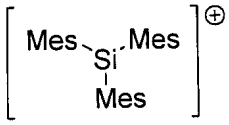

76^{+}

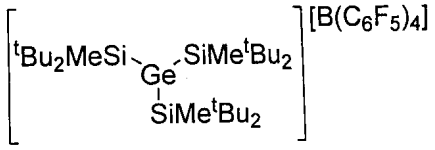

77[$B(C_6F_5)_4$]

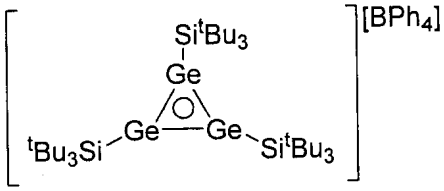

78[BPh_4]

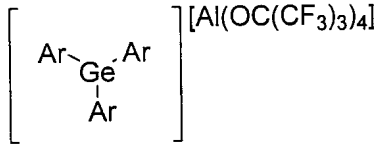

Ar=2,6-(O^tBu)$_2C_6H_3$

79[$Al(OC(CF_3)_3)_4$]

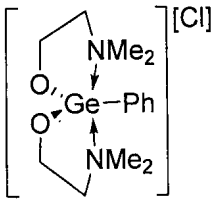

80[Cl]

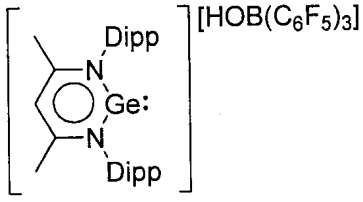

81[$HOB(C_6F_5)_3$]

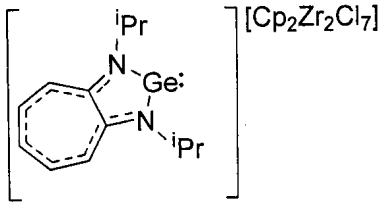

82[$Cp_2Zr_2Cl_7$]

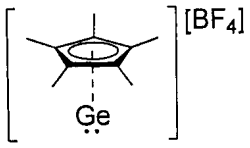

83[BF_4]

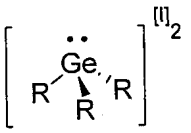

84[I]$_2$

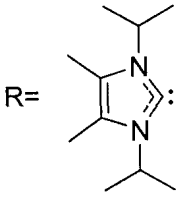

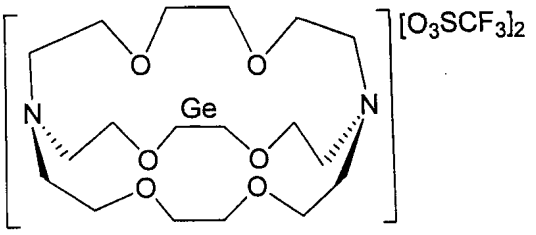

85[OTf]$_2$

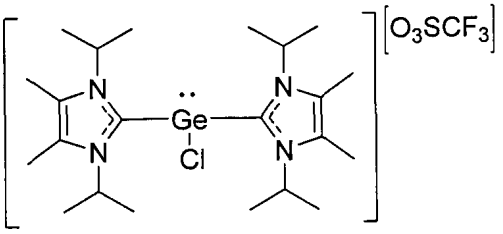

86[OTf]

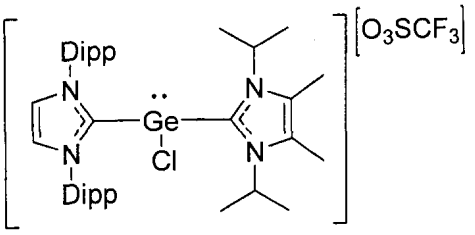

87[OTf]

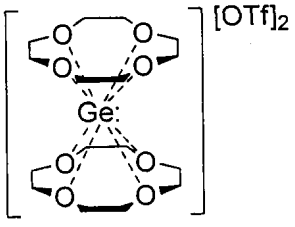

88[OTf]$_2$

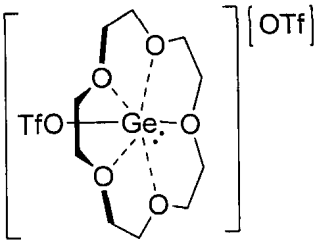

89[OTf]

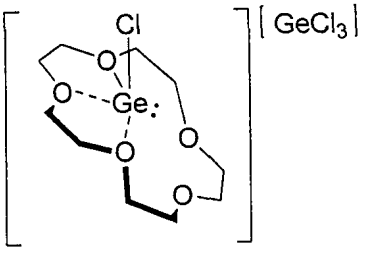

90[GeCl$_3$]

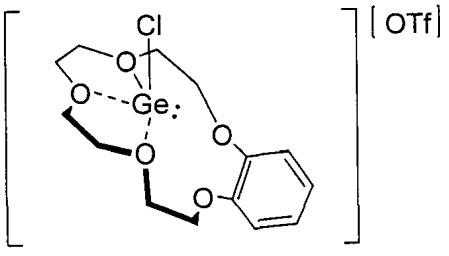

91[OTf]

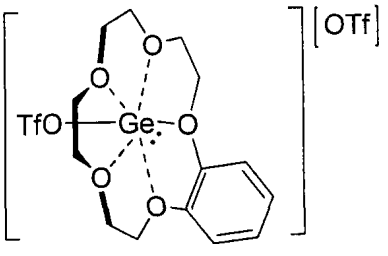

92[OTf]

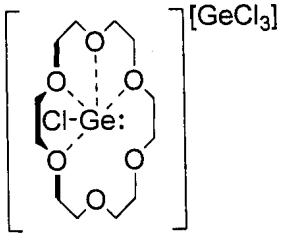

93[$GeCl_3$]

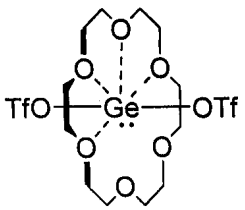

94

Chapter 1

An Introduction to the Chemistry of Germanium(II)

1.1 General Introduction

As a third row element, the chemistry of Ge has similarities with both the lighter group 14 elements, carbon and silicon, and the heavier group 14 elements, tin and lead. Tetravalent germanium, like carbon and silicon, is the most common valence state encountered in germanium chemistry. As with silicon, tin, and lead, hypercoordinate germanium compounds, in which germanium is bonded to five or six substituents, are known and are stable, particularly when electronegative elements are attached to the germanium centre.[1]

Group 14
6 C 12.0
14 Si 28.1
32 **Ge** 72.6
50 Sn 118.7
82 Pb 207.2

Although four coordinate germanium is the most prevalent, germylenes, divalent germanium containing compounds, are important both as reactive intermediates and as synthetically useful precursors.[2] As germylenes play a central role in this thesis, the chemistry of germanium(II) containing compounds is reviewed.

1.1.1 Germylenes

The chemistry of germanium(II) is somewhat of a hybrid between the extremely reactive carbene and silicon(II) species and the thermodynamically more stable tin(II) and lead(II) compounds. Unlike divalent carbon, which can have a singlet or triplet ground state, the ground state electronic configuration of germylenes, as well as all other heavy divalent group 14 elements, rests entirely in the singlet state.[3, 4]

Chart 1.1

Resembling singlet carbenes, the frontier molecular orbitals of Ge(II) species consist of a lone pair of electrons and an empty π-orbital, making the germanium amphoteric in nature (Chart 1.1). As a result of their amphoteric properties and the fact that they are in an intermediate oxidation state, simple Ge(II) compounds such as germylene (GeH_2) and the related organogermylenes (GeR_2, where R=small alkyl or aryl) are, in general, very reactive and not stable in the condensed phase.[5]

Although organogermylenes are unstable, the dihalogermylenes, GeX_2 (where X= F, Cl, Br, or I), are less reactive and are "bottle-able substances" under an inert atmosphere.[2] The stability of dihalogermylenes has been attributed to deactivation of the lone pair of electrons through inductive effects and π donation from the electron lone pairs on the halides into the empty p-orbital on germanium.[2] The ability to fill the empty p-orbital through the intermolecular association with a lone pair of electrons belonging to a neighbouring halogen atom also contributes to the increased stability of dihalogermylenes (Chart 1.2).

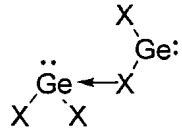

Chart 1.2

1.2 Techniques for the Stabilization of Germylenes

The pursuit of stable germylenes, especially diorganogermylenes, through the judicious selection of the substituents on germanium, is an active area of research in germanium(II) chemistry. Two general approaches for the stabilization of germylenes are possible: shielding the reactive centre though steric protection or deactivation of the divalent germanium via electronic effects.

1.2.1 Stabilization of Germylenes Through Steric Protection

The kinetic instability of germylenes is a consequence of their tendency to rapidly oligomerize.[6] Diorganogermylenes tend to be especially reactive and quickly polymerize. By installing sterically bulky groups on the germanium, kinetic stabilization can be achieved. Depending on the size of the substituents placed on germanium, either a digermene, a doubly bonded germanium compound, or a diorganogermylene can be isolated. Often an equilibrium exists between the two and both can be observed in solution (Scheme 1.1).

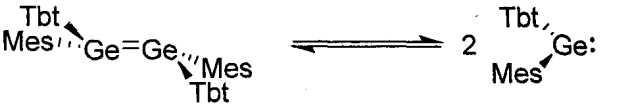

1

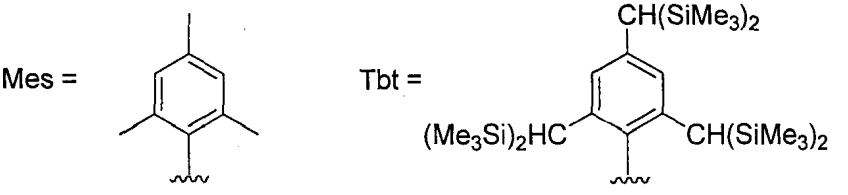

Scheme 1.1

For example, digermene **1** and its corresponding germylene can be detected simultaneously by UV-Visible spectroscopy at room temperature in solution (Scheme 1.1).[7] Extremely large groups on germanium, such as supermesityl (tris-2,4,6-^{t}butylphenyl), can stabilize monomeric GeR_2 species and prevent dimer formation (for example **2**, Chart 1.3).[8] 2,6-Dimesitylphenyl and the related terphenyls are also capable of preventing germylene dimerization.[9]

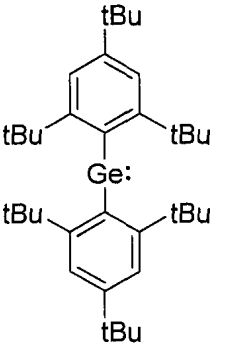

2

Chart 1.3

1.2.2 Electronic Stabilization of Germylenes

The most prevalent method for the stabilization of Ge(II) compounds is by electronic stabilization via the transfer of electron density into the empty π-orbital. There are three primary ways to accomplish the transfer of electron density: π donation from an adjacent atom (Chart 1.4 **A**), through space donation from an intramolecular donor (Chart 1.4 **B**), or through space donation from an intermolecular donor (Chart 1.4 **C**).

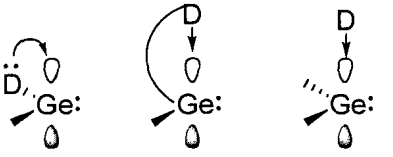

A **B** **C**

Chart 1.4

Germylenes stabilized by π donation have neighbouring atoms that possess electron lone pairs α to the germanium. Such atoms transfer electron density into the empty p-orbital on germanium (Chart 1.4 **A**). The prototypical example of a germylene stabilized via π donation is **3**,[10] which features two electron rich $(Me_3Si)_2N$ substituents (Chart 1.5). Other common examples include N-heterocyclic germylenes, such as **4**.[2g, 11] Although the presence of electron rich groups next to the germanium greatly contributes to the stability of these compounds, steric protection is often still required, as illustrated by the four bulky trimethylsilyl groups in **3** and the ^{t}butyl substituent on the nitrogen atoms of **4**.

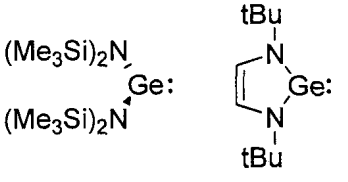

3 **4**

Chart 1.5

In addition to placing electron rich atoms α to the Ge(II) centre, substituents with electron lone pairs in the correct spatial orientation will form an intramolecular donor-acceptor bond with the germanium by transferring electron density into the empty p-orbital (Chart 1.4 **B**). The majority of intramolecularly stabilized germylenes employ either nitrogen, oxygen, or sulfur atoms as the electron donor (Chart 1.6).[12] As evident in **5**[13] and **6**,[14] the Lewis basic atom is typically held in proximity of the germanium by a rigid group, such as a phenyl ring. The fluorinated **7**[15] is an unusual case, where the solid state structure clearly shows the fluorine atoms of the *o*-CF_3 substituents coordinating the Ge(II) centre. Compound **7** is interesting in that it is stabilized by steric protection, electron donation into the p-orbital on germanium, and by the electron withdrawing inductive effects of the CF_3 groups, which deactivate the lone pair of electrons on germanium.

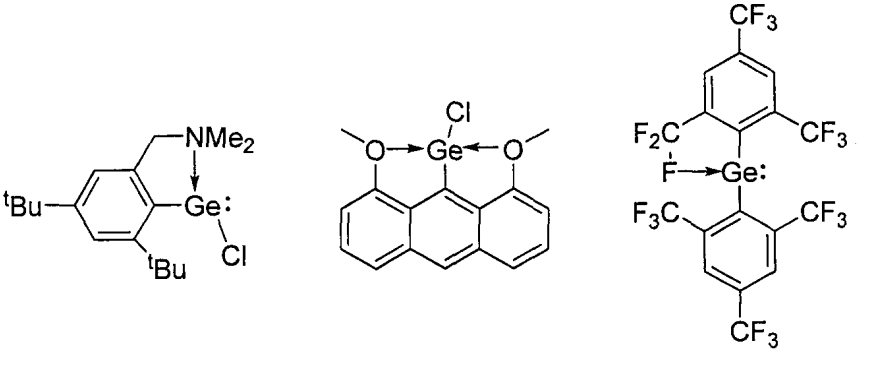

5 **6** **7**

Chart 1.6

Although conceptually similar to the intramolecularly stabilized Ge(II) species, few intermolecularly stabilized complexes of GeR_2 are known and those that have been characterized invariably contain intrinsically stable germylenes. First synthesized in the mid 1960's by Nefedov and coworkers, $GeCl_2$•dioxane (**8**) is the most well-known

example of an intermolecularly stabilized germylene and is an important reagent in the chemistry of germanium(II) (Chart 1.7).[16] Stabilization of dichlorogermylene is achieved by the donation of electron density from the Lewis base, 1,4-dioxane, into the empty p-orbital on germanium. A relatively weak donor is sufficient to produce a stable complex because of the inherent stability of dichlorogermylene.[2] Another illustration of an intermolecularly stabilized germylene is the triphenylphosphine-GeI_2 complex **9** which, unlike **8**, is monomeric because of the stronger donor properties and steric bulk of the triphenylphosphine compared to 1,4-dioxane.

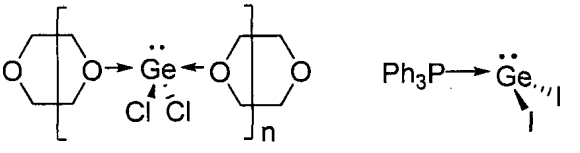

8 **9**

Chart 1.7

1.3 Synthesis of Germylenes

The synthesis of germanium(II) compounds is usually accomplished by either extrusion of a GeR_2 fragment from a precursor or through substitution chemistry with a preexisting Ge(II) species. Reduction of Ge(IV) to Ge(II) with metallic reducing agents is less often employed because the harsh reaction conditions often result in poor yields and complex reaction mixtures.

Transient diorganogermylenes are almost exclusively produced by elimination of a GeR_2 fragment, often from a strained ring system (Scheme 1.2). As shown in Scheme 1.2, retrocyclizations, initiated photochemically or thermally, are a common method for the generation of transient germylenes.

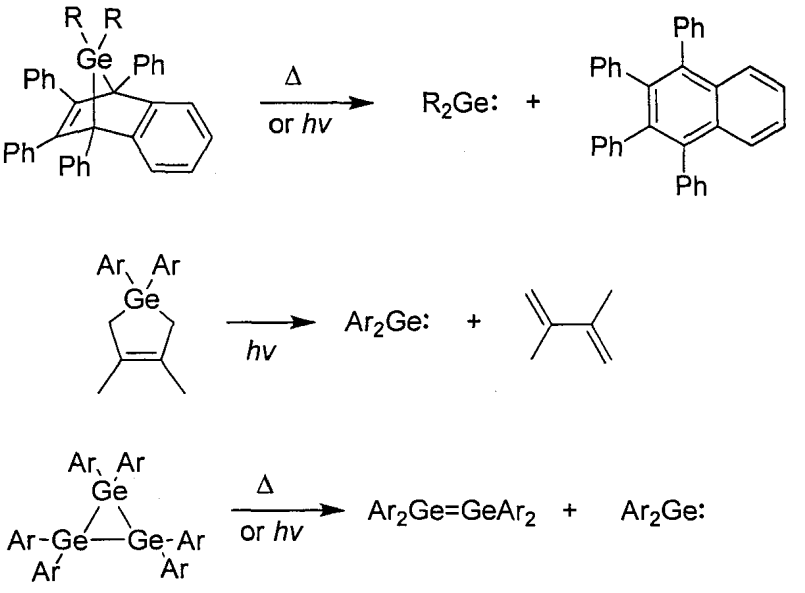

Scheme 1.2

Stable germylenes are usually made from nucleophilic substitution, typically of $GeCl_2$·dioxane (**8**), with either an organolithium or Grignard reagent (Scheme 1.3).[17] $GeCl_2$·dioxane (**8**) itself is readily synthesized through the reduction of $GeCl_4$ by tetramethyldisiloxane (Scheme 1.3).[18]

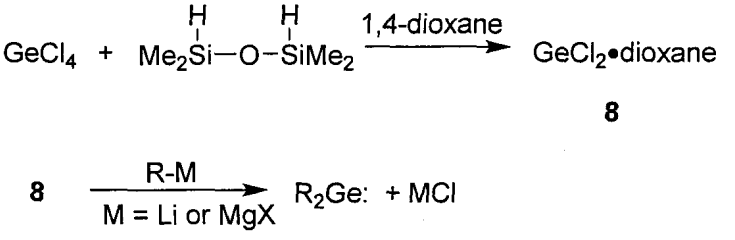

Scheme 1.3

1.4 Reactivity of Germylenes

The chemistry of germylenes is diverse and is highly dependent on the substituents on germanium. Nevertheless, there are a number of reactions (Scheme 1.4) common to both stable and transient Ge(II) species. In the case of transient compounds, identification of the products from the reactions shown in Scheme 1.4 can often be used as evidence for

the formation of the transient species, particularly since the reactions are often selective and high yielding. The common driving force amongst these reactions is the creation of two new covalent bonds to germanium during the transformation of a Ge(II) species to a Ge(IV) compound.

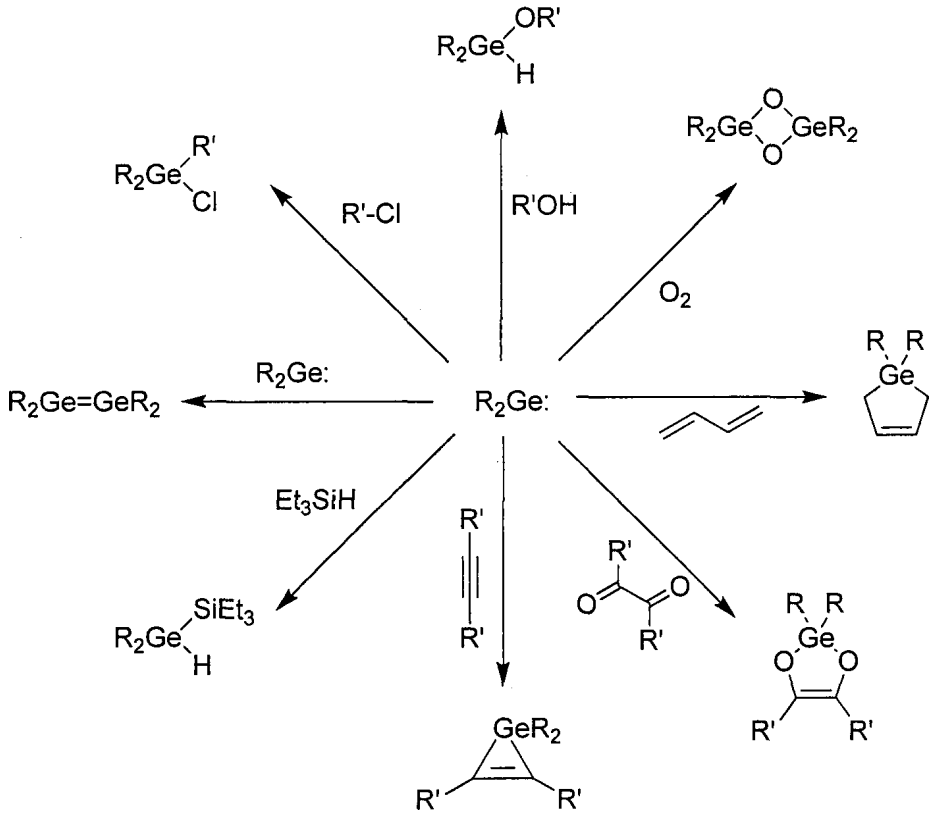

Scheme 1.4

1.5 Project Overview

Given the central role germylenes play in germanium chemistry and the prevalence of intramolecularly stabilized Ge(II) compounds, it is surprising that strong neutral donors have never been employed in the intermolecular stabilization of reactive GeR_2 compounds. While there are no examples of a transient germylene stabilized by an intermolecular donor, precedence for the moderation of the reactivity of short lived GeR_2

species using donor solvents (i.e. THF) has been demonstrated.[19] We believe that through the use of strong neutral donors, complexes of unstable germylenes may also be isolable. Such complexes are likely to have useful applications as ligands in coordination chemistry,[20] as novel precursors for the generation of uncoordinated germylenes, as well as in the synthesis of novel germanium polymers. This project will demonstrate that neutral donors can indeed coordinate and stabilize a number of otherwise reactive germanium(II) species.

In Chapter 2, the reaction between tetramesityldigermene and two different strong Lewis bases, an anionic gallium(I) and an N-heterocyclic carbene (NHC), is explored. In both cases, a stable complex with $GeMes_2$ is formed, the reactivity of which is also examined. Chapter 3 expands on Chapter 2 and shows that a variety of NHC complexes of GeR_2 can be synthesized. By starting with a chloride substituted germanium(II) complex, NHC-GeR_2 species are formed and structurally characterized. The nature of the bonding between the N-heterocyclic carbene and the germylene is examined computationally and the limitation of NHCs in the stabilization of simple diorgano-substituted GeR_2 species is demonstrated.

The chemistry of selected NHC-Ge(II) complexes is examined in Chapter 4. Their reactivity towards a number of reagents is described with an emphasis on the comparative chemistry with other germanium(II) species.

Chapter 5 will examine the role of neutral donors in the formation of cationic germanium(II) complexes. In addition to NHC complexes of cationic Ge(II), a number of polydentate ligands are explored, which results in the isolation of a number of

unprecedented cationic germanium compounds. Finally, a summary of the thesis is given in Chapter 6.

1.6 References

1. Weinert, C. S. In *Comprehensive Organometallic Chemistry III, Vol 3*; Mingos, D. M. P., Crabtree, R. H., Housecroft, C. E., Eds; Elsevier: Oxford, **2007**; pp. 699 – 808.
2. Reviews on germanium(II) chemistry: (a) Neumann, W. P. *Chem. Rev.* **1991**, *91*, 311. (b) Barrau, J.; Rima, G. *Coord. Chem. Rev.* **1998**, *178-180*, 593. (c) Weidenbruch, M. *Eur. J. Inorg. Chem.* **1999**, 373. (d) Satgé, J. *Chem. Heterocyclic Comp.* **1999**, *35*, 1013. (e) Boganov, S. E.; Faustov, V. I.; Egorov, M. P.; Nefedov, O. M. *Russ. Chem. Bull., Int. Ed.* **2004**, *53*, 960. (f) Zemlyanskii, N. N.; Borisova, I. V.; Nechaev, M. S.; Khrustalev, V. N.; Lunin, V. V.; Antipin, M. Y.; Ustynyuk, Y. A. *Russ. Chem. Bull., Int. Ed.* **2004**, *53*, 980. (g) Kühl, O. *Coord. Chem. Rev.* **2004**, *248*, 411. (h) Leung, W. P.; Kan, K. W.; Chong, K. H. *Coord. Chem. Rev.* **2007**, *251*, 2253. (i) Saur, I.; Alonso, S. G.; Barrau, J. *Appl. Organomet. Chem.* **2005**, *19*, 414. (j) Nagendran, S.; Roesky, H. *Organometallics*, **2008**, *27*, 457.
3. For example, the singlet-triplet gap for germylene (GeH_2) has been calculated at 96 kJ/mol. See Jacobsen, H.; Ziegler, T. *J. Am. Chem. Soc.* **1994**, *116,* 3667.
4. There is a single example of a triplet silylene. See Sekiguchi, A.; Tanaka, T.; Ichinohe, M.; Akiyama, K.; Tero-Kubota, S. *J. Am. Chem. Soc.* **2003**, *125*, 4962.
5. Examples of reactive germylenes being trapped in low temperature matrices are well known. See Boganov, S. E.; Egorov, M. P.; Faustov, V. I.; Nefedov, O. M. In *The*

Chemistry of Organic Germanium, Tin and Lead Compounds, Vol. 2; Rappoport, Z., Ed; John Wiley & Sons Ltd.: West Sussex, England, **2002**; pp 749. – 841.

6. For example, the rate of dimerization of Ph_2Ge has been estimated as 1.1 (±0.2) x 10^{10} $M^{-1}s^{-1}$ in hexanes at room temperature. See: Leigh, W. L.; Harrington, C. R.; Vargas-Baca, I. *J. Am. Chem. Soc.* **2004**, *126*, 16105.

7. Tokitoh, N.; Kishikawa, K.; Okazaki, R.; Sasamori, T.; Nakata, N.; Takeda, N. *Polyhedron* **2002**, *21*, 563.

8. (a) Lange, L.; Meyer, B.; Du Mont, W. W. *J. Organomet. Chem.* **1987**, *329,* C17. (b) Jutzi, P.; Schmidt, H.; Neumann, B.; Stammler, H. *Organometallics* **1996**, *15*, 741.

9. Spikes, G. H.; Peng, Y.; Fettinger, J.C. ; Power, P. P. *Z. Anorg. Allg. Chem.* **2006**, *632*, 1005.

10. Davidson, P. J.; Harris, D. H.; Lappert, M. F. *J. Chem. Soc., Dalton Trans.* **1976**, 2268.

11. (a) Hermann, W. A.; Denk, M.; Behm, J.; Scherer, W.; Klingan, F.; Bock, H.; Solouki, B.; Wagner, M. *Angew. Chem. Int. Ed. Engl.* **1992**, *31*, 1485. (b) Tomasik, A. C.; Hill, N. J. West, R. *J. Organomet. Chem.* **2009**, *694*, 2122.

12. Barrau, J.; Rima, G.; El-Amraoiu, T. *J. Organomet. Chem.* **1998**, *561*, 167.

13. Jutzi, P.; Keitemeyer, S.; Neumann, B.; Stammler, H. *Organometallics* **1999**, *18*, 4778.

14. Yamashita, M.; Murakami, H.; Unrin-in, T.; Kawachi, A.; Akiba, K.; Yamamoto, Y. *Chem. Lett.* **2005**, *34,* 690.

15. Bender, J. E.; Banaszak Holl, M. M.; Kampf, J. W. *Organometallics* **1997**, *16*, 2743.

16. Kolesnikov, S. P.; Shiryaev, V. I.; Nefedov, O. M. *Izv. Akad. Nauk SSSR, Ser. Khim.* **1966**, 584.

17. (a) Cissell, J. A.; Vaid, T. P.; DiPasquale, A. G.; Rheingold, A. L. *Inorg. Chem.* **2007**, *46*, 7713. (b) Cissell, J. A.; Vaid, T. P.; DiPasquale, A. G.; Rheingold, A. L. *J. Am. Chem. Soc.* **2007**, *129*, 7841. (c) Lee, V. Y.; Takanashi, K.; Kato, R.; Matsuno, T.; Ichinohe, M.; Sekiguchi, A. *J. Organomet. Chem.* **2007**, *692*, 2800. (d) Segmueller, T.; Schlueter, P. A.; Drees, M.; Schier, A.; Nogai, S.; Mitzel, N. W.; Strassner, T.; Karsch, H. H. *J. Organomet. Chem.* **2007**, *692*, 2789. (e) Zabula, A. V.; Hahn, F. E.; Pape, T.; Hepp, A. *Organometallics* **2007**, *26*, 1972. (f) Hahn, F. E.; Zabula, A. V.; Pape, T.; Hepp, A. *Eur. J. Inorg. Chem.* **2007**, 2405. (g) Gushwa, A. F.; Richards, A. F. *J. Chem. Cryst.* **2006**, *36*, 851. (h) Fedushkin, I. L.; Hummert, M.; Schumann, H. *Eur. J. Inorg. Chem.* **2006**, 3266. (i) Eichler, J. F.; Just, O.; Rees, W. S., Jr. *Inorg. Chem.* **2006**, *45*, 6706. (j) Pampuch, B.; Saak, W.; Weidenbruch, M. *J. Organomet. Chem.* **2006**, *691*, 3540. (k) Fedushkin, I. L.; Khvoinova, N. M.; Baurin, A.; Yu.; Chudakova, V. A.; Skatova, A. A.; Cherkasov, V. K.; Fukin, G. K.; Baranov, E. V. *Russ. Chem. Bull.* **2006**, *55*, 74. (l) West, R.; Moser, D. F.; Guzei, I. A.; Lee, G.; Naka, A.; Li, W.; Zabula, A.; Bukalov, S.; Leites, L. *Organometallics* **2006**, *25*, 2709. (m) Leung, W.; Wong, K.; Wang, Z.; Mak, T. C. W. *Organometallics* **2006**, *25*, 2037. (n) Schoepper, A.; Saak, W.; Weidenbruch, M. *J. Organomet. Chem.* **2006**, *691*, 809. (o) Stanciu, C.; Richards, A. F.; Stender, M.; Olmstead, M. M.; Power, P. P. *Polyhedron* **2006**, *25*, 477.

18. Leigh, W. J.; Harrington, C. R.; Vargas-Baca, I. *J. Am. Chem. Soc.* **2004**, *126*, 16105.

19. Leigh, W. J.; Lollmahomed, F.; Harrington, C. R.; McDonald, J.M. *Organometallics* **2006**, *25*, 5424.

20. (a) Petz, W. *Chem. Rev.* **1986**, *86*, 1019. (b) Jutzi, P.; Leue, C. *Organometallics* **1994**, *13*, 2898. (c) Litz, K. E.; Henderson, K.; Gourley, R. W.; Banaszak Holl, M. M. *Organometallics* **1995**, *14*, 5008. (d) Litz, K. E.; Bender, J. E.; Kampf, J. W.; Banaszak Holl, M. M. *Angew. Chem. Int., Ed. Engl.* **1997**, *36*, 496. (e) Agustin, D.; Rima, G.; Gornitzka, H.; Barrau, J. *Inorg. Chem.* **2000**, *39*, 5492. (f) Agustin, D.; Rima, G.; Gornitzka, H.; Barrau, J. *Eur. J. Inorg. Chem.* **2000**, 693. (g) Bibal, C.; Mazières, S.; Gornitzka, H.; Couret, C. *Organometallics* **2002**, *21*, 2940. (h) Cygan, Z. T.; Kampf, J. W.; Banaszak Holl, M. M. *Inorg. Chem.* **2003**, *42*, 7219. (i) Saur, I.; Rima, G.; Miqueu, K.; Gornitzka, H.; Barrau, J. *J. Organomet. Chem.* **2003**, *672*, 77. (j) Usui, Y.; Hosotani, S.; Ogawa, A.; Nanjo, M.; Mochida, K. *Organometallics* **2005**, *24*, 4337. (k) Zabula, A. V.; Hahn, F. E.; Pape, T.; Hepp, A. *Organometallics* **2007**, *26*, 1972.

Chapter 2

The Stabilization of Dimesitylgermylene by an N-Heterocyclic Gallium(I) Anion and an N-Heterocyclic Carbene*

2.1 Introduction

The Baines research group has a long standing interest in germanium and mixed germanium-silicon small ring systems as they have proven to be valuable precursors for the easy synthesis of a variety of germanium containing compounds.[1] As part of these research efforts, methods for the incorporation of group 13 elements, such as gallium, into strained germanium rings systems were investigated. One possible route towards such compounds involves the formal [2+2] cycloaddition of a low valent group 13 compound with a digermene (Scheme 2.1).

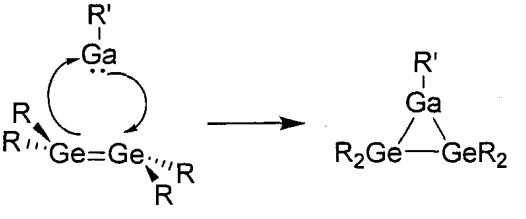

Scheme 2.1

Recently, the group of Prof. Cameron Jones reported the reaction of an anionic gallium(I) containing[2] species, **10**,[3] with digermenes **11** and **12** (Scheme 2.2).[4] Rather than the formation of a germanium-gallium ring as envisioned, the addition of **10** to a solution of **11** gave the complex **13** which was isolated and subsequently characterized by single crystal X-ray diffraction. As illustrated in Scheme 2.2, the structure of **13** consists

---

* This chapter is a combination of two separate publications: Rupar, P. A.; Jennings, M. C.; Baines, K. M. *Can. J. Chem.* **2007**, *85*, 141 and Rupar, P. A.; Jennings, M. C.; Ragogna, P. J.; Baines, K. M. *Organometallics* **2007**, *26*, 4109.

of the germylene fragment coordinated by the N-heterocyclic gallium moiety. A possible interpretation of the nature of **13**, which is alluded to by the authors, is that of a base stabilized germylene, in which the anionic gallium is donating electron density into the empty p-orbital on the germanium.[4]

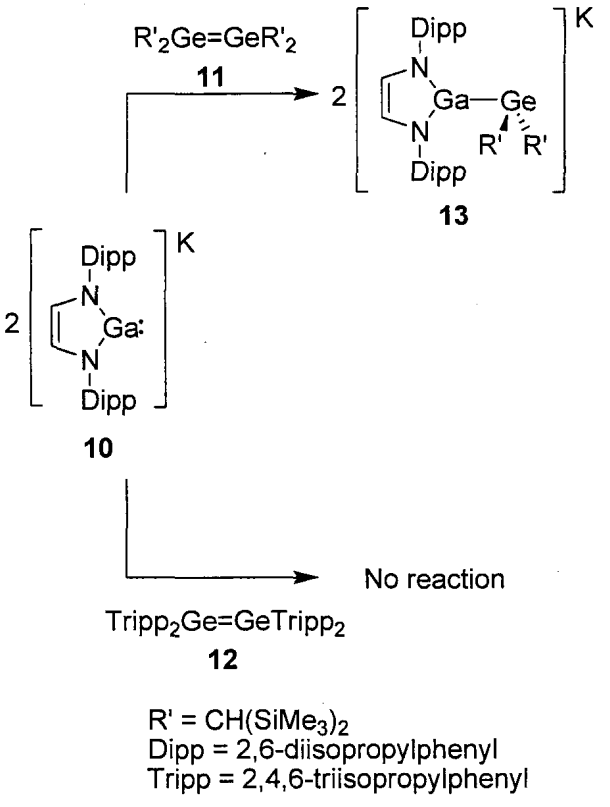

Scheme 2.2

The analogous reaction of **10** with the triisopropylphenyl-substituted digermene **12** did not proceed; the formation of a gallium complex was not observed (Scheme 2.2). Jones *et al.* argued that since digermene **11** readily dissociates to its corresponding germylene[5] in solution (see Chapter 1.2.1), the formation of the anionic complex **13** is most likely due to the direct reaction of **10** with germylene **14** (Scheme 2.3). Unlike digermene **11**, digermene **12** does not readily dissociate in solution at room temperature,[6]

providing a plausible explanation for the difference in reactivity between the two doubly bonded germanium species (Scheme 2.3).

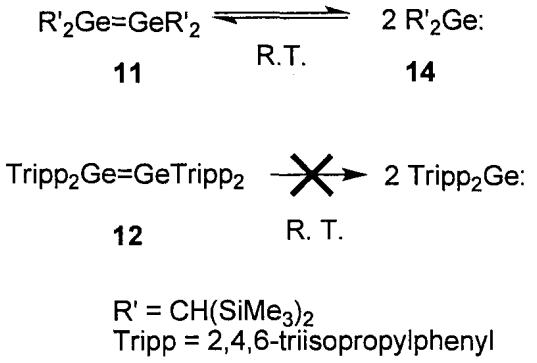

Scheme 2.3

Among the stable aryl substituted digermenes, tetramesityldigermene (**15**) is the least sterically hindered (Scheme 2.4).[7] Like digermene **12**, it does not dissociate in solution, and therefore, reacts as a digermene rather than as a germylene (Scheme 2.4).[7] We were interested in exploring the reaction of **10** with digermene **15** because the decreased size of the aryl substituents of **15** may allow it to react with **10**, whereas the more sterically encumbered digermene **12** did not. The reaction between **10** and tetramesityldigermene (**15**) is now reported and the results are compared to those of the previous study.

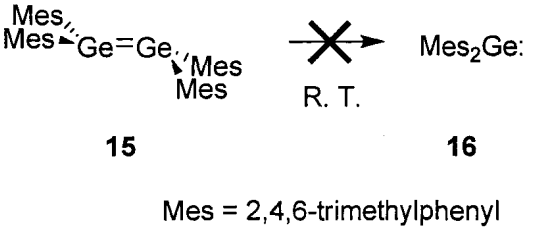

Scheme 2.4

2.2 Results and Discussion

2.2.1 A Gallium(I) Complex of $GeMes_2$

The addition of two equivalents of **10** to a yellow THF solution of **15** initially forms a dark red solution, which rapidly changes colour to orange (Scheme 2.5). After removal of the solvent, analysis of the product mixture by ^{1}H NMR spectroscopy revealed the presence of a new compound, **17**, and hexamesitylcyclotrigermane (**18**) in a 9:1 ratio. The ^{1}H NMR spectrum of compound **17** established that it contained a $\{N(Dipp)CH\}_2$ ligand and two equivalent mesityl groups. Compound **17** was purified by successive washes with hexanes. Crystals of **17** were grown from toluene at -30 °C and unambiguously identified by X-ray crystallography as the anionic, donor-stabilized germylene **17** (Figure 2.1).

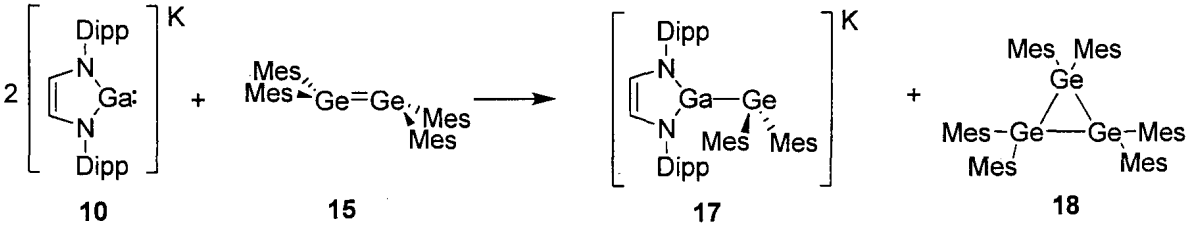

10 **15** **17** **18**

Dipp = 2,6-diisopropylphenyl

Scheme 2.5

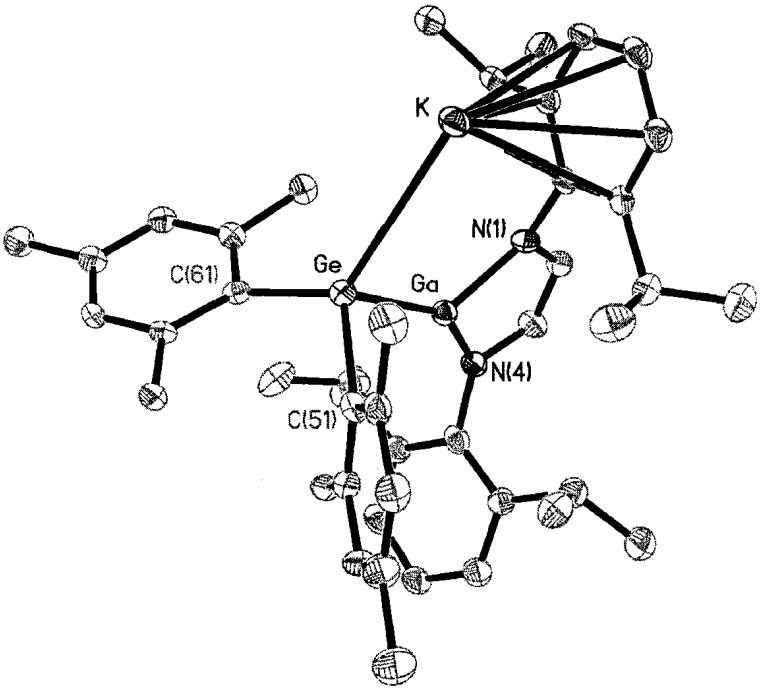

Figure 2.1. Thermal ellipsoid plot (30% probability surface) of the asymmetric unit of **17**. Hydrogen atoms have been omitted for clarity. Selected bond lengths (Å) and angles (deg): Ge-Ga = 2.4600(8), Ge-K = 3.3987(15), Ge-C51 = 2.021(6), Ge-C61 = 2.030(6), Ga-Ge-C51 = 99.01(16), Ga-Ge-C61 = 102.85(15), Ga-Ge-K = 90.02(3), C51-Ge-K = 119.28(17), C61-Ge-K = 126.9716, C51-Ge-C61 = 109.2(2), N1-Ga-N4 = 85.8(2), Ge-Ga-N4 = 149.47(15), Ge-Ga-N1 = 123.88(14).

Compound **17** crystallized as a symmetrical dimer, half of which is shown in Figure 2.1. The structural metrics of **17** are similar to those previously reported for **13**.[4] The unsolvated potassium is directly associated with the germanium at a distance of 3.3987(15) Å. Furthermore, the potassium bridges between the aromatic diisopropylphenyl group of one molecule and the aromatic ring of the mesityl group of a second molecule (not shown in Figure 2.1). The metrics of the $\{N(Ar)CH\}_2$ backbone are typical of those found in other gallium NHC complexes: the N-Ga bond length

(average: 1.886 Å) is significantly shorter and the N-Ga-N bond angle is larger (85.8(2)°) in comparison to the uncomplexed anionic gallium NHC (approximately 2.01 Å and 82°, respectively).[3] The gallium-germanium bond length in **17** is 2.4600(8) Å, which is typical of other gallium-germanium single bonds,[8] but shorter than that found in **13**. The long gallium-germanium bond length in **13** (2.5396(8) Å) was attributed to increased steric congestion around the germanium centre.[4] The geometry about the germanium in **17** is pyramidal and the Ga-Ge-Mes bond angles are more acute (99.01(16) Å and 102.85(15) Å) than expected given the steric bulk. These features are consistent with the previous report, suggesting that the germanium centre can be described as sp^2-hybridized with the gallium donating into the empty p-orbital on the germanium[4] and can be regarded as a base-stabilized germylene.

Unlike digermene **11**, digermene **15** does not dissociate to the corresponding germylene in solution. Thus, we do not believe that the major pathway to compound **17** is by the direct reaction of germylene **16** with the N-heterocyclic **10**. We propose that the addition of **10** to digermene **15** initially yields the germyl anion **19**, which then eliminates the transient dimesitylgermylene (**16**) (Scheme 2.6).

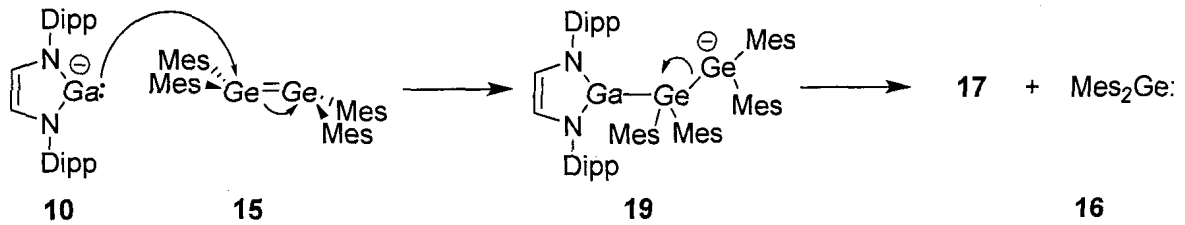

Scheme 2.6

Germylene **16** can then dimerize to give **15**,[9] react with a molecule of **10** forming **17**, or insert into the double bond of **15** resulting in the formation of cyclotrigermane **18** (Scheme 2.7).[10] Since digermene **15** is generated by photolysis of cyclotrigermane **18**,[7] the observation of the cyclotrigermane in the product mixture may also be attributed to incomplete photolysis. However, careful examination of the ^{1}H NMR spectrum of the solution of **15** prior to the addition of **10** revealed the complete absence of cyclotrigermane **18**. Thus, the amount of cyclotrigermane **18** present must be less than 5% (the assumed upper detection limit of the NMR experiment). This is much less than the 10% of **18** generated during the reaction of **15** with **10**.

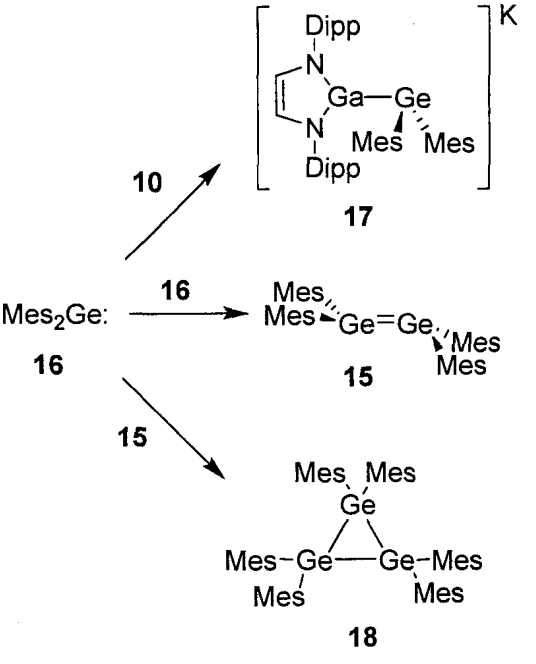

Scheme 2.7

A similar mechanism has been proposed to explain the results of the addition of Grignard reagents to tetramesityldigermene (**15**).[1a,h] The nucleophilic addition of RMgX to the digermene **15** resulted in the formation of a germyl Grignard reagent which underwent subsequent elimination of MesMgX to give a germylene. Our results show

that direct addition of **10** to digermenes is possible and the reaction of **10** with a digermene does not require prior dissociation to a germylene.

The isolation of **17** is remarkable because it is the first example of the stabilization of a *transient* germylene by intermolecular coordination. The chemistry of dimesitylgermylene (**16**) has been well studied but only through trapping reactions or laser flash photolysis experiments.[1, 11] Normally, when **16** is generated, it dimerizes to the digermene **15** on route to forming high oligomers. The rate of this process is extremely rapid; it has been estimated to be $5 \times 10^9 M^{-1}s^{-1}$.[12]

We have also investigated the reactivity of two additional gallium(I) species (**20** and **21**)[13,14] and a N-heterocyclic germylene **22**[15] towards **15** (Chart 2.1). However, in each case, no reaction was observed, likely due to the decreased nucleophilicity of compounds **20 - 22**. The reactivity of two other common Lewis bases was also examined, pyridine and PMe_3, but again, the formation of a complex was not observed. Interestingly, the addition of PMe_3 accelerated the conversion of the digermene **15** to the cyclotrigermane **18**.

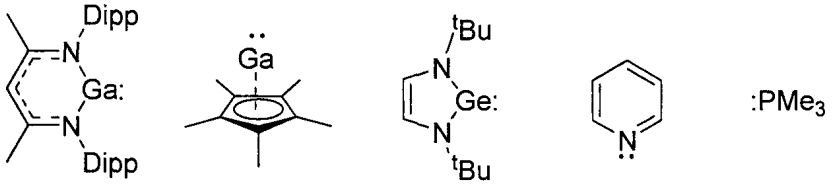

20 **21** **22**

Chart 2.1

2.2.2 Salt Elimination Reactions of 17

To explore the reactivity of **17**, CH_3I and Me_3SiCl were added to the new complex (Scheme 2.8). The addition of CH_3I to a solution of **17** dissolved in THF resulted in the

instantaneous formation of a white precipitate. Analysis of the reaction mixture by ^{1}H NMR spectroscopy revealed the quantitative conversion of **17** to a new species, **23**. The product was unambiguously identified by mass spectrometry and NMR spectroscopy. The EI mass spectrum of **23** revealed a highest mass ion at *m/z* 772, with the expected isotopic distribution corresponding to the molecular ion of methylated **23**. The ^{1}H-^{13}C gHMBC spectrum of **23** showed a correlation between the signal at 0.77 ppm in the ^{1}H dimension, assigned to the Ge-CH_3 group, and the signal at 136.20 ppm in the ^{13}C dimension, assigned to the *ipso*-mesityl carbon. All signals in the ^{1}H and ^{13}C NMR spectra of **23** were entirely consistent with the proposed structure.

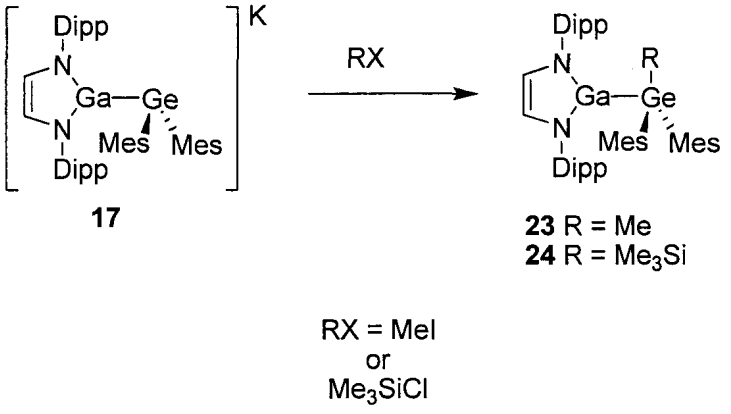

Scheme 2.8

The addition of $(CH_3)_3SiCl$ to a THF solution of **17** resulted in the rapid change in colour of the solution from orange to yellow (Scheme 2.8). NMR spectroscopic analysis (^{1}H, ^{13}C, and ^{29}Si) of the solid isolated after solvent removal was consistent with formation of the trimethylsilyl adduct of **17**. Yellow crystals of **24** were grown from a solution of toluene and acetonitrile at -30 °C and analyzed by X-ray diffraction. Compound **24** crystallizes with two distinct molecules in the asymmetric unit. Although chemically identical, they differ structurally by the orientation of the mesityl substituents and the length of the gallium-germanium bond. The difference in the gallium-germanium

bond length (2.4082(9) Å vs. 2.4312(10) Å) is most likely due to increased steric demands caused by the rotation of one of the mesityl substituents. Only one of the molecules from the unit cell is presented in Figure 2.2.

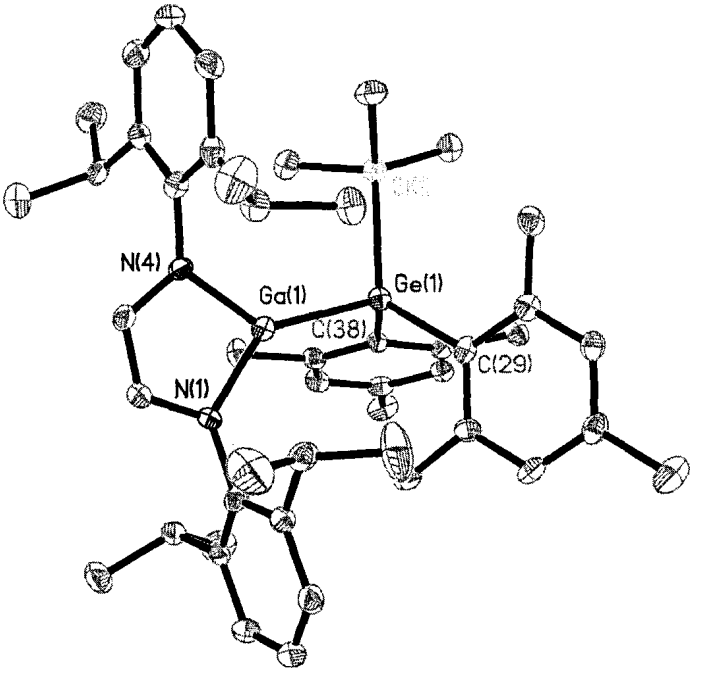

Figure 2.2 Thermal ellipsoid plot (30% probability surface) of **24**. Hydrogen atoms have been omitted for clarity. Selected bond lengths (Å) and angles (deg): Ge1-Ga1 = 2.4311(10), Ge1-Si1 = 2.4162(19), Ge1-C29 = 2.011(3), Ge1-C38 = 2.026(3), Ga1-Ge1-Si1 = 107.65(5), Ga1-Ge1-C29 = 103.31(12), Ga1-Ge1-C38 = 113.63(11), Si1-Ge1-C29 = 125.33(13), Si1-Ge1-C38 = 99.15(13), C29-Ge1-C38 = 108.13(16).

The structure of **24** is similar to that of **17**, except the potassium has been replaced with $(CH_3)_3Si$. The metrics of the N-heterocyclic backbone are essentially unchanged from **17**. The geometry about the germanium is now a distorted tetrahedron. The Ga-Ge-*ipso*-C angles have increased from 99.01(16)° and 102.85(15)° in **17** to 103.31(12)° and 113.63(11)° in **24**. The gallium-germanium bond length has decreased from 2.4600(8) Å

in **10** to 2.4312(10) Å in **24**, despite the added steric bulk of the $(CH_3)_3Si$ group. The transformation of the non-bonding pair of electrons on germanium to a bonding pair would reduce electron-electron repulsion, thereby promoting a decrease in the gallium-germanium bond length.

2.2.3 The Stabilization of $GeMes_2$ by an N-Heterocyclic Carbene

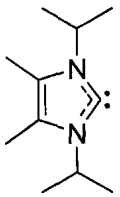

25

Chart 2.2

Based on the successful synthesis of **17**, a strong donor, such as the gallium(I) **10**, can stabilize dimesitylgermylene (**16**) by transferring electron density into the empty p-orbital on germanium. An intermolecularly stabilized germylene is expected to be synthetically useful (c.f. $GeCl_2$·dioxane) however, a more accessible donor, compared to a Ga(I) ligand, is desirable. Although a selection of other Lewis bases was not successful in stabilizing **16** (Chart 2.1), *N*-heterocyclic carbenes (NHCs), which are amongst the strongest neutral donors known,[16] may be suitable for this task. While NHCs are predominantly used in transition metal chemistry,[17] there has been an increase in the successful use of *N*-heterocyclic carbenes in the stabilization of main group compounds.[18, 19, 20, 21, 22, 23, 24, 25] Therefore, we examined NHC **25**[26] for the base stabilization of transient germylenes (Chart 2.2).

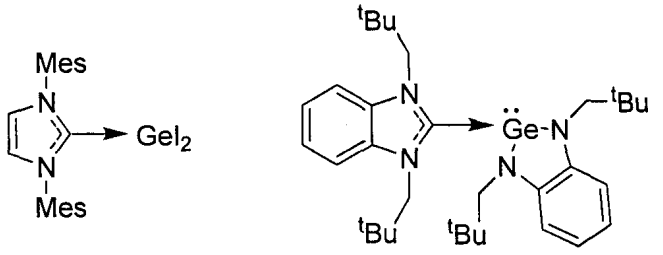

26 **27**

Chart 2.3

Prior to this work, only two NHC-GeR_2 species have been structurally characterized: NHC-GeI_2 (**26**)[27] and NHC-*N*-heterocyclic germylene complex **27** (Chart 2.3).[28] In both cases, the uncoordinated, free germanium(II) compounds are intrinsically stable and have been isolated and characterized independent of coordination.[28]

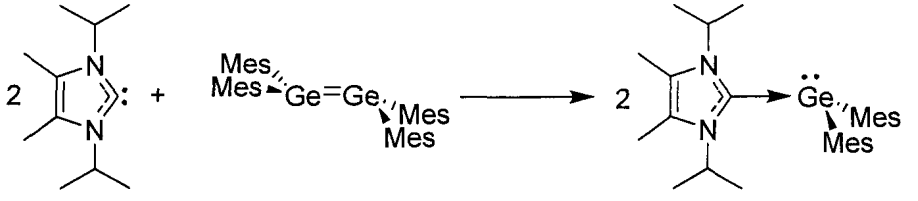

25 **15** **28**

Scheme 2.9[29]

Two equivalents of carbene **25** were added to a yellow solution of tetramesityldigermene (**15**) (Scheme 2.9). No visible change was observed. ^1H and $^{13}C\{^1H\}$ NMR spectroscopic analysis of the yellow residue, obtained after removal of the solvent, indicated quantitative conversion of the starting materials to a single product. The ^1H NMR spectrum of the product revealed the carbene and dimesitylgermylene moieties to be in a 1:1 ratio and the ^{13}C signal attributable to the carbenic carbon shifted upfield from 206 ppm to 176 ppm, which is indicative of carbene coordination. Crystals suitable for X-ray crystallographic analysis were grown from a concentrated toluene

solution at -30 °C. The molecular structure of the product was unambiguously determined to be **28** by single crystal X-ray diffraction analysis (Figure 2.3).

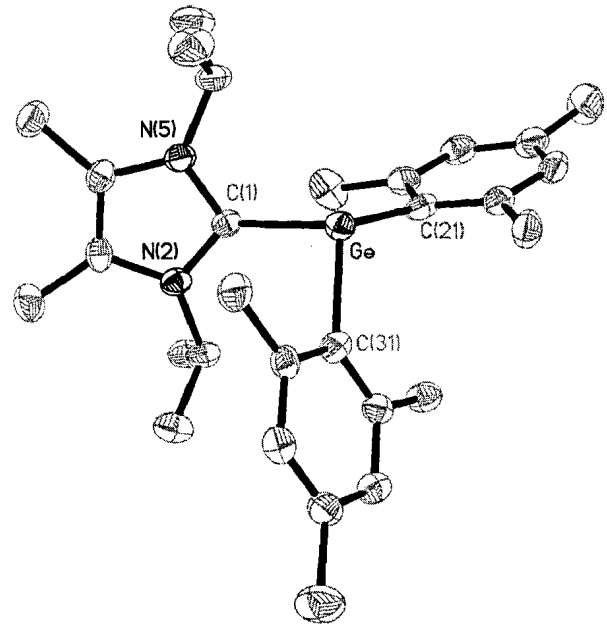

Figure 2.3. Thermal ellipsoid plot (50% probability surface) of **28**. Hydrogen atoms have been omitted for clarity. Selected bond distances (Å) and angles (°): Ge-C1 = 2.078(4), Ge-C21 = 2.065(2), Ge-C31 = 2.072(2), C1-N2 = 1.359(4), C1-N5 = 1.357(5), C1-Ge-C21 = 109.2(1), C1-Ge-C31 = 95.9(1), C21-Ge-C31 = 112.6(1).

The carbenic carbon-germanium bond length of 2.078(4) Å is consistent with a carbon-germanium single bond and the germanium centre is pyramidal, which is indicative of the presence of a stereochemically active lone pair of electrons. The same trends were observed in the related NHC-tin(II) and lead(II) complexes.[21, 22]

Unlike what was observed in the formation of **17** (Scheme 2.5 and 2.7), hexamesitylcyclotrigermane (**18**) was not detected in the reaction between **15** and **25**. We propose that the mechanism for the formation of **28** is comparable to that of **17**. Specifically, carbene **25** nucleophilically attacks **15** and forms **28** while displacing

dimesitylgermylene (**16**). Since NHC **25** is a stronger, less hindered, base than **10**, the rate at which **25** coordinates to **16** is faster than the rate at which **16** cyclizes with unreacted **15** to form **18** (Scheme 2.7).

2.2.4 Preliminary Reactivity Studies of 28

2,3-Dimethylbutadiene (DMB), a well known germylene trap, is often used to verify the presence of reactive germylenes; the diene undergoes rapid formal [2 + 4] cycloaddition with the germylene to give a germacyclopentene.[30, 31, 32] Addition of DMB to a THF solution of **28** at room temperature resulted in no observable reaction, suggesting that the carbene-germanium bond is stable under these conditions. Heating the THF solution to 70 °C in a sealed tube resulted in the quantitative formation of DMB-trapped germylene **29**, along with a stoichiometric equivalent of free NHC **25** (Scheme 2.10).[33] We believe that **28** dissociates to the free carbene and the free germylene under these conditions.

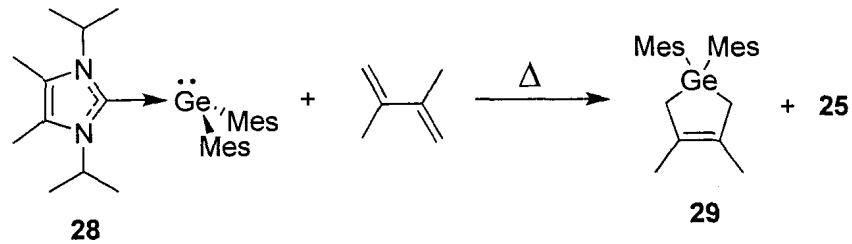

28 **29**

Scheme 2.10

The germanium centre in **28** has three bonds to carbon and a lone pair, and thus, is an isovalent analogue of phosphines (R_3Ge^- c.f. R_3P:). To evaluate the potential of **28** to act as a Lewis base, one equivalent of BH_3•THF was added to a THF solution of **28** (Scheme 2.11), resulting in the formation of a clear and colourless solution. Removal of the solvent *in vacuo* gave a white, air-stable powder. The ^1H NMR spectrum of the powder

indicated that the carbene and dimesitylgermylene moieties remain in a 1:1 ratio. In addition, a broad signal, which integrates for three hydrogens, was observed at 1.9 ppm. The FT-IR spectrum of the powder showed a series of signals centred at 2300 cm^{-1}, which is in the expected range for boron-hydrogen bond vibrations. High resolution mass spectrometric analysis of the sample revealed an M^+ ion consistent with a BH_3 adduct of **28**. A single crystal suitable for X-ray diffraction was grown by slow evaporation of a benzene solution of the reaction product and was confirmed to be **30**.

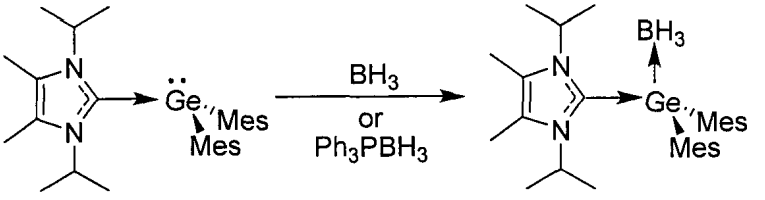

Scheme 2.11

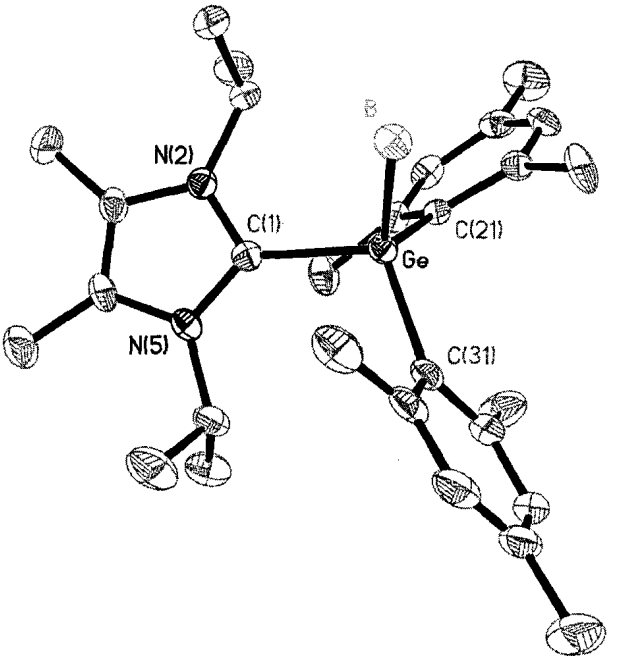

Figure 2.4 Thermal ellipsoid plot (50% probability surface) of **30**. Hydrogen atoms omitted for clarity. Selected bond distances (Å) and angles (°): C1-Ge = 2.047(3), Ge-B =

2.095(3), Ge-C21 = 2.005(2), Ge-C31 = 2.002(3), C1-N2 = 1.363(3), C1-N5 = 1.353(3), C1-Ge-B = 104.6(1), C1-Ge-C21 = 102.7(1), C1-Ge-C31 = 109.5(1), C21-Ge-C31 = 112.9(1).

The molecular structure of **30** is shown in Figure 2.4. Complex **30** can be viewed as a carbene-germylene-borane "in-series" coordination complex, where the germanium is simultaneously an electron pair acceptor and an electron pair donor (Scheme 2.11). The metrics of **30** are similar to **28**; however, the NHC-Ge-Mes angles are slightly more obtuse[34] and the germanium-carbon bond lengths are somewhat decreased.[35] Both observations are consistent with the conversion of the lone pair of electrons on the germanium centre into a bonding pair of electrons.[36] The Ge-B bond length is 2.095(3) Å. Heating **28** in the presence of $Ph_3P{\bullet}BH_3$ resulted in the formation of **30** and the recovery of free PPh_3, demonstrating that **28** is a stronger donor than PPh_3 (Scheme 2.11). Remarkably, **30** is air stable, which is in striking contrast to the parent **28**.

Finally, in an effort to displace the carbene from the germanium, methyllithium was added to a solution of **28**. After an aqueous workup, compound **31**[37] was isolated (Scheme 2.12). Furthermore, when 0.5 equiv of methyllithium is added to **28**, a mixture of **31** and **32** is isolated following aqueous workup.

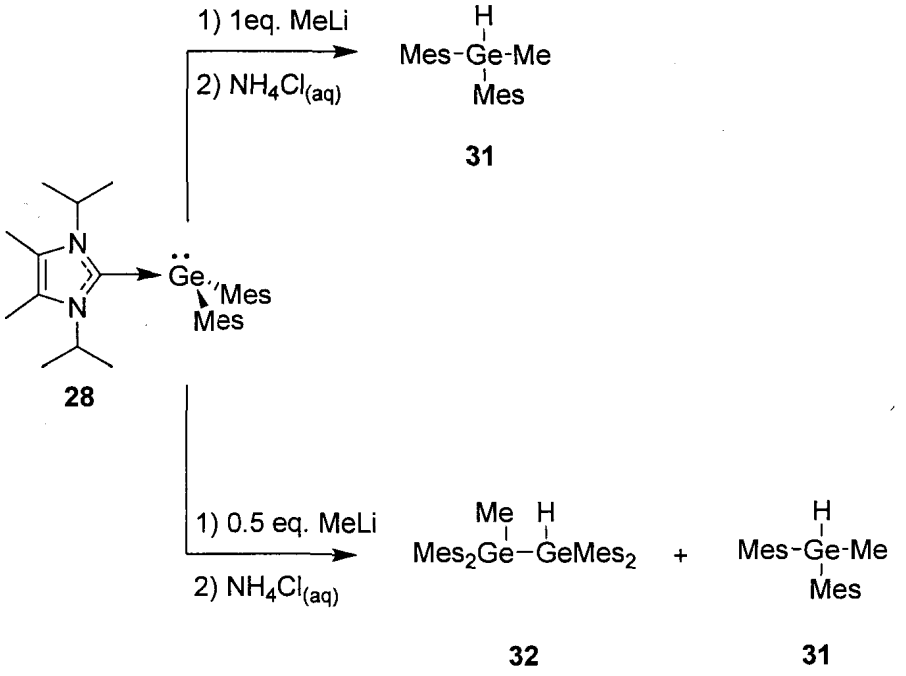

Scheme 2.12

The formation of **31** and **32** is believed to occur by the mechanism shown in Scheme 2.13. Initially, methyllithium does a nucleophilic attack on **28**, displacing **25** and forming germyl lithum **33**. The germyl lithium **33** is then able to nucleophilically attack a second molecule of **28**, displacing another molecule of **25** and forming the digermyl lithium **34**. Upon aqueous workup, both **33** and **34** are protonated to give the observed **31** and **32**. Liberated NHC **25** is also protonated to give **35** which is washed away in the aqueous phase and is not isolated.

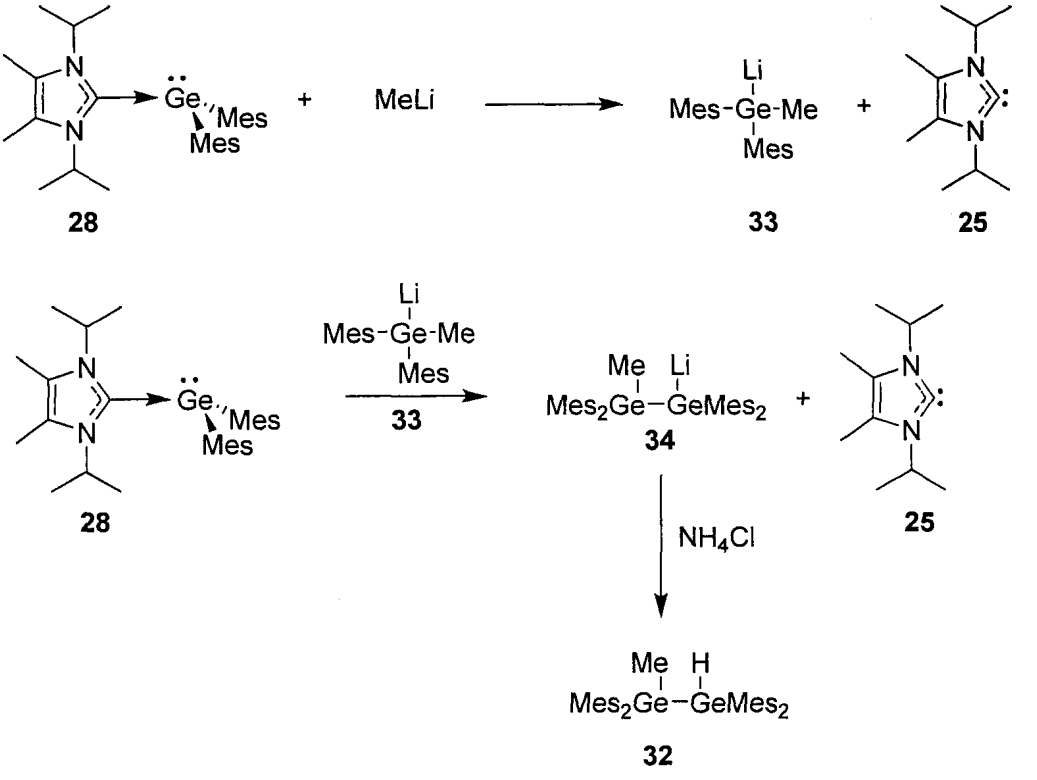

Scheme 2.13

The mechanism shown in Scheme 2.13 is similar to what occurs in a living anionic polymerization.[38] Unfortunately, attempts at forming higher oligomers by the reaction of substoichiometric amounts of methyllithium with **28** were not successful; only complex mixtures were obtained. We believe that there are three compounding factors. First, the reaction is very slow: the reaction of stoichiometric MeLi with **28** to form **31** takes over 18 hr to complete. Second, germyl anions tend to be unstable and probably decompose either by proton abstraction or through alpha elimination of a mesityl anion. Finally, if larger oligomers do begin to form, the steric bulk of the mesityl groups would be additive and further slow the growth of the polymer chain.

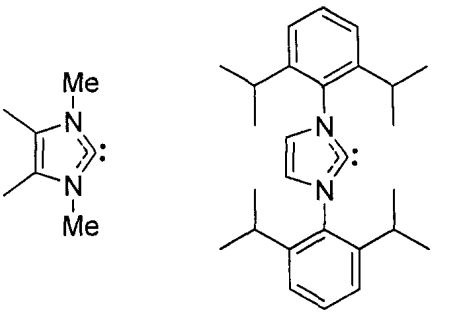

Chart 2.4

Given the ability of **25** to stabilize $GeMes_2$ (**16**), the reactivity of two other N-heterocyclic carbenes with tetramesityldigermene (**15**) was examined (Chart 2.4). The less bulky tetramethyl substituted NHC behaved similarly to **25** and is discussed briefly in Chapter 3 of this thesis. The larger, diisopropylphenyl substituted NHC did not react with **15** (Chart 2.4).

36 **37**

Chart 2.5

The reactivity of two other heavy alkene analogues with **25** was examined (Chart 2.5). The addition of **25** to a yellow solution of tetramesityldisilene[39] (**36**) produced a red solution. Analysis of the solution by ^1H NMR spectroscopy showed signals with identical chemical shifts as those of **25** and **36**. The species responsible for the red colour must be present in amounts lower than the detection limit of the NMR experiment. Attempts to grow crystals from the solution were not successful.

The addition of **25** to a solution of **37**[40] resulted in the rapid dimerization of **37** into **38** (Scheme 2.14). The dimerization of **37** was previously reported, however, it took

many days to go to completion;[41] the carbene appears to catalytically accelerate the dimerization.

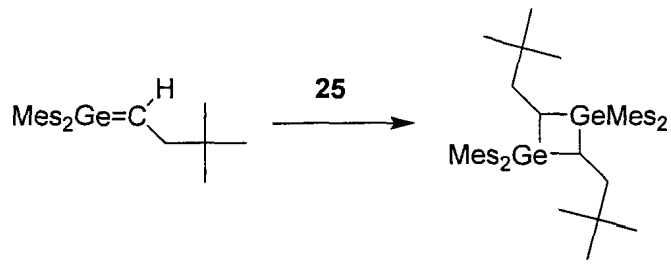

37 **38**

Scheme 2.14

2.3 Conclusions

In summary, the addition of the gallium NHC analogue **10** to the solution stable digermene **15** resulted in the formation of complex **17**. The molecular structure of **17** was determined and found to be similar to the previously reported gallium NHC complex **13**. The formation of **17** from **15** demonstrates that the gallium NHC analogue **10** is able to add directly to digermenes and cause subsequent cleavage of the germanium-germanium double bond; dissociation of digermenes into germylenes is not a prerequisite for a reaction to occur with **10**. **17** is the first example of a transient germylene being stabilized intermolecularly by a Lewis base.

The anionic complex **17** was derivatized with CH_3I and $(CH_3)_3SiCl$, forming compounds **23** and **24** respectively. The molecular structure of the $(CH_3)_3Si$ adduct **24** was determined and the gallium-germanium bond length was less than the parent compound **17**.

We have also synthesized the first example of a carbene-stabilized transient diorganogermylene, **28**, from readily available starting materials. Complex **28** acts as a

strong Lewis base towards BH_3 to give **30**. The carbene-germylene complex **28** is a thermal source of dimesitylgermylene (**16**) and reacts with MeLi to displace the carbene.

Compounds **17** and **28** represent a novel class of Ge(II) compounds: stable Lewis acid/base adducts of a transient germylene. The ease of synthesis, especially of the NHC supported **28**, suggests that other reactive GeR_2 may be stabilized using similar techniques.

2.4 Experimental

All manipulations were carried out under a dry N_2 environment at room temperature in a glove box. Solvents were dried by passing through an alumina column and were subsequently degassed.[42] Compounds **10**,[3] **15**,[7] **20**,[13] **21**,[14] **22**,[15] **25**,[26] **36**,[39] and **37**[40] were synthesized following literature procedures. All other chemicals were purchased from commercial sources and used without further purification. NMR chemical shifts are reported in ppm with coupling constants in Hz. All spectra were acquired using C_6D_6 as the solvent. ^1H NMR spectra were referenced to residual C_6D_5H (7.15 ppm). ^{13}C spectra were referenced to the ^{13}C central transition (128.0 ppm) of C_6D_6. ^{13}C signals were unambiguously assigned using ^1H-^{13}C gHSQC and ^1H-^{13}C gHMBC spectroscopy. ^{29}Si chemical shifts were obtained using ^1H-^{29}Si gHMBC spectroscopy and referenced externally to $(CH_3)_4Si$ (0.0 ppm). Melting points were determined under a N_2 atmosphere and are uncorrected. Elemental analyses were performed at Guelph Chemical Laboratories, Guelph, Ontario, Canada.

2.4.1 Preparation of 17

To a yellow solution of Mes_4Ge_2 (**15**) (0.161 mmol, from the photolysis of 100 mg of Mes_6Ge_3 **18**) dissolved in THF (5 mL) was added a red THF (2 mL) solution of **10** (0.32 mmol, 0.16 g) dissolved in THF (2 mL) to give a dark red solution. After 5 min, the colour of the solution changed to orange. The solvent was removed under vacuum yielding an orange residue. The residue was taken up in hexanes and a centrifuge was used to remove suspended salts. The yellow precipitate was collected and washed with hexanes repeatedly. Compound **17** was collected as a yellow powder in 60% yield (0.15 g, 0.19 mmol). Crystals suitable for X-ray analysis were grown from a concentrated toluene solution stored at -30 °C. M.P. 98 °C (dec); ^{1}H NMR: 1.02 (d, $^3J_{HH}$= 6 Hz, 12 H, *i*-Pr CH_3), 1.23 (d, $^3J_{HH}$= 6 Hz, 12 H, *i*-Pr CH_3), 2.15 (s, 6 H, *p*-Mes-CH_3), 2.21 (s, 12 H, *o*-Mes-CH_3), 3.58 (sept, $^3J_{HH}$= 7 Hz, 4 H, *i*-Pr CH), 6.30 (s, 2 H, C_2H_2), 6.67 (s, 4 H, *m*-Mes-H), 7.01 (s, 6 H, *m,p*-Ar-H); ^{13}C {^{1}H} NMR: 20.96 (*p*-Mes-CH_3), 24.40 (*i*-Pr-CH_3), 25.56 (*i*-Pr-CH_3), 27.04 (*o*-Mes-CH_3), 28.30 (*i*-Pr-CH), 121.40 (C_2H_2), 122.86 (*m*-Ar-CH), 124.86 (*p*-Ar-CH), 128.28 (*m*-Mes-CH), 134.36 (*p*-Mes-C), 143.14 (*o*-Mes-C), 147.02 (*o*-Ar-C), 148.47 (*i*-Ar-C), 150.83 (*i*-Mes-C); MS/ESI neg ion: *m/z* 376 [{N(Ar)CH}$_2^-$, 100%].

2.4.2 Preparation of 23

Excess methyl iodide (0.1 mL) was added to an orange THF (5 mL) solution of **17** (0.16 mmol, 130 mg). A white precipitate formed instantly and the solution turned yellow. The solvent was removed under vacuum and the residue was extracted with hexanes. The suspended salts were removed by centrifuge yielding a yellow hexanes

solution. The solvent was removed under vacuum to give **23** as a yellow powder in a yield of 97% (0.12 g, 0.155 mmol). ^{1}H NMR: 0.77 (s, 3 H, CH_3-Ge), 1.13 (d, $^3J_{HH}$=7 Hz, 12 H, *i*-Pr CH_3), 1.26 (d, 12 H, $^3J_{HH}$= 6 Hz, *i*-Pr CH_3), 2.02 (s, 6 H, *p*-Mes-CH_3), 2.15 (s, 12 H, *o*-Mes-CH_3), 3.57 (sept, 4 H, $^3J_{HH}$ = 7 Hz, *i*-Pr CH), 6.32 (s, 2 H, C_2H_2), 6.57 (s, 4 H, *m*-Mes-H), 7.13-7.20 (m, 6 H, *m,p*-Ar-H); ^{13}C{^{1}H} NMR: 5.35 (Ge-Me), 20.84 (*p*-Mes-CH_3), 23.84 (CH(CH_3)$_2$), 24.58 (*o*-Mes-CH_3), 25.98 (CH(CH_3)$_2$), 28.68 (CH(CH_3)$_2$), 121.94 (C_2H_2), 123.30 (*m*-Ar-CH), 125.96 (*p*-Ar-CH), 129.54 (*m*-Mes-CH), 136.20 (*i*-Mes-C), 138.22 (*p*-Mes-C), 142.22 (*o*-Mes-C) 145.63 (*o*-Ar-C), 145.70 (*i*-Ar-*C*); MS/EI: *m/z* 772 [M^+, 50%], 564 [M^+ - GeMesMe, 70%], 445 [Ga{N(Ar)CH}$_2^+$, 30%], 327 [$GeMes_2Me^+$, 100%]; High resolution MS/EI for $C_{45}H_{61}{}^{69}Ga^{74}GeN_2$ calc. 772.331, found 772.328.

2.4.3 Preparation of 24

Excess $(CH_3)_3SiCl$ (50 μL, 0.39 mmol) was added to an orange THF solution (2 mL) of **17** (100 mg, 0.12 mmol). The colour of the solution immediately turned to yellow; the solution was allowed to stir for 5 min. The solvent was removed under vacuum yielding a yellow residue. The residue was taken up in hexanes (5 mL) and the suspended solids were removed by centrifugation. The hexanes were removed under vacuum leaving behind a yellow/orange residue of essentially pure **24** with a yield of 67% (0.07 g, 0.08 mmol). Crystals suitable for X-ray analysis were grown from a concentrated toluene/acetonitrile solution stored at -30 °C. M.P. 190 - 192 °C; ^{1}H NMR: -0.01 (s, 9 H, Si(CH_3)$_3$), 1.14 (d, $^3J_{HH}$ = 7 Hz, 12 H, *i*-Pr CH_3), 1.27 (d, $^3J_{HH}$= 7 Hz, 12 H, *i*-Pr CH_3), 2.05 (s, 6 H, *p*-Mes-CH_3), 2.08 (s, 12 H, *o*-Mes-CH_3), 3.53 (sept, $^3J_{HH}$= 7 Hz, 2 H, *i*-Pr-

CH), 6.31 (s, 2 H, C_2H_2), 6.82 (s, 4 H, *m*-Mes-CH), 7.12 - 7.21 (m, 6 H, *m,p*-Ar-CH); $^{13}C\{1H\}$ NMR: 1.36, 14.34, 20.85, 23.37, 26.29, 26.52, 28.85, 122.58, 123.31, 125.88, 129.15, 136.58, 137.45, 142.37, 145.80, 146.42; ^{29}Si NMR: -2.3; MS/EI: *m/z* 830 [M^+, 58%], 564 [M^+ - $(CH_3)_3SiGeMes$, 21%], 445 [M^+ - $(CH_3)_3SiGeMes_2$, 43%], 385 [$(CH_3)_3SiGeMes_2$, 100%].

2.4.4 Synthesis of 28

To a yellow solution of **15** (0.161 mmol, from the photolysis of 100 mg of **16**) dissolved in THF (5 mL) was added NHC **25** (0.32 mmol, 0.06 g) dissolved in THF (5 mL). The reaction was allowed to stir for 5 min. The solvent was removed under vacuum yielding a yellow powder of essentially pure **28** in 96% yield (0.15 g, 0.31 mmol). Crystals suitable for X-ray analysis were grown from a concentrated toluene solution stored at -30 °C. M.P. 144-146 °C; ^1H NMR: 0.96 (d, $^3J_{HH}$ = 7 Hz, 12 H), 1.50 (s, 6 H), 2.29 (s, 6 H), 2.59 (s, 12 H), 5.73 (sept, $^3J_{HH}$ = 7 Hz, 2 H), 6.93 (s, 4 H); $^{13}C\{^1H\}$ NMR: 9.99, 20.79, 21.20, 25.54, 51.91, 125.88, 128.51, 134.37, 143.97, 152.31, 176.06; EI-MS: *m/z* 311 [Mes_2Ge, 6%], 180 [C{[N(*i*-Pr)C$(CH_3)]_2$}, 34%], 138 [C{[N(*i*-Pr)C$(CH_3)]_2$} - *i*-Pr, 40%].

2.4.5 Reaction of 28 with DMB

To a THF (10 mL) solution of **28** (0.15 g, 0.31 mmol) was added excess 2,3-dimethylbutadiene (5 mL). The reaction mixture was allowed to stir for 24 hr at room temperature. ^1H NMR spectroscopy of the crude reaction mixture showed that no reaction had occurred. The reaction was heated to 70 °C in a sealed tube for 24 hr and

allowed to stir. After cooling, a small aliquot was removed from the reaction mixture. The solvent was removed from the aliquot and ^{1}H NMR spectroscopy of the residue showed clean conversion of **28** to **29** and **25**. A saturated $NH_4Cl_{(aq)}$ solution (20 mL) was added to the reaction mixture and the organic layer was separated from the aqueous layer. The aqueous layer was extracted with diethyl ether (3 x 10 mL). The organic layers were combined and the solvent removed *in vacuo* giving **29** as a white solid in 79% yield (0.10 g, 0.25 mmol). Compound **29** was identified by comparison of the ^{1}H NMR spectrum of the product to that of an authentic sample.[43]

2.4.6 Synthesis of 30

To a yellow solution of **28** (0.15 g, 0.31 mmol) dissolved in THF (10 mL) was added a 1 M solution of BH_3•THF in THF (0.31 mL, 0.31 mmol). The yellow solution faded to a clear and colourless solution after 15 min. The solvent was removed under vacuum yielding a white powder of pure **30** in a quantitative yield. Crystals suitable for X-ray analysis were grown by the slow evaporation of a saturated C_6H_6 solution. M.P. 155-162 °C (dec); ^{1}H NMR: 1.00 (d, $^3J_{HH}$ = 7 Hz, 12 H), 1.51 (s, 6 H), 1.70 – 2.10 (broad, 3 H), 2.18 (s, 6 H), 2.52 (s, 12 H), 5.55 (broad, 2 H), 6.82 (s, 4 H); ^{13}C{^{1}H}NMR: 10.12, 21.04, 21.39, 26.02, 51.41, 127.55, 129.42, 136.97, 143.01, 144.46, 164.60; ^{11}B: -28.49 (broad); IR: 847 (m), 1035 (s), 1374 (s), 1457 (broad, s), 1600 (m), 2268 (s), 2298 (s), 2349 (s), 2375 (m), 2731 (w), 2867 (s), 2921 (s), 2874 (s); EI-MS: *m/z* 505 [M^+, 5%], 492 [M^+ - BH_3, 100%], 373 [C{[N(*i*-Pr)C(CH_3)]$_2$}GeMes, 10%], 311 [Mes_2Ge, 20%]. High resolution EI-MS calcd. for $C_{29}H_{45}{}^{11}B^{74}GeN_2$ 505.2818. Found: 505.2820. Anal. Calcd For $C_{29}H_{45}BGeN_2$: C, 68.96; H, 8.98. Found: C, 68.62; H, 9.45.

2.4.7 Reaction of 28 with PPh_3BH_3

A 1 M solution of BH_3•THF in THF (0.32 mL, 0.32 mmol) was added to a solution of PPh_3 (0.09 g, 0.32 mmol) dissolved in THF (5 mL). The solution was allowed to stir at room temperature for 20 min. **28** (0.15 g, 0.32 mmol) was then added to the reaction mixture. After stirring for 18 hr at room temperature, no reaction was observed upon analysis of the crude reaction mixture by ^1H & ^{31}P NMR spectroscopy. The solution was heated to 70 °C in a sealed tube and then allowed to stir for 18 hr at that temperature. ^1H NMR spectroscopic analysis of the crude product mixture showed conversion of **28** to **30**. ^{31}P NMR spectroscopy of the crude reaction mixture revealed the formation of PPh_3.

2.4.8 Reaction of 28 with MeLi

28 (0.15 g, 0.31 mmol) was dissolved in THF (3 mL). A solution of methyllithium in diethyl ether (1.6 M, 0.3 mL) was added to the THF solution of **28**. The reaction mixture was allowed to stir for 4 hr at room temperature. During this time, the colour of the solution changed from bright yellow to green . The reaction mixture was cooled to 0 °C, and a saturated $NH_4Cl_{(aq)}$ solution (20 mL) was added. The two layers were separated. The aqueous layer was extracted with diethyl ether (3 x 15mL). The organic layers were combined and the solvent was removed *in vacuo* yielding **31** as an off white solid in a 49% yield (0.05 g). Compound **31** was identified by comparison of its ^1H NMR spectral data to those of an authentic sample.[44]

2.4.9 Reaction of 28 with ½ equivalent of MeLi

To a solution of **28** (0.48 mmol) in THF (5 mL) was added a 1.6 M solution of methyllithium (0.15 mL, 0.24 mmol). The reaction mixture was allowed to stir for 18 hr after which a solution of 1 M NH_4Cl (10 mL) was added. The two layers were separated. The aqueous layer was extracted with diethyl ether (3 x 15mL). The organic layers were combined and the solvent was removed *in vacuo* yielding a white residue (0.13 g). Analysis of the residue by ^1H NMR spectroscopy was consistent with a mixture of **31** and **32** in an approximately 50:50 ratio.

2.4.10 Reaction of 25 with Tetramesityldisilene (36)

$(Me_3Si)_2SiMes_2$ (0.100 g, 0.243 mmol) dissolved in hexanes (10 mL) was combined with NHC **25** (0.05 g, 0.28 mmol) in a quartz Schlenk tube under a nitrogen atmosphere. The tube was cooled to -70° C and irradiated (254 nm) for 24 hr. After irradiation, the reaction solution was a bright red colour. An aliquot (1 mL) was removed from the solution and the solvent was evaporated under vacuum. Analysis of the residue by ^1H NMR spectroscopy was consistent with the presence of **36**[39] and unreacted **25**.

2.4.11 Reaction of 25 with 37

To a solution of **37** (0.15 mmol) dissolved in hexanes (3 mL) was added a solution of **25** (0.03 g, 0.17 mmol) in THF (5 mL). The solution turned pale brown. After stirring for 2 hr, the solvent was removed under vacuum leaving a pale brown residue. The residue was examined by ^1H NMR spectroscopy. The ^1H NMR spectrum of the residue showed signals consistent with **25** and **38**.[41]

2.4.12 Single Crystal X-ray Diffraction Experimental Details

Data were collected at low temperature (-123 °C) on a Nonius Kappa-CCD area detector diffractometer with COLLECT. The unit cell parameters were calculated and refined from the full data set. Crystal cell refinement and data reduction were carried out using HKL2000 DENZO-SMN.[45] Absorption corrections were applied using HKL2000 DENZO-SMN (SCALEPACK).

The SHELXTL/PC V6.14 suite of programs was used to solve the structures by direct methods.[46] Subsequent difference Fourier syntheses allowed the remaining atoms to be located. All of the non-hydrogen atoms were refined with anisotropic thermal parameters with the exception of a molecule of toluene in the unit cell of **24** which was located on a symmetry site and modeled at ½ occupancy. The hydrogen atom positions were calculated geometrically and were included as riding on their respective carbon atoms.

The crystallographic information files (CIFs) can be obtained free of charge, via www.ccdc.cam.ac.uk/consts/retrieving.html or from the Cambridge Crystallographic Data Centre, 12 Union Road, Cambridge CB2 1EZ, U.K. (Fax: 44-1223-336033 or email: deposit@ccdc.cam.ac.uk). The Cambridge Crystallographic Data Centre (CCDC) retrieval numbers for each compound are listed in Table 2.1

Table 2.1 Crystallographic data for compounds **17**, **24**, **28**, and **30**.

Compound	**17**	**24**	**28**	**30**
CCDC #	632305	632306	643704	643705
Empirical formula	$C_{58}H_{74}Ga\ Ge\ KN_2$	$C_{55.75}H_{77}Ga\ GeN_2Si$	$C_{32.50}H_{46}Ge\ N_2$	$C_{32}H_{48}BGe\ N_2$
Formula weight	980.60	945.59	537.30	544.12
Crystal system	orthorhombic	triclinic	triclinic	monoclinic
Space group	P b c a	P-1	P-1	P 21/c

a (Å)	33.7506(7)	12.1913(6)	8.8091(9)	22.0634(5)
b (Å)	24.7122(5)	19.5294(10)	13.7282(17)	8.6076(2)
c (Å)	12.7699(3)	22.1905(14)	14.061(2)	16.2745(5)
α (°)	90	95.785(3)	63.736(5)	90
β (°)	90	94.883(3)	80.017(7)	93.0960(10)
γ (°)	90	95.664(3)	81.165(8)	90
Volume (Å^3)	10650.8(4)	5206.6(5)	1496.1(3)	3086.23(14)
Z	8	4	2	4
Data/restraints/ parameters	9398/8 /544	17669/1 /989	4990/ 329 / 328	5429/344/ 21
Goodness-of-fit (all data)	1.024	0.950	0.992	1.090
R [$I>2\sigma(I)$]	0.0709	0.0663	0.0509	0.0365
wR^2 (all data)	0.1817	0.1516	0.1347	0.0924
Largest diff. peak and hole (e Å^{-3})	0.756 -0.573	0.745 -0.649	0.751 -0.788	0.520 -0.390

2.5 References

1. Selected examples: (a) Fujdala, K.L.; Gracey, D.W.K.; Wong, E.F.; Baines, K.M. *Can. J. Chem.* **2002**, *80*, 1387. (b) Samuel, M. S.; Baines, K. M. *J. Am. Chem. Soc.* **2003**, *125*, 12702. (c) Sulkes, M.; Fink, M. J.; Gottschling, S. E.; Baines, K. M.; *Organometallics* **2002**, *21*, 2438. (d) Samuel, M. S.; Jennings, M. C.; Baines, K. M. *J. Organomet. Chem.* **2001**, *636*, 130. (e) Samuel M. S.; Jennings, M. C.; Baines, K. M. *Organometallics* **2001**, *20*, 590. (f) Dixon, C. E.; Hughes, D. W.; Baines, K. M. *J. Am. Chem. Soc.* **1998**, *120*, 11049. (g) Dixon, C. E.; Cooke, J. A.; Baines, K. M. *Organometallics* **1997**, *16*, 5437. (h) Dixon, C.E.; Netherton, M.R.; Baines, K. M. *J. Am. Chem. Soc.* **1998**, *120*, 10365. (i) Baines, K. M.; Cooke, J. A.; Dixon, C. E.; Liu, H. W.; Netherton, M. R. *Organometallics* **1994**, *13*, 631.
2. (a) Uhl., W. *Naturwissenschaften* **2004**, *91*, 305. (b) Hardman, N.J.; Phillips, A.D.; Power, P.P. *ACS Symp. Ser.* **2002**, *822*, 2. (c) Baker, R.J.; Jones, C *Coord. Chem.*

Rev. **2005**, *249*, 1856. (d) Gemel, C.; Steinke, T.; Cokoja, M.; Kempter, A.; Fischer, R. A. *Eur. J. Inorg. Chem.* **2004**, 4161.

3. Baker, R. J.; Farley, R. D.; Jones, C.; Kloth, M.; Murphy, D. M. *J. Chem. Soc., Dalton Trans.* **2002**, 3844.

4. Green, S. P.; Jones, C.; Lippert, K.; Mills. D. P.; Stasch. A. *Inorg. Chem.* **2006,** *45,* 7242.

5. (a) Goldberg, D.E.; Harris, D.H.; Lappert, M.F.; Thomas, K.M. *J. Chem. Soc., Chem. Commun.* **1976**, 261. (b) Davidson, P.J.; Harris, D.H.; Lappert, M.F. *J. Chem. Soc., Dalton Trans.* **1976**, 2268. (c) Hitchcock, P.B.; Lappert, M.F.; Miles, S.J.; Thorne, A.J. *J. Chem. Soc., Chem. Commun.* **1984**, 480.

6. (a) Weidenbruch, M. *J. Organomet. Chem.* **2002**, *646,* 39. (b) Meiners, F.; Saak, J; Weidenbruch, M. *Z. Anorg. Allg. Chem.* **2002**, *628*, 2821. (c) Tsumuraya, T.; Sato, S.; Ando, W. *Organometallics* **1990**, *9,* 2061. (d) Schäfer, H.; Saak, W.; Weidenbruch, M. *Organometallics* **1999**, *18*, 3159.

7. Hurni, K. L.; Rupar, P. A.; Payne, N. C.; Baines, K. M. *Organometallics* **2007**, *26*, 5569.

8. A survey of the Cambridge Crystallographic Database revealed a Ga-Ge single bond length average of 2.46 Å.

9. (a) Ando, W.; Tsumuraya, T.; Sekiguchi, A. *Chem. Lett.* **1987,** 317. (b) Ando, W.; Itoh, H.; Tsumuraya, T.; Yoshida, H. *Organometallics* **1988**, *7,* 1880. (c) Ando, W.; Itoh, H.; Tsumuraya, T. *Organometallics* **1989**, *8*, 2759.

10. Tsumuraya, T.; Kabe, Y.; Ando, W. *J. Organomet. Chem.* **1994**, *483*, 131.

11. (a) Leigh, W. J.; Lollmahomed, F.; Harrington, C. R.; McDonald, J. M. *Organometallics* **2006**, *25*, 5424. (b) Tsumuraya, T.; Kabe, Y.; Ando, W. *J. Organomet. Chem.* **1994**, *482*,131.

12. (a) Leigh, W. J.; Harrington, C. R.; Vargas-Baca, I. *J. Am. Chem. Soc.* **2004**, *126*, 16105.

13. Hardman, N. J.; Eichler, B.; Power, P. P. *J. Chem. Soc., Chem. Commun.* **2000**, 1991.

14. Jutzi, P.; Schebaum, L. O. *J. Organomet. Chem.* **2002**, *654*, 176.

15. Hermann, W. A.; Denk, M.; Behm, J.; Scherer, W.; Klingan, F.; Bock, H.; Solouki, B.; Wagner, M. *Angew. Chem. Int. Ed. Engl.* **1992**, *31*, 1485.

16. For a recent comparison of different neutral donors and their Lewis basicity see: Gusev, D. G. *Organometallics* **2009**, *28*, 763.

17. Selected recent reviews: (a) Hahn, F. E.; Jahnke, M. C. *Angew. Chem., Int. Ed.* **2008**, *47*, 3122. (b) de Fremont, P.; Marion, N.; Nolan, S. P. *Coord. Chem. Rev.* **2009**, *253*, 862. (c) Kuhl, O. *Chem. Soc. Rev.* **2007**, *36*, 592. (d) Cavallo, L.; Correa, A.; Costabile, C.; Jacobsen, H. *J. Organomet. Chem.* **2005**, *690*, 5407.

18. (a) Kirmse, W. *Eur. J. Org. Chem.* **2005**, 237. (b) Diez-Conzalez, S.; Nolan, S. P. *Annu. Rep. Prog. Chem., Sect. B* **2005**, *101*, 171.

19. (a) Kuhn, N.; Al-Sheikh, A. *Coord. Chem. Rev.* **2005**, *249*, 741. (b) Graham, T. W.; Udachin, K. A.; Carty, A. J. *Chem. Commun.* **2006**, 2699. (c) Ellis, B. D.; Dyker, C. A.; Decken, A.; Macdonald, C. L. B. *Chem. Commun.* **2005**, 1965. (d) Burford, N.; Dyker, C. A.; Phillips, A. D.; Spinney, H. A.; Decken, A.; McDonald, R.; Ragogna, P. J.; Rheingold, A. L. *Inorg. Chem.* **2004**, *43*, 7502. (e) Ellis, B. D.; Ragogna, P. J.; Macdonald, C. L. B. *Inorg. Chem.* **2004**, *43*, 7857. (f) Burford, N.; Ragogna, P. J. *J.*

Chem. Soc., Dalton Trans. **2002**, 4307. (g) Hardman, N. J.; Abrams, M. B.; Pribisko, M. A.; Gilbert, T. M.; Martin, R. L.; Kubas, G. J.; Baker, R. T.; *Angew. Chem., Int. Ed.* **2004**, *43*, 1955. (h) Burford, N.; Cameron, T. S.; LeBlanc, D. J.; Phillips, A. D. *J. Am. Chem. Soc.* **2000**, *122*, 5413. (i) Cowley, A. H. *J. Organomet. Chem.* **2001**, *617-618*, 105.

20. Frison, G.; Sevin, A. *J. Chem. Soc., Perkin Trans. 2* **2002**, 1692.

21. Schäfer, A.; Weidenbruch, M.; Saak, W.; Pohl, S. *J. Chem. Soc., Chem. Commun.* **1995**, 1157.

22. Stabenow, F.; Saak, W.; Weidenbruch, M. *Chem. Commun.* **1999**, 1131.

23. (a) Wang, Y.; Quillian, B.; Wei, P.; Wannere, C. S.; Xie, Y.; King, R. B.; Schaefer III, H. F.; Schleyer, P. V. R.; Robinson, G. H. *J. Am. Chem. Soc.* **2007**, *129*, 12412. (b) Wang, Y.; Xie, R. B.; King, R. B.; Schaefer III, H. F.; Schleyer, P. V. R.; Robinson, G. H. *J. Am. Chem. Soc.* **2008**, *130*, 14970. (c) Wang, Y.; Xie, Y.; Wei, P.; King, R. B.; Schaefer III, H. F.; Schleyer, P. V. R.; Robinson, G. H. *Science,* **2008**, *321*, 1069.

24. (a) Fillippou, A. C.; Chernov, O.; Schnakenburg, G. *Angew. Chem., Int. Ed.* **2009**, DOI: 10.1002/anie.200902431. (b) Ghadwai, R. S.; Roesky, H. W.; Merkel, S.; Henn, J.; Stalke, D. *Angew. Chem., Int. Ed.* **2009**, DOI: 10.1002/anie.200901766.

25. Dutton, J. L.; Tuononen, H. M.; Ragogna, P. J. *Angew. Chem., Int. Ed.* **2009**, *48*, 4409.

26. Kuhn, N.; Kratz, T. *Synthesis* **1993**, 561.

27. Arduengo III, A. J.; Dia, V. R.; Calabrese, J. C.; Davidson, F. *Inorg. Chem.* **1993**, *32*, 1541.

28. Gehrhus, B.; Hitchcock, P. B.; Lappert, M. F. *J. Chem. Soc., Dalton Trans.* **2000,** 3094.

29. Throughout this thesis the carbenic carbon-germanium bond in the NHC-GeR_2 complexes are drawn using a dative bond. In our opinion, this better represents the nature of these complexes. A zwitterionic depiction, in which the NHC moiety carries a positive charge while the germanium is formally anionic, is also possible. The IUPAC Compendium of Chemical Terminology (2006) defines a dative bond as "The coordination bond formed upon interaction between molecular species, one of which serves as a donor and the other as an acceptor of the electron pair to be shared in the complex formed. In spite of the analogy of dative bonds with covalent bonds, in that both types imply sharing a common electron pair between two vicinal atoms, the former as distinguished by their significant polarity, lesser strength, and greater length. The distinctive feature of dative bonds is that their minimum-energy rupture in the gas phase or in inert solvent follows the heterolytic bond cleavage path."

30. (a) Tsumuraya, T.; Kabe, Y.; Ando, W. *J. Organomet. Chem.* **1994**, *482*, 131 (b) Rivière, P.; Satgé, J. *J. Organomet. Chem.* **1982**, *232*, 123.

31. Hurni, K. L.; Baines, K. M. *Can. J. Chem.* **2007**, *85*, 668.

32. Baines, K. M.; Cooke, J. A.; Dixon, C. E.; Liu, H. W.; Netherton, M. R. *Organometallics* **1994**, *13*, 631.

33. NHC **25** does not react with DMB under these conditions.

34. Sum of bond angles around Ge in **30** is 325°. Sum of C-Ge-C bond angles around Ge in **28** is 318°.

35. Sum of C-Ge bond lengths in **30** is 6.063 Å. Sum of C-Ge bond lengths in compound **28** is 6.215 Å.

36. Similar bond angle shifts have been noted in a carbene-phosphinidene complex upon coordination to BH_3. See Arduengo III, A.J.; Carmalt, C. J.; Clyburne, J. A. C.; Cowley, A. H.; Pyati, R. *J. Chem. Soc., Chem. Commun.* **1997**, 981.

37. **31** was previously synthesized by a different method. See Castel, A.; Rivière, P.; Satgé, J.; Ko, Y. *J. Organomet. Chem.* **1988**, *342*, C1.

38. (a) Szwarc, M.; Levy, M.; Milkovich, R. *J. Am. Chem. Soc.* **1956**, *78*, 2656. (b) Szwarc, M. *Nature* **1956**, *178*, 1168.

39. West, R.; Fink, M. J.; Michl, J. *Science* **1981,** *214*, 1343.

40. Couret, C.; Escudié, J.; Delpon-Lacaze, G.; Satgé, J. *Organometallics* **1992**, *11*, 3176.

41. Pavelka, L. C.; Holder, S. J.; Baines, K. M. *Chem. Commun.* **2008**, 2346.

42. Pangborn, A. B.; Giardello, M. A.; Grubbs, R. H.; Rosen, R. K.; Timmers, F. J. *Organometallics* **1996**, *15*, 1518.

43. Rivière, P; Satgé, J. *J. Organomet. Chem.* **1982**, *232*, 123.

44. Castel, A.; Rivière, P.; Satgé, J.; Ko, Y. *J. Organomet. Chem.* **1988**, *342*, C1.

45. Otwinowski, Z; Minor, W. In *Methods in Enzymology. Vol. 276: Macromolecular Crystallography, Part A.*; Carter, Jr, C.W., Sweet, R.M., Eds; Academic Press: New York. **1997**, pg 307.

46. Sheldrick, G.M. *Acta Cryst.* **2008**, *A64*, 112.

Chapter 3

The Synthesis and Characterization of N-Heterocyclic Carbene Complexes of Germanium(II)*

3. 1 Introduction

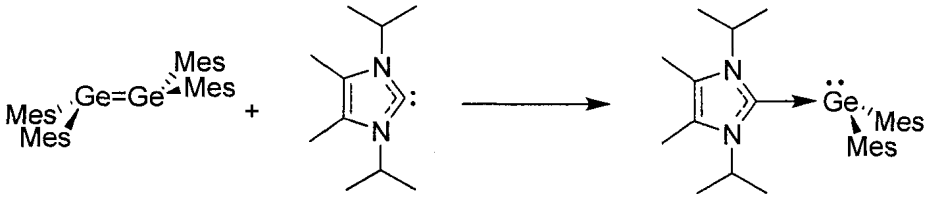

15 25 28

Scheme 3.1

The isolation of the carbene complex of $GeMes_2$, **28**,[1] clearly demonstrated that N-heterocyclic carbenes (NHCs) are capable of stabilizing reactive Ge(II) species. The use of a strong σ-donor was key as, in general, intermolecular complexes of simple diarylgermylenes exist only as transient intermediates.[2] Although occupation of the p-orbital on Ge by the carbene lone pair is clearly necessary for the stabilization of **28**, steric shielding provided by the mesityl groups most likely also plays a role. We desired to synthesize additional NHC complexes of Ge(II) to determine if other reactive germylenes could also be stabilized and to further explore the chemistry of these species. Unfortunately, the synthesis of **28**, using tetramesityldigermene (**15**) as a precursor (Scheme 3.1), restricts the nature of the substituents on Ge because of the limited number

* This chapter is a combination of two separate publications and additional unpublished results: Rupar, P. A.; Jennings, M. C.; Baines, K. M. *Organometallics* **2008**, *27*, 5043 and Rupar, P. A.; Staroverov, V.N.; Ragogna, P. J.; Baines, K. M. *J. Am. Chem. Soc.* **2007**, *129*, 15138.

of stable and readily available doubly-bonded germanium compounds. A more general approach for the synthesis of carbene-germylene complexes was needed.

In this chapter, the synthesis and structural characterization of a number of NHC-stabilized Ge(II) compounds is described. The goal is to produce versatile reagents for the facile delivery of synthetically useful germylenes. Chapter 4 will report on the reactivity of the complexes described herein and their ability to act as germylene synthons.

3.2 Results and Discussion

Two different approaches were examined in the synthesis of NHC-stabilized Ge(II) compounds. The first method examined was the reduction of R_2GeX_2 in the presence of carbene **25** (Scheme 3.2). Using Mes_2GeCl_2 as the germanium source, a number of reducing agents were examined, including Na, K, Mg and tetramethyldisiloxane. Excess carbene **25** was also examined because it has been shown to be a mild reducing agent for the synthesis of other low valent p-block elements.[3] Unfortunately, regardless of the reaction conditions employed, either complex reaction mixtures were obtained or the reducing agents failed to induce any detectable chemical transformations.

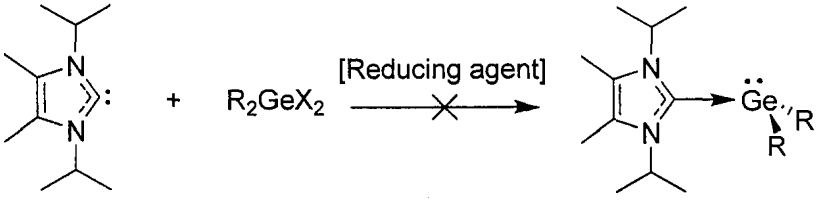

25

Scheme 3.2

The second method examined for the synthesis of novel NHC-Ge(II) complexes proved to be more successful. By first installing a stable germylene on **25**, the carbene

could then act as a scaffold, supporting the Ge(II) centre during substitution reactions (Scheme 3.3).

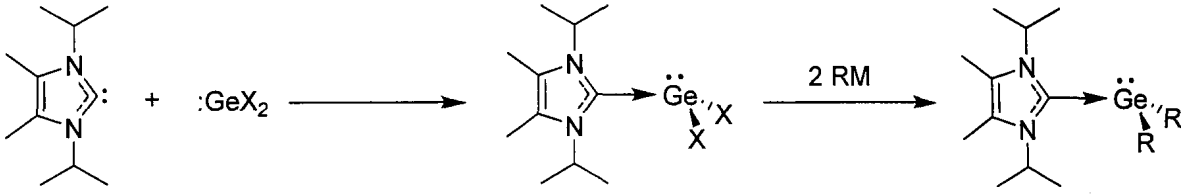

25

Scheme 3.3

3.2.1 Synthesis of NHC complexes of GeR_2

The 1,4-dioxane complex of dichlorogermylene (**8**) was used as the starting germylene source. The direct reaction of $GeCl_2$·dioxane (**8**) with **25** gave the desired complex **39** by displacement of the dioxane from the germanium centre. Compound **39** was isolated in excellent yield as a white powder (Scheme 3.4).

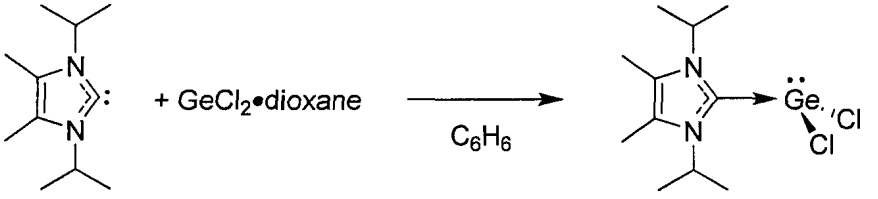

25 8 39

Scheme 3.4

Using **39** as a starting material, the remaining NHC-Ge(II) dihalo derivatives were synthesized. Reaction of **39** with excess potassium fluoride and a catalytic amount of [18]crown-6 resulted in the formation of the difluoro-substituted derivative **40** (Scheme 3.5).

The addition of either excess Me_3SiBr or Me_3SiI to **39** resulted in the formation of the dibromo **41** or the diiodo analog **42**, respectively (Scheme 3.5). The chemical shifts of

the signals in the ^{1}H NMR spectra of the halogen derivatives **39** - **42** are very similar, and thus, are not diagnostic. However, the four compounds, **39** - **42**, can be easily differentiated on the basis of the wavenumber for the Ge-X stretching vibration observed by FT-Raman spectroscopy (F = 530 cm^{-1}, Cl = 316 cm^{-1}, Br = 232 cm^{-1}, I = 205 cm^{-1}).[4]

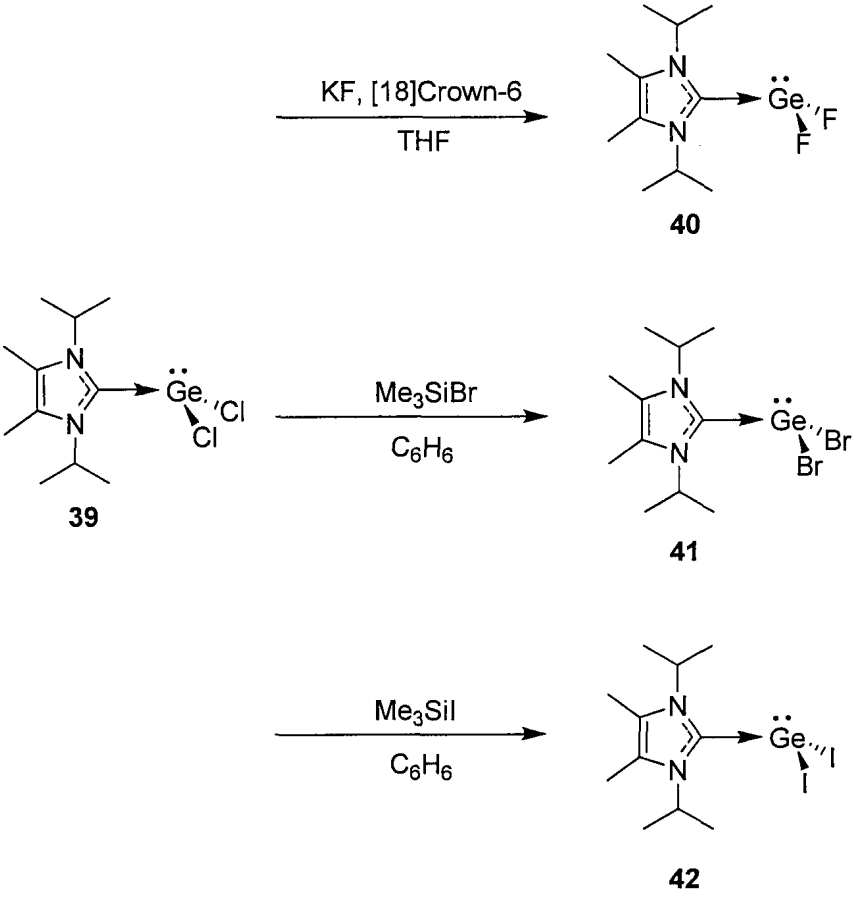

Scheme 3.5

The structures of all four of the halogen derivatives **39** - **42** were verified by single crystal x-ray diffraction (Figure 3.1). In general, the halide derivatives are monomeric in the solid state, showing no significant intermolecular interactions. However, the germanium atoms of opposing molecules in the unit cell of **41** are within the sum of their van der Waals radii (4.30 Å)[5] at 3.67 Å. This value greatly exceeds the bond length of a Ge-Ge single bond (typical range: 2.41 – 2.46 Å)[6] and is, most likely, a consequence of

crystal packing, rather than any meaningful bonding interaction. The structures of **39 - 42** are strikingly similar (Figure 3.1) with comparable metrics (Table 3.1).

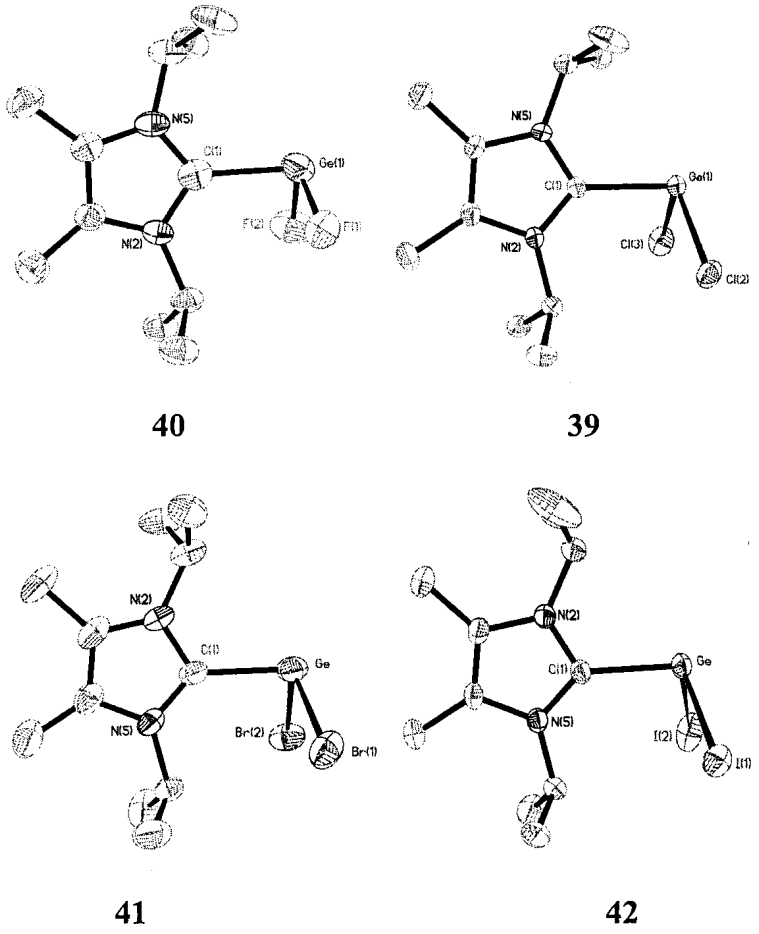

Figure 3.1: Thermal ellipsoid plot (50% probability surface) of **39 - 42**. Hydrogen atoms are omitted for clarity.

Table 3.1: Selected bond lengths (Å) and angles (°) of compounds **39 - 42**.

Compound	C1-Ge (Å)	Ge-X (Å)	X-Ge-X (°)	C(1)-Ge-X (°)
40 (-F)	2.117(7)	1.829(5), 1.829(5)	95.1(3)	91.2(3), 94.6(3)
39 (-Cl)	2.106(3)	2.2927(9), 2.2953(8)	97.82(3)	93.74(8), 95.74(8)
41 (-Br)	2.089(5)	2.4514(9), 2.4572(8)	99.67(3)	94.78(14), 95.73(14)
42 (-I)	2.086(3)	2.6578(5), 2.6863(7)	99.865(17)	97.07(9), 97.93(11)

A NHC dihalogermylene complex was previously structurally characterized. This diiodo derivative with a bulkier NHC (mesityl groups on nitrogen and unsubstituted at the alkenyl carbons) was found to have similar metrics to **39** – **42** (See compound **26**, Chart 2.3 in Chapter 2.2.3).[7]

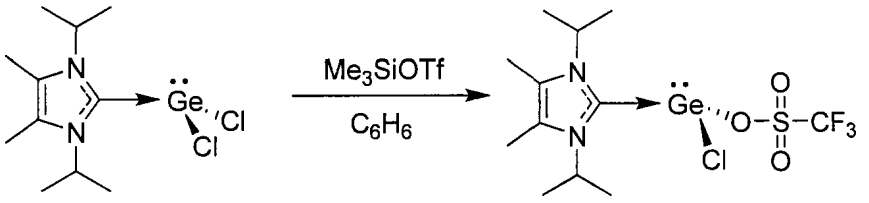

39 **43**

Scheme 3.6

Since a triflate-germanium bond (triflate = OTf = O_3SCF_3) is expected to ionize quite readily, and thus be synthetically useful, we attempted to make a ditriflate derivative of the complex. Addition of Me_3SiOTf to **39**, followed by removal of the solvent yielded a white powder (Scheme 3.6). The ^1H NMR spectrum of the white powder was, predictably, similar to that of **39**, while the ^{19}F NMR spectrum of the solid showed a signal whose chemical shift was consistent with a triflate moiety. Surprisingly, a signal attributable to a Ge-Cl bond stretch at 315 cm^{-1} was apparent in the FT-Raman spectrum of the powder. Crystals of the product were obtained; single crystal x-ray diffraction confirmed the formation of **43**, an NHC-germylene complex with both a chloride and a triflate substituent present on the germanium centre (Figure 3.2). The triflate is covalently bound to the germanium with a Ge-O bond length of 2.0342(16) Å (cf. 1.75 - 1.85 Å for a typical Ge-O bond).[6] The carbenic carbon-germanium bond is reduced in length to 2.068(2) Å (from 2.106(3) Å in **39**) and the chlorine-germanium bond length has decreased to 2.2680(6) Å (from an average of 2.294 Å in **39**). These observations are consistent with a δ^+ charge on germanium due to the electron withdrawing triflate group.

As observed in the solid state structure of **41**, the germanium atoms in opposing molecules of **43** are within the sum of their van der Waals radii at 3.75 Å but, once again, far outside the distance expected of a Ge-Ge bond (typical range: 2.41 – 2.46 Å).[6]

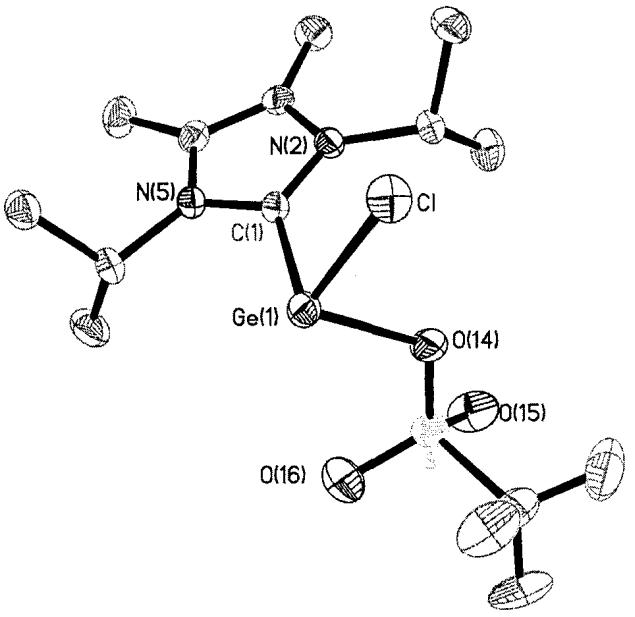

Figure 3.2: Thermal ellipsoid plot (50% probability surface) of **43**. Hydrogen atoms are omitted for clarity. Selected bond lengths (Å) and angles (°): C1–Ge = 2.068(2), Ge-Cl = 2.2680(6), Ge-O14 = 2.0342(16), S-O14 = 1.4914(16), S-O15 = 1.4273(19), S-O16 = 1.4914(16), C1-Ge-Cl = 95.51, C1-Ge-O14 = 89.81(8), Cl-Ge-O14 = 92.69(6).

Efforts to replace both chlorides on **39** using a large excess of Me_3SiOTf were not successful; only **43** was isolated. Attempts to use AgOTf to facilitate chloride/triflate metathesis also failed; complex mixtures were formed and no single compound was identified.

Unlike most Ge(II) compounds, many N-heterocyclic germylenes are indefinitely stable due to partial occupation of the empty p-orbital on germanium by the nitrogen lone pair of electrons.[8] This partial occupation makes N-heterocyclic germylenes less Lewis

acidic and, as a result, it was expected that the strength of a coordination complex with **25** would be weakened. Indeed, the addition of the dilithium salt **44** to a solution of **39** resulted in the formation of two compounds: free carbene **25** and N-heterocyclic germylene **4**[9] (Scheme 3.7). Complete dissociation of the carbene was confirmed by NMR spectroscopy: the ^{1}H NMR chemical shifts of the signals in the reaction mixture are identical to an independently prepared solution of **25** and **4**, and to the chemical shifts of the signals in the ^{1}H NMR spectra of the isolated compounds. In addition, the ^{13}C NMR spectrum of the reaction mixture showed a signal at 207 ppm, attributed to the carbenic carbon, which is identical to the ^{13}C chemical shift of the carbenic carbon in a pure sample of **25**. The reaction between a benzannulated NHC with a benzannulated N-heterocyclic germylene has been previously examined; a weak bonding interaction between the two fragments was observed both in solution and in the solid state (see compound **27**, Chart 2.3, Chapter 2).[10] The substituents on the nitrogen atoms of the N-heterocyclic germylene are N-neopentyl rather than N-^{t}butyl, as in **4**. The difference in the extent of complexation with an NHC between the two germylenes is likely due to a combination of the ring annulation, which increases Lewis acidity of the germanium,[11] and the increased flexibility of the neopentyl group, which reduces steric bulk in comparison to the ^{t}butyl group.

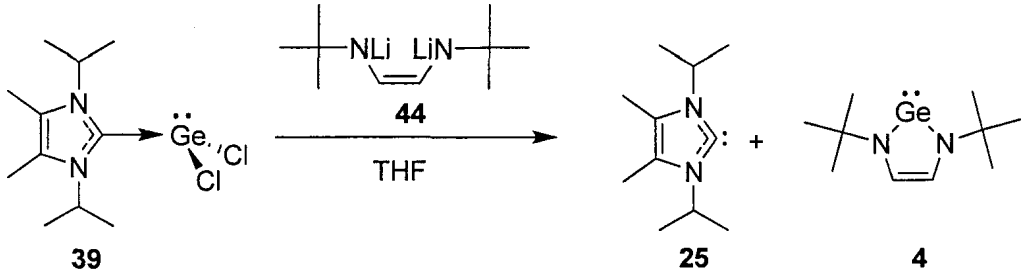

39 **25** **4**

Scheme 3.7

In general, $Ge(OR)_2$ compounds rapidly oligomerize, which makes isolation and characterization of such germylenes difficult. Even the sterically encumbered $Ge(ODipp)_2$ (Dipp = 2,6-diisopropylphenyl) forms a dimer in the solid state.[12] However, a few discrete dialkoxy[13] and diaryloxy[12,14,15,16,17,18] germylenes have been structurally characterized. An NHC could potentially stabilize the reactive dialkoxygermylenes through occupation of the p-orbital on the germanium and allow isolation of monomeric molecular complexes.[19] Nucleophilic substitution of the chlorides in **39** using two equivalents of potassium ^{t}butoxide proceeded cleanly (Scheme 3.8). The ^{1}H NMR spectrum of the white powder isolated from the reaction was consistent with the di(*tert*-butoxy)-substituted carbene-germylene complex **45**. The structure of the product was confirmed by x-ray crystallography (Figure 3.3). Two monomeric molecules of **45** were present in the asymmetric unit. Both molecules have identical connectivity and orientation, but differ significantly in the carbenic carbon-Ge bond length (2.120(9) Å vs 2.224(14) Å).

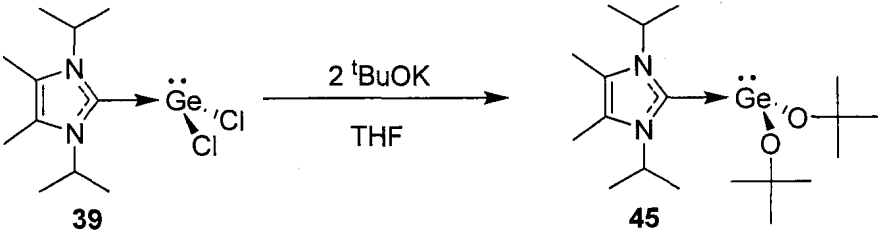

Scheme 3.8

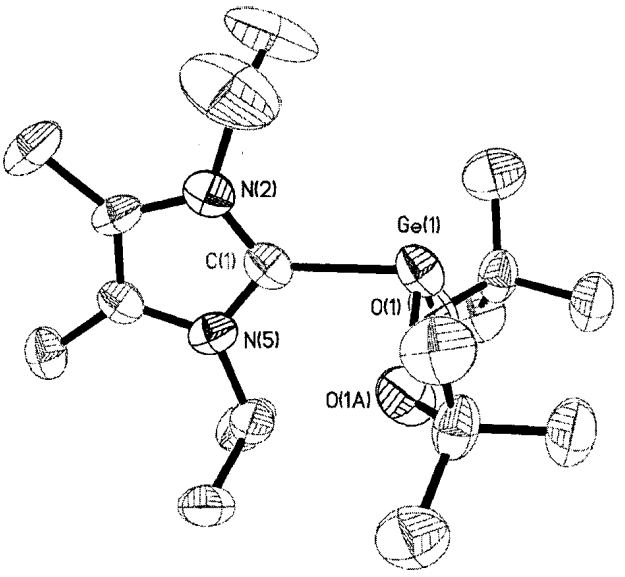

Figure 3.3: Thermal ellipsoid plot (50% probability surface) of **45**. Only one of the two molecules in the asymmetric unit is shown. Hydrogen atoms are omitted for clarity. Selected bond lengths (Å) and angles (°): C1–Ge1 = 2.120(9), O1–Ge1 = 1.874(5), O1-Ge1-O1A = 95.4(4), O1-Ge1-C1 = 89.5(2).

Attempts were also made to synthesize the dimethoxy derivative through the reaction of **39** with MeOK or MeONa. Signals consistent with the MeO substituted species were detected but unfortunately, we were unable to isolate the species and reproducibility was problematic.

$Ge(NCS)_2$ has been studied previously; the germylene is stable in dilute solution but polymerizes rapidly upon isolation.[20] Again, coordination of the NHC should allow isolation of a monomeric, base-stabilized $Ge(NCS)_2$. Two equivalents of KSCN underwent a reaction with **39** to form complex **46** as determined by FT-Raman and x-ray crystallography (Scheme 3.9). Four chemically identical, but crystallographically unique molecules of **46** are found in the asymmetric unit. Each molecule shows the same

connectivity with two N-bonded thiocyanates attached to the germanium centre (Figure 3.4). The central C1–Ge bond lengths vary (2.105(9), 2.072(9), 2.075(10), and 2.062(9) Å) with an average value of 2.078 Å. There are also short intermolecular contacts between the sulfur atoms and neighboring germanium atoms. The closest S-Ge approach is 3.61 Å, which is much longer than the length of a typical S-Ge single bond (the average S-Ge single bond length is 2.21-2.29 Å).[6] In contrast to $Ge(NCS)_2$,[20] **46** is stable under an inert atmosphere in both the solid state or in solution. Both $Ge(NCS)_2$ and **46** show Ge-N connectivity rather than Ge-S connectivity, which indicates that Ge(II) has a preference for the harder nitrogen atom over the softer sulfur atom. Only one other structurally characterized thiocyanato germanium compound, a tetraazacyclotetradecane Ge(IV) complex, is known; this compound also shows a preference for Ge-N bonding.[21]

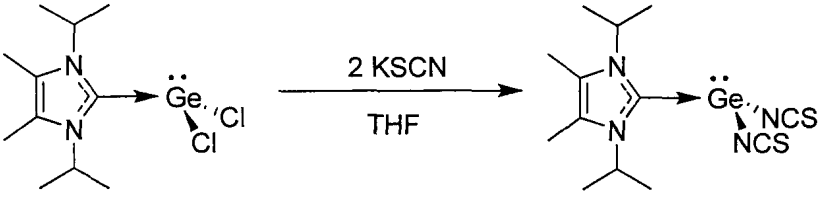

39 **46**

Scheme 3.9

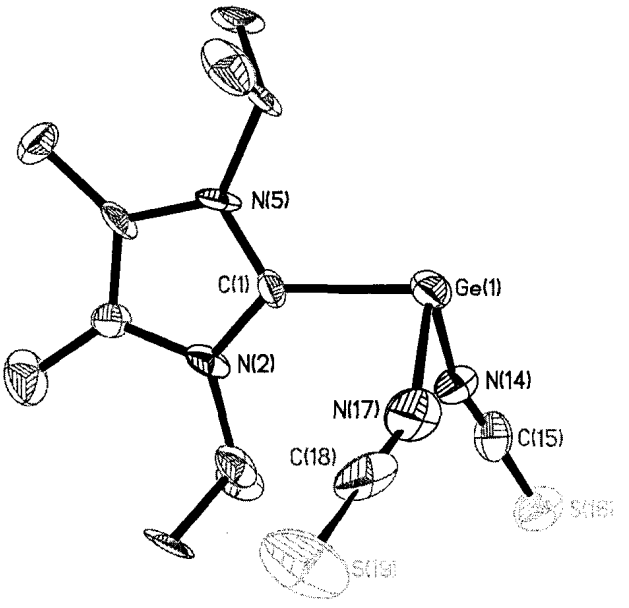

Figure 3.4: Thermal ellipsoid plot (50% probability surface) of **46**. Only one of the four molecules from the asymmetric unit is shown. Hydrogen atoms are omitted for clarity. Selected bond lengths (Å) and angles (°): C1-Ge1 = 2.105(9), Ge1-N14 = 1.983(8), Ge1-N17 = 1.998(9), N14-C15 = 1.146(11), N17-C18 = 1.207(13), N14-Ge1-N17 = 89.7(4), N14-Ge1-C1 = 93.1(4), N17-Ge1-C1 = 90.0(4).

Simple dialkylgermylenes are extremely reactive intermediates and cannot be isolated under standard conditions. Experimental evidence suggests that transient dialkylgermylenes form reversible donor-acceptor complexes with Lewis bases in solution.[22] NHCs are among the strongest known neutral Lewis bases, and therefore, should form strong coordination complexes with dialkylgermylenes. Indeed, the isolation of **28** demonstrated that an unstable diarylgermylene can be isolated using NHC complexation. We attempted to form NHC complexes of GeR_2 (where R = small alkyl) by the reaction of **39** with alkyl Grignard or lithium reagents. Invariably, and independent of reaction conditions, only complex mixtures formed.[23] Broad signals in

the ^{1}H NMR spectra of the crude reaction mixtures suggested that some polymeric material may be formed.

In addition to dialkyl complexes, the synthesis of other diaryl systems was also attempted. The reaction of Tol_2Mg with **39** gave **47** as the only isolated tolyl containing product (Scheme 3.10). The cyclotetragermane **47** likely results from the oligomerization of four $Ge(Tol)_2$ fragments. Broad signals attributable to tolyl groups in the ^{1}H NMR spectrum of the crude reaction mixture suggest that larger oligomers are also formed. The identity of **47** was confirmed by ^{1}H NMR spectroscopy and x-ray crystallography (Figure 3.5).[24] The Grignard reagent Mes_2Mg[25] was reacted with **39** to produce complex **28**, and thus, provides an alternate route to **28** that does not require the use of tetramesityldigermene (**15**) as a starting material (Scheme 3.10). The reaction proceeds slowly, taking three days at room temperature to complete.

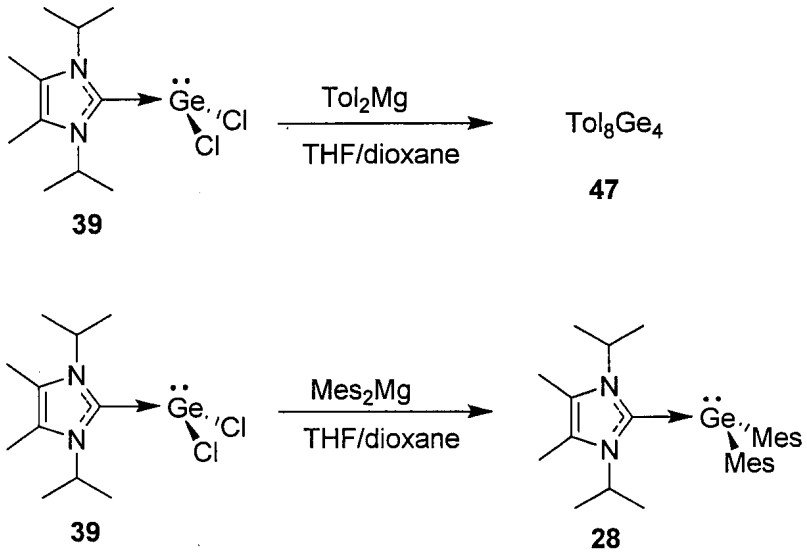

Scheme 3.10

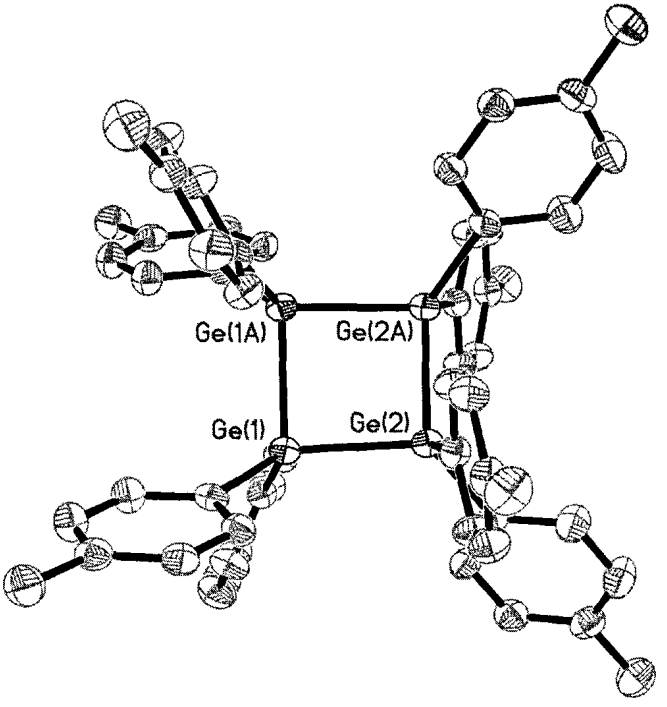

Figure 3.5: Thermal ellipsoid plot (50% probability surface) of **47**. Hydrogen atoms are omitted for clarity. Selected bond lengths (Å) and angles (°): Ge1-Ge1A = 2.4587(7), Ge1-Ge2 = 2.4632(5), Ge2-Ge2A = 2.4555(7), Ge1A-Ge1-Ge2 = 88.987(11), Ge2A-Ge2-Ge1 = 89.061(11).

The results from the attempted substitution reactions with organometallic reagents demonstrate that nucleophilic displacement of the chlorides from **39** is possible, but the NHC-diorganogermylene products are apparently unstable under the reaction conditions. In addition to coordination of a strong Lewis base, steric protection of the germanium centre must be necessary for the isolation of complexed diorganogermylenes. By virtue of its isolation and characterization, compound **28** meets these requirements.

Additional substitution reactions with **39** were attempted using a variety of organometallic reagents (Chart 3.1). The reaction with lithium diphenylphosphide

produced complex mixtures regardless of reaction conditions, while 4-trifluoromethylphenylmagnesium bromide failed to react with **39**. One equivalent of $(Me_3Si)_3SiLi$ did, in fact, react with **39**; however, the reaction was not clean and attempts to isolate a product were not successful. A salt metathesis with MesCu was unsuccessful with evidence of redox processes occurring under the reaction conditions employed.

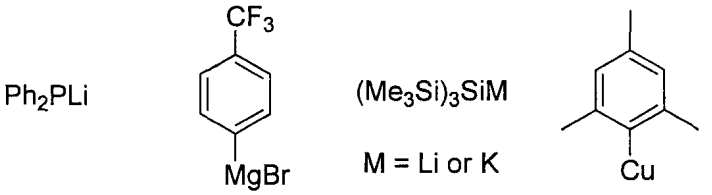

Chart 3.1

A carbene-germanium(II) complex with both a mesityl and a chloro substituent would be useful in the synthesis of NHC coordinated heteroleptic germylenes. Intermolecular ligand redistributions between germanium(II) compounds are known to occur between aryl and chloro substituents,[26] and therefore, compounds **28** and **39** were dissolved in THF to determine if exchange would occur (Scheme 3.11). The ^1H NMR spectrum of the mixture was complex. Signals attributable to unreacted **28** were observed in addition to signals consistent with several compounds containing mesityl and carbene fragments. The formation of a thin metallic-like film, presumably elemental germanium, on the wall of the reaction vessel was also observed. A white powder precipitated upon addition of pentane to a C_6H_6 solution of the crude products. The ^1H NMR spectrum of the precipitate showed signals consistent with two non-equivalent mesityl groups in a 1:1 ratio and a carbene moiety. Crystals were grown and the structure was determined by x-ray crystallography to be germylgermylene **48** (Scheme 3.11, Figure 3.6). The compound contains two germanium atoms: a three coordinate Ge with a vacant coordination site that

is presumably occupied by a lone pair of electrons, and a coordinately saturated Ge. Compound **48** is a rare example of a donor stabilized germylgermylene; such compounds are important intermediates in a number of reactions involving germanium. Few have been directly observed and structurally characterized.[27, 28]

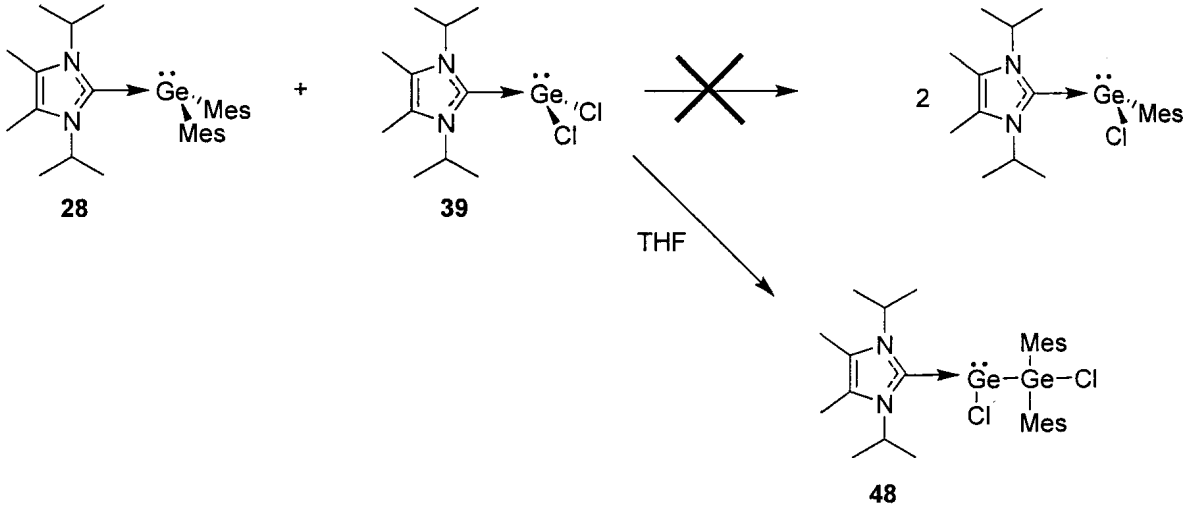

Scheme 3.11

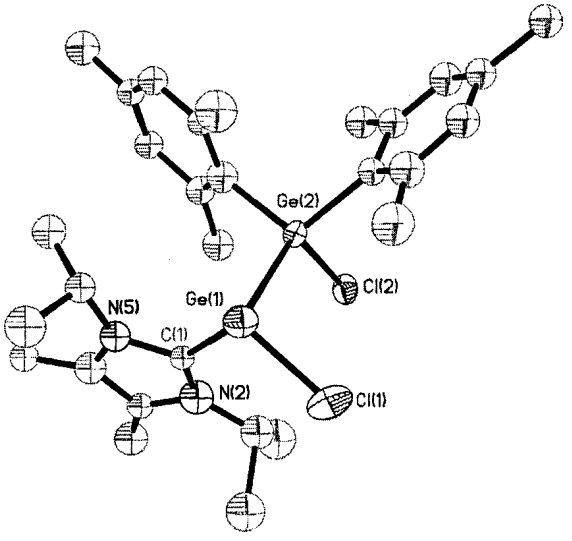

Figure 3.6: Thermal ellipsoid plot (50% probability surface) of **48**. Hydrogen atoms are omitted for clarity. Selected bond lengths (Å) and angles (°): Ge1-Ge2 = 2.5355(19), C1-Ge1 = 2.147(12), Ge2-C21 = 2.017(5), Ge2-C31 = 2.013(5), Ge1-Cl1 = 2.147(12), Ge2-

Cl2 = 2.230(3), C1-Ge1-Cl1 = 101.8(3), Cl1-Ge1-Ge2 = 88.6(4), Cl2-Ge2-Ge1 = 108.30(10), Cl2-Ge2-C21 = 110.8(2), Cl2-Ge2-C31 = 98.6(2), C21-Ge2-C31 = 107.4(3).

In the reaction producing **48**, compounds **28** and **39** are combined in an equal molar ratio; however, the ^{1}H NMR spectrum of the crude reaction mixture showed signals attributable to unreacted **28**. The low isolated yield of **48** (25 %) and the complex product mixture indicates that other products are formed under the reaction conditions. The formation of a metallic-like film implies that redox chemistry is occurring. Unfortunately, efforts to identify other reaction products were unsuccessful. The reduction of main group compounds by NHCs has been reported. The reduction appears to be driven by the formal elimination of X_2 (X = halogen) from the main group element.[3]

The formation of **48** was unexpected and arises, presumably, by the insertion of a molecule of **28** into the Ge-Cl bond of a molecule of **39**, with concommittal loss of a carbene. Germylenes are known to readily insert into many different types of bonds (See Scheme 1.4 in Chapter 1). The formation of both **47** and **48** provides some insight into why our attempts to synthesize carbene-germylene complexes with smaller aryl or alkyl groups on germanium failed. Presumably, the insertion reactions are more facile with smaller R groups on Ge, and thus, oligomerization occurs during the attempted syntheses of carbene-stabilized GeR_2 complexes.

Secondary insertions reactions do not appear to be taking place during the synthesis of compounds **39** - **43**, **45**, and **46**, all of which have electron withdrawing substituents bonded to germanium. Electron withdrawing groups, which stabilize the germanium electron lone pair, may be inhibiting further reaction chemistry.

3.2.2 Variable Temperature ^{1}H NMR Spectroscopy of NHC Complexes of GeR_2

The signals observed in the room temperature ^{1}H NMR spectra of compounds **39** - **43**, **45**, and **46** are broad. As expected, the signal assigned to the vinylic methyls of the carbene is a singlet and the signal assigned to the methyls of the isopropyl moiety is a doublet. However, the signal assigned to the methyne ^{1}H is not the expected septet; instead, it is very broad, often disappearing into the baseline of the spectrum.

Variable temperature ^{1}H NMR spectroscopy was performed on compounds **39** - **43**, **45**, and **46**; the results obtained were similar, and thus, only the results for compound **39** will be discussed. At -90 °C, the broad signal assigned to the methyne ^{1}H resolved into three septets which integrated in a 1:2:1 ratio (Figure 3.7). To explain this observation, the following model is proposed: at 26 °C, hindered rotation about the C1-Ge bond results in line broadening in the ^{1}H NMR spectrum. At -90 °C, this rotation halts and two conformations predominate. In one conformation, depicted as rotamer **A** in Chart 3.2, the methyne ^{1}H's are not equivalent because of the orientation of the $GeCl_2$ moiety. The second conformation, rotamer **B** in Chart 3.2, occurs with the $GeCl_2$ moiety in such an orientation that the methyne ^{1}Hs are equivalent. The upfield region of the ^{1}H NMR spectrum of **39** at -90 °C showed numerous, overlapping signals consistent with the reduced symmetry of the rotamers. All of the remaining halogenated complexes (**40**, **41**, and **42**) showed the same behavior as **39**. Compound **45** also displayed three different methyne ^{1}H signals at low temperature in the ^{1}H NMR spectrum, although complete resolution of the septets was not achieved. For compounds **43** and **46**, the broad signals did not completely resolve into different signals at low temperatures. Presumably, resolution of the rotamers would be achieved at temperatures lower then -90 °C.

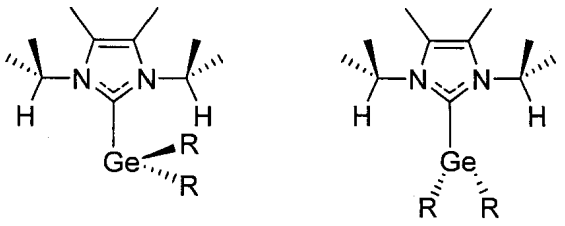

Rotamer **A** Rotamer **B**

Chart 3.2

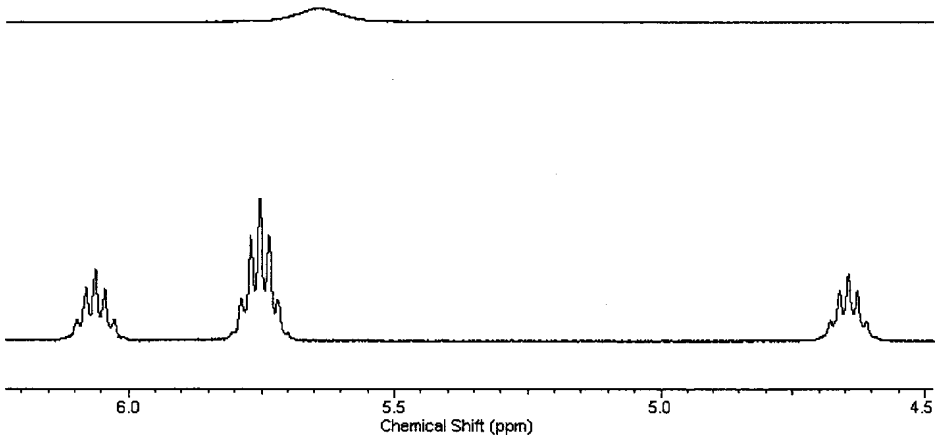

Figure 3.7: ^{1}H NMR spectra of compound **39** focusing on the isopropyl methyne region (4.5 - 6.2 ppm) at 26 °C (top) and at -90 °C (bottom) in THF-d_8.

Intermolecular exchange between the carbene and germylene moieties on the NMR timescale is an alternative explanation for the line broadening observed with the signals in the ^{1}H NMR spectra of **39** - **43**, **45**, and **46** at room temperature. Either a dissociative exchange or an associative exchange is possible. No reaction was observed at room temperature when 2,3-dimethylbutadiene (DMB), a well-known germylene trap, was added to solutions of **39** - **43**, **45**, and **46** in C_6H_6. Thus, the formation of free germylene in solution is unlikely at room temperature and the dissociative mechanism was discarded. The possibility of associative exchange occurring is more difficult to rule out.

In the most sterically hindered compounds **28** and **48**, the multiplets in their room temperature ^{1}H NMR spectra are well resolved. A possible interpretation is that the compounds with less sterically bulky substituents (**39** - **43**, **45**, and **46**) undergo an associative exchange that is active on the NMR time scale, while individual molecules (**28** and **48**) of the bulkier complexes are unable to approach each other, thus rendering the associative exchange mechanism inoperative. Further evidence for an associative mechanism comes from the isolation of **48**, which forms presumably through successive associations of NHC-GeR_2 fragments.

Although the variable temperature ^{1}H NMR spectra of compounds **39** - **43**, **45**, and **46** are consistent with the rotamer model, the spectra of **28** and **48** suggest an associative exchange process. Depending on the temperature and the NHC-GeR_2 complex involved, both mechanisms could operate simultaneously.

3.2.3 Structural Comparisons of NHC Complexes of GeR_2

The NHC-germylene complexes described in this work have similar solid state structures, with metrics consistent with Ge(II) donor/acceptor complexes. The R-Ge-R bond angles are approximately 90 °; the planes of the carbenic rings are orthogonal to the R-Ge-R planes and bisect the other substituents on the germanium atoms. The metrics of compound **28** differ slightly from the metrics of the other complexes: the angles around germanium are more obtuse, which is likely due to the steric bulk of the mesityl substituents.

Oláh *et al.* have recently examined the nature of Lewis acid-base interactions between silicon(II) or germanium(II) compounds with the neutral donors NH_3, PH_3, and

AsH_3.[29] In general, π donating substituents on the heavy group 14 element reduce the energy of complexation (ΔE_{comp})[30] between the substituted germylene and a donor, presumably by transferring electron density into the empty p-orbital. For germanium, the ΔE_{comp} decreases in the following order: (forms energetically most favorable complex) GeH_2, > HGeMe > $GeCl_2$ $\approx GeF_2$ > $Ge(OH)_2$ > $Ge(NH_2)_2$ (forms least energetically favorable complex) (Table 3.2).[29]

Table 3.2: Calculated ΔE_{comp} of Germylenes with NH_3 and PH_3[29]

Germylene	NH_3 (kJ/mol)	PH_3 (kJ/mol)
GeH_2	-95.31	-78.24
HGeMe	-78.78	-55.65
$Ge(NH_2)_2$	-13.51	Not stable
$Ge(OH)_2$	-44.27	-6.82
GeF_2	-83.64	-28.53
$GeCl_2$	-82.17	-32.47

A trend in the variation of the carbenic C-Ge bond length with respect to the π donating ability of atoms located on germanium was observed in compounds **28**, **39** - **43**, **45** and **46**. This is best illustrated by comparing the metrics of **28** (Mes-substituted) with **40** (F-substituted). Based on steric arguments and the electronegativity of the substituents, **40** may be expected to have the shortest C1-Ge bond length since fluorine has a very small atomic radius and is more electron withdrawing than mesityl. Instead, **40** was observed to have one of the longest carbenic C1-Ge bond lengths, while **28** has one of the shortest (Table 3.3). This observation is consistent with Oláh *et al.*'s findings:[29] the lone pairs of electrons on fluorine donate electron density into the σ^* orbital of the carbenic carbon-germanium bond and, consequently, the bond length between the carbene C1 and Ge is elongated compared to the other compounds. In

contrast, the π-electrons of the mesityl substituents are relatively poor electron donors and the carbenic carbon-germanium bond is one of the shortest in the series. Further evidence for the weakening of the carbene C1-Ge bond by competing π donation is apparent in the formation of **4**,[9] where the strong electron donating ability of the two nitrogen substituents on germanium provides enough electron density to the p-orbital to completely dislodge the carbene.

Table 3.3: Bond lengths between the carbenic carbon and germanium in selected NHC-GeR_2 complexes.

Substitution (R_2)	Bond Length (Å)			
$(OtBu)_2$	**45**	2.120(9), 2.224(14)	**49**[31]	2.110(5)
F_2	**40**	2.117(7)		N/A
Cl_2	**39**	2.106(3)	**50**[31]	2.088(4), 2.106(7)
Br_2	**41**	2.089(5)	**51**[31]	2.085(5)
I_2	**42**	2.086(3)	**52**[31]	2.103(7), 2.099(7)
$(NCS)_2$	**46**	2.105(9), 2.062(9), 2.075(10), 2.072(9)		N/A
Mes_2	**28**	2.078(3)	**53**[31]	2.067(3)
Cl, OTf	**43**	2.068(2)		N/A

In spite of the foregoing discussion, the trends observed for the bond lengths in the NHC-GeR_2 complexes may be a result of crystal packing effects rather than electronic effects. Recently, a series of related NHC complexes of GeR_2 were synthesized (Chart 3.3) and did not show a distinct trend in the carbenic carbon-germanium bond length (Table 3.3).[31] Moreover, in the work of Oláh *et al.*, only the ΔE_{comp} between a Lewis base and a germylene were examined; bond lengths of the complexes were not reported. Therefore, in an effort to help better interpret our experimental results, we examined the

energy of complexation and bond lengths in NHC complexes of germanium(II) computationally.

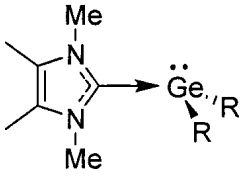

49 R = O^{t}Bu
50 R = Cl
51 R = Br
52 R = I
53 R = Mes

Chart 3.3

To reduce the complexity of the systems under study, a series of simplified complexes was used (Chart 3.4), where the vinylic methyl groups and isopropyl groups of the carbene were replaced with hydrogen atoms and methyl groups, respectively. Two different model chemistries were employed: MP2/6-311+G(d,p) and PBE1PBE/6-311+G(d,p).[32]

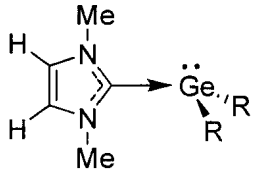

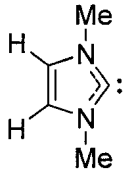

54 R = H
55 R = OH
56 R = NH_2
57 R = CH_3
58 R = F
59 R = Cl

60

Chart 3.4

The ΔE_{comp} for a given complex was determined in the following manner: the geometries of the uncoordinated model carbene **60** and uncoordinated model germylene (GeH_2, GeF_2, etc) were optimized independently. The two species were then oriented in

the analogous positions observed in the experimentally determined structures. The geometry of the model complex was then optimized. The ΔE_{comp} was determined by the difference between the total energy of the uncoordinated species and the total energy of the complex (Table 3.4). Included within the calculation of ΔE_{comp} are corrections for zero point energy (ZPE). The basis set superposition errors (BSSEs) were calculated but not included in the final results as they were found to be negligible.[33] The results from the two different model chemistries (PBE1PBE and MP2) employed found similar complexation energies and bond lengths (Table 3.4). For simplicity, only the results from the PBE1PBE calculations will be discussed.

Table 3.4: Calculated ΔE_{comp} and bond lengths of the carbenic carbon-germanium bond in model NHC-GeR_2 complexes **54 - 59**

Compound (Substitution)	PBE1PBE/6-311+G(d,p)		MP2/6-311+G(d,p)	
	ΔE_{comp} (kJ/mol)	Bond length (Å)	ΔE_{comp} (kJ/mol)	Bond length(Å)
54 (H)	-192.6	2.021	-190.8	2.037
55 (OH)	-108.2	2.107	-114.3	2.114
56 (NH_2)	-63.2	2.114	-72.2	2.123
57 (CH_3)	-133.4	2.047	-149.3	2.061
58 (F)	-144.0	2.150	-148.0	2.149
59 (Cl)	-154.7	2.129	-174.7	2.116

As shown in Figure 3.8, in which the C1-Ge bond length is plotted against complexation energy, there is no apparent correlation between the complexation energy and the carbenic carbon – germanium bond length for the model compounds **54 - 59**.

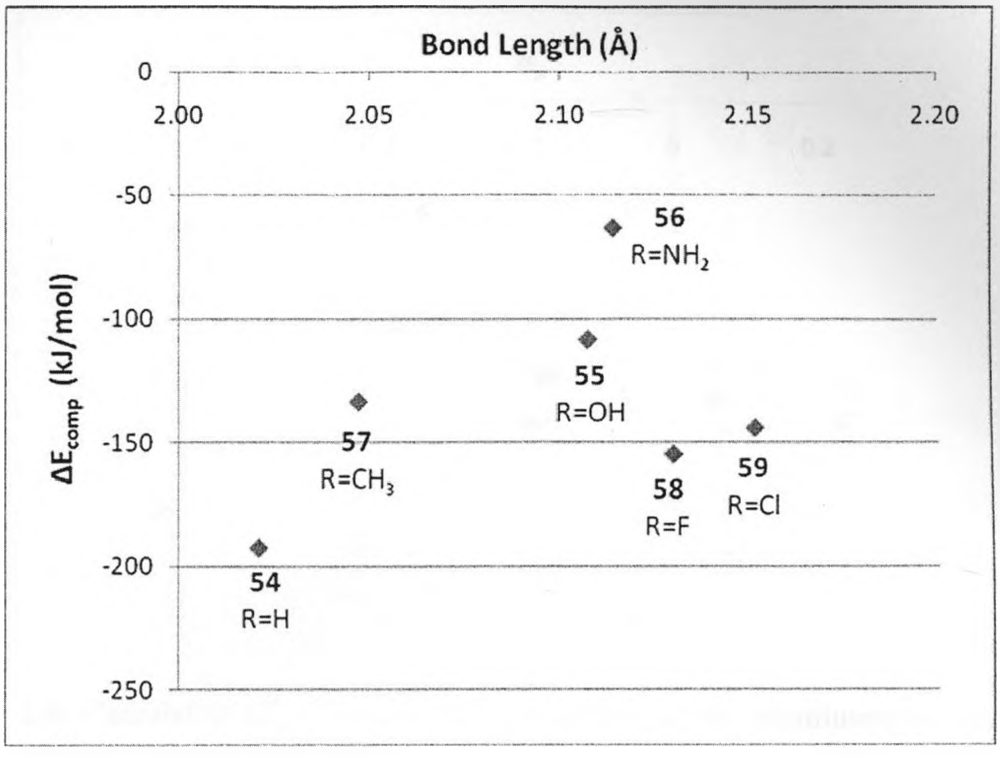

Figure 3.8: Calculated ΔE_{comp} versus carbenic carbon-Ge bond length in model compounds **54 – 59**.

Oláh *et al.* observed that π donors situated next to germanium decrease complexation energy; we also observed the same trend using both DFT and MP2 methods. Hammett's σ_p values can be used as an empirical measure of a substituent's effect on a charge localized on a neighbouring atom. A plot of the calculated ΔE_{comp} vs the σ_p constants is shown in Figure 3.9 and exhibits a negative correlation between ΔE_{comp} and the σ_p constants of the substituents on germanium. This dependence is somewhat linear, only the parent germylene (R=H) is significantly off the line of best fit. These results are similar to Oláh *et al.*'s observations and show that ligands which are suitable for stabilizing nearby negative charges also provide a stabilizing effect on ΔE_{comp} for the model NHC-GeR_2 complexes.

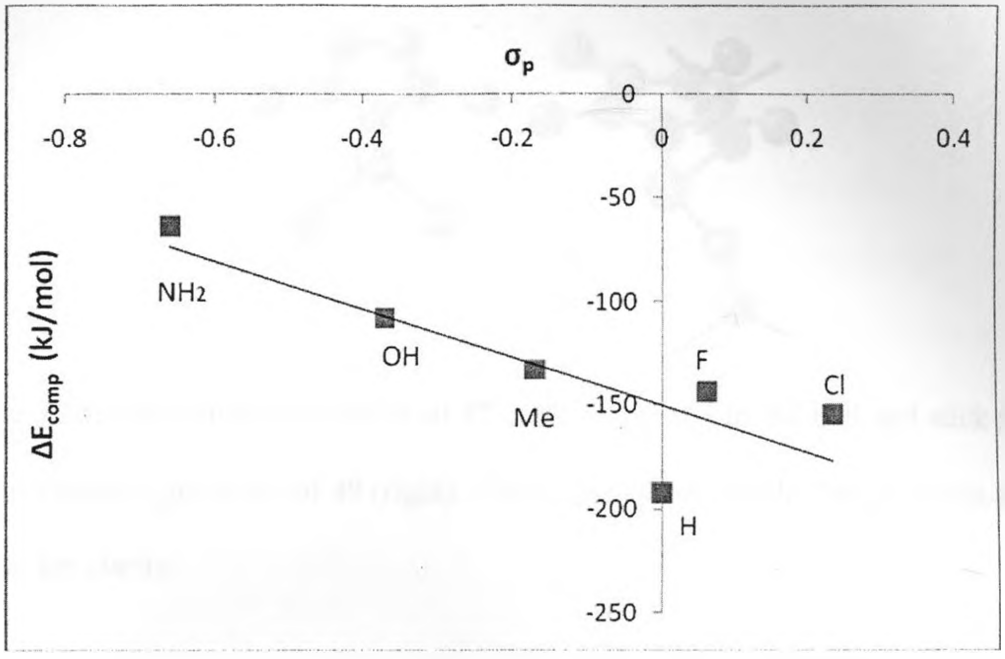

Figure 3.9: Calculated ΔE_{comp} versus the σ_p constants of the substituents on germanium in model compounds **54** – **59**.

According to the computational models, there is no apparent correlation between the substituent on germanium and the carbenic carbon-germanium bond length. Therefore, we conclude that any trend that was present in the x-ray structures of **28**, **39** - **43**, **45** and **46** was purely fortuitous.

In the optimized structures of model compounds **54**, **56**, **57**, but not **55**, **58** or **59**, the orientation of the GeR_2 fragment is twisted approximately 90° along the carbene C1-Ge bond from what was observed in the experimental structures as shown in the comparison in Figure 3.10. To determine if the conformational difference greatly influences ΔE_{comp}, a relaxed potential energy scan was performed where the dihedral angle between the substituents on germanium and the plane of the carbene was varied.

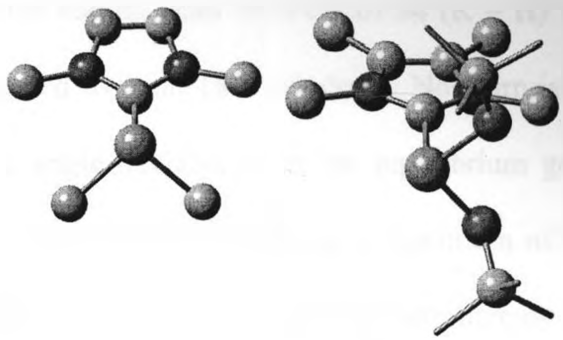

Figure 3.10: Calculated geometries of **57** (left) compared to the ball and stick model of the experimental geometry of **49** (right). Hydrogen atoms and the ^{t}butyl carbon atoms are omitted for clarity.

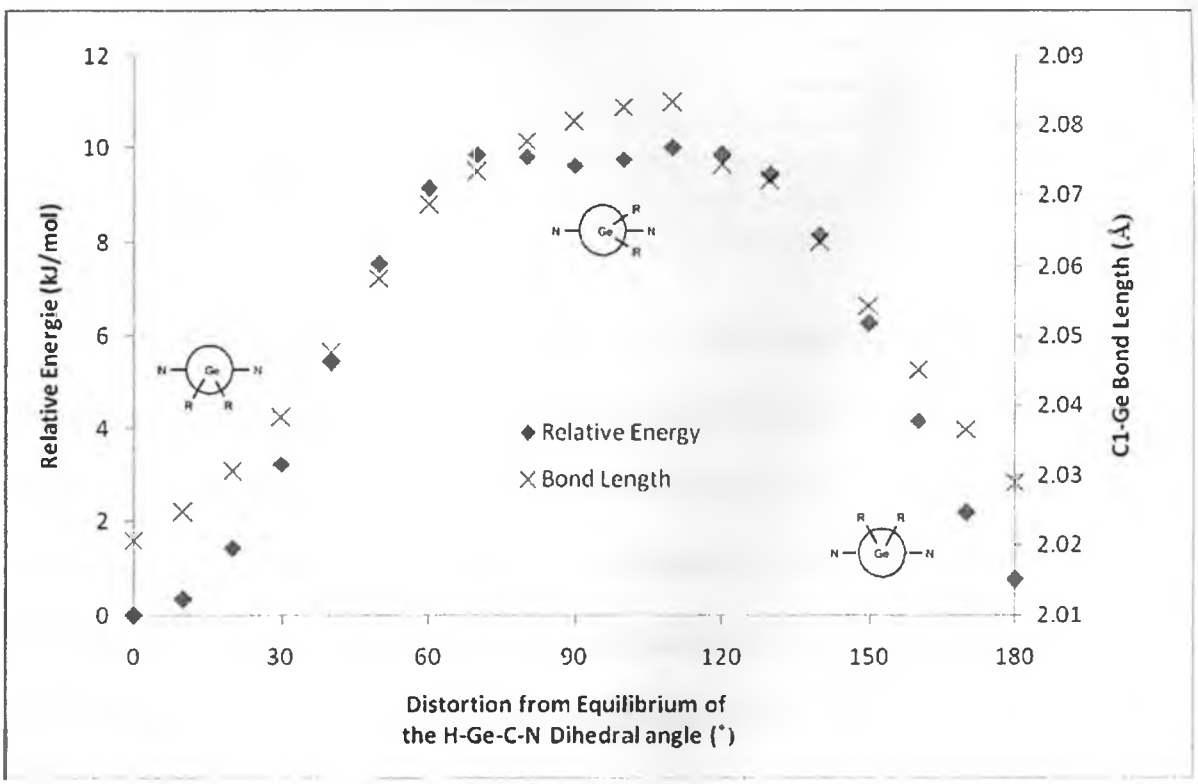

Figure 3.11. Calculated change in C1-Ge bond length and relative energy verse H-Ge-C-N dihedral angle for model compound **54**.

Figure 3.11 shows the results from the PES of **54** (R = H) in which the H-Ge-C-N dihedral angle was scanned over an 180° window. Not surprisingly, the energy of the system increases as the angle deviates from the equilibrium geometry. However, the energy differences are fairly minimal, reaching a maximum of 10.0 kJ/mol. The bond length between the carbenic carbon and the germanium increases to 2.08 Å from 2.02 Å, the value calculated at the equilibrium geometry.

Table 3.5: Calculated variations in relative energy and C1-Ge bond length during a relaxed PES sweep of the R-Ge-C-N dihedral angle.

Compound	Maximum increase in energy (kJ/mol)	Maximum increase in Ge-C bond length (Å)
54 (R = H)	10.0	0.06
55 (R= OH)	5.8	0.01
56 (R = NH_2)	15.7	0.06
57 (R = CH_3)	6.9	0.07
58 (R = F)	6.6	0.02
59 (R = Cl)	11.9	0.02

PESs on the R-Ge-C-N dihedral angle of model compounds **55** - **59** produced comparable results to what was observed for model compound **54**. A summary of the results is presented in Table 3.5. Overall, the results in Table 3.5 demonstrate that the calculated energy differences between the conformations of the GeR_2 groups relative to the plane of the NHC are minimal. The small increase in energy and bond length as the dihedral angle is altered from equilibrium would have little impact on the trends observed in Figure 3.8 and Figure 3.9.

The shallow potential energy surface for the twisting of the R-Ge-C-N dihedral angle is of similar magnitude to crystal packing forces,[34] and thus, provides a possible justification for the discrepancies in the R-Ge-C-N dihedral angle in the calculated

geometry versus the experimentally determined x-ray geometries. Finally, although the steric environments are different in the model compounds compared to the experimental compounds, a calculated shallow potential energy surface of the R-Ge-C-N dihedral angle is consistent with the multiple conformers present in solution as was observed by ^{1}H NMR spectroscopy (see Section 3.2.2).

3.3 Conclusions

In summary, **39** is a versatile reagent which we have used to synthesize a series of stable N-heterocyclic carbene complexes of germanium(II) via substitution chemistry. The goal of stabilizing transient germylenes with an NHC was partially successful: complexes **39** - **43**, **45**, and **46** are all stable derivatives of otherwise transient germylenes. NHC **25** appears to be unsuitable for the stabilization of simple diorganogermylenes; perhaps a more basic[35] or sterically encumbered[36] carbene would allow the formation of stable Ge(II) complexes. An attempted ligand exchange between **28** and **39** to form a complexed heteroleptic germylene resulted in the unexpected formation of germylgermylene **48**.

Compounds **39** - **43**, **45**, and **46** display broad signals in their room temperature ^{1}H NMR spectra. Using variable temperature NMR spectroscopy, two rotamers were observed at low temperature. The origin of the line broadening in the room temperature ^{1}H NMR spectra of **39** - **43**, **45**, and **46** is believed to be due to either hindered rotation and/or an associative exchange mechanism.

The structural characterization of the carbene-germylene complexes **39** - **43**, **45**, and **46** suggested that the length of the carbenic carbon-germanium bond is significantly

influenced by the nature of the substituents on germanium. However, subsequent computational modeling showed that although the ΔE_{comp} between the carbene and germylene is influence by the substituents, the bond length does not vary systematically. A correlation was observed between the σ_p constants of the substituents on germanium and ΔE_{comp}.

3.4 Experimental Procedures

Reactions were performed under an inert atmosphere of nitrogen using standard techniques. Solvents were purified according to literature procedures[37] and stored over 4 Å molecular sieves under N_2. All NMR spectra were acquired using C_6D_6 or THF-d_8 as the solvent. ^1H NMR spectra were referenced to residual C_6D_5H (7.15 ppm) or the upfield THF-d_7 transition (3.58 ppm). ^{13}C spectra were referenced to the ^{13}C central transition (128.0 ppm) of C_6D_6. ^{19}F spectra were referenced externally to C_6H_5F (-113.1 ppm relative to $CFCl_3$). The signals in the ^{13}C NMR spectra of the complexes were broad at both room temperature and -90 °C and thus, the data are not listed. Melting points were determined under an N_2 atmosphere and are uncorrected. FT-Raman spectra were acquired on bulk samples sealed in a melting point tube under nitrogen. Mes_2Mg and Tol_2Mg were prepared using modified literature procedures.[25] Elemental analyses were performed at Guelph Chemical Laboratories, Guelph, Ontario, Canada. Compounds **8**[38] and **25**[39] were synthesized according to literature procedures.

3.4.1 Synthesis of 39

Carbene **25** (1.0 g, 5.56 mmol) was dissolved in C_6H_6 (5 mL). $GeCl_2$·dioxane (**8**) (1.28 g, 5.56 mmol) was added directly to the carbene solution. The resulting mixture was clear and colourless. After stirring for 30 min, a white precipitate was observed. Hexanes (10 mL) was then added to the mixture. The precipitate was collected and then washed with hexanes (2 x 5 mL). The white solid was dried under high vacuum and identified as **39**. Yield: 1.54 g (88%). M.P. 160 – 163 °C (dec). ^{1}H NMR: 1.01 (d, $^3J_{HH}$ = 7, 12 H), 1.40 (s, 6 H), 5.58 (broad, 2 H). FT-Raman (cm^{-1}): 111 (m), 169 (m), 293 (m), 316 (s) (Ge – Cl), 529 (w), 748 (w), 884 (w), 1138 (w), 1434 (w), 1633 (m), 2928 (s), 2981 (s); EI-MS (m/z): 324 (M^+, 0.4). High-resolution EI-MS: exact mass calcd for $C_{11}H_{20}{}^{74}GeN_2{}^{35}Cl_2$ 324.021, found 324.022. Anal. Calcd for $C_{11}H_{20}N_2GeCl_2$: C, 40.53; H, 6.23; N, 8.65; Found: C, 40.53; H, 6.43; N, 8.91.

3.4.2 Synthesis of 40

To a colourless solution of **39** (0.77 mmol, 0.25 g) in THF (4 mL) was added KF (2.0 mmol, 0.12 g) and 18-crown-6 (0.03 mmol, 0.01g). The reaction mixture was stirred for 2 days at room temperature. After this time, a white precipitate (presumed to be KCl) was removed by centrifugation and was discarded. The solvent was removed under high vacuum to yield a white powder that was triturated with Et_2O (2 mL X 2). The white powder was dried under high vacuum to give **40** (0.15 g, 67%). Crystals suitable for single crystal x-ray diffraction analysis were obtained by slow diffusion of pentane into a saturated C_6H_6 solution. M.P. 103 - 108 °C (dec). ^{1}H NMR (C_6D_6): δ 1.15 (d, $^3J_{HH}$ = 7 Hz, 12 H), 1.42 (s, 6 H), 5.46 (broad, 2 H). ^{19}F NMR: δ -112. FT-Raman: 209 (s), 530

(m), 888 (m), 1084 (w), 1142 (w), 1286 (w), 1324 (w), 1352 (w), 1399 (m), 1458 (m), 1637 (m), 2941 (s), 2985 (s).

3.4.3 Synthesis of 41

To a colourless solution of **39** (1.0 mmol, 0.32 g) in C_6H_6 (5 mL) was added Me_3SiBr (0.52 mL, 4.0 mmol, 0.12 g). The reaction mixture was stirred for 24 hr and then hexanes (10 mL) was added. A white precipitate was collected, triturated with hexanes (2 mL x 2), and dried under high vacuum to give **41** (0.29 g, 71 %). Crystals suitable for single crystal x-ray diffraction analysis were obtained by slow diffusion of pentane into a saturated C_6H_6 solution. M.P. 150 °C (dec). ^{1}H NMR (C_6D_6): δ 1.09 (d, $^3J_{HH}$ = 7 Hz, 12 H), 1.37 (s, 6 H), 5.52 (broad, 2 H). FT-Raman (cm^{-1}): 106 (m), 133 (w), 213 (m), 232 (s), 886 (w), 1284 (m), 1414 (m), 1443 (m), 1624 (m), 2940 (s), 2982 (m). Anal. Calcd for $C_{11}H_{20}N_2GeBr_2$: C, 32.01; N, 6.79; H, 4.88. Found: C, 32.08; N, 6.42; H, 5.24.

3.4.4 Synthesis of 42

39 (0.32 g, 1 mmol) was dissolved in C_6H_6 (5 mL) to give a clear and colourless solution. Me_3SiI (0.30 mL, 2 mmol) was added to the solution. The colour of the solution became yellow. The solution was allowed to stir for 1 hr, after which a yellow precipitate began to form. Hexanes (5 mL) was then added to the solution. The yellow precipitate was collected and dried under high vacuum. Yield: 0.35 g (69%). M.P. 162 °C (dec). ^{1}H NMR: 1.14 (d, $^3J_{HH}$ = 7, 12 H), 1.45 (s, 6 H), 5.51 (broad, 2 H). FT-Raman (cm^{-1}): 115 (s), 205 (s) (Ge – I), 273 (w), 458 (w), 540 (w), 764 (w), 883 (w), 992 (m),

1282 (m), 1440 (m), 1625 (m), 2936 (m), 2972 (m); EI-MS (m/z): 508 (M^+, 0.5), 463 (M^+ - C_3H_7, 10), 340 (M^+ - C_3H_7I, 10). High-resolution EI-MS: exact mass calcd for $C_{11}H_{20}{}^{72}GeN_2I_2$ 507.893, found 507.893. Anal. Calcd for $C_{11}H_{20}N_2GeI_2$: C, 26.07; H 3.98; N, 5.53; Found: C, 25.94; H, 3.84; N, 5.73.

3.4.5 Synthesis of 43

To a colourless solution of **39** (1.0 mmol, 0.32 g) in C_6H_6 (6 mL) was added Me_3SiOTf (2 mmol, 0.36 mL). The reaction mixture was allowed to stir for 2 hr, after which time the solvent was removed under high vacuum to yield a white powder. The powder was triturated with hexanes (3 mL x 2) and was dried under high vacuum. The white powder was identified as **43** (0.36 g, 62 %). Crystals suitable for single crystal x-ray diffraction analysis were grown by slow diffusion of pentane into a saturated C_6H_6 solution. M.P. 101-103 °C (dec). ^1H NMR (C_6D_6): δ 1.08 (d, $^3J_{HH}$ = 7 Hz, 12 H), 1.30 (s, 6 H), 5.18 (broad, 2H). ^{19}F NMR (C_6D_6): -78. FT-Raman (cm^{-1}): 100 (m), 315 (s), 585 (w), 764 (m), 888 (m), 973 (m), 1235 (w) 1287 (m), 1447 (m), 1623 (m), 2949 (s), 2994 (m). Anal. Calcd for $C_{12}H_{20}N_2GeClF_3O_3S$: C, 32.95; N, 6.40; H, 4.61. Found: C, 33.05; N, 6.42; H, 4.91.

3.4.6 Addition of 44 to 39

A solution of **44** (1 mmol) dissolved in THF (3 mL) was added dropwise to a stirring solution of **39** (0.36 g, 1.1 mmol) dissolved in THF (10 mL) which was cooled in a Dry Ice/acetone bath. The reaction mixture was stirred for 18 hr during which time it was allowed to warm to room temperature. After this time, the reaction mixture was orange

in colour. The solvent was evaporated under high vacuum, leaving behind an orange residue. The residue was taken up in C_6D_6. Insoluble salts (presumed to be LiCl) suspended in the C_6D_6 solution were removed by centrifugation. ^1H and ^{13}C NMR spectra of the solution were consistent with the quantitative formation of **25** and **4**.[9]

3.4.7 Synthesis of 45

^{t}BuOK (1.8 mmol, 0.20 g) was added to a colourless solution of **39** (0.93 mmol, 0.30 g) dissolved in THF (3 mL). The reaction mixture was allowed to stir for 18 hr at room temperature, after which time a white precipitate (presumed to be KCl) was collected by centrifugation and discarded. The solvent was removed under vacuum yielding **45** (0.32 g, 89 %). Crystals suitable for single crystal x-ray diffraction were grown by placing a saturated Et_2O solution in a freezer at -20 °C for one week. M.P. 94-102 °C (dec). ^1H NMR (C_6H_6): δ 1.28 (d, $^3J_{HH}$ = 7 Hz, 12 H), 1.53 (s, 6 H), 1.67 (s, 18 H), 6.07 (broad, 2H). FT-Raman (cm^{-1}): 84 (m), 120 (m), 295 (w), 464 (w), 531 (w), 608 (w), 765 (m), 887 (w), 1233 (w), 1295 (w), 1451 (s), 1628 (w), 2912 (s), 2937 (s), 2970 (s). Anal. Calcd for $C_{19}H_{38}GeN_2O_2$: C, 57.17; N, 7.02; H, 9.60. Found: C, 56.88; N, 6.84; H, 9.68.

3.4.8 Synthesis of 46

To a colourless solution of **39** (0.93 mmol, 0.3 g) in THF (5 mL) was added KSCN (1.86 mmol, 0.18g). The reaction mixture was allowed to stir for 2 days at room temperature, after which time the solvent was removed under vacuum to yield a white residue. The residue was suspended in C_6H_6 (6 mL); a white solid (presumed to be KCl)

was removed by centrifugation and then discarded. Hexanes was added to the C_6H_6 solution; the white precipitate was collected. The solid was dried under vacuum to give **46** (82%, 0.28 g). Crystals suitable for single crystal x-ray diffraction analysis were grown by slow diffusion of pentane into a saturated C_6H_6 solution. M.P. 122-124 °C (dec). ^{1}H NMR (C_6D_6): δ 0.94 (d, $^3J_{HH}$ = 7 Hz, 12 H), 1.27 (s, 6 H), 4.94 (broad, 2H). FT-Raman (cm^{-1}): 152 (w), 191 (w), 226 (w), 290 (m), 457(w), 486 (w), 584 (w), 863 (m), 887 (m), 1287 (m), 1359 (w), 1442 (m), 1623 (m), 2046 (s), 2059 (s), 2936 (s), 2973 (m). Anal. Calcd for $C_{13}H_{20}N_4GeS_2$: C, 42.30; N,15.18; H, 5.46. Found: C, 42.33; N, 14.82; H, 6.49.

3.4.9 Synthesis of 28 via 39

Compound **39** (0.13 g, 0.4 mmol) was added to a stirring solution of Mes_2Mg (0.4 mmol) in THF/dioxane (4 mL THF, 1 mL dioxane). The solution became yellow in colour and was allowed to stir for 3 days at room temperature. A white precipitate (presumed to be $MgCl_2$·dioxane) was removed by centrifugation. The ^{1}H NMR spectrum of the bright yellow solution was consistent with quantitative formation of **28**.

3.4.10 Reaction of Tol_2Mg with 39

To a solution of **39** (0.16 g, 0.5 mmol) dissolved in THF (4 mL) was added Tol_2Mg (0.5 mmol) dissolved in THF/dioxane (4 mL THF, 2 mL dioxane). The colour of the solution became yellow and was allowed to stir for 18 hr at room temperature. After 18 hr, the white precipitate (presumed to be $MgCl_2$·dioxane) was removed by centrifugation. The solvent was removed to yield a pale yellow residue. The residue was dissolved in

C_6H_6 (3 mL). Vapor diffusion of Et_2O into the C_6H_6 solution resulted in the formation of crystals of **47**. Crystals suitable for single crystal x-ray diffraction analysis were grown by slow diffusion of pentane into a saturated C_6H_6 solution. ^1H NMR (C_6D_6): δ 2.00 (s, 24 H), 6.92 (d, $^3J_{HH}$ = 7 Hz, 16 H), (d, $^3J_{HH}$ = 7 Hz, 16 H).

3.4.11 Synthesis of 48

To a deep yellow solution of **28** (0.32 mmol) dissolved in THF (10 mL) was added **39** (0.10 g, 0.32 mmol). The reaction mixture was stirred for 2 days, after which time it became orange in colour. The solvent was removed under vacuum to yield an orange/yellow residue which was then resuspended in C_6H_6 (2 mL). The orange solution was turbid; the fine particulates were removed by centrifugation and discarded. Pentane (4 mL) was added to the C_6H_6 solution and a pale yellow solid precipitated. The pale yellow solid was collected, triturated with pentane (2 x 2 mL), and dried under high vacuum to give **48** (0.06 g, 25 %). Crystals suitable for single crystal x-ray diffraction analysis were grown by slow diffusion of pentane into a saturated C_6H_6 solution. M.P. 180-183 °C (dec). ^1H NMR (C_6H_6): δ 0.79 (d, $^3J_{HH}$ = 7 Hz, 6 H), 1.23 (d, $^3J_{HH}$ = 7 Hz, 6 H), 1.47 (s, 6 H), 2.07 (s, 3 H), 2.09 (s, 3 H), 2.62 (s, 6 H), 2.84 (s, 6 H), 5.61 (sept, $^3J_{HH}$ = 7 Hz, 2 H), 6.66 (s, 2 H), 6.71 (s, 2 H). FT-Raman (cm^{-1}): 102 (s), 276 (w), 324 (w), 354 (w), 534 (w), 561 (m), 584 (w), 760 (w), 887 (w), 992 (w), 1284 (s), 1344 (m), 1380 (m), 1442 (m), 1601 (m), 1628 (m), 2730 (w), 2916 (m), 2978 (w). Anal. Calcd for $C_{29}H_{42}N_2GeCl_2$: C, 54.87; N, 4.41; H, 6.67. Found: C, 54.58; N, 4.06; H, 6.75.

3.4.12 Computational Details

Calculations were performed using Gaussian03.[40] All optimized geometries did not have any imaginary frequencies, and therefore, are minima on the potential energy surface. For the DFT calculations, tight convergence criteria for the self consistent field (SCF=Tight) and an ultra fine integration grid (Int=Grid=Ultrafine) were used during the calculations. For the MP2 calculations, tight convergence criteria for the self consistent field (SCF=Tight) were used during the calculations. The basis set superposition error was calculated using the Counterpoise keyword in Gaussian03. Appendix A1.1-A1.3 contains the Gaussian03 input files.

3.4.13 Single Crystal X-ray Diffraction

Data were collected at low temperature (-123 °C) on a Nonius Kappa-CCD area detector diffractometer with COLLECT. The unit cell parameters were calculated and refined from the full data set. Crystal cell refinement and data reduction were carried out using HKL2000 DENZO-SMN.[41] Absorption corrections were applied using HKL2000 DENZO-SMN (SCALEPACK).

The SHELXTL/PC V6.14 suite of programs was used to solve the structures by direct methods.[42] Subsequent difference Fourier syntheses allowed the remaining atoms to be located. All of the non-hydrogen atoms were refined with anisotropic thermal parameters. The hydrogen atom positions were calculated geometrically and were included as riding on their respective carbon atoms.

Both compounds **46** and **48** showed signs of non-merohedral twinning in the E-statistics and the F_{obs} values were consistently higher than the F_{calcs}. WinGX[43] was used

to "detwin" the data. ROTAX[44] found the Twin Law. "Make HKLF5" was used to generate the detwinned file used in further refinement.

Table 3.6: Crystallographic data for compounds **39** - **43** and **45** - **48**.

	39	**40**	**41**	**42**· benzene
CCDC#		709071	709072	
Empirical formula	$C_{11}H_{20}Cl_2GeN_2$	$C_{11}H_{20}N_2GeF_2$	$C_{11}H_{20}N_2GeBr_2$	$C_{11}H_{20}N_2Ge$, I_2 0.5(C_6H_6)
Formula weight	323.78	290.88	412.70	545.73
Crystal system	Monoclinic	Monoclinic	Orthorhombic	Monoclinic
Space group	Cc	Cc	Pccn	C 2/c
a (Å)	14.0114(4)	12.124(2)	14.3290(4)	21.4774(7)
b (Å)	9.3901(3)	9.830(2)	17.6782(3)	8.6709(3)
c (Å)	11.5641(4)	11.487(2)	12.3781(5)	20.2449(7)
α (°)	90	90	90	90
β (°)	106.168(2)	103.38(3)	90	100.7940(14)
γ (°)	90	90	90	90
Volume (Å^3)	1461.30(8)	1331.8(5)	3135.51(16)	4385.25(14)
Z	4	4	8	4
Data/restraints/ parameters	3226/2/152	1877/2/152	3644/0/151	4236/0/180
Goodness-of-fit	1.031	1.068	1.049	1.062
R [$I>2\sigma(I)$]	R_1 = 0.0291,	0.0578	0.0569	R_1 = 0.0354,
wR^2 (all data)	wR_2 = 0.0715	0.1501	0.1668	wR_2=0.0927
Largest diff. peak and hole (e Å^{-3})	0.432 -0.534	0.754, -0.905	1.420, -1.237	0.810 -1.405

	43	**45**	**46**	**47**
CCDC #	709073	709074	709075	709076
Empirical formula	$C_{12}H_{20}N_2GeClF_3O_3S$	$C_{19}H_{38}GeN_2O_2$	$C_{13}H_{20}GeN_4S_2$	$C_{56}H_{56}Ge_4$
Formula weight	574.46	399.10	369.04	1019.37
Crystal system	Triclinic	Monoclinic	Triclinic	Monoclinic
Space group	P-1	Pm	P-1	C2/c
a (Å)	8.9383(3)	8.7579(6)	10.3332(4)	21.5323(8)
b (Å)	9.2138(3)	14.0465(11)	19.2660(7)	10.8763(3)
c (Å)	11.3287(5)	9.2646(6)	19.3942(9)	20.9354(5)
α (°)	95.712(2)	90	105.353(2)	90
β (°)	105.712(2)	102.212(4)	104.885(2)	97.4440(16)
γ (°)	96.726(6)	90	104.763(2)	90
Volume (Å^3)	883.50(6)	1113.92(14)	3375.2(2)	4861(3)
Z	2	2	8	4

Data/restraints/ parameters	4047/0/214	4752/2/261	15215/0/746	5577/0/275
Goodness-of-fit	1.070	1.046	1.121	1.058
R [$I>2\sigma(I)$]	0.0396	0.0709	0.0742	0.0424
wR^2 (all data)	0.0914	0.1997	0.2476	0.1218
Largest diff. peak and hole (e $Å^{-3}$)	0.594, -1.058	2.725, -0.707	3.00, -1.842	0.853, -1.046

	48
CCDC#	709077
Empirical formula	$C_{29}H_{42}Cl_2Ge_2N_2$
Formula weight	634.73
Crystal system	Monoclinic
Space group	$P2_1/c$
a (Å)	20.4418(6)
b (Å)	9.6341(2)
c (Å)	15.6432(4)
α (°)	90
β (°)	93.422(2)
γ (°)	90
Volume ($Å^3$)	3075.25(14)
Z	4
Data/restraints/ parameters	5363/0/305
Goodness-of-fit	1.040
R [$I>2\sigma(I)$]	0.1090
wR^2 (all data)	0.2846
Largest diff. peak and hole (e $Å^{-3}$)	3.534, -2.359

3.5 References

1. Rupar, P. A.; Jennings, M. C.; Ragogna, P. J.; Baines, K. M. *Organometallics* **2007**, *26*, 4109.

2. (a) Leigh, W. J.; Lollmahomed, F.; Harrington, C. R.; McDonald, J. M. *Organometallics* **2006**, *25*, 5424. (b) Huck, L. A.; Leigh, W. J. *Organometallics* **2007**, *26*, 1339.

3. (a) Ellis, B. D.; Dyker, C. A.; Decken, A.; Macdonald, C. L. B. *Chem. Commun.* **2005**, 1965. (b) Dutton, J. L.; Tabeshi, R.; Jennings, M. C.; Lough, A. J.; Ragogna, P. J. *Inorg. Chem.* **2007**, *46*, 8594.

4. Boganov, S. E.; Egorov, M. P.; Faustov, V. I.; Nefedov, O. M. In *The Chemistry of Organic Germanium, Tin and Lead Compounds,* Vol. 2; Rappoport, Z., Ed; John Wiley & Sons Ltd.: West Sussex, England, **2002**; pp. 749 – 841.

5. Chauvin, R. *J. Phys. Chem.* **1992**, *96*, 9194.

6. Baines, K. M.; Stibbs, W. G. *Coord. Chem. Rev.* **1995**, *145*, 157.

7. Arduengo, III, A. J.; Dias, H. V. R.; Calabrese, J. C.; Davidson, F. *Inorg. Chem.* **1993**, *32*, 1541.

8. Kühl, O. *Coord. Chem. Rev.* **2007**, *251,* 2253.

9. N-heterocyclic germylene **4** has been reported previously. See: Hermann, W. A.; Denk, M.; Behm, J.; Scherer, W.; Klingan, F.; Bock, H.; Solouki, B.; Wagner, M. *Angew. Chem., Int. Ed. Engl.* **1992**, *31*, 1485.

10. Gehrhus, B.; Hitchcock, P. B.; Lappert, M. F. *J. Chem. Soc., Dalton Trans.* **2000**, 3094.

11. Kühl, O; Lifson, K.; Langel, W. *Eur. J. Org. Chem.* **2006**, 2336.

12. Weinert, C. S.; Fenwick, A. E.; Fanwick, P. E.; Rothwell, I. P. *J. Chem. Soc., Dalton Trans.* **2003**, 532.

13. Fjeldberg, T.; Hitchcock, P. B.; Lappert, M. F.; Smith, S. J.; Thorne, A. J. *J. Chem. Soc., Chem. Commun.* **1985**, 939.

14. Weinert, C.S.; Fanwick, P. E.; Rothwell, I. P. *J. Chem. Soc., Dalton Trans.* **2002**, 2948.

15. Cetinkaya, B.; Gümrükcü, I.; Lappert, M. F.; Atwood, J. L., Rogers, R. D.; Zaworotko, M. J. *J. Am. Chem. Soc.* **1980**, *102*, 2088.

16. Barrau, J.; Rima, G.; El Amraoui, T. *Organometallics* **1998**, *17*, 607.

17. Barrau, J.; Rima, G.; El Amraoui, T. *J. Organomet. Chem.* **1998**, *570*, 163.

18. Gerung, H.; Boyle, T. J.; Tribby, L. J.; Bunge, S. D.; Brinker, C. J.; Han, S. M. *J. Am. Chem. Soc.* **2006**, *128*, 5244.

19. Using an intermolecular coordinating donor to stabilize a $Ge(OR)_2$ species has been previously reported. For example, $Ge(OMes)_2$ forms a monomer when coordinated by an amine. See: Bonnefille, E.; Mazières, S.; El Hawi, N.; Gornitzka, H.; Couret, C. *J. Organomet. Chem.* **2006**, *691*, 5619.

20. Onyszchuk, M.; Castel, A.; Rivière, P.; Satgé, J. *J. Organomet. Chem.* **1986**, *317*, C35.

21. Shen, X.; Sakata, K.; Hashimoto, M. *Polyhedron* **2002**, *21*, 969.

22. Leigh, W. J.; Lollmahomed, F.; Harrington, C. R.; McDonald, J.M. *Organometallics* **2006**, *25*, 5424.

23. Substitution reactions with all of the dihalo derivatives were attempted and gave similar results.

24. For examples of other R_8Ge_4 ring systems, see: Ando, W.; Tsumuraya, T. *J. Chem. Soc., Chem. Commun.* **1987**, 1514.

25. For the preparation of the mesityl Grignard reagent, the Schlenk equilibrium was driven towards Mes_2Mg by the precipitation of $MgBr_2$·dioxane. The addition of this Grignard reagent to **39** resulted in a higher yield for the formation of **28** in comparison to the addition of MesMgBr. See Cannon, K. C.; Krow, G. R. In *Handbook of*

Grignard Reagents; Silverman, G. S., Rakita, P. E., Eds; Marcel Dekker: New York, **1996**.

26. Richards, A. F.; Brynda, M.; Power, P. P. *J. Chem. Soc., Chem. Commun.* **2004**, 1592.

27. Power, P.P. In *Modern Aspects of Main Group Chemistry*; Lattman, M., Kemp, R. A., Eds; American Chemical Society: Washington, DC, **2006**; pp. 179 - 191.

28. (a) Richards, A. F.; Phillips, A. D.; Olmstead, M. M.; Power, P. P. *J. Am. Chem. Soc.* **2003**, *125*, 3204. (b) Fukaya, N.; Sekiyama, H.; Ichinohe, M.; Sekiguchi, A. *Chem. Lett.* **2002**, 802. (c) Fukaya, N.; Ichinohe, M.; Kabe, Y.; Sekiguchi, A. *Organometallics* **2001**, *20*, 3364. (d) Setaka, W.; Sakamoto, K.; Kira, M.; Power, P. P. *Organometallics* **2001**, *20*, 4460. (e) Baines, K. M.; Cooke, J. A.; Vittal, J. J. *J. Chem. Soc., Chem. Commun.* **1992**, 1484. (f) Fujdala, K. L.; Gracey, D. W. K.; Wong, E. F.; Baines, K. M. *Can. J. Chem.* **2002**, *80*, 1387. (g) Dixon, C. E.; Netherton, M. R.; Baines, K. M. *J. Am. Chem. Soc.* **1998**, *120*, 10365. (h) Dixon, C. E.; Liu, H. W.; VanderKant, C. M.; Baines, K. M. *Organometallics* **1996**, *15*, 5701.

29. Oláh, J.; Proft, F. D.; Veszprémi, T.; Geerlings, P. *J. Phys. Chem. A.* **2005**, *109*, 1608.

30. The energy of complexation (ΔE_{comp}) was determined by subtracting the total energy of the uncoordinated species from the total energy of the complex.

31. Ruddy, A. Chemistry 4490 Thesis, The University of Western Ontario, **2009**.

32. DFT has been endorsed as an excellent method for predicting bond lengths and bond dissociation energies of NHC complexes of metals. See: Jacobsen, H.; Correa, A.; Poater, A.; Costabile, C.; Cavallo, L. *Coord. Chem. Rev.* **2009**, *253*, 687.

33. Using PBE1PBE/6-311+G(d,p) model chemistry: For R=H, BSSE = 2.3 kJ/mol; R=CH_3, BSSE=3.2 kJ/mol; R=NH_2, BSSE=5.9 kJ/mol; R=OH, BSSE = 8.2 kJ/mol; R = F, BSSE = 6.3 kJ/mol; R = Cl, BSSE = 6.7 kJ/mol.

34. (a) Tiekink, E. R. T. *Rigaku J.,* **2002**, *19*, 14. (b) Steed, J. W. In *Frontiers in Crystal Engineering;* Tiekink, E. R. T., Vittal, J. J., Eds; John Wiley & Sons, Ltd: Chichester, England, **2006**; pp. 68 - 90.

35. Nakafuji, S.; Kobayashi, J.; Kawashima, T. *Angew. Chem., Int. Ed.* **2008**, *47*, 1141.

36. Jafarpour, L.; Stevens, E. D.; Nolan, S. P. *J. Organomet. Chem.* **2000**, *606*, 49.

37. Pangborn, A. B.; Giardello, M. A.; Grubbs, R. H.; Rosen, R. K.; Timmers, F. J. *Organometallics* **1996**, *15*, 1518.

38. Leigh, W. J.; Harrington, C. R.; Vargas-Baca, I. *J. Am. Chem. Soc.* **2004**, *126*, 16105.

39. Kuhn, N.; Kratz, T. *Synthesis* **1993**, 561.

40. Gaussian 03, Revision C.02, Frisch, M. J.; Trucks, G. W.; Schlegel, H. B.; Scuseria, G. E.; Robb, M. A.; Cheeseman, J. R.; Montgomery, Jr., J. A.; Vreven, T.; Kudin, K. N.; Burant, J. C.; Millam, J. M.; Iyengar, S. S.; Tomasi, J.; Barone, V.; Mennucci, B.; Cossi, M.; Scalmani, G.; Rega, N.; Petersson, G. A.; Nakatsuji, H.; Hada, M.; Ehara, M.; Toyota, K.; Fukuda, R.; Hasegawa, J.; Ishida, M.; Nakajima, T.; Honda, Y.; Kitao, O.; Nakai, H.; Klene, M.; Li, X.; Knox, J. E.; Hratchian, H. P.; Cross, J. B.; Bakken, V.; Adamo, C.; Jaramillo, J.; Gomperts, R.; Stratmann, R. E.; Yazyev, O.; Austin, A. J.; Cammi, R.; Pomelli, C.; Ochterski, J. W.; Ayala, P. Y.; Morokuma, K.; Voth, G. A.; Salvador, P.; Dannenberg, J. J.; Zakrzewski, V. G.; Dapprich, S.; Daniels, A. D.; Strain, M. C.; Farkas, O.; Malick, D. K.; Rabuck, A. D.; Raghavachari, K.; Foresman, J. B.; Ortiz, J. V.; Cui, Q.; Baboul, A. G.; Clifford, S.; Cioslowski, J.; Stefanov, B. B.;

Liu, G.; Liashenko, A.; Piskorz, P.; Komaromi, I.; Martin, R. L.; Fox, D. J.; Keith, T.; Al-Laham, M. A.; Peng, C. Y.; Nanayakkara, A.; Challacombe, M.; Gill, P. M. W.; Johnson, B.; Chen, W.; Wong, M. W.; Gonzalez, C.; and Pople, J. A.; Gaussian, Inc., Wallingford CT, **2004.**

41. Otwinowski, Z; Minor, W. In *Methods in Enzymology. Vol. 276: Macromolecular Crystallography, Part A.*; Carter, Jr, C.W., Sweet, R.M., Eds; Academic Press: New York, **1997**; pg 307.

42. Sheldrick, G.M. *Acta Cryst.* **2008**, *A64*, 112.

43. Farrugia, L. J. *J. Appl. Cryst.* **1999**, *32*, 837.

44. Cooper, R. I.; Gould, R. O.; Parsons, S.; Watkin, D. J. *J. Appl. Cryst.* **2002**. *35*, 168.

Chapter 4

Reactivity Studies of N-Heterocyclic Carbene Complexes of Germanium(II)

4.1 Introduction

Simple germylenes are amphoteric because of their unoccupied p-orbital and lone pair of electrons. The addition of electron density to the empty p-orbital, either by a donor ligand or by π donation, reduces the Lewis acidity, while simultaneously increasing the nucleophilicity of the electron lone pair. As such, electronically stabilized germylenes often react primarily through their electron lone pair rather than as a Lewis acid.

The chemistry of intermolecularly stabilized germylenes, with exception of the substitution chemistry of $GeCl_2$·dioxane (**8**), is poorly studied.[1, 2] Since N-heterocyclic carbenes are amongst the strongest known neutral donors[3] they are expected to significantly alter the reactivity of GeR_2 upon complexation. Specifically, NHC-GeR_2 species are anticipated to be more nucleophilic and less electrophilic in comparison with non-coordinated germylenes. Nevertheless, the NHC-GeR_2 complexes retain some Lewis acidity, as demonstrated by the reaction of MeLi with **28** to form Mes_2GeMeH (**31**) (Chapter 2).

In this chapter, the reactivity of three NHC-Ge(II) complexes is examined (Chart 4.1). Compounds **39**, **45**, and **28** were chosen because they are representative of NHC complexes of three different germylenes. **39** is a complex of dichlorogermylene: dihalogermylenes are intrinsically stable and amongst the least reactive GeR_2 compounds. Compound **45** is a complex of a dialkoxygermylene which are intermediate

in their reactivity. Compound **28** is a complex of a highly reactive and transient diarylgermylene.

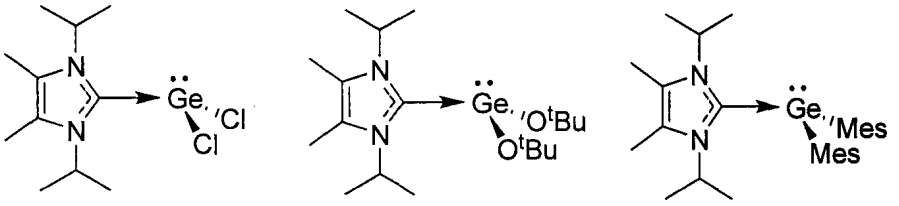

39 **45** **28**

Chart 4.1

Germylenes are valuable building blocks for the synthesis of germanium-containing compounds. Unfortunately, their potential utility is often limited by their non-specific reactivity. The NHC-GeR_2 complexes may act as synthons of GeR_2 while being easier to handle and isolate. Therefore, the reactivity of **39**, **45**, and **28** will be compared to the reactivity of uncoordinated germylenes and the potential of using **39**, **45**, and **28** as synthetic equivalents of GeR_2 will be evaluated.

4.2 Results and Discussion

4.2.1 Reaction with Dimethylbutadiene

2,3-Dimethylbutadiene (DMB) is commonly used as a trapping reagent for transient[4] and stable[5] germylenes since they undergo cycloaddition[6] with DMB to form a germacyclopentene cleanly and in high yield.[1]

Complex **28** acts as a synthetic equivalent of $GeMes_2$: when it was heated with DMB (Chapter 2), germacyclopentene **29** was isolated (Scheme 4.1). It was proposed that, upon heating, uncoordinated $GeMes_2$ (**16**) was released from **28** which then rapidly cyclized with DMB to give **29**. To ascertain the generality of the reaction of DMB with NHC-Ge(II) species, the reactivity of **39** and **45** with DMB was examined.

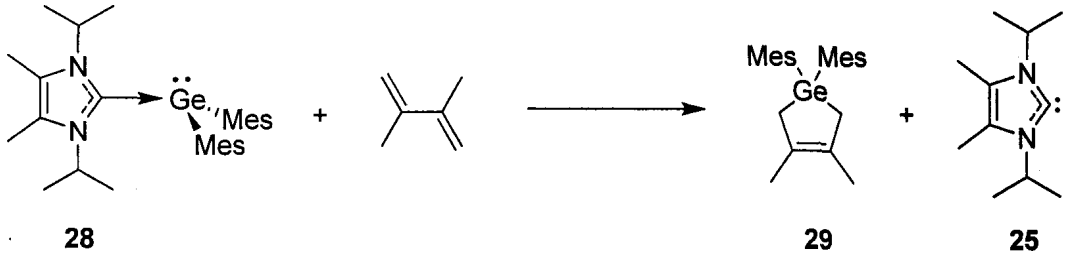

Scheme 4.1

A solution of **39** and DMB did not undergo any observable reaction as determined by ^{1}H NMR spectroscopy, even after prolonged heating and in the presence of excess DMB (Scheme 4.2). In contrast, $GeCl_2$·dioxane (**8**) readily reacts with DMB to form **61** under similar conditions.[7] If it is assumed that for $GeCl_2$ to react with DMB it must be dissociated from any neutral donors, then the difference in reactivity between **8** and **39** towards DMB can be attributed to the much stronger coordination of NHC to $GeCl_2$ compared to 1,4-dioxane. Under these conditions, the dissociation of $GeCl_2$ from the carbene in **39** is apparently not favoured kinetically. The reaction may also not be thermodynamically favorable: $GeCl_2$ may prefer to coordinate with the NHC rather than form a germacyclopentene.

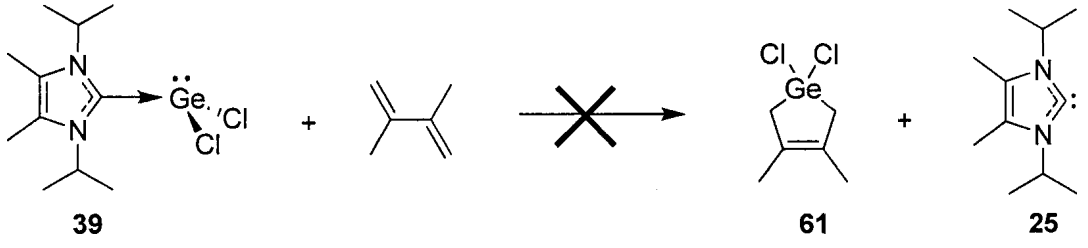

Scheme 4.2

Interestingly, when **61** was added to a solution of the free NHC **25**, complex **62** was isolated from the reaction mixture (Scheme 4.3). The structure of complex **62** consists of a molecule of **61** coordinated by the carbene (Figure 4.1). Given that the germanium centre in **61** has two electron-withdrawing chloride substituents, it is not surprising that

the germanium is able to form a hypercoordinated species.[8] Upon heating a solution of **62** in THF in a sealed tube for 3 days, DMB and **39** were formed as determined by ^{1}H NMR spectroscopy. Thus, the formation of **61** by the reaction between **39** and DMB may not be thermodynamically favourable.

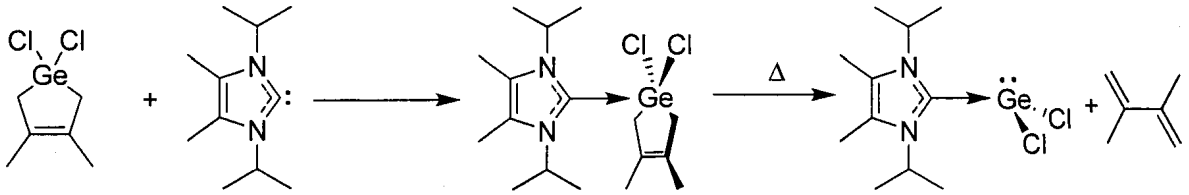

61 **25** **62** **39**

Scheme 4.3

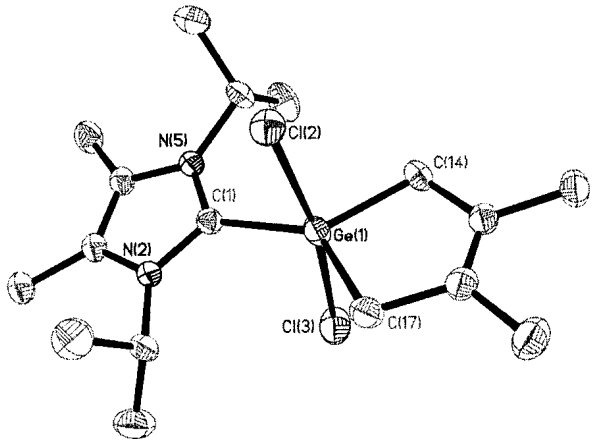

Figure 4.1: Thermal ellipsoid plot (50% probability surface) of **62**. Hydrogen atoms are omitted for clarity. Selected bond lengths (Å) and angles (°): Ge1-C1 = 1.965(2); Ge1-C14 = 1.942(2); Ge1-C17 = 1.943(3); Ge1-Cl2 = 2.4007(7); Ge1-Cl3 = 2.5093(7); Cl2-Ge1-Cl3 = 169.09(3); C14-Ge1-C17 = 96.87(11); C1-Ge-Cl2 = 87.16(7); C1-Ge-Cl3 = 82.06(7).

Heating a solution of complex **45** and excess DMB at 80 °C for 18 hr resulted in the formation of **63** and free carbene **25** (Scheme 4.4).[9] Unlike **39**, a coordination complex

between the NHC and **45** was not observed and heating **63** in the presence of free NHC did not result in any retrocyclization.

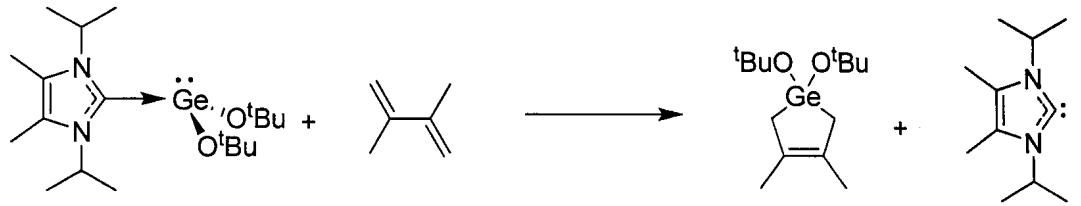

45 **63** **25**

Scheme 4.4

Based on the results illustrated in Schemes 4.1 – 4.4, the favorability of the reaction of a NHC-GeR_2 complex with DMB appears to be strongly substituent dependent: both the Mes and O^{t}Bu substituted compounds form the corresponding germacyclopentene, while the germanium dichloride complex favoured coordination to NHC **25**. Using the same model chemistry employed in Chapter 3 (PBE1PBE/6-311+G(d,p)), the energetics of a model system were examined to gain further insight into the reaction of butadiene with a series of NHC-GeR_2 complexes.[10]

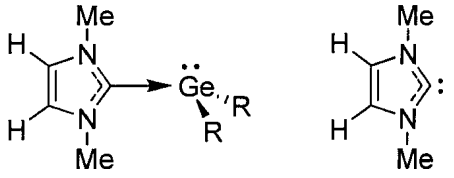

54 R = H
55 R = OH
56 R = NH_2
57 R = CH_3
58 R = F
59 R = Cl

60

Chart 4.2

To reduce the complexity of the systems under study, a series of simplified carbene complexes (the same used in Chapter 3.2.2) were employed and butadiene was used in place of DMB (Chart 4.2). The energetics of the reactions of the NHC complexes of

GeR_2 with butadiene were examined by comparing the three systems shown in Chart 4.3. The total energy of System A, the $NHCGeR_2$ complex plus butadiene, was used as the reference point. System B, modeled after **62** (Scheme 4.3, Figure 4.1), consists of a complex of the NHC with the germacyclopentene. System C is the germacyclopentene with free carbene.

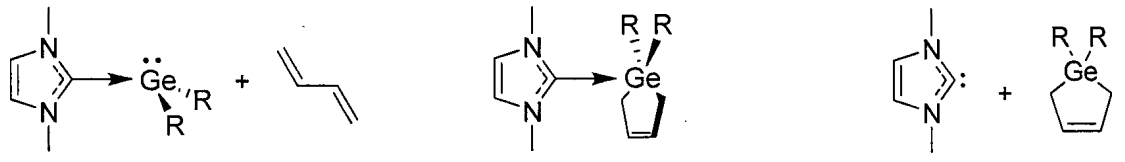

System A **System B** **System C**

Chart 4.3

Table 4.1: Calculated relative energies for the reaction of model NHC-GeR_2 complexes with butadiene.

Substitution on germanium	Relative ΔG° for System A (kJ/mol)	Relative ΔG° for System B (kJ/mol)	Relative ΔG° for System C (kJ/mol)
R = F	0	5.6	30.8
R = Cl	0	8.6	25.0
R = OH	0	12.3	-13.0
R = H	0	Not stable	-30.8
$R = NH_2$	0	Not stable	-44.3
R = Me	0	Not stable	-88.9

The results are tabulated in Table 4.1 and reveal a number of interesting trends. With four of the six substitution patterns (R = OH, H, NH_2 or Me), System C is the most stable. However, when the substituent on germanium is either fluorine or chlorine, System A is energetically preferred. System B is stable only when electronegative substituents (R = F, Cl or OH) are on germanium.[8] With less electron withdrawing substituents on germanium (R = H, NH_2 or Me), System B is not stable and, upon

geometry optimization, separates into uncoordinated carbene and germacyclopentene (System C).

The results from the computational analysis reveal that when the germanium is halogenated, the carbene complex with free butadiene (System A) is thermodynamically favoured over the germacyclopentene and carbene (System C). The computational results are consistent with the experimental results. The formation of a dichlorogermacyclopentene was not observed in the reaction between **39** and DMB; the reaction of dichlorogermacyclopentene (**61**) with NHC **25** produced the hypercoordinate **62**. Based on the computational results, complex **62** is expected to be thermodynamically unstable towards the release of butadiene. Indeed, **62** dissociates upon heating by releasing DMB (Scheme 4.3) and forming **39**.

The computations indicate that System B may be experimentally accessible when R = OH; however, in the R = O^{t}Bu system, the corresponding pentacoordinated complex was not observed (Scheme 4.4). Presumably, the increased steric bulk of the O^{t}Bu substituent compared to the OH group disfavours the formation of a pentacoordinate germanium species.

Both the experimental and computational results show that a dihalogenated germylene prefers to be coordinated to a NHC, rather than form an adduct with butadiene, whereas the dialkoxy- and diorgano-germylenes prefer the formation of a germacyclopentene. The origin of this contrasting behavior between the halogenated and non-halogenated germylenes is not immediately obvious. A possible explanation could be that the NHC-germanium complexation energy was found to be more favourable when R = F or Cl compared to when R = Me, NH_2 or OH (See Chapter 3, Table 3.4 or Table

4.2).[11] However, this rationalization fails to explain the dihydrogermylene system which prefers to bond with DMB even though complexation with the NHC is more exothermic than what was calculated for the halogenated systems.

The energetics of the reaction between butadiene and the uncoordinated germylenes to form germacyclopentenes were calculated at the PBE1PBE/6-311+G(d,p) level (Scheme 4.5, Table 4.2). The free energy of the reaction is exothermic and strongly substituent dependent (Table 4.2). The origin of the differences between the different germylenes in Table 4.2 appears to be related to the relative intrinsic stability of the germylenes. The hydroxyl, amino, and halogen substituted germylenes are relatively stable species and form thermodynamically less stable complexes with butadiene (See Chapter 1.1.1). Conversely, the cyclization of dihydro- and dimethylgermylene with butadiene is much more exothermic.[12]

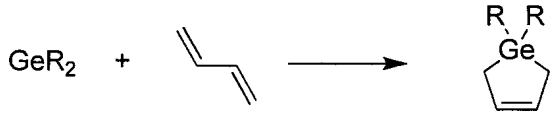

Scheme 4.5

Table 4.2: Calculated energetics for the reaction of GeR_2 with butadiene; calculated ΔG° of complexation with NHC **60**.

Substitution on Germanium	ΔG° of Cyclization with Butadiene (kJ/mol)	ΔG° of Complexation with NHC (kJ/mol)
H	-183.4	-150.3
F	-67.2	-91.8
Cl	-81.5	-99.7
Me	-171.0	-82.2
OH	-72.8	-54.3
NH_2	-53.6	-3.4

The free energy of the reaction between butadiene and NHC complexes of GeR_2 appears to be governed by two competing factors: the relative stability of the NHC-GeR_2

complexes versus the relative stability of the germacyclopentenes. Due to the increased Lewis acidity of difluoro- and dichlorogermylene, coordination of a strong donor is energetically preferred. The free energy of the reaction of GeH_2 and $GeMe_2$ is greater with butadiene than with the NHC, although both ligands form strong complexes. Finally, the dihydroxy- and diamino-substituted germylenes form relatively weak cycloadducts with butadiene, but even weaker complexes with the NHC.

In summary, both **45** and **28** react with DMB in a manner similar to what would be expected for the corresponding uncoordinated germylene. On the contrary, and unlike $GeCl_2$, **39** does not react with DMB as the reaction appears to be thermodynamically not favoured.

4.2.2 Reactions with an Orthoquinone

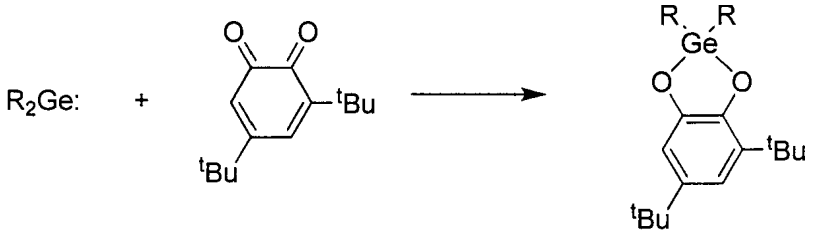

Scheme 4.6

As with DMB, 3,5-di-^{t}butyl-orthoquinone reacts rapidly and in high yield with germylenes, and therefore, can be used as a trapping reagent for reactive divalent germanium compounds (Scheme 4.6).[13] Due to the formation of two germanium-oxygen bonds and the aromatization of the quinone (Scheme 4.6), the reaction of 3,5-di-^{t}butyl-orthoquinone with complexes **39**, **45**, and **28** is expected to be more thermodynamically favourable compared to the analogous reactions with DMB.

Addition of the red 3,5-di-^{t}butyl-orthoquinone to a colourless solution of **39** resulted in rapid discolouration of the quinone (Scheme 4.7). A white solid was isolated and was identified as **64** by X-ray crystallography. Figure 4.2 shows the solid state structure of the cycloadduct: notably, the NHC remains coordinated to the germanium.[8]

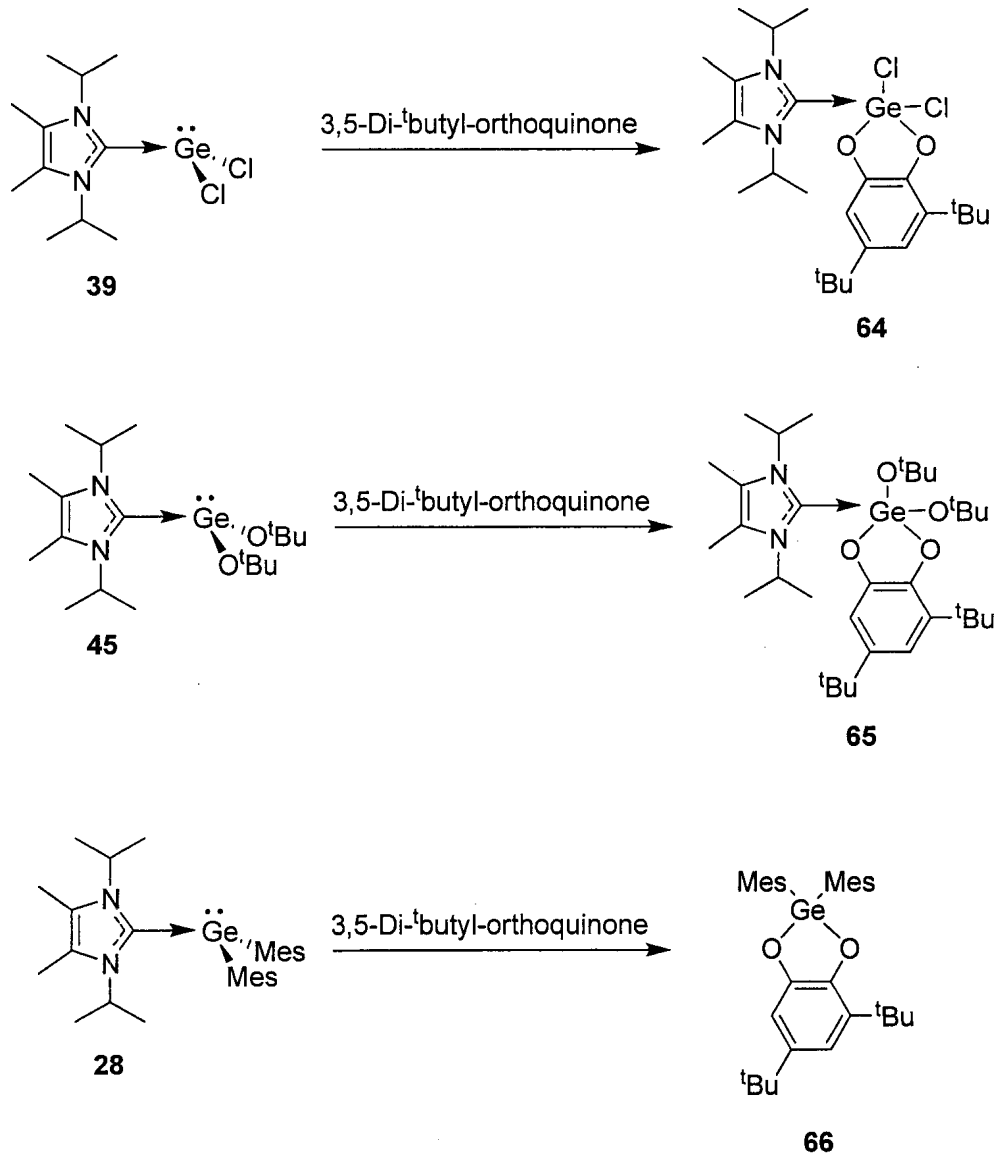

Scheme 4.7

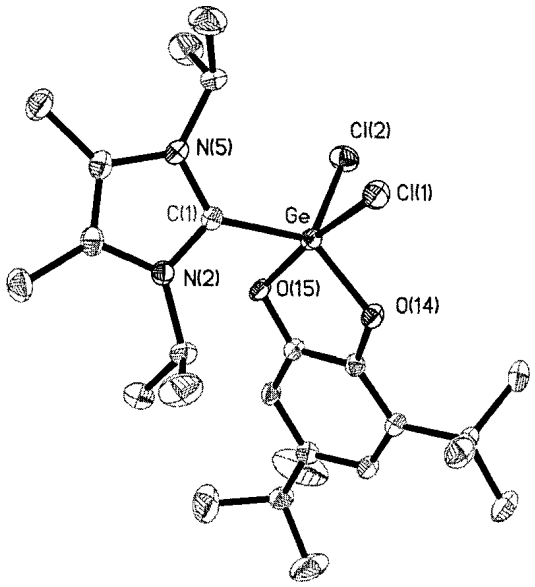

Figure 4.2: Thermal ellipsoid plot (50% probability surface) of **64**. Hydrogen atoms are omitted for clarity. Selected bond lengths (Å) and angles (°): C1-Ge = 1.995(2); Ge-Cl1 = 2.2738(10); Ge-Cl2 = 2.1541(9); Ge-O14 = 1.8136(16); Ge-O15 = 1.8906(17); O14-Ge-O15 = 86.86(7); O14-Ge-C1 = 132.33(8); O15-Ge-C1 = 87.42(8); O14-Ge-Cl2 = 113.95(6); O15-Ge-Cl2 = 94.33(6); C1-Ge-Cl2 = 113.66(7); O14-Ge-Cl1 = 85.58(6); O15-Ge-Cl1 = 168.48(5); C1-Ge-Cl1 = 91.25(7).

The reaction of **45** and 3,5-di-^{t}butyl-orthoquinone behaved in exactly the same manner as with **39** (Scheme 4.7). A white solid was isolated and analysis by ^{1}H NMR spectroscopy confirmed the formation of a 1:1 adduct of the quinone with the NHC coordinated germylene. Attempts to grow crystals of **65** suitable for single crystal X-ray diffraction were not successful.

The addition of 3,5-di-^{t}butyl-orthoquinone to a yellow solution of **28** resulted in the formation of a deep-blue reaction mixture. The ^{1}H NMR spectrum of the solution was complex, but clearly showed the presence of **66** (Scheme 4.7), which was subsequently

isolated and characterized.[14] Signals that could be clearly attributed to an NHC moiety, either coordinated or uncoordinated, were not visible in the ^{1}H NMR spectrum of the crude reaction mixture. Under the reaction conditions, the NHC appears to be reacting with the quinone; however, attempts to determine the fate of the NHC failed. The direct reaction of the NHC with 3,5-di-^{t}butyl-orthoquinone also resulted in a visually similar deep blue solution. The ^{1}H NMR spectrum of the solution exhibited a multitude of signals indicating a complex mixture of products. Efforts to identify any of the products derived from the reaction between the carbene and 3,5-di-^{t}butyl-orthoquinone were not successful. Possibly, the quinone is abstracting an electron from the NHC, leading to the formation of a radical anion/cation pair which then undergoes further chemistry. The formation of a NHC radical cation upon exposure of **25** to oxidants has been reported previously.[15]

In summary, 3,5-di-^{t}butyl-orthoquinone reacts readily with **39**, **45**, and **28** to give a cycloadduct in a manner similar to that observed with the corresponding germylenes. The rapid rate at which the orthoquinone reacts with the NHC complexes suggests that 3,5-di-^{t}butyl-orthoquinone is able to cyclize directly with germanium while it is still complexed to the NHC. This is in contrast to DMB which reacted slowly with **45** and **28**, only after extended periods of heating.

4.2.3 Reactions with Methyl Iodide

The reaction of germylenes with methyl iodide has been reported and usually results in the insertion of the germylene into the carbon-iodine bond and the formation of tetravalent germanium.[16] If the germylene is stabilized by an intramolecular donor,

nucleophilic attack of the germylene on MeI can result in the formation of a cationic germanium complex.[17] Since intermolecularly stabilized Ge(II) are less well studied, reports of their reactivity towards MeI or related electrophiles are limited.[18] In Chapter 2, it was demonstrated that the lone pair of electrons on Ge is chemically active by coordination of **28** to BH_3. The reactions of methyl iodide with **39**, **45**, and **28** are now presented.

Addition of an excess of MeI to a solution of **39** in C_6H_6 resulted in the appearance of several new signals in the ^1H NMR spectrum consistent with the formation of methylated adducts of **39**. ESI-MS (+ mode) of the reaction mixture showed signals attributable to the expected adduct, as well as signals attributable to species in which one or both of the chlorides were replaced with iodides (Scheme 4.8). Also evident in both the mass spectrograph and the ^1H NMR spectra were signals attributable to the methylated NHC cation, **25-Me$^+$**.[19] The origin of **25-Me$^+$** is not entirely clear, but could arise from the elimination of GeI_2 from **67$^+$**.

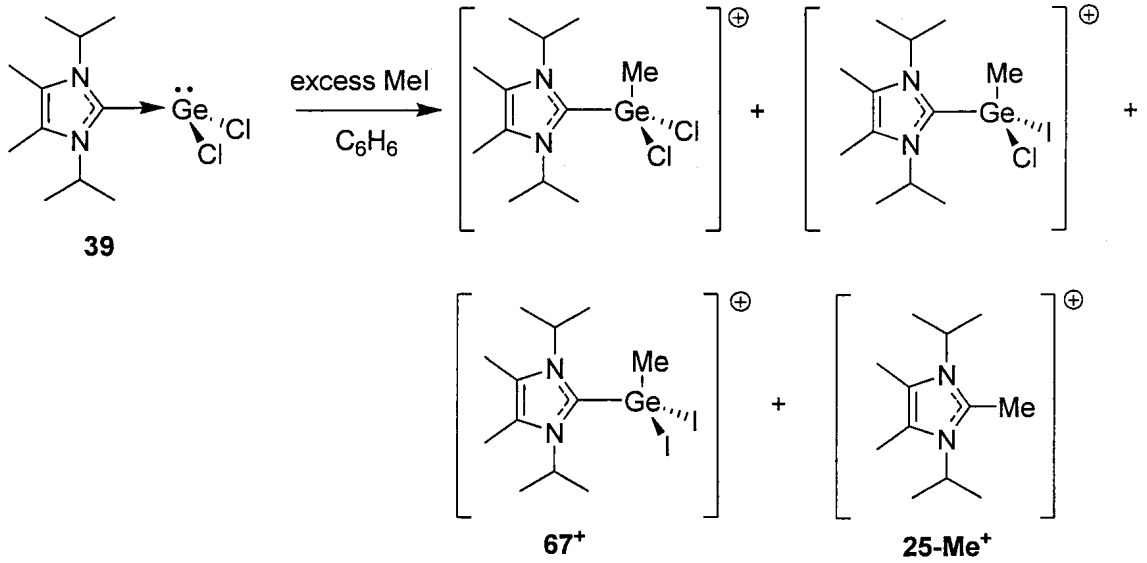

Scheme 4.8

Although separation of the reaction products was not successful, **67**[I] could also be formed by the reaction of **42** with excess MeI (Scheme 4.9). Again, the formation of **25-Me**[I] wasobserved. Pale green crystals of **67**[I] were mechanically separated by inspection under an optical microscope. The structure of **67**[I] was confirmed by single crystal X-ray diffraction (Figure 4.3); as expected, a methyl group occupies the empty coordination site that was evident in the structure of **42**. The germanium complex is cationic; the cation is separated from the iodide counter ion with the closest Ge – I approach being 4.305(1) Å . The Ge-C1 and Ge-I bond lengths are contracted in comparison to those in **42** (see Table 3.1 and Figure 4.3), which can be understood given the conversion of the electron lone pair on germanium to a bonding electron pair and the cationic charge.

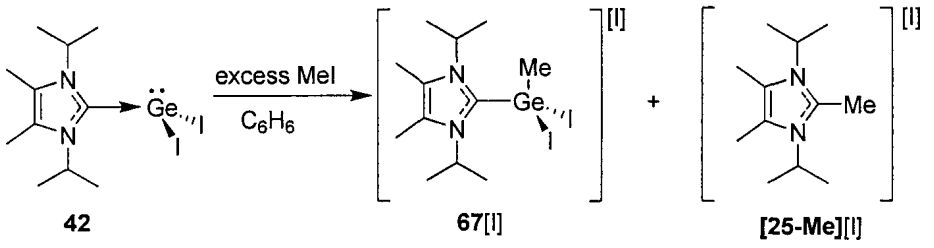

42 **67**[I] **[25-Me][I]**

Scheme 4.9

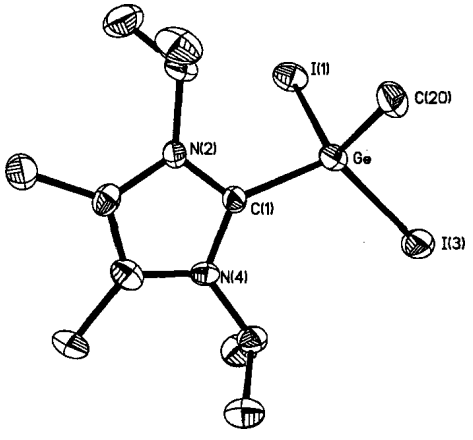

Figure 4.3: Thermal ellipsoid plot (50% probability surface) of 67^{+}. Hydrogen atoms and iodide counter anions are omitted for clarity. Selected bond lengths (Å) and angles

(°): Ge-C1 = 1.994(9); Ge-C20 = 1.930(8); Ge-I1 = 2.5405(10), Ge-I2 = 2.5299(13); C20-Ge-C1 = 112.9(4); C20-Ge-I2 = 108.1(3); C1-Ge-I2 = 118.2(3); C20-Ge-I1 = 111.3(3); C1-Ge-I1 = 101.3(2); I2-Ge-I1 = 104.57(4).

Complexes **45** and **28** both react rapidly with methyl iodide (Scheme 4.10). In each case, a white powder formed upon addition of a stoichiometric amount of methyl iodide to a solution of either **45** or **28**. The precipitates were identified as **68**[I] and **69**[I] respectively, by ^{1}H NMR spectroscopy, mass spectrometry and single crystal X-ray diffraction (Figures 4.4 and 4.5).

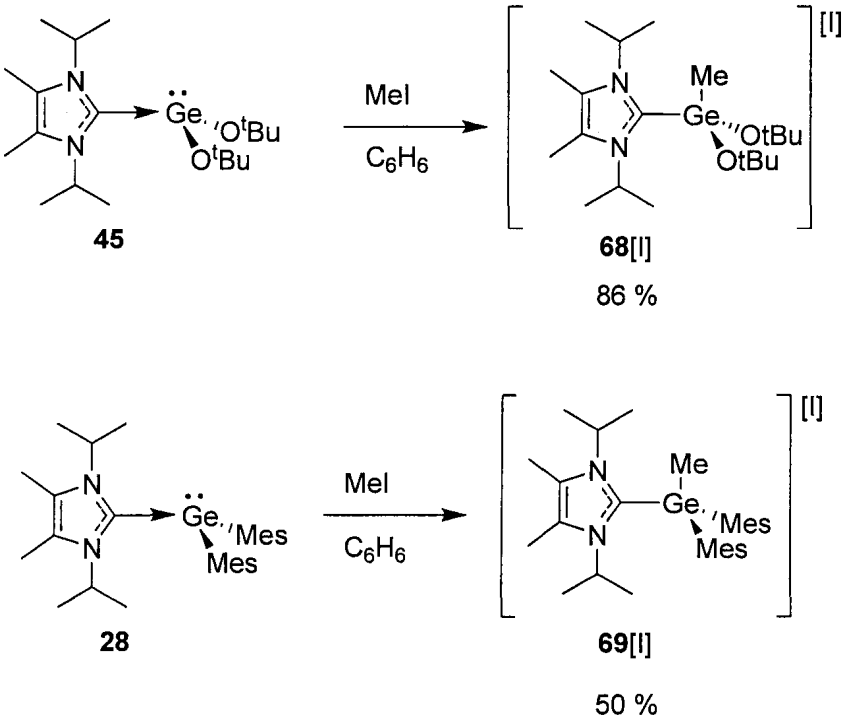

Scheme 4.10

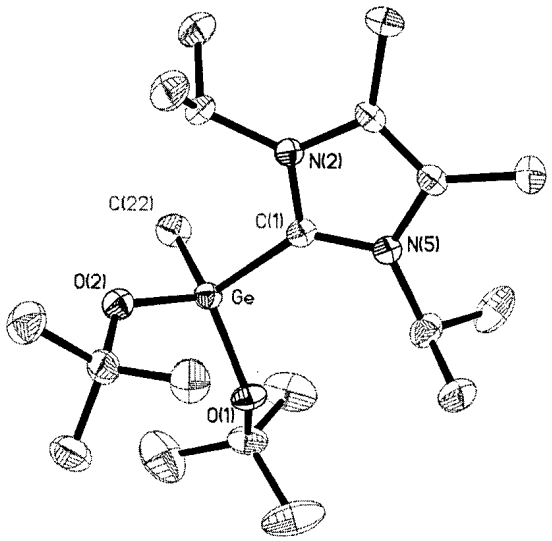

Figure 4.4: Thermal ellipsoid plot (50% probability surface) of $\mathbf{68}^{+}$. Hydrogen atoms and iodide counter anions are omitted for clarity. Selected bond lengths (Å) and angles (°): Ge-C1 = 1.998(5); Ge-O1 = 1.764(3); Ge-O2 = 1.762(4); Ge-C22 = 1.924(5); O2-Ge-O1 = 109.18(18); O2-Ge-C22 = 106.8(2); O1-Ge-C22 = 119.7(2); O2-Ge-C1 = 106.71(19); O1-Ge-C1 = 105.46(19); C22 – Ge - C1 108.3(2).

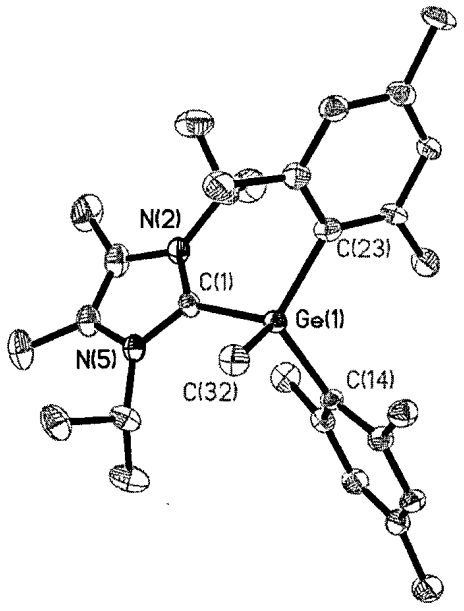

Figure 4.5: Thermal ellipsoid plot (50% probability surface) of $\mathbf{69}^{+}$. Hydrogen atoms and iodide counter anions are omitted for clarity. Selected bond lengths (Å) and angles

(°): Ge1 - C1 = 2.014(5); Ge1 - C32 = 1.962(5); Ge1 - C23 = 1.971(5); Ge1- C14 = 1.977(5); C32 - Ge1 - C23 = 109.4(2); C32 - Ge1 - C14 = 107.0(2); C23 - Ge1 - C14 = 116.4(2); C32 - Ge1 - C1 = 105.3(2); C23 - Ge1 - C1 = 110.0(2).

Qualitatively, compounds **39**, **45**, and **28** react at noticeably different rates with methyl iodide. In solution, a precipitate (**69**[I]) was observed instantly upon addition of MeI to a solution of **28**. The reaction of MeI and **45** was also quick, with precipitate formation occurring within a couple of minutes. Finally, **39** reacted very slowly with methyl iodide. The reaction took days to go to completion even in the presence of excess MeI; furthermore, the chemistry of **39** and MeI was complicated by halogen exchanges (Scheme 4.8). Examination of the calculated energies of the HOMOs of model compounds (Table 4.3) shows a good correlation between the energy of the HOMO and the reactivity of the related experimental systems towards MeI.

Table 4.3: Calculated energy of the HOMO of model compounds **55**, **57**, and **59** and the qualitative reaction rate of related experimental systems.

Substitution of model compound	Equivalent Experimental Compound	Qualitative Reaction rate with MeI	HOMO Energy (eV) of model compound (Lone Pair on Ge)
59 (R = Cl)	**39** (R = Cl)	Slow	-6.21
55 (R = OH)	**45** (R = O^{t}Bu)	Fast	-5.23
57 (R = CH_3)	**28** (R = Mes)[20]	Fastest	-4.41

Complex **69**[I] reacts rapidly with $CDCl_3$, resulting in dissociation of the carbene moiety and the quantitative formation of **70**,[21] which was subsequently characterized (Scheme 4.11).[22] Overall, the methylation of **28** followed by chlorination to give **70** is the synthetic equivalent of the insertion of $GeMes_2$ into MeCl, an otherwise difficult transformation to perform with a transient germylene.

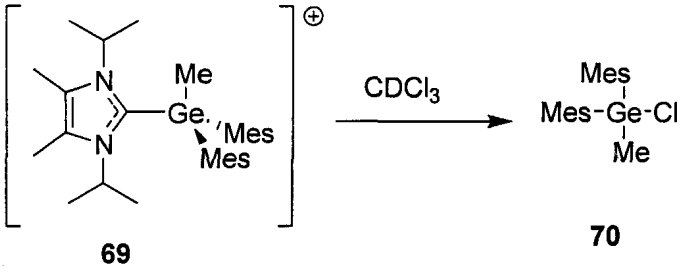

69 70

Scheme 4.11

The reaction of **28** with other alkyl halides was also examined. Ethyl iodide reacts with **28**, forming the expected ethylated species **71**[I]. Cation $\mathbf{71}^{+}$ also underwent a similar chlorination reaction to give **72** (Scheme 4.12). Secondary and tertiary alkyl iodides did not react cleanly with **28**, nor did primary bromides or chlorides. Complex **45** is unreactive towards more highly substituted alkyl iodides at room temperature. Since substituted alkyl iodides (beyond ethyl iodide) appear to be unreactive, the synthetic scope of this reaction is limited.

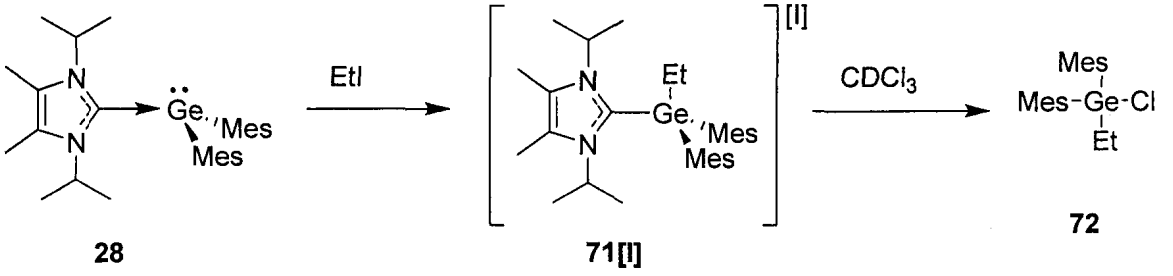

28 71[I] 72

Scheme 4.12

4.2.4 Reaction with Pivalic Acid

Germylenes react with a carboxylic acid by insertion into the oxygen-hydrogen bond resulting in the generation of a germyl ester.[23] To determine if NHC coordinated germylenes will behave in the same manner, the reactivity of **39**, **45**, and **28** towards a carboxylic acid was investigated.

Addition of pivalic acid to solutions of **39** and **45** formed complex mixtures as ascertained by ^{1}H NMR spectroscopy. Attempts to identify any of the products were not successful. In contrast, **28** reacted cleanly with pivalic acid to form two different germanium containing compounds: **73** and **74** (Scheme 4.13) in addition to the conjugate acid of the carbene (**35**). Compound **73** is the same compound expected from the reaction of pivalic acid with free dimesitylgermylene (**16**); compound **74** was not anticipated as a product and the mechanism for its formation is not clear.[24]

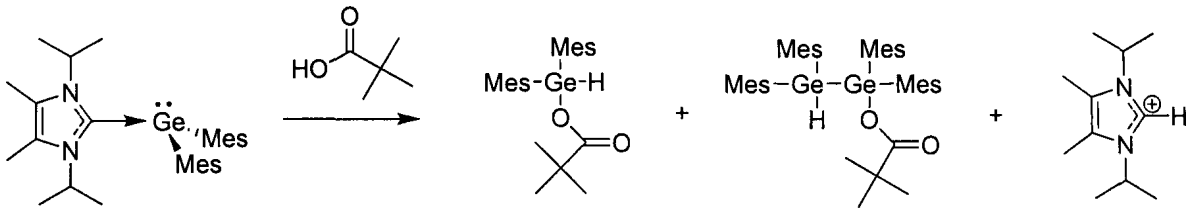

Scheme 4.13

The ratio of **73** to **74** varied with the stoichometry used in the reaction. Compound **73** is formed exclusively when **28** was added dropwise to a solution containing an excess of pivalic acid. Conversely, if an equivalent of pivalic acid is slowly added to a solution of **28**, **74** is the only germanium containing compound detected by ^{1}H NMR spectroscopy.

Based on these observations, it appears as if compound **74** is formed by the reaction of **73** with **28**. Indeed, when **73** and **28** are combined in solution, both **74** and **25** were detected as products by ^{1}H NMR spectroscopy (Scheme 4.14).

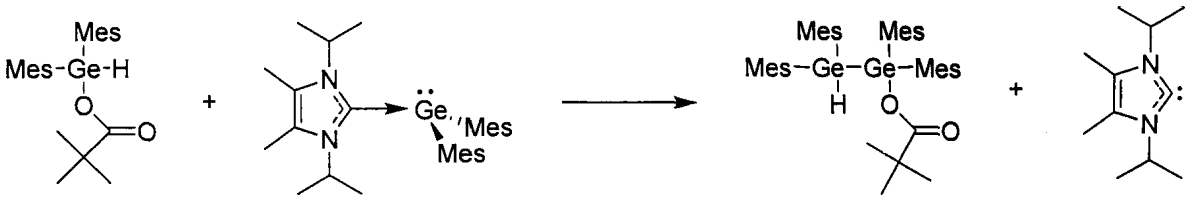

73 **28** **74** **25**

Scheme 4.14

Previous work has demonstrated that the mechanism for the addition of transient organogermylenes to carboxylic acids proceeds initially by complexation of the carbonyl oxygen to the germanium followed by proton transfer.[23] However, this mechanism is probably not operative in the formation of **73** since the formally empty p-orbital on the NHC-GeR_2 complex is occupied by the carbene, and therefore, the Lewis acidity is greatly diminished. Complex **28** is a strong Lewis base (see section 2.2.4 and 4.2.3), and thus the formation of **73** through initial proton transfer followed by displacement of the carbene by pivalate is proposed.

4.2.5 Reaction with Benzophenone

The stable germylene, $Ge[CH(SiMe_3)_2]_2$ (**14**) reacts rapidly with phenones at room temperature to yield conjugated trienes.[25] Therefore, the reactivity of **39**, **45**, and **28** with benzophenone was examined to see if the NHC base stabilized germylenes react in the same manner as **14**.

While neither **39** nor **45** showed any reactivity towards benzophenone even at elevated temperatures, complex **28** was found to react slowly with benzophenone over 24 hr at 100 °C to form **75**, which was isolated as a colourless powder after chromatographic separation (Scheme 4.15). Integration of the ^1H NMR spectrum of **75** clearly showed the

formation of a 1:1 adduct of the Mes_2Ge moiety with benzophenone. Mass spectrometric data were also consistent with the formation of a 1:1 adduct.

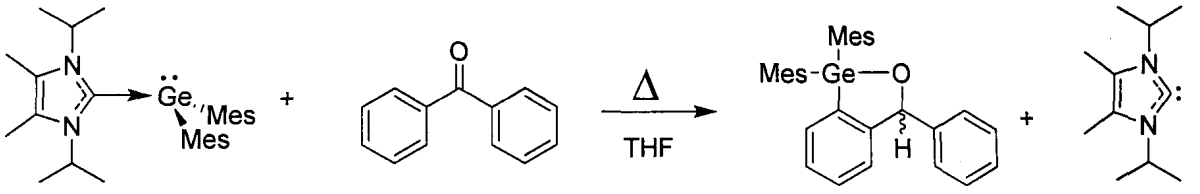

28 **75** **25**

Scheme 4.15

The structure of **75** was determined by 1D and 2D NMR techniques. In the ^1H and ^{13}C NMR spectrum of **75**, signals attributable to two different mesityl and two different phenyl moieties were detected. The ^1H-^{13}C gHSQC spectrum of **75** was consistent with a 1,2-substitution pattern on one of the aromatic rings originating from benzophenone. The other phenone phenyl ring remained monosubstituted. The presence of the doubly benzylic proton was confirmed by gCOSY and ^1H-^{13}C gHMBC spectroscopy.

Based on experimental evidence, the reaction of $Ge[CH(SiMe_3)_2]_2$ (**14**) with phenones was proposed to occur via a concerted [4 + 2] cycloaddition.[25] A similar mechanism is likely operative in the formation of **75**. As was previously proposed, **28** dissociates to **16** and **25** (Scheme 4.16) at elevated temperature. Dimesitylgermylene (**16**) can then react with benzophenone, presumably via [4+2] cycloaddition. Subsequent rearomatization of the ring by a hydrogen shift results in the formation of **75**. Attempts to observe the postulated triene intermediate by ^1H NMR spectroscopy were unsuccessful; the [1,3] hydrogen shift is most likely catalyzed by the NHC **25**, a strong base.[26] The reactions of the related R_2Si with benzophenone have also been studied; the formation of both conjugated trienes ($R= C_5Me_5$)[27] and rearomatized products ($R = NR'_2$ or $R = Me$)[28, 29, 30] have been reported.

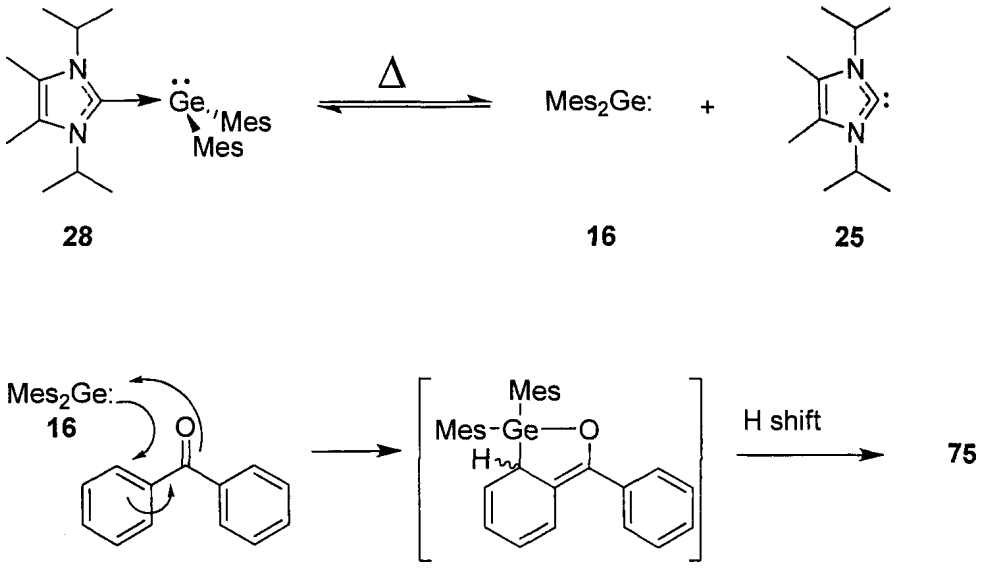

Scheme 4.16

4.2.6 Reactions that Did Not Proceed or Resulted in Intractable Mixtures

In addition to the chemistry described in sections 4.2.1 – 4.2.5, the reactions of **39**, **45**, and **28** with a number of additional reagents were explored. The results are summarized in Table 4.4. Essentially, **39** and **45** were found to be unreactive towards many reagents under the reaction conditions examined. The NHC complex **28** was found to react with a wider array of reagents; however, the product mixtures were often complex. Typically, the ^{1}H NMR spectra of the crude reaction mixtures displayed either broad peaks indicative of the formation of polymeric material (benzaldehyde, P_4) or a large number of peaks suggesting a multitude of products. Attempts to separate the products through selective crystallization, selective precipitation, or chromatography were not successful.

One of the contributing factors that may be leading to the complicated reaction mixtures is that NHC **25** can be released from germanium. Since NHCs are versatile

organic catalysts for a wide range of reactions, the presence of free NHC **25** may lead to undesirable side reactions.[31]

Table 4.4 Summary of the outcome of reactions between $NHCGeR_2$ and various reagents

Reagent	**39**	**45**	**28**
TEMPO[32]	N/R[a]	N/R[a]	Decomposition[b,c]
Benzaldehyde[33]	N/R[a]	N/R[a]	Decomposition[b,c]
Bis(trimethylsilyl) acetylene	N/R[a]	N/R[a]	N/R[a]
Phenylacetylene[34]	N/R[a]	N/R[a]	Decomposition[a]
Triethylsilane[1]	N/R[a]	N/R[a]	N/R[a]
P_4[35]	N/R[a]	N/R[a]	Decomposition[b,c]
C-H activation with phenyl iodide[36]	N/R[a]	N/R[a]	N/R[a]

a) reaction performed at 70 °C in THF; b) attempted at room temperature in THF; c) attempted at -30 °C.

4.3 Conclusions

In summary, the chemistry of **39**, **45**, and **28** towards a variety of reagents was explored. In some cases, the NHC-GeR_2 complexes formed reaction products similar to those of uncoordinated germylenes while in other situations, the NHC-GeR_2 complexes behaved significantly different to uncoordinated germylenes.

The dimesityl **28** and the di^{t}butoxy germylene **45** NHC complexes reacted with DMB to give germacyclopentenes **29** and **63** in a manner identical to uncoordinated germylenes. The dichloro derivative **39** did not react with DMB. DFT calculations showed that dichlorogermylene thermodynamically prefers to be coordinated by the NHC than the diene.

3,5-Di-^{t}butyl-orthoquinone was found to react quickly with **39**, **45**, and **28** to produce a cycloadduct. The qualitatively fast reaction of the quinone with **39**, **45**, and **28** suggests

that the reaction occurs while the NHC remains coordinated to the germanium; in the case of **39** and **45**, the NHC ligand remained coordinated to germanium even after cycloaddition. With the mesityl substituted system, **28**, the NHC was released from the germanium upon reaction with the orthoquinone. The uncoordinated NHC reacted rapidly with available 3,5-di-^{t}butyl-orthoquinone producing a complex reaction mixture.

Like intramolecularly stabilized germylenes, complexes **39**, **45**, and **28** acted as nucleophiles towards methyl iodide by quaternizing the germanium and forming cationic complexes. The qualitative rate of the reaction was inversely proportional to the energy level of the HOMO of model germanium compounds. The alkylation reaction is limited to unhindered alkyl iodides as substrates. Alkyl chlorides and alkyl bromides were found to be unreactive towards **39**, **45**, and **28**. Treatment of **69**[I] or **71**[I] with $CDCl_3$ chlorinated the germanium to give **70** and **72**, respectively.

Pivalic acid formed a complex product mixture upon addition with **39** and **45.** In the mesityl system **28**, two products were formed and subsequently isolated and characterized. The expected germylene/pivalic acid adduct **73** was isolated, along with the unexpected **74** which can also be formed by the addition of **28** to **73**. The formation of either **73** or **74** can be favoured by manipulation of the reaction conditions.

Benzophenone was found to be unreactive with both **39** and **45** under the reaction conditions examined. Upon prolonged heating, **28** reacted with benzophenone to give **75** which likely arises from a [4+2] cycloaddition between dimesitylgermylene (**16**) and benzophenone, followed by a hydrogen shift. The reactivity of **28** towards benzophenone is similar to what was reported for uncoordinated germylenes and silylenes.

The reactivity of several additional reagents towards **39**, **45**, and **28** was examined. In general, **39** and **45** were found to be unreactive. The mesityl-substituted **28** did react in some cases, but the identities of the products were not determined because of the complexity of the reaction mixtures.

In general, the substituent effects on the reactivity of uncoordinated germylenes are similar to those observed for the NHC germylene complexes. As a result of the intrinsic stability of the corresponding dichlorogermylene and a HOMO stabilized by the electronegative chlorines on the germanium centre, **39** was the least reactive of the complexes. Compound **28** was the most reactive, likely because of the inherent instability of the related uncoordinated germylene **16** and the higher energy of its HOMO as a result of having less electronegative carbon substituents on the germanium centre. The reactivity of the O^{t}Bu substituted **45** was intermediate between **39** and **28**.

After examining the reactivity of **39**, **45**, and **28**, and comparing them to the reactivity of the uncomplexed GeR_2 compounds, the possibility of using NHC-GeR_2 as synthons for GeR_2 appears to be situation specific. The release of carbene **25** is a concern given the strongly basic nature of the NHC which may lead to undesired side reactions.

4.4 Experimental

Reactions were performed under an inert atmosphere of nitrogen using standard techniques. Solvents were purified according to literature procedures[37] and stored over 4 Å molecular sieves under N_2. All NMR spectra were acquired using C_6D_6, THF-d_8 or CD_3CN as the solvent. ^{1}H NMR spectra were referenced to residual C_6D_5H (7.15 ppm), residual CD_2HCN (1.94 ppm) or the upfield THF-d_7 (3.58 ppm). Melting points were

determined under a N_2 atmosphere and are uncorrected. FT-Raman spectra were acquired on bulk samples sealed in a melting point tube under nitrogen. All chemicals were purchased from commercial suppliers. Pivalic acid was dried prior to use by first dissolving it in THF and storing over 4 Å molecular sieves under N_2. Elemental analyses were performed at Guelph Chemical Laboratories, Guelph, Ontario, Canada.

4.4.1 Attempted Reaction of 39 with DMB

In a screw cap vial filled with THF (2 mL) was added **39** (0.05 g, 0.155 mmol) and DMB (0.113 mL, 1 mmol). The reaction mixture was stirred for 18 hr at room temperature. Analysis of an aliquot by ^{1}H NMR spectroscopy showed that no reaction had occurred. The screw cap vial was sealed and heated to 100 °C for 3 days after which analysis of an aliquot by ^{1}H NMR spectroscopy showed no reaction.

4.4.2 Synthesis of 62

To a solution of **61** (0.1g, 0.44 mmol) in C_6H_6 (3 mL) was added **25** (0.08 g, 0.44 mmol). The solution was stirred for 10 min. Hexanes (10 mL) was added to induce the formation of a white precipitate. The precipitate was identified as **62** (0.14 g, 78 %). Crystals suitable for single crystal X-ray diffraction were grown by the slow diffusion of pentane into a concentrated solution of **62** in C_6H_6. M.P. 136-142 °C. ^{1}H NMR (C_6D_6): 1.28 (d, $^3J_{HH}$ = 7 Hz, 12 H), 1.36 (s, 6 H), 1.87 (s, 6 H), 2.97 (s, 4 H), 5.13 (sept, $^3J_{HH}$ = 7 Hz, 2 H). FT-Raman (cm^{-1}): 137 (m), 161 (w), 250 (m), 460 (w), 526 (w), 581 (w), 695 (s), 780 (w), 891 (w), 1166 (w), 1305 (w), 1394 (m), 1447 (m), 1625 (m), 2915 (s), 2944

(s), 2984 (s). Anal. Calcd for $C_{17}H_{31}Cl_2GeN_2$: C, 50.17; N, 6.88; H, 7.68. Found: C, 49.79; N, 6.99; H, 7.86.

4.4.3 Thermolysis of 62

A solution of **62** (0.02g, 0.11 mmol) dissolved in C_6H_6 (5 mL) was heated in a sealed screw cap bottle for 3 days. Analysis of an aliquot by ^{1}H NMR spectroscopy showed the quantitative formation of **39** and DMB.

4.4.4 Reaction of 45 with DMB

To a solution of **45** (0.05 g, 0.13 mmol) in THF (2 mL) was added excess 2,3-dimethylbutadiene (1 mL, 8.8 mmol). The reaction mixture was placed in a sealed tube and heated to 70 °C for 4 days. Analysis of an aliquot by ^{1}H NMR spectroscopy showed the quantitative formation of **63** and **25**.

4.4.5 Synthesis of 63

To a solution of **61** (0.1 g, 0.44 mmol) dissolved in THF (3 mL) was added KO^{t}Bu (0.1 g, 0.88 mmol). The reaction mixture was allowed to stir overnight. The solvent was removed under vacuum yielding a colourless residue. The residue was taken up in Et_2O (10 mL). A white suspension, presumed to be KCl, was removed by centrifugation. The solvent was removed under vacuum to yield a colourless liquid that was identified as **63** (0.11 g, 85 %). ^{1}H NMR (C_6D_6): δ 1.38 (s, 18 H), 1.60 (s, 6 H), 1.73 (s, 4 H). EI/MS *m/z*: 302 [M^+, 29%], 287 [M^+-Me, 18%], 205 [$^+$Ge(O^{t}Bu)$_2$ - Me, 100%], 147 [GeO^{t}Bu, 85%],

82 [$^{+}$DMB, 35 %]. High resolution EI/MS for $C_{14}H_{28}{}^{74}GeO_2$ calc 302.1303, found 302.1292.

4.4.6 Reaction of 39 with 3,5-Di-^{t}butyl Orthoquinone

3,5-Di^{t}butyl-orthoquinone (0.07 g, 0.31 mmol) dissolved in THF (5 mL) was added drop wise over 2 min to a solution of **39** (0.10 g, 0.31 mmol) in THF (2 mL). During the addition, the red colour of the orthoquinone quickly faded. After the addition was complete, the solvent was evaporated under high vacuum to yield an off-white powder. The powder was washed with hexanes (2 mL) to give a brilliant white solid identified as **64** (0.16 g, 94%). Crystals suitable for single crystal X-ray diffraction were acquired by the slow diffusion of Et_2O into a saturated solution of **64** in C_6H_6. M.P. 196 – 202 °C. ^{1}H NMR (C_6D_6): δ 1.06 (d, $^{3}J_{HH}$ = 7 Hz, 12 H), 1.28 (s, 6 H), 1.37 (s, 9 H), 1.71 (s, 9 H), 5.67 (sept, $^{3}J_{HH}$ = 7 Hz, 2 H), 7.06 (s, 1 H), 7.26 (s, 1 H). FT-Raman (cm^{-1}): 109 (s), 177 (w), 243 (s), 270 (w), 319 (m) 381 (m), 547 (w), 642 (w), 812 (w), 888 (w), 915 (m), 1029 (w), 1103 (w), 1201 (w), 1292 (w), 1330 (w), 1424 (s), 1447 (s), 1581 (w), 1598 (w), 1625 (m), 2874 (s), 2942 (s), 2986 (s). Anal. Calcd for $C_{29}H_{42}N_2GeCl_2$: C, 55.08; N, 5.14; H, 7.58. Found: C, 55.29; N, 4.90; H, 7.85.

4.4.7 Reaction of 45 with 3,5-Di-^{t}butyl Rrthoquinone

3,5-Di-^{t}butyl orthoquinone (0.04 g, 0.18 mmol) dissolved in hexanes (5 mL) was added drop wise over 2 min to a solution of **45** (0.07 g, 0.18 mmol) in hexanes (5 mL). During the addition, the colour of the orthoquinone solution (green) quickly faded. After the addition was complete, the solvent was evaporated under high vacuum leaving behind

an off-white powder. The powder was determined to be **65** (0.10 g, 91 %). M.P. 120 – 122 °C. ^{1}H NMR (C_6D_6): δ 1.13 (d, $^3J_{HH}$ = 7 Hz, 12 H), 1.41 (s, 6 H), 1.42 (s, 9 H), 1.66 (s, 18 H), 1.82 (s, 9 H), 5.56 (sept, $^3J_{HH}$ = 7 Hz, 2 H), 6.98 (d, $^4J_{HH}$ = 2 Hz, 1 H), 7.10 (d, $^4J_{HH}$ = 2 Hz, 1 H). Raman (cm^{-1}): 138 (w), 229 (m), 271 (w), 451 (w), 599 (m), 780 (w), 831 (w), 887 (w), 918 (w), 1108 (w), 1202 (m), 1238 (m), 1331 (w), 1448 (s), 1597 (w), 1636 (w), 2700 (w), 2924 (s), 2967 (s).

4.4.8 Reaction of 28 with 3,5-Di-^{t}butyl-Orthoquinone

Compound **28** (0.16 g, 0.32 mmol) was dissolved in THF (10 mL) resulting in a yellow solution. 3,5-Di-^{t}butyl-orthoquinone (0.07 g, 0.32 mmol), dissolved in THF (5 mL), was added dropwise to the THF solution of **28**. During the addition, the colour of the reaction mixture turned from yellow to dark blue. The reaction mixture was extracted with an NH_4Cl aqueous solution (10 mL). The aqueous layer was extracted with Et_2O (10 mL x 3). The organic layers were combined, dried over $MgSO_4$ and filtered. Evaporation of the solvent yielded compound **66** (0.11 g, 65%) as a white residue which was identified by ^{1}H NMR spectroscopy and EI/MS.[14]

4.4.9 Reaction of 39 with Methyl Iodide

To a solution of **39** (0.10 g, 0.31 mmol) in C_6H_6 (4 mL) was added excess methyl iodide (0.19 mL, 3.1 mmol). The solution was allowed to stir overnight after which time it was pale green in colour. Hexanes (10 mL) was added to the reaction mixture causing a pale yellow solid to precipitate. The precipitate was collected, redissolved in THF (3

mL) and analyzed by ESI/MS (+ mode). See Section 4.2.3 for a discussion of the ESI/MS spectrum.

4.4.10 Reaction of 42 with Methyl Iodide

To a solution of **42** (0.08 g, 0.15 mmol) in C_6H_6 (6 mL) was added MeI (80 μL, 1.2 mmol). The reaction mixture was stirred for 3 days. Hexanes (10 mL) was added to induce precipitation of a pale green solid which was collected. Crystals suitable for single crystal X-ray diffraction were acquired by the slow diffusion of Et_2O into a saturated solution CH_3CN solution. Both yellow and pale green single crystals were grown. The yellow crystals were identified to be **25-Me[I]** by comparison of the unit cell of the crystals to the reported literature values for **25-Me[I]**.[19] The pale green crystals were analyzed by single crystal X-ray diffraction and found to be **67[I]**.

4.4.11 Reaction of 45 with Methyl Iodide

To a solution of **45** (0.05 g, 0.13 mmol) in C_6H_6 (2 mL) was added methyl iodide (8 μL, 0.13 mmol). After 5 min, a white precipitate formed. The solution was stirred for an additional 10 min. Hexanes (10 mL) was added to the reaction solution to complete the precipitation. The white precipitate was collected and identified as **68[I]** (0.06 g, 86 %). Crystals suitable for single crystal X-ray diffraction were acquired by the slow diffusion of Et_2O into a saturated solution CH_3CN solution of **68[I]**. M.P. 160 – 165 °C. ^{1}H NMR (CD_3CN): δ 1.30 (s, 3 H), 1.35 (s, 18 H), 1.56 (d, $^3J_{HH}$ = 7 Hz, 12 H), 2.35 (s, $^3J_{HH}$ = 7 Hz, 6 H), 5.37 (s, $^3J_{HH}$ = 7 Hz, 2 H). ESI-MS (+ mode) *m/z*: 415 [**68**$^+$, 100%] Raman (cm^{-1}): 597 (m), 1293 (w), 1447 (m), 1459 (m), 1629 (m), 2910 (s), 2973 (s).

4.4.12 Reaction of 28 with Methyl Iodide

To a yellow solution of **28** (0.08g, 0.16 mmol) in C_6H_6 (5 mL) was added MeI (10 μL, 0.16 mmol). A white precipitate formed immediately. Hexanes (10 mL) was added to the reaction solution to complete the precipitation of **69**[I] (0.05 g, 50 %). The ^1H NMR spectrum of **69**[I] taken in CD_3CN was complicated at room temperature with numerous broad signals and was difficult to interpret. As the temperature was varied, the spectrum changed but was still complicated. High temperature NMR experiments were also attempted but resulted in compound decomposition. Crystals suitable for single crystal X-ray diffraction were grown by diffusing pentane into a concentrated THF solution of **28**. M.P. 198 – 202 °C. ^1H NMR (CD_3CN) (RT): 1.29 (s), - 1.31 (bs, 15 H total), 2.13 (bs, 12 H), 2.28 (s, 6H), 2.36 (s, 6H), 4.57 (bs, 2 H), 6.78 (s, 4H). Raman (cm^{-1}): 106 (w), 229 (w), 557 (m), 596 (m), 887 (w), 1047 (w), 1292 (m), 1384 (m), 1450 (m), 1604 (m), 1629 (w), 2736 (w), 2927 (s), 2982 (s). ESI-MS (+ mode) *m/z*: 507 [**69**$^+$, 100%] Anal. Calcd for $C_{30}H_{45}GeIN_2$: C, 56.90; N, 4.42; H, 7.16. Found: C, 56.78; N, 4.29; H, 7.29.

4.4.13 Reaction of 69[I] with $CDCl_3$

69[I] (2.00 g, 0.32 mmol) was dissolved in $CDCl_3$ (2 mL) resulting in a colourless solution. After 10 minutes the reaction mixture turned brown. The solvent was extracted with a saturated NH_4Cl solution (10 mL). The aqueous layer was extracted with CH_2Cl_2 (3x10 mL). The organic layers were combined, dried over $MgSO_4$ and filtered. Removal of the solvent yielded a brown residue. The residue was redissolved in hexanes and passed through a short silica plug. Removal of the hexanes yielded a colourless residue

identified as **70** (0.08 g, 70 %). The identity of **70** was confirmed by comparison of the ^{1}H NMR spectral and EI/MS data to the literature values.[21]

4.4.14 Reaction of 28 with Ethyl Iodide

To a yellow solution of **28** (0.17 g, 0.32 mmol) in C_6H_6 (5 mL) was added EtI (26 μL, 0.32 mmol). The reaction was stirred for 2 h over which time the bright yellow solution of **28** faded to a pale straw colour. Hexanes (5 mL) was added to induce the precipitation of **71**[I] which was collected as an off-white sticky residue. As with **69**[I], the ^{1}H NMR spectra of **71**[I] was complicated at room temperature with numerous broad signals. ESI-MS (+ mode) *m/z*: 521 [M^+, 35 %], 209 [**25-Et**$^+$, 90 %], 181 [**25-H**$^+$, 100%].

4.4.15 Synthesis of 72

71[I] (0.07 g, 0.1 mmol) was dissolved in $CDCl_3$ (2 mL) resulting in a colourless solution. After 10 minutes the reaction mixture turned brown. The solvent was extracted with a saturated NH_4Cl solution (10 mL). The aqueous layer was extracted with CH_2Cl_2 (3x10 mL). The organic layers were combined, dried over $MgSO_4$ and filtered. Removal of the solvent yielded a brown residue. The residue was redissolved in hexanes and passed through a short silica plug. Removal of the hexanes yielded a colourless residue identified as **72** (0.035 g, 94 %). ^{1}H NMR (C_6D_6): δ 1.19 (t, $^3J_{HH}$ = 8 Hz, 3H), 1.64 (q, $^3J_{HH}$ = 7 Hz, 2 H), 2.04 (s, 6 H), 2.38 (s, 12 H), 6.64 (s, 4). EI/MS: *m/z* 376 [M^+, 18 %], 347 [M^+ - Et, 100%], 311 [$GeMes_2$ - H]. High resolution MS/EI for $C_{20}H_{27}{}^{70}Ge^{35}Cl$ calc 372.1043, found 372.1028.

4.4.16 Reaction of 28 with Excess Pivalic Acid

To a solution of pivalic acid (0.14 g, 1.4 mmol) in THF (2 mL) was added dropwise a solution of **28** (0.08 g, 0.16 mmol) in THF (1 mL) over 5 min. The rate of addition was such that the yellow colour of **28** was allowed to dissipated before the next drop was added. The solvent was removed under vacuum yielding a colourless residue. An ^1H NMR spectrum of the residue revealed the presence of **73**, **35**$^+$, and pivalic acid. The residue was suspended in Et_2O (10 mL) and then extracted with a concentrated NH_4Cl solution (10 mL). The organic layer was separated, dried over $MgSO_4$ and evaporated under vacuum leaving a colourless waxy residue. The residue was placed under high vacuum for one week to remove most of the pivalic acid; however, it was not possible to completely remove all traces of pivalic acid from **73**. ^1H NMR (C_6H_6): δ 1.19 (s, 9 H), 2.04 (s, 6 H), 2.44 (s, 12 H), 6.67 (s, 4 H), 7.33 (s, 1 H). EI-MS: *m/z* 413 [M^+, 20 %], High resolution MS/EI for $C_{23}H_{31}{}^{74}GeO_2$ calc 413.1539, found 413.1519.

4.4.17 Reaction of 28 with Limiting Pivalic Acid

Pivalic acid (8 mg, 0.08 mmol), dissolved in THF (0.45 mL), was added dropwise to a solution of **28** (0.08 g, 0.16 mmol) in THF (10 mL) over 5 min. During this time the yellow colour of **28** faded to give a colourless solution. After the addition was complete the solvent was evaporated under high vacuum leaving behind a colourless residue. The residue was redissolved in Et_2O (10 mL). The Et_2O solution was extracted with NH_4Cl (10 mL x2) and then dried over $MgSO_4$. After filtration and removal of the solvent by evaporation under vacuum, **74** was isolated (0.04 g, 67 %). The identity of **74** was confirmed by comparisons with an authentic sample.[24]

4.4.18 Reaction of 28 with Benzophenone

To a solution of **28** (0.08 g, 0.16 mmol) in THF (5 mL) was added benzophenone (0.03 g, 0.16 mmol) in a screw capped sealed vial. The reaction mixture was heated to 80 °C and stirred for 18 hr. The reaction mixture was extracted with NH_4Cl (10 mL x 2) which in turn was extracted with Et_2O (10 mL x 3). The organic layers were combined, then dried over $MgSO_4$ and then filtered. Removal of the solvent by evaporation under vacuum gave a colourless residue which was purified by silica gel chromatography using 90 % CH_2Cl_2/ 10% hexanes) as the eluent to give **75** (0.02 g, 25 %). ^1H NMR (CD_2Cl_2): δ 2.23 (s, 3H, $C^{23}H_3$), 2.28 (s, 3H, $C^{22}H_3$), 2.41 (s, 6H, $C^{20}H_3$), 2.43 (s, 6H, $C^{21}H_3$), 6.20 (s, 1H, $C^{19}H$), 6.81 (s, 2H, $C^{12}H$), 6.86 (s, 2H, $C^{13}H$), 7.05-7.07 (m, 1H, $C^{10}H$), 7.15 - 7.24 (m, 5H, $C^{17}H + C^{14}H + C^{16}H$), 7.27 – 7.31 (m, 2H, $C^{11}H + C^{15}H$), 7.84 -7.86 (m, 1H, $C^{18}H$). ^{13}C NMR (CD_2Cl_2): δ 21.27 (C23), 21.39 (C22), 23.18 (C21), 24.21 (C20), 83.87 (C19), 125.16 (C18), 127.62 (C17), 127.81 (C16), 128.04 (C15), 128.86 (C14), 129.37 (C13), 129.59 (C12), 129.78 (C11), 132.28 (C10), 135.47 (C9), 136.23 (C8), 137.82 (C7), 139.90 (C6), 140.18 (C5), 143.05 (C4), 143.09 (C3), 146.38 (C2), 152.81 (C1). High resolution EI/MS for $C_{31}H_{32}{}^{74}GeO$ calc 494.1665, found 494.1649.

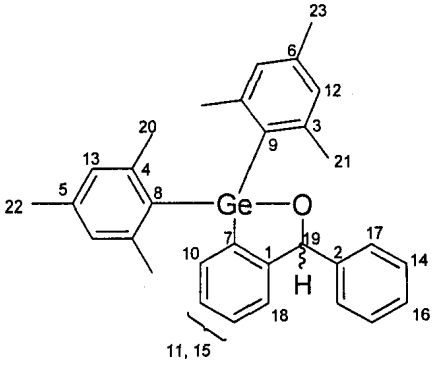

75

4.4.19 Computational Details

The geometries of the model compounds were optimized using the PBE1PBE density functional and the 6-311+G(d,p) basis set using Gaussian03.[38] Tight convergence criteria for the self consistent field (SCF=Tight) and an ultra fine integration grid (Int=Grid=Ultrafine) was used during the calculations. All optimized geometries did not have any imaginary frequencies, and therefore, are minima on the potential surface. Appendix A1.4 – A1.6 contains the commands issued to Gaussian 03 for the calculations.

4.4.20 Single Crystal X-ray Diffraction Experimental Details

Data were collected at low temperature (-123 °C) on a Nonius Kappa-CCD area detector diffractometer with COLLECT. The unit cell parameters were calculated and refined from the full data set. Crystal cell refinement and data reduction were carried out using HKL2000 DENZO-SMN.[39] Absorption corrections were applied using HKL2000 DENZO-SMN (SCALEPACK).

The SHELXTL/PC V6.14 suite of programs was used to solve the structures by direct methods.[40] Subsequent difference Fourier syntheses allowed the remaining atoms to be located. All of the non-hydrogen atoms were refined with anisotropic thermal parameters. The hydrogen atom positions were calculated geometrically and were included as riding on their respective carbon atoms.

Table 4.5: Crystallographic data for compounds **62**, **64**, **67**[I], **68**[I] and **69**[I]

	62	**64**	**67[I]**	**68[I]**
Empirical formula	C17 H30 Cl2 Ge N2	C25 H40 Cl2 Ge N2 O2	C12 H23 Ge I3 N2	C20 H41 Ge I N2 O2
Formula weight	405.92	544.10	648.61	541.06
Crystal system	Monoclinic	Triclinic	orthorhombic	monoclinic

Space group	P 21/c	P-1	P 21 21 21	P 21/c
a (Å)	15.9298(5)	8.5449(17)	10.246(2)	11.821(2)
b (Å)	8.3530(2)	8.8873(18)	12.522(3)	13.765(3)
c (Å)	16.5558(5)	18.880(4)	14.850(3)	15.378(3)
α (°)	90	78.89(3)	90	90.00
β (°)	115.8120(14)	79.44(3)	90	92.14(3)
γ (°)	90	81.13(3)	90	90.00
Volume (Å^3)	1983.15(10)	1372.5(5)	1905.2(7)	2500.6(9)
Z	4	2	4	4
Data/restraints/ parameters	4554/0/204	6266/0/301	5559/0/171	5678/0/248
Goodness-of-fit	1.066	1.043	0.994	1.155
R [$I>2\sigma(I)$]	0.0409	0.0380	0.0526	0.0526
wR^2 (all data)	0.1084	0.0958	0.1357	0.1582
Largest diff. peak and hole (e Å^{-3})	0.570, -0.738	0.544, -0.696	1.266 -1.759	3.340 -1.171

	69[I]
Empirical formula	C30 H45 Ge I N2
Formula weight	633.19
Crystal system	monoclinic
Space group	P 21
a (Å)	11.251(2)
b (Å)	18.190(4)
c (Å)	15.163(3)
α (°)	90
β (°)	107.22(3)
γ (°)	90
Volume (Å^3)	2964.1(11)
Z	4
Data/restraints/ parameters	13307/1/641
Goodness-of-fit	1.057
R [$I>2\sigma(I)$]	0.0428
wR^2 (all data)	0.1042
Largest diff. peak and hole (e Å^{-3})	0.732, -0.979

4.5 References

1. (a) Neumann, W. P. *Chem. Rev.* **1991**, *91*, 311. (b) Barrau, J.; Rima, G. *Coord. Chem. Rev.* **1998**, *178-180*, 593. (c) Weidenbruch, M. *Eur. J. Inorg. Chem.* **1999**, 373. (d) Satgé, J. *Chem. Heterocyclic Comp.* **1999**, *35*, 1013. (e) Boganov, S. E.; Faustov, V. I.; Egorov, M. P.; Nefedov, O. M. *Russ. Chem. Bull., Int. Ed.* **2004**, *53*, 960. (f) Zemlyanskii, N. N.; Borisova, I. V.; Nechaev, M. S.; Khrustalev, V. N.; Lunin, V. V.; Antipin, M. Y.; Ustynyuk Y. A. *Russ. Chem. Bull., Int. Ed.* **2004**, *53*, 980. (g) Kühl, O. *Coord. Chem. Rev.* **2004**, *248*, 411. (h) Leung, W. P.; Kan, K. W.; Chong, K. H. *Coord. Chem. Rev.* **2007**, *251*, 2253. (i) Weinert, C. S. In *Comprehensive Organometallic Chemistry III, Vol 3;* Mingos, D. M. P., Crabtree, R. H., Housecroft, C. E., Eds; Elsevier: Oxford, **2007**; pp. 699 – 808. (j) Saur, I.; Alonso, S. G.; Barrau, J. *Appl. Organomet. Chem.* **2005**, *19*, 414. (j) Nagendran, S.; Roesky, H. *Organometallics* **2008**, *27*, 457.

2. (a) Cissell, J. A.; Vaid, T. P.; DiPasquale, A. G.; Rheingold, A. L. *Inorg. Chem.* **2007**, *46*, 7713. (b) Cissell, J. A.; Vaid, T. P.; DiPasquale, A. G.; Rheingold, A. L. *J. Am Chem. Soc.* **2007**, *129*, 7841. (c) Lee, V. Y.; Takanashi, K.; Kato, R.; Matsuno, T.; Ichinohe, M.; Sekiguchi, A. *J. Organomet. Chem.* **2007**, *692*, 2800. (d) Segmueller, T.; Schlueter, P. A.; Drees, M.; Schier, A.; Nogai, S.; Mitzel, N. W.; Strassner, T.; Karsch, H. H. *J. Organomet. Chem.* **2007**, *692*, 2789. (e) Zabula, A. V.; Hahn, F. E.; Pape, T.; Hepp, A. *Organometallics* **2007**, *26*, 1972. (f) Hahn. F. E.; Zabula, A. V.; Pape, T.; Hepp, A. *Eur. J. Inorg. Chem.* **2007**, 2405. (g) Gushwa, A. F.; Richards, A. F. *J. Chem. Cryst.* **2006**, *36*, 851. (h) Fedushkin, I. L.; Hummert, M.; Schumann, H. *Eur. J. Inorg. Chem.* **2006**, 3266. (i) Eichler, J. F.; Just, O.; Rees, W. S., Jr. *Inorg. Chem.*

2006, *45*, 6706. (j) Pampuch, B.; Saak, W.; Weidenbruch, M. *J. Organomet. Chem.* **2006**, *691*, 3540. (k) Fedushkin, I. L.; Khvoinova, N. M.; Baurin, A.; Yu. A.; Chudakova, V. A.; Skatova, A. A.; Cherkasov, V. K.; Fukin, G. K.; Baranov, E. V. *Russ. Chem. Bull.* **2006**, *55*, 74. (l) West, R.; Moser, D. F.; Guzei, I. A.; Lee, G.; Naka, A.; Li, W.; Zabula, A.; Bukalov, S.; Leites, L. *Organometallics* **2006**, *25*, 2709. (m) Leung, W.; Wong, K.; Wang, Z.; Mak, T. C. W. *Organometallics* **2006**, *25*, 2037. (n) Schoepper, A.; Saak, W.; Weidenbruch, M. *J. Organomet. Chem.* **2006**, *691*, 809. (o) Stanciu, C.; Richards, A. F.; Stender, M.; Olmstead, M. M.; Power, P. P. *Polyhedron* **2006**, *25*, 477.

3. For a recent comparison of different neutral donors and their Lewis basicity see: Gusev, D. G. *Organometallics* **2009**, *28*, 763.
4. (a) Hurni, K. L.; Baines, K. M. *Can. J. Chem.* **2007**, *85*, 668. (b) Neumann, W. P.; Schriewer, M. *Tetrahedron Lett.* **1980**, *21*, 3273. (c) Riviere, P.; Castel, A.; Satgé, J. *J. Organomet. Chem.* **1982**, *232*, 123. (d) Schriewer, M.; Neumann, W. P. *J. Am. Chem. Soc.* **1983**, *105*, 7. (e) Baines, K. M.; Cooke, J. A.; Dixon, C. E.; Liu, H. W.; Netherton, M. R. *Organometallics* **1994**, *13*, 631. (f) Tokitoh, N.; Okazaki, R. *Coord. Chem. Rev.* **2000**, *210*, 251. (g) Jenkins, R. L.; Kedrowski, R A.; Elliott, L. E.; Tappen, D. C.; Schlyer, D. J.; Ring, M. A. *J. Organomet. Chem.* **1975**, *86*, 347.
5. Bonnefille, E.; Mazières, S.; El Hawi, N.; Gornitzka, H.; Couret, C. *J. Organomet. Chem.* **2006**, *691*, 5619.
6. Recent evidence suggests that the reaction proceeds via a concerted [4+2] cycloaddition which is in contradiction with previous work. (a) Huck, L. A.; Leigh, W. J. *2009 Silicon Symposium* Long Branch, NJ., **2009** (b) Leigh, W. J.; Harrington,

C. R. *J. Am. Chem. Soc.* **2005**, *127*, 5084. (c) Bobbitt, K. L.; Maloney, V. M.; Gaspar, P. P. *Organometallics* **1991**, *10*, 2772.

7. Leigh, W.; Harrington, C. R.; Vargas-Baca, I. *J. Am. Chem. Soc.* **2004**, *126*, 16105.

8. Baukov, Y. I; Tandura, S. N. In *The Chemistry of Organic Germanium, Tin and Lead Compounds, Vol. 2;* Rappoport, Z., Ed; John Wiley & Sons Ltd.: West Sussex, England, **2002**; pp. 963-1239.

9. Compound **63** can also be synthesized by the reaction of two equivalents of KO^tBu with **61**.

10. Since the results from the MP2 calculations in Chapter 3 were very similar to the PBE1PBE results, only DFT was used.

11. Please note that the energies of complexation calculated in Chapter 3 did not include enthalpic or entropic corrections whereas those presented in this Chapter do.

12. The energies of cyclization of GeR_2 and ethylene have been calculated and exhibit similar substituent effects. See: Boganov, S. E.; Egorov, M. P.; Faustov, V. I.; Nefedov, O. M. In *The Chemistry of Organic Germanium, Tin and Lead Compounds, Vol. 2*; Rappoport, Z., Ed; John Wiley & Sons Ltd.: West Sussex, England, **2002**; pp. 749-842.

13. (a) Rivière, P.; Castel, A.; Satgé, J.; Guyot, D. *J. Organomet. Chem.* **1986**, *315*, 157. (b) Mazières, S.; Lavayssière, H.; Dousse, G.; Satgé, J. *Inorg. Chim. Acta* **1986**, *252*, 25. (c) Michels, E.; Neumann, W. P. *Tet. Lett.* **1986**, *27*, 2455.

14. Compound **66** has been reported previously. See reference 13a.

15. Radical cations derived from **25** were formed by one electron oxidation of the NHC by tetracyanoethylene and ferrocenium. See Ramnial, T.; Mckenzie, I.; Gorodetsky, B.; Tsang, E. M.; Clyburne, J. A. C. *Chem. Commun.,* **2004**, 1054.

16. (a) Bonnefille, E.; Mazières, S.; El Hawi, N.; Gornitzka, H.; Couret, C. *J. Organomet. Chem.* **2006**, *691*, 5619. (b) Weinert, C. S.; Fenwick, A. E.; Fanwick, P. E.; Rothwell, I. P. *Dalton Trans.* **2003**, *532.*

17. (a) Jutzi, P.; Keitemeyer, S.; Neumann, B.; Stammler, H. *Organometallics* **1999**, *18*, 4778. (b) Schmidt, H.; Keitemeyer, S.; Neumann, B.; Stammler, H.; Schoeller, W. W.; Jutzi, P. *Organometallics* **1998**, *17*, 2149.

18. To the best of our knowledge, the reaction of **17** with MeI is the only example. See Chapter 2.

19. **25-Me**$^+$ has been reported before and was synthesized by the direct reaction of **25** with MeI. See Kuhn, N.; Göhner, M.; Steimann, M. *Z. Naturforsch. B* **2002**, *57*, 631.

20. Using **57** (R = CH_3) as a model for the mesityl substituted **28** is a fairly poor approximation. It would be expected the HOMO in **28** would receive additional stabilization as a result of the sp^2 hybridization of the ipso mesityl carbon substituents.

21. **70** was previously reported and was synthesized by the addition of MeLi to Mes_2GeCl_2. See Duverneuil, G.; Mazerolles, P.; Perrier, E. *App. Organomet. Chem.* **1995**, *9*, 37.

22. **25** is believed to form a salt of Cl_2 as was observed previously in the reaction of **25** with hexachloroethane. See Kuhn, N.; Abu-Rayyan, A.; Göhner, M.; Steimann, M. *Z. Anorg. Allg. Chem.* **2002**, *628*, 1721.

23. Huck, L. A.; Leigh, W. J. *Organometallics* **2007**, *26*, 1339.

24. Adduct **74** has been previously reported and was formed by the direction reaction of tetramesityldigermene with pivalic acid. Hurni, K. L.; Rupar, P. A.; Payne, N. C.; Baines, K. M. *Organometallics* **2007**, *26*, 5569.

25. (a) Sweeder, R. D.; Edwards, F. A.; Miller, K. A.; Banaszak Holl, M. M.; Kampf, J. W. *Organometallics* **2002**, *21*, 457. (b) Sweeder, R. D.; Cygan, Z. T.; Banaszak Holl, M. M.; Kampf, J. W. *Organometallics* **2003**, *22*, 4613.

26. As a reference, the pKa of the conjugate acid of the NHC used in this study has been calculated as approximately 36 in acetonitrile. See: Magill, A. M.; Cavell, K. J.; Yates, B. F. *J. Am. Chem. Soc.* **2004**, *126*, 8717.

27. Jutzi, P.; Eikenberg, D.; Bunte, E. A.; Möhrke, A.; Neumann, B.; Stammler, H.G. *Organometallics* **1998**, *15*, 1930.

28. Gehrhus, B.; Hitchcock, P. B.; Lappert, M. F. *Organometallics* **1997**, *16*, 4861.

29. Ando, W.; Ikeno, M.; Sekiguchi A. *J. Am. Chem. Soc.* **1977**, *99*, 6447.

30. Xiong, Y.; Yao, S.; Driess, M. *Chem. Eur. J.* **2009**, *15*, 5545.

31. (a) Marion, N.; Diez-Gonzalez, S.; Nolan, S. P. *Angew. Chem. Int. Ed.* **2007**, *46*, 2988. (b) Ender, D.; Niemeier, O.; Henseler, A. *Chem. Rev.* **2007**, *107*, 5606.

32. Iwamoto, T.; Masuda, H.; Ishida, S.; Kabuto, C.; Kira, M. *J. Organomet. Chem.* **2004**, *689*, 1337.

33. (a) Xiong, Y.; Yao, S.; Driess, M. *Chem. Eur. J.* **2009**, *15*, 5545. (b) Baines, K. M.; Cooke, J. A.; Vittal, J. J. *Heteroat. Chem.* **1994**, *5*, 293.

34. Yao, S.; van Wüllen, C.; Driess, M. *Chem. Commun.* **2008,** 5393.

35. Xiong, Y.; Yao, S.; Brym, M.; Driess, M. *Angew. Chem., Int. Ed.* **2007**, *46*, 4511.

36. (a) Walker, R. H.; Miller, K. A.; Scott, S. L.; Cygan, Z. T.; Bartolin, J. M.; Kampf, J. W.; Holl Banaszak, M. M. *Organometallics* **2009**, *28*, 2744.

37. Pangborn, A. B.; Giardello, M. A.; Grubbs, R. H.; Rosen, R. K.; Timmers, F. J. *Organometallics* **1996**, *15*, 1518.

38. Gaussian 03, Revision B.05, Frisch, M. J.; Trucks, G. W.; Schlegel, H. B.; Scuseria, G. E.; Robb, M. A.; Cheeseman, J. R.; Montgomery, Jr., J. A.; Vreven, T.; Kudin, K. N.; Burant, J. C.; Millam, J. M.; Iyengar, S. S.; Tomasi, J.; Barone, V.; Mennucci, B.; Cossi, M.; Scalmani, G.; Rega, N.; Petersson, G. A.; Nakatsuji, H.; Hada, M.; Ehara, M.; Toyota, K.; Fukuda, R.; Hasegawa, J.; Ishida, M.; Nakajima, T.; Honda, Y.; Kitao, O.; Nakai, H.; Klene, M.; Li, X.; Knox, J. E.; Hratchian, H. P.; Cross, J. B.; Bakken, V.; Adamo, C.; Jaramillo, J.; Gomperts, R.; Stratmann, R. E.; Yazyev, O.; Austin, A. J.; Cammi, R.; Pomelli, C.; Ochterski, J. W.; Ayala, P. Y.; Morokuma, K.; Voth, G. A.; Salvador, P.; Dannenberg, J. J.; Zakrzewski, V. G.; Dapprich, S.; Daniels, A. D.; Strain, M. C.; Farkas, O.; Malick, D. K.; Rabuck, A. D.; Raghavachari, K.; Foresman, J. B.; Ortiz, J. V.; Cui, Q.; Baboul, A. G.; Clifford, S.; Cioslowski, J.; Stefanov, B. B.; Liu, G.; Liashenko, A.; Piskorz, P.; Komaromi, I.; Martin, R. L.; Fox, D. J.; Keith, T.; Al-Laham, M. A.; Peng, C. Y.; Nanayakkara, A.; Challacombe, M.; Gill, P. M. W.; Johnson, B.; Chen, W.; Wong, M. W.; Gonzalez, C.; and Pople, J. A.; Gaussian, Inc., Wallingford CT, **2004.**

39. Otwinowski, Z; Minor, W. In *Methods in Enzymology. Vol. 276: Macromolecular Crystallography, Part A.*; Carter, Jr, C.W., Sweet, R.M., Eds; Academic Press: New York. **1997**, pg 307.

40. Sheldrick, G.M. *Acta Cryst.* **2008**, *A64*, 112.

Chapter 5

The Synthesis of Cationic Complexes of Ge(II)*

5.1 Introduction

Understanding the structure and reactivity of carbenium ions has been critical in the development of many areas of organic chemistry. Given the long-standing interest in the fundamental differences and similarities between carbon and its heavier congeners, cationic compounds of the heavier group 14 elements, particularly in the condensed phase, have also been the subject of intense research.[1]

Based on the reduced electronegativity of the heavier group 14 elements relative to carbon, the formation of heavy group 14 cationic species may be expected to be facile. In the gas phase, this is indeed the case and cations of the type $^{+}ER_3$ (E = heavy group 14 element) are observable.[1e] However, in the condensed phase, heavier group 14 cations are difficult to synthesize due to a number of compounding factors. First, the larger atomic radius of the heavy group 14 atom makes them difficult to shield from nucleophilic attack from solvent and anions. Second, the stabilizing influences of resonance, inductive, and hyperconjugative effects, which play crucial roles in carbenium cation isolation, are much weaker with heavier elements. Finally, due to the reduced electronegativity of the heavier group 14 elements compared to carbon, organic ligands on the group 14 element provide a destabilizing effect on group 14 cations.[1]

---

* This chapter is a combination of three separate publications and additional unpublished results: (a) Rupar, P. A.; Staroverov, V. N.; Ragogna, P. J.; Baines, K. M. *J. Am. Chem. Soc.* **2007**, *129*, 15137. (b) Rupar, P. A.; Staroverov, V. N.; Baines, K. M. *Science* **2008**, *322*, 1360. (c) Rupar, P. A.; Bandyopadhyay, R.; Cooper, B. F. T.; Stinchcombe M. R.; Macdonald, C. L. B.; Ragogna, P. J.; Baines, K. M. *Angew. Chem., Int. Ed.* **2009**, *48*, 5155.

It was not until 2002 that the first example of a fully ionized $^{+}ER_3$ cation, without anion or solvent coordination, was isolated and structurally characterized in the condensed phase. Silyl cation **76**$^{+}$ was synthesized by the electrophilic attack of $Et_3Si(HCB_{11}Me_5Br_6)$ on a vinyl silane as shown in Scheme 5.1.[2] The use of sterically protecting mesityl groups on silicon, a weakly coordinating carborane counter anion, and a relatively non-nucleophilic solvent were critical for the successful isolation of **76**$^{+}$.

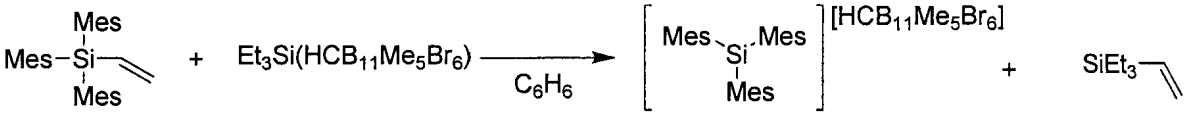

76[$HCB_{11}Me_5Br_6$]

Scheme 5.1

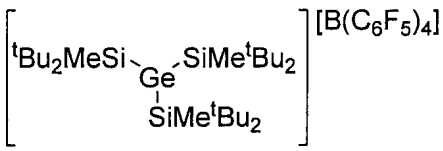

77[$B(C_6F_5)_4$]

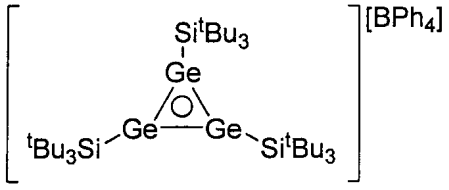

78[BPh_4]

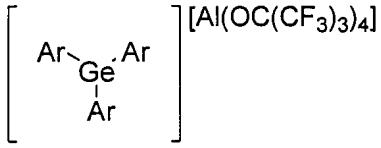

Ar=2,6-(O^tBu)$_2C_6H_3$

79[$Al(OC(CF_3)_3)_4$]

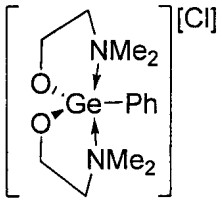

80[Cl]

Chart 5.1

Three-coordinate germyl cations, such as **77**$^{+}$ – **79**$^{+}$, have been synthesized using strategies similar to those employed with **76**$^{+}$; specifically, cations **77**$^{+}$ – **79**$^{+}$ rely on steric protection and weakly coordinating counter anions.[3, 4, 5] The electron rich silyl groups on

77$^+$ and **78**$^+$ and the alkoxy-substituted aryl rings of **79**$^+$ provide additional electronic stabilization. The cyclopropenium analog **78**$^+$ is interesting in that a two electron aromatic system provides charge delocalization.[4]

Although three coordinate germyl cations such as **77**$^+$ – **79**$^+$ have received more attention in the scientific community, hypercoordinate germanium centered cations are also known and, in general, are more synthetically accessible.[6] In hypercoordinate germanium centered cations, the problem of protecting the germanium centre is solved by installing neutral donor atoms onto the germanium. The hypercoordination also moderates the electrophilic centre, thus making the germanium centre less sensitive to nucleophilic anions and solvent. Cation **80**$^+$ is a typical example where two amine ligands are providing electron density to the otherwise electron deficient germanium centre (Chart 5.1).[7]

Although they have no known carbon analog, cations of Ge(II) represent another important class of positively charged germanium compounds. Germanium(II) cations differ from the three coordinate Ge(IV) cations in that Ge(II) cations, in their simplest form, not only have empty p-orbitals but also have a lone pair of electrons. Two different types of Ge(II) cations can be envisioned, a Ge(II) monocation and a Ge(II) dication (Chart 5.2). The germanium(II) monocations are well represented in the literature. Common amongst all reported germanium(II) monocations are ligands that stabilize the germanium by transferring electron density into the two formally empty p-orbitals on germanium. The most common type of ligands used are N-heterocycles, with **81**$^+$ and **82**$^+$ being representative.[8] The pentamethylcyclopentadienyl **83**$^+$ is an example of a

carbon-substituted Ge(II) monocation: the pentadienyl group provides both steric protection and electronically saturates the p-orbitals on germanium via π interactions.[9]

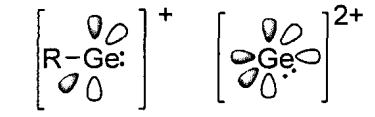

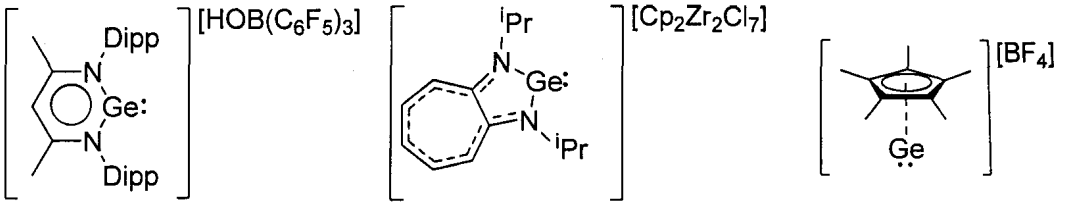

81[HOB(C_6F_5)$_3$] **82**[$Cp_2Zr_2Cl_7$] **83**[BF_4]

Chart 5.2

Despite the progress made with the monocationic germanium(II) systems, prior to this work, germanium(II) dications have not been reported in the literature. With three empty p-orbitals and an occupied s-orbital (Chart 5.2), the prospect of isolating such a reactive species seemed remote and was presumed impossible. This chapter will demonstrate that by using intermolecular donors, including N-heterocyclic carbenes (NHCs), both germanium centred mono and, for the first time, dications can be generated and characterized.

5.2 Results and Discussion

5.2.1 Synthesis of a Ge(II) Dication Supported by Three NHCs

Due to the lack of protection and stabilization, a naked Ge(II) dication is presumably unisolable in the condensed phase. Our objective was to use strong neutral donor ligands to occupy the empty p-orbitals on the Ge^{2+} to provide electronic stability to the electrophilic centre (Chart 5.3) in a manner similar to that used in the isolation of the

neutral germylene complexes discussed in Chapters 2-4. The synthetic pathway envisioned involved the heterolytic displacement of labile substituents on a germanium(II) centre by strong intermolecular donors.[10] The halogenated carbene complexes **39, 41** and **42** are good candidates for such a reaction since the Ge-X bonds are susceptible to displacement due their polarized nature and ability to produce the relatively stable halide anions.

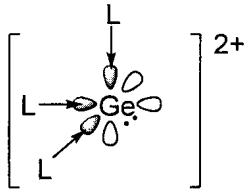

Chart 5.3

Using the NHC **25** as the nucleophile, the reaction of excess **25** with the halogenated **39**, **41** and **42** was examined (Scheme 5.2). No reaction between **39** and **25** was while the addition of **25** to a solution of **41** resulted in the formation of a complex reaction mixture. However, upon addition of excess **25** to a yellow THF solution of **42**, the colour of the solution quickly faded and a white precipitate formed. Colourless crystals were grown from the white powder by diffusion of diethyl ether into a saturated pyridine solution of the bulk powder and were analyzed by single crystal X-ray diffraction. The structure was determined to be the diiodide salt of $\mathbf{84}^{2+}$ in which three crystallographically identical carbenes are bonded to the germanium centre, forming a pyramidal C_3 propeller consistent with an AX_3E[11] configuration (Figure 5.1). The carbenic C-Ge bond length of 2.070(6) Å is slightly longer than an average C-Ge single bond (range 1.90 - 2.05 Å).[12]

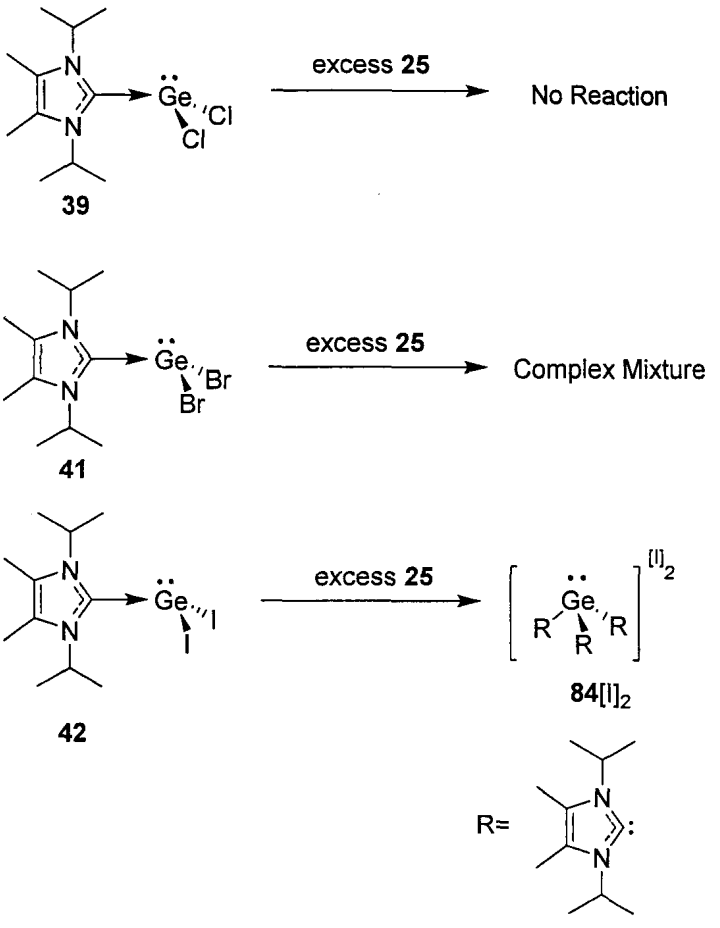

Scheme 5.2

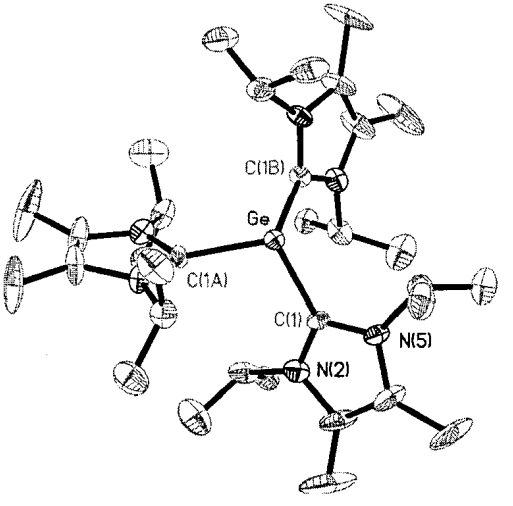

Figure 5.1: Thermal ellipsoid plot (30% probability surface) of $\mathbf{84}^{2+}$. Hydrogen atoms are omitted for clarity. Selected bond lengths (Å) and angles (°): C1–Ge = 2.070(6), N2-C1 = 1.319(9), N5-C1 = 1.358(9), N2-C1-N5 = 106.5(6), C1-Ge-C1A = 103.1(2).

The two iodide anions in the asymmetric unit show no significant bonding interaction with the germanium of $\mathbf{84}^{2+}$. The closest approach of the iodides is 3.11 Å from a methyl hydrogen, which is barely within the sum of the van der Waals radii (3.18 Å).[13] Iodide is usually considered a nucleophilic anion; exclusion of iodide from germanium (the closest Ge - I approach is 5.96 Å) can be attributed to steric protection of the germanium centre from the carbenes and the stereochemically active lone pair of electrons. A disordered pyridine solvate is also present in the unit cell, but is distant from the germanium with the closest approach being 3.78 Å.

As expected, the FT-Raman spectrum of the bulk powder of $\mathbf{84}[I]_2$ lacked a signal attributable to a germanium-iodine covalent bond which was clearly evident in the FT-Raman spectrum of **42**. The ^{1}H NMR spectrum of $\mathbf{84}[I]_2$ is rather complex at room temperature showing multiple broad signals (Figure 5.2) which, at 90 °C, simplify into resonances consistent with one type of carbene moiety. The ^{1}H NMR spectrum of a solution containing both **25** and $\mathbf{84}[I]_2$ at room temperature shows sharp signals attributable to free carbene **25** superimposed on the signals attributable to $\mathbf{84}^{2+}$, suggesting that ligand exchange is not responsible for the broadening of the ^{1}H NMR signals of $\mathbf{84}^{2+}$. At -20 °C, the ^{1}H NMR spectrum of $\mathbf{84}^{2+}$ revealed signals attributable to two non-equivalent isopropyl methyne ^{1}H's, four isopropyl methyl groups, and two backbone methyl groups, which is consistent with the C_3 symmetry of $\mathbf{84}^{2+}$ in the solid state (Figure 5.3). Therefore, it can be concluded that hindered rotation is the most likely explanation for the complex ^{1}H NMR spectrum of $\mathbf{84}^{2+}$ observed at room temperature.

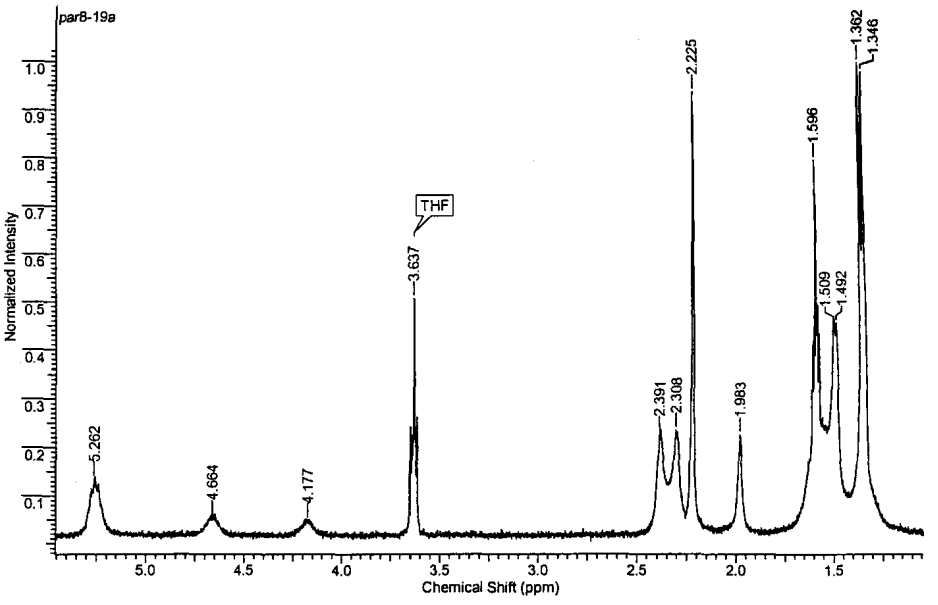

Figure 5.2: ^{1}H NMR spectrum of **84**$[I]_2$ at 26 °C in C_5D_5N

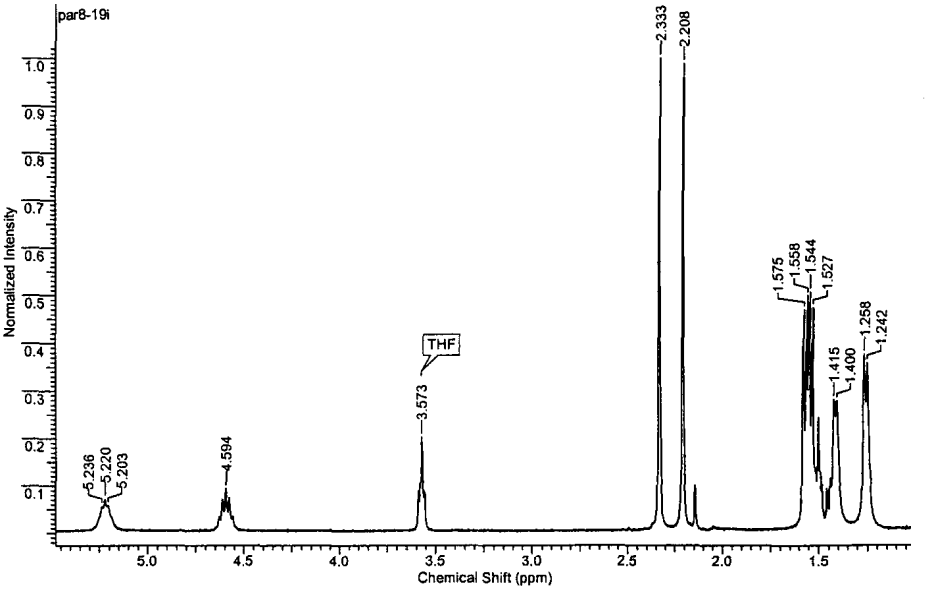

Figure 5.3: ^{1}H NMR spectrum of **84**$[I]_2$ at -20 °C in C_5D_5N

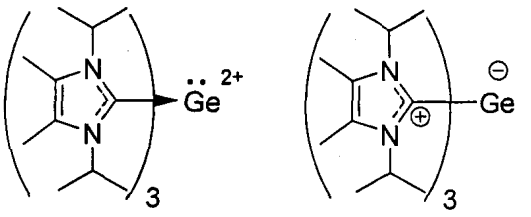

A B

Chart 5.4

Conceptually, there are two different cannonical models for the representations of $\mathbf{84}^{2+}$, a dative[14] bonding model where the germanium has a formal 2+ charge (Chart 5.4, **A**), and a zwitterionic bonding model where the germanium has a formal 1^- charge (Chart 5.4, **B**). Although models **A** and **B** are not true contributing resonance structures (no electron pairs are being moved), the exact electronic nature of $\mathbf{84}^{2+}$ is probably a hybrid between the two models. Electronic structure calculations reveal that the HOMO of $\mathbf{84}^{2+}$ is the lone electron pair on germanium, which is consistent with a Ge(II) species, while the LUMO is a pair of degenerate π^* orbitals localized on the carbenes (Figure 5.4). The natural population anaylsis[15] charge on $\mathbf{84}^{2+}$ is +0.64 and is consistent with the hybrid model.

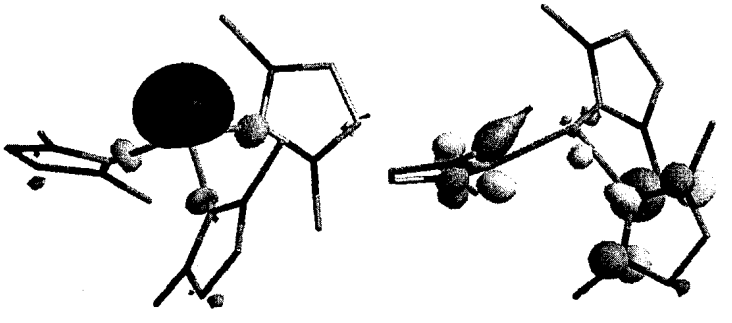

Figure 5.4 The HOMO and one of the degenerate LUMOs at an isosurface value of 0.075 for $\mathbf{84}^{2+}$. For clarity, the methyl groups and hydrogen atoms are not shown.

Efforts at studying the chemistry of **84**$[I]_2$ were hampered by its poor solubility. **84**$[I]_2$ was found to be insoluble in aliphatic and aromatic hydrocarbons, Et_2O, THF, and DCM, and **84**$[I]_2$ decomposed in CH_3CN. The only solvent that **84**$[I]_2$ was soluble in and did not cause decomposition was pyridine. Attempts to increase the solubility of $\mathbf{84}^{2+}$ by changing its counter ions were not successful.

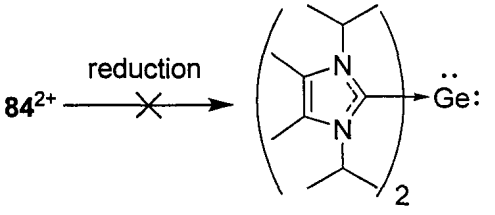

Scheme 5.3

The synthesis of a zero valent germanium compound stabilized by NHC ligands would be highly desirable since there are no examples of such compounds in the literature. Although $\mathbf{84}^{2+}$ seemed like an ideal candidate for reduction, attempts at reducing **84**$[I]_2$ to form a zero valent germanium compound supported by NHCs were not successful (Scheme 5.3). Numerous attempts using a variety of different reducing agents led only to the formation of a black precipitate, presumed to be elemental germanium.

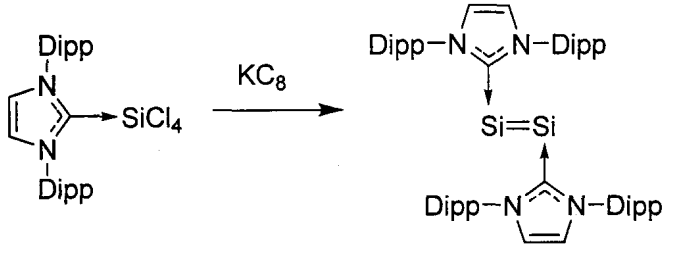

Dipp = 2,6-diisopropylphenyl

Scheme 5.4

Recently it was reported that the reduction of a diisopropylphenyl substituted NHC complex of $SiCl_4$ resulted in the formation of an NHC stabilized elemental silicon complex (Scheme 5.4).[16] Increasing the steric bulk of the NHC used in Scheme 5.3 will likely be an important factor in the stabilization of germanium(0) species. In the future, it may be worthwhile to investigate the reduction of a NHC-Ge(II) complex using a similar, sterically bulky carbene.

5.2.2 Synthesis of a Cryptand Supported Germanium(II) Dication

Although some analogies between $\mathbf{84}^{2+}$ and naked Ge^{2+} can be made, the strong donor properties of the three NHC ligands drastically alter the electronic structure of the central germanium. If the desired goal is to create a complex which retains as much of the electronic character of a Ge(II) dication as possible, neutral donors weaker than a NHC are necessary. An ideal ligand would provide multiple weak stabilizing interactions, while providing protection from nucleophilic anions and solvents.

A class of ligands that fulfill the requirements of having relatively weaker donor atoms while providing a three dimensional protective environment are the cryptands. Cryptands are bicyclic macromolecular polyether cages commonly used to sequester metallic cations.[17] Surprisingly, with the exception of protonated species (for example NH_4^+),[17] there are no reports of a cryptand containing a mononuclear metalloid or non-metal element carrying a cationic charge.[18] Given the success of cryptands in binding metallic cations, it was postulated that a cationic germanium could be isolated and stabilized using an appropriately-sized cryptand. Since cryptands can completely encapsulate their host cation and protect it from nucleophilic counterions and solvents,

the use of cryptands may allow for the isolation of a more highly charged germanium species. Thus, the reaction between cryptand [2.2.2], which is known to accommodate a diverse range of positively-charged species,[17] and NHC complex **43** was investigated. Complex **43** was selected because the Ge-$O_{triflate}$ bond is expected to be labile and conducive to ionization.

The addition of cryptand [2.2.2] to a solution of **43** in THF resulted in the rapid precipitation of a white powder (Scheme 5.5). After stirring the reaction mixture for 24 hours, the precipitate was collected and then redissolved in deuterated acetonitrile (CD_3CN) for study by nuclear magnetic resonance (NMR) spectroscopy. The ^1H NMR spectrum of the product showed only three distinct signals which were assigned to the cryptand moiety. The simplicity of the spectrum suggests that the macrocycle remains in a highly symmetrical environment. Signals attributable to a carbene moiety were not observed. The ^{19}F NMR spectrum of the product showed a single resonance typical of a triflate anion.

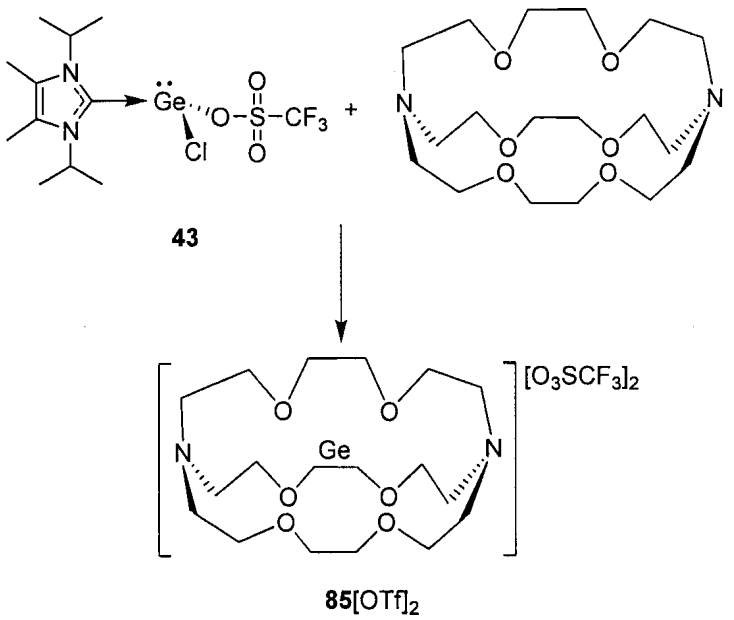

Scheme 5.5

Crystals of the precipitate were grown and identified by single crystal X-ray diffraction as the salt **85**$[OTf]_2$. The primary species in the unit cell is a dicationic germanium located inside the cavity of the cryptand (Figure 5.5). The (Ge·cryptand [2.2.2])$^{2+}$ complex has D_3 symmetry with the germanium directly in the centre of the cage. No solvent molecules are occluded within the crystal. The triflate counterions show no interaction with the germanium; the closest triflate–oxygen–germanium approach is 5.32 Å. Previous examples of unsaturated cations of group 14 utilized very weakly or non-coordinating anions to maintain discrete cation/anion separation in the condensed phase;[1] triflate is not considered a weakly or non-coordinating anion.[19] The observation that the cryptand [2.2.2] is able to exclude the triflates from the coordination sphere of the dicationic germanium attests to the stabilizing effect of the cryptand on the cation and its ability to provide steric shielding.

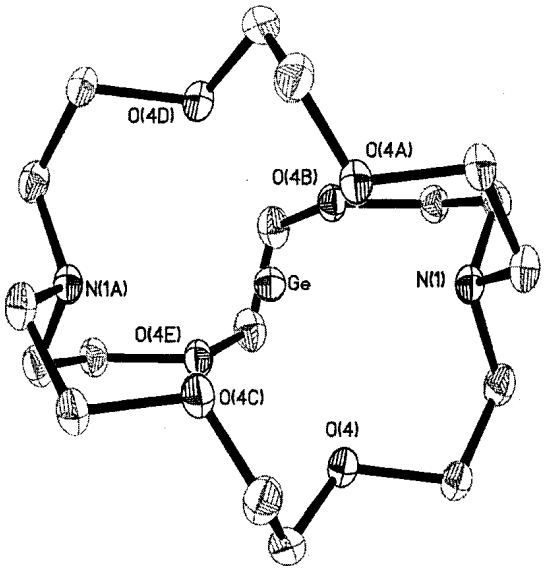

Figure 5.5 Thermal ellipsoid plot (30% probability surface) of **85**$^{2+}$. Triflate anions and hydrogen atoms have been omitted for clarity. Selected distances between atoms (Å): Ge–N1 = 2.524(3), Ge–O4 = 2.4856(16).

The electron-rich cryptand cavity contributes significantly to the ability of cryptands to attract and stabilize guest cations. Cryptand [2.2.2] has six oxygen and two nitrogen atoms, all of which have electron lone pairs oriented into the cavity of the macrocycle. The experimental Ge–N and Ge–O distances in the crystals of $\mathbf{85}^{2+}$ are 2.524(3) Å and 2.4856(16) Å respectively, values which are considerably greater than the distances of typical Ge–N and Ge–O single bonds, at 1.85 Å and 1.80 Å, respectively.[12, 20, 21] The long interatomic distances suggest that the Ge atom does not have significant bonding interactions with any of the cryptand atoms and that, to a first approximation, compound $\mathbf{85}^{2+}$ is a cryptand-protected salt of Ge^{2+} with two triflate anions. Calculations confirmed this supposition: the Wiberg bond index (WBI)[22] for each G-N and Ge-O interaction was found to be 0.11 and 0.10, respectively. Furthermore, by using natural population analysis,[15] the estimated residual charge on germanium was determined to be +1.38, which suggests that much of the cationic charge remains on the encapsulated Ge atom despite the interactions with the cryptand.

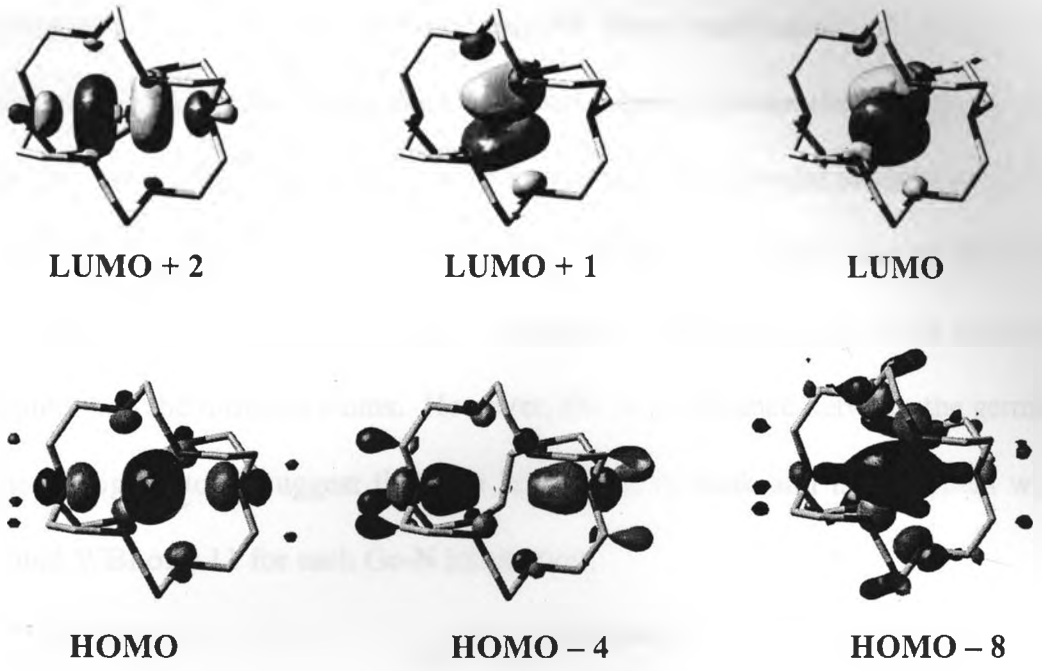

Figure 5.6 Kohn-Sham orbitals of $\mathbf{85}^{2+}$ that are dominated by the contributions from the Ge and N atoms. Isosurface value of 0.075. Hydrogen atoms have been omitted for clarity.

Visualization of the frontier molecular orbitals of $\mathbf{85}^{2+}$ show that the electronic structure of the orbitals are similar to an idealized germanium(II) dication: the first three LUMOs have significant contributions from the $4p_x$, $4p_y$ and $4p_z$ orbitals on germanium while the HOMO has contribution from the *4s* orbital (Figure 5.6). However, stating that the germanium in $\mathbf{85}^{2+}$ is the same as a naked Ge^{2+} ion is a gross simplification as the nitrogen and oxygen atoms of the cryptand are clearly providing electronic stabilization to the germanium centre. A qualitative molecular orbital diagram was constructed to help better understand the complex shape of Kohn-Sham orbitals (Figure 5.7); for simplicity, only the frontier orbitals of germanium and nitrogen atoms were considered for Figure 5.7. In the qualitative MO diagram, the occupied *4s* and unoccupied $4p_z$ atomic orbitals

on germanium mix with two symmetry-adapted linear combinations (SALCs) from the two nitrogen-based electron lone pairs. The interaction between the germanium and the nitrogen atoms results in the formation of three occupied molecular orbitals: two bonding and one antibonding. Since the antibonding interaction negates one of the bonding interactions, there is an overall single 3-centered-2-electron (3c2e) bond between the germanium and the nitrogen atoms. However, the large distance between the germanium and the nitrogen atoms suggest that this 3c2e bond is weak and is consistent with the calculated WBI of 0.11 for each Ge-N interaction.

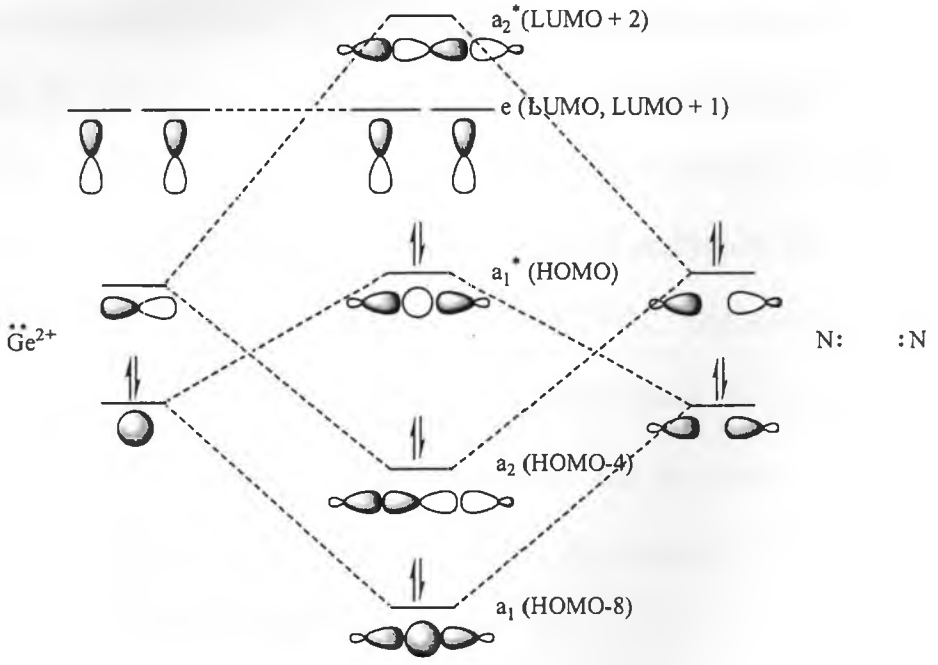

Figure 5.7 Qualitative molecular orbital diagram of the interactions between the germanium dication and the lone pairs of electrons on the nitrogen atoms in the D_3 point group for compound **85**$^{2+}$. The remaining atoms of the cryptand were excluded for clarity. The labels in parentheses are in reference to the Kohn-Sham orbitals in Figure 5.6.

Natural bond orbital analysis was performed on $\mathbf{85}^{2+}$ to obtain another interpretation of the electronics of this unusual cation. The NBO method determines the best possible Lewis-type structure for a given molecule by identifying all core orbitals, localized two-electron two-centre bonds, one-centre nonbonding orbitals (lone pairs), and other conventional covalency effects.[15] The NBO calculations suggest that the Ge atom does not participate in any covalent bonding interactions. The most direct evidence of this is the fact that the highest-occupied NBOs on the germanium and the heteroatoms are all nonbonding lone electron pairs.

Considering that cryptand [2.2.2] has a strong affinity for metallic ions, the possibility exists that the central atom within the cryptand is not germanium, but is instead an adventitious metallic cation. Evidence that germanium is present was obtained by three different analytical techniques. Combustion elemental analysis of the bulk powder was consistent with the molecular formula of $\mathbf{85}[OTf]_2$: $GeC_{20}N_2O_{12}F_3S_2$. Second, electrospray ionization mass spectrometry (ESI-MS) shows the expected mass/charge (*m/z*) signals for $\mathbf{85}^{2+}$, with an isotopic distribution that is characteristic of germanium (Figure 5.8). Finally, energy dispersive X-ray spectroscopy (EDX) showed signals confirming the presence of germanium (Figure 5.9).

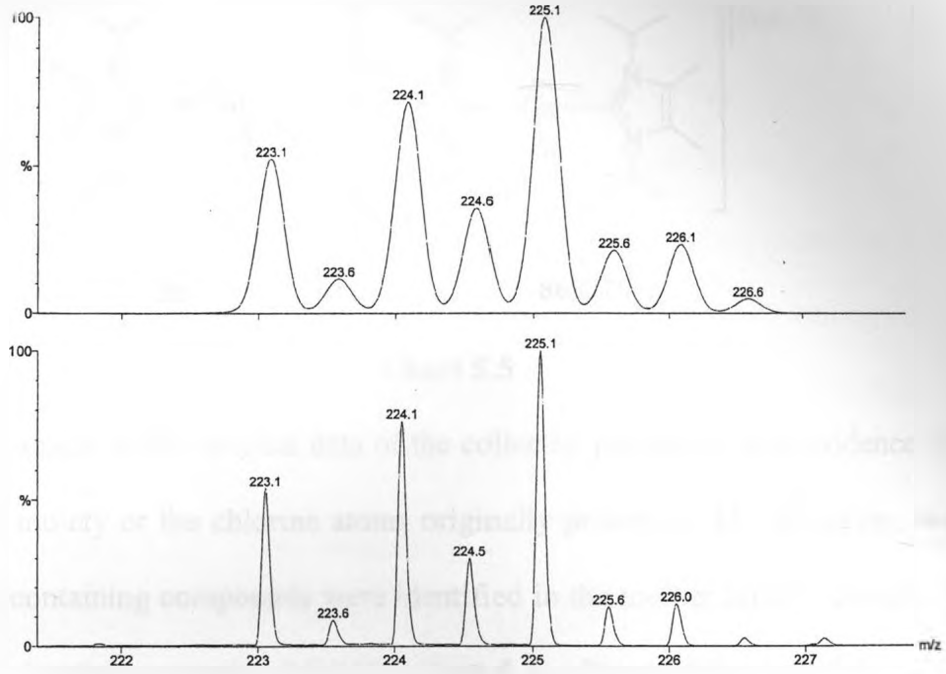

Figure 5.8 Top, predicted electrospray ionization mass spectrometric graph of the $(GeC_{18}H_{36}O_6N_2)^{2+}$ ion $\mathbf{85}^{2+}$. Bottom, measured electrospray ionization mass spectrometric graph of the $(GeC_{18}H_{36}O_6N_2)^{2+}$ ion ($\mathbf{85}^{2+}$).

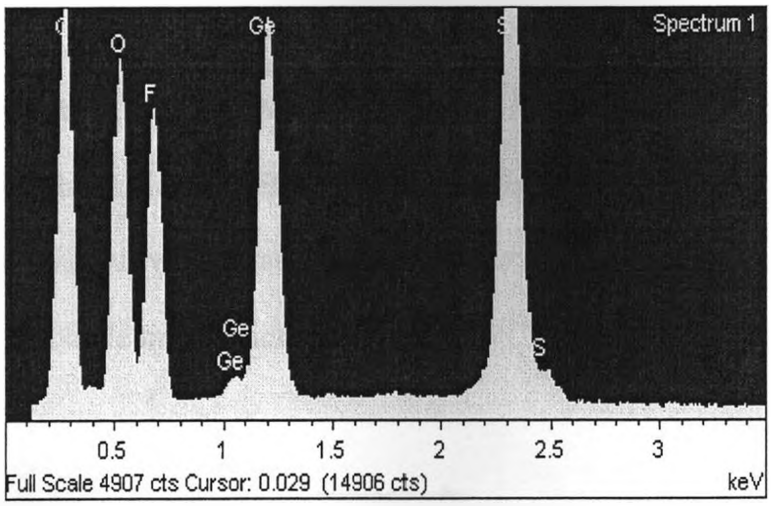

Figure 5.9 Energy Dispersive X-ray Spectrum (EDX) of $\mathbf{85}[OTf]_2$.

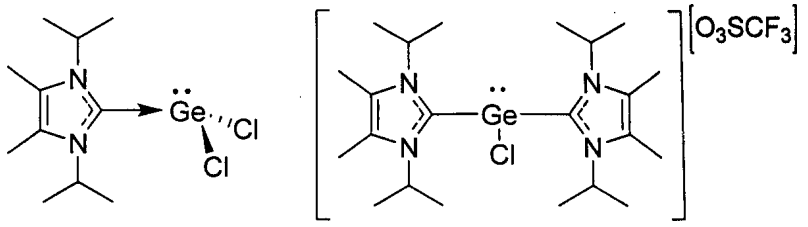

39 **86**[OTf]

Chart 5.5

Notably absent in the spectral data of the collected precipitate was evidence of either the carbene moiety or the chlorine atoms originally present in **43**. However, two other germanium containing compounds were identified in the mother liquor: complex **39** and the cationic dicarbene complex **86**[OTf] (Chart 5.5). Presumably, with the precipitation of **85**$[OTf]_2$, the displaced chloride and carbene react rapidly with two equivalents of **43** displacing the labile triflate and forming **39** and **86**[OTf], respectively. Based on compounds **85**$[OTf]_2$, **39**, and **86**[OTf] being the primary products of the reaction, the stoichiometry of the reaction shown in Scheme 5.5 is three equivalents of **43** per equivalent of cryptand[2.2.2]. When the reaction is carried out with the correct stoichiometry, the isolated yields of **85**$[OTf]_2$, **39**, and **86**[OTf] are 88%, 81%, and 96%, respectively. A possible driving force for the reaction is the precipitation of the $\mathbf{85}^{2+}$ complex which is insoluble in the reaction solvent, THF.

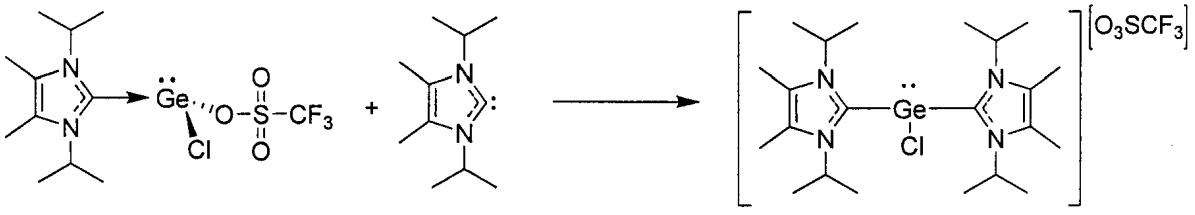

43 **25** **86**[OTf]

Scheme 5.6

The identity of **39** was confirmed by comparison with an authentic sample. The identity of **86**[OTf] was elucidated using ^{1}H NMR spectroscopy, Raman spectroscopy, elemental analysis, and ESI mass spectrometry. Complex **86**[OTf] was synthesized independently by the reaction of **43** and **25** (Scheme 5.6) providing additional support for the proposed mechanism of its formation. Compound **86**[OTf] did not crystallize, and thus its molecular structure could not be determined. However, using a bulkier carbene, the related **87**[OTf] was synthesized and its structure determined by single crystal X-ray diffraction (Scheme 5.7). The connectivity of $\mathbf{87}^{+}$ was as expected, with two NHCs coordinated to a GeCl fragment (Figure 5.10). The anion, a triflate, is separated from the germanium containing complex and shows no bonding interactions with the cationic fragment.

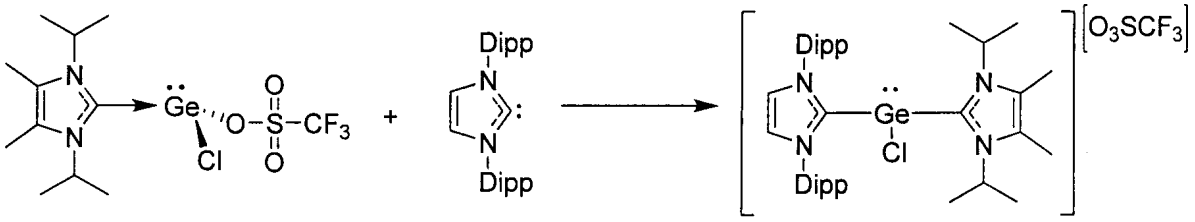

43 **87**[OTf]

Dipp = 2,6-diisopropylphenyl

Scheme 5.7

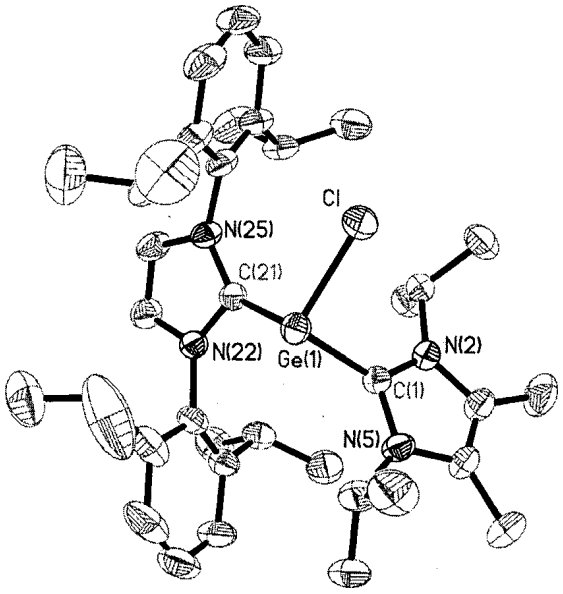

Figure 5.10: Thermal ellipsoid plot (30% probability surface) of $\mathbf{87}^{+}$. Hydrogen atoms and the triflate anion are omitted for clarity. Selected bond lengths (Å) and angles (°): Cl – Ge1 = 2.086(3); C21 – Ge1 = 2.071(2); Cl – Ge1 = 2.2560(8); C21 – Ge1 – Cl = 99.42(10); C21 – Ge1 – Cl = 98.53(7); C1 – Ge1 – Cl = 94.71(7).

$$\underset{\mathbf{8}}{GeCl_2\bullet dioxane} + Me_3SiOTf + cryptand[2.2.2] \longrightarrow \mathbf{85}[OTf]_2$$

Scheme 5.8

Although the synthesis of $\mathbf{85}[OTf]_2$ shown in Scheme 5.5 is simple to perform, the reaction is not atom economical. Alternatively, $\mathbf{85}[OTf]_2$ can be synthesized directly from $GeCl_2$·dioxane (**8**). By combining **8**, cryptand [2.2.2], and Me_3SiOTf in a solution of THF, the desired $\mathbf{85}[OTf]_2$ was formed in high yield (Scheme 5.8). The only byproducts, Me_3SiCl and 1,4-dioxane, are volatile and easily removed.

The poor solubility of $\mathbf{85}^{2+}$ makes it difficult to study. Like $\mathbf{84}^{2+}$, attempts at reducing $\mathbf{85}^{2+}$ with alkali metals were not successful and appeared to only produce

elemental germanium. Further work is still required to assess the scope of the reactivity of $\mathbf{85}^{2+}$.

5.2.3 Synthesis of Crown Ether Supported Germanium(II) Cations

The dicationic $\mathbf{85}^{2+}$ is the first example of a non-metallic cation entombed in a cryptand and represents not only a new approach to the isolation of germanium cations, but potentially other light p-block element cations as well. Cryptands are only one example of a large family of macrocyclic polyethers which are commonly used for the sequestering of metal cations. Perhaps the most commonly encountered macrocyclic polyethers are the crown ethers. Given the success in isolating the cryptand complex $\mathbf{85}^{2+}$, the synthesis and characterization of crown ether complexes of Ge(II) was pursued.

Coordination complexes between crown ethers and every type of metal ion on the periodic table have been described.[23] In the p-block, reported examples of crown ether complexes with metallic cations include Al,[24] Ga,[25] In,[25,26,27,28] Tl,[29] Sn,[30] Pb,[23] and Bi.[23] Neutral crown ether complexes of non-metals are also known, although the non-metal atom is usually situated outside of the cavity of the macrocycle.[23, 31, 32] Only a single example of a non-metal p-block cation has been reported, namely a [15]crown-5 complex of $[Sb\text{-}Cl]^{2+}$.[33]

Many different bonding modes are possible between crown ethers and guest cations. This originates from the relationship between the crown ether cavity size and the ionic radius of the guest. As a consequence, complexes of the same cation with different crown ethers of varying dimensions often exhibit strikingly different structures. For example, $In(I)^{+}$ readily fits into the cavity of [18]crown-6, but forms a "crown ether

sandwich" with two molecules of [15]crown-5.[26 - 28, 34] Given the unpredictable nature with which different sized crown ethers bind, three sizes of crown ethers were examined: [12]crown-4, [15]crown-5, and [18]crown-6.[35]

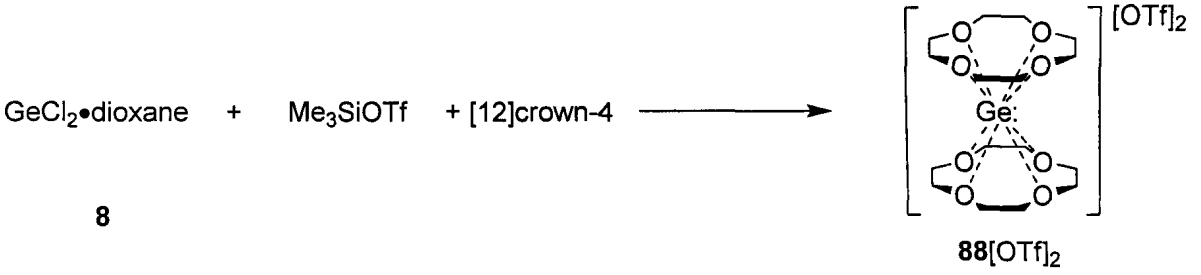

Scheme 5.9

Addition of [12]crown-4 to a solution of $GeCl_2$·dioxane (**8**) and Me_3SiOTf in THF resulted in the formation of a white precipitate that was characterized by elemental analysis, spectroscopic methods, and X-ray crystallography (Scheme 5.9). The powder was characterized as **88**$[OTf]_2$ which consists of a Ge^{2+} sandwiched by two [12]crown-4 moieties. The X-ray data were unambiguous, but were of poor quality and therefore preclude discussion of the metrical parameters (Figure 5.11).

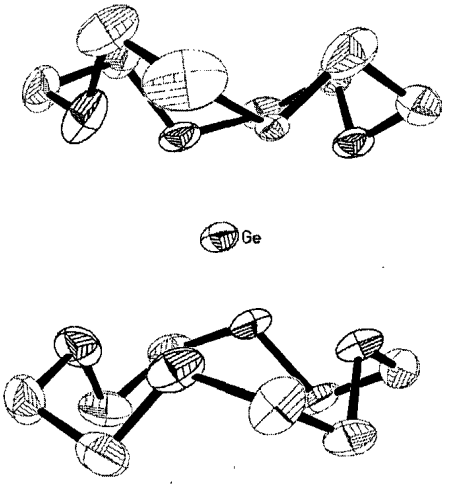

Figure 5.11 Thermal ellipsoid plot (30% probability surface) of $\mathbf{88}^{2+}$. Hydrogen atoms and triflate counter anions are omitted for clarity. The poor quality of the data set precludes discussion of the metrical parameters.

The $\mathbf{88}^{2+}$ ion can also be made as the $GeCl_3^-$ salt ($\mathbf{88}[GeCl_3]_2$) by the direct reaction of $GeCl_2$·dioxane (**8**) with [12]crown-4.[35] The structure of $\mathbf{88}[GeCl_3]_2$, like $\mathbf{88}[OTf]_2$, consists of a Ge^{2+} sandwiched by two [12]crown-4 moieties with the anions, $[GeCl_3]^-$, showing no significant interactions with the cationic fragment. The Ge-O distances in $\mathbf{88}[GeCl_3]_2$ range from 2.383(6) Å to 2.489(7) Å. These are comparable to the Ge-O distances in $\mathbf{85}^{2+}$ at 2.4856(16) Å, and are much longer than typical Ge-O single bond distances which range from 1.75 to 1.85 Å.[12, 36, 37]

The structure of $\mathbf{88}^{2+}$ clearly shows germanium residing outside the cavity of the two [12]crown-4 moieties, suggesting that [12]crown-4 is too small to accommodate a Ge^{2+} ion within its cavity. In order to determine how a larger crown ether interacts with Ge(II), the synthesis of a [15]crown-5 derivative was studied next.

Using a method similar to that used in the synthesis of $\mathbf{85}[OTf]_2$, **43** was combined with [15]crown-5 to produce small quantities of a white precipitate (Scheme 5.10).[38] Crystals suitable for single crystal X-ray diffraction were grown and the identity of the precipitate was found to be **89**[OTf] (Figure 5.12).

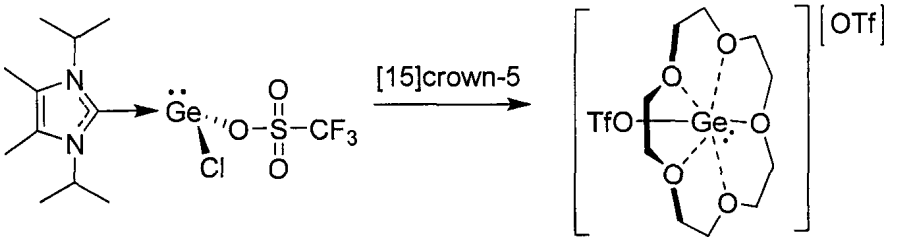

43 **89**[OTf]

Scheme 5.10

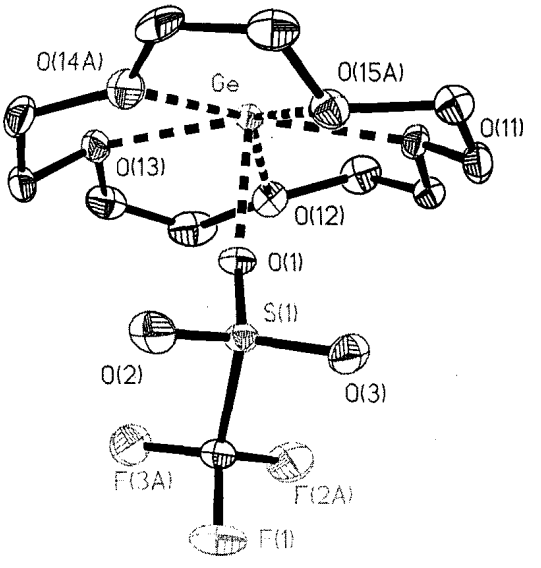

Figure 5.12 Thermal ellipsoid plot (30% probability surface) of **89**$^{+}$. Hydrogen atoms and the $^{-}$OTf counter ion are omitted for clarity. Selected distances between atoms (Å): Ge-O11 = 2.260(4), Ge-O12 = 2.233(5), Ge-O13 = 2.308(6), Ge-O14 = 2.289 (8), Ge-O15 = 2.349(6), Ge-O1 = 2.015 (3), S1-O1 = 1.451(3), S1-O2 = 1.416(6), S1-O3 = 1.423(6).

As shown in Figure 5.12, the crown ether moiety in **89**[OTf] adopts a coplanar conformation. The germanium is situated near the centroid of the ring, with Ge-O_{crown} distances ranging from 2.260(4) Å to 2.349(6) Å. One of the triflate groups in **89**[OTf] remains in close proximity to the germanium cation. Although the Ge-$O_{triflate}$ distance of 2.015(3) Å is longer than a typical Ge-O bond of 1.75-1.85 Å,[12] it is comparable to other known Ge-$O_{triflate}$ covalent interactions (i.e. in compound **43**). Furthermore, the S1-O1 bond length of 1.451(3) Å, is longer than the remaining other two sulfur-oxygen bonds at 1.416(6) and 1.423(6) Å, respectively, which is characteristic of a triflate with at least partial covalent bonding to a substituent. The second triflate group in **89**[OTf] is present

as a distinctly separate anion in the unit cell, with the closest Ge-$O_{triflate}$ distance at 3.169(6) Å.

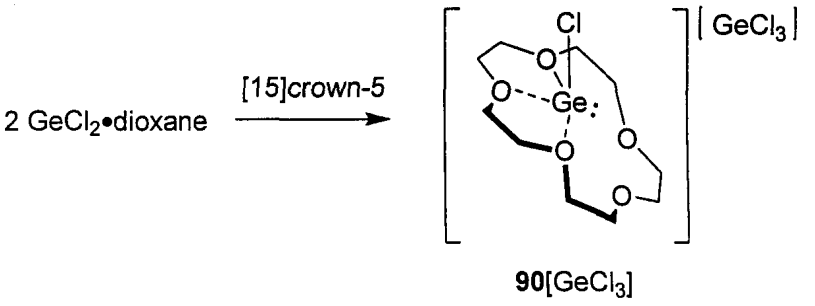

90[$GeCl_3$]

Scheme 5.11[35]

The direct reaction of $GeCl_2$·dioxane (**8**) with [15]crown-5 also produced a germanium monocationic [15]crown-5 complex (Scheme 5.11). Complex **90**[$GeCl_3$] was isolated as a white solid and characterized by single crystal X-ray diffraction (Figure 5.13).[35] The structure of $\mathbf{90}^+$ is strikingly different from $\mathbf{89}^+$ in that the crown ether adopts a bent conformation. The plane defined by Ge4, O41, O42 and O43 is almost perpendicular to the plane defined by Ge4, O45 and O44. The $^+$GeCl fragment is situated closest to O42 at a distance of 2.104(6) Å, much closer than what was observed in $\mathbf{85}^{2+}$ and $\mathbf{88}^{2+}$; two other oxygen atoms, O41 and O43, also show close contacts of 2.363(7) Å and 2.433(10) Å.

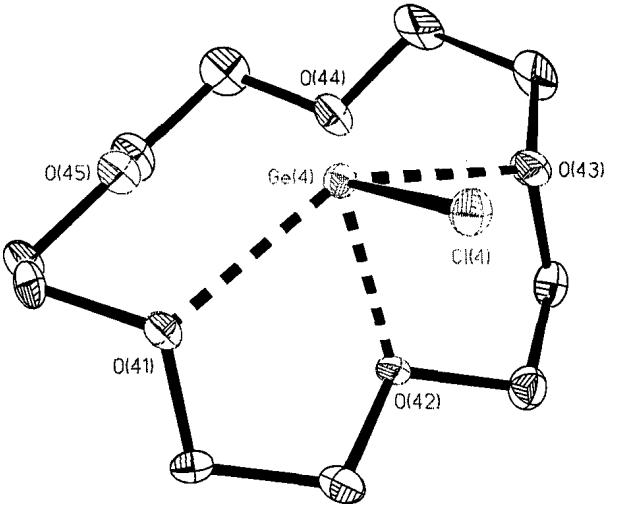

Figure 5.13 Thermal ellipsoid plot (30% probability surface) of $\mathbf{90}^+$. Only one of the four crystallographically-independent cations is illustrated; hydrogen atoms and the $^-GeCl_3$ counter ion are omitted for clarity. Selected distances between atoms (Å) (average for all 4 cations in brackets): Ge4-Cl4 = 2.293(2) [2.308(6)], Ge4-O41 = 2.363(7) [2.353(18)], Ge4-O42 = 2.104(6) [2.128(15)], Ge4-O43 = 2.433(10) [2.380(13)], Ge4-O44 = 3.044(8) [2.985(17)], Ge4-O45 = 2.835(8) [2.916(15)].[35]

The difference in structure between $\mathbf{89}^+$ and $\mathbf{90}^+$ was unexpected. The origins of this phenomenon may be due to electronic differences in the $^+$GeCl and $^+$GeOTf cations. Alternatively, crown ethers are notoriously flexible molecules and the observed geometrical differences between $\mathbf{89}^+$ and $\mathbf{90}^+$ could be a result of crystal packing effects. To help differentiate between these possibilities the benzo-crown ether derivatives of $\mathbf{89}^+$ and $\mathbf{90}^+$ were synthesized and characterized.

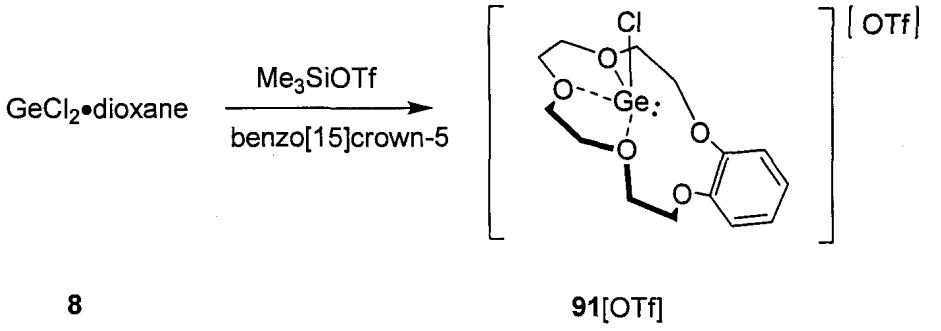

8 **91**[OTf]

Scheme 5.12

The benzo[15]crown-5 derivative of $\mathbf{90}^+$ was made from the reaction of $GeCl_2$·dioxane (**8**), Me_3SiOTf and benzo[15]crown-5 (Scheme 5.12). The solid state structure of $\mathbf{91}^+$, as a triflate salt, was determined and found to be very similar to the structure of $\mathbf{90}^+$ (Figure 5.14). Specifically, the benzo-crown is bent with a folded conformation with an angle of 89.3° (the planes are defined by Ge, O12, O13 and O15 versus Ge, O15 and O11). Like $\mathbf{90}^+$, the $^+$GeCl fragment in $\mathbf{91}^+$ is bound asymmetrically by the crown ether and is situated closest to O13 at a distance of 2.147(4) Å. Two other oxygen atoms, O12 and O14, also show close contacts of 2.232(4) Å and 2.473(10) Å. The two remaining oxygen atoms, O11 and O15, are situated significantly farther away at 2.889(4) Å and 2.971(3) Å as a result of the folding of the ring.

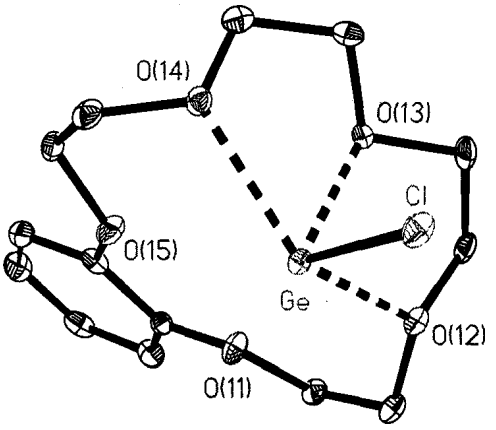

Figure 5.14: Thermal ellipsoid plot (30% probability surface) of $\mathbf{91}^+$. Hydrogen atoms and the $^-$OTf counter ion are omitted for clarity. Selected distances between atoms (Å): Ge-O13 = 2.147(4), Ge-O12 = 2.232(4), Ge-O14 = 2.473(4), Ge-O11 = 2.889(4), Ge-O15 = 2.971(3), Ge-Cl = 2.2880(16).

The benzo[15]crown-5 derivative of $\mathbf{89}^+$ was synthesized by the exchange of the chloride in $\mathbf{91}^+$ using **43** to give **92**[OTf] (Scheme 5.13). Although the poor quality of the data set for **92**[OTf] precludes discussion of the metrical parameters, the data did show unambiguously that the crown ether adopts a planar conformation (Figure 5.15).

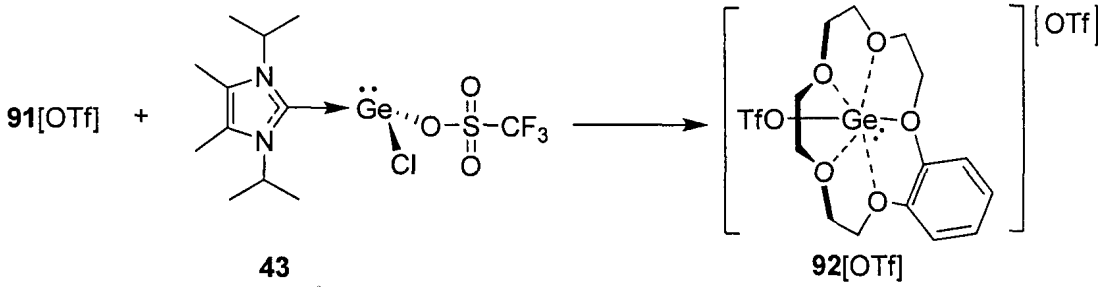

Scheme 5.13

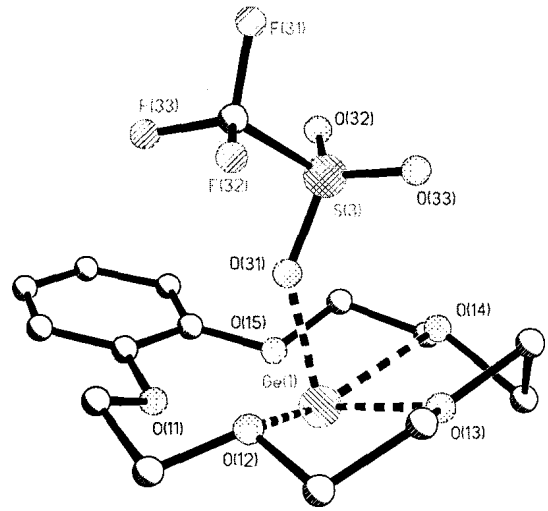

Figure 5.15: Isotropic thermal ellipsoid plot (30% probability surface) of **92**$^{+}$. Hydrogen atoms and triflate counter anions are omitted for clarity. The poor quality of the data set precludes discussion of the metrical parameters.

Since both the [15]crown-5 and benzo[15]crown-5 adopt the same bent conformations towards the $^{+}$GeCl cation while maintaining a planar conformation when bound to the $^{+}$GeOTf cation it can be concluded that these differences are probably not due to crystal packing effects. A possible explanation for these observed differences is that the Ge-Cl bonds in **90**$^{+}$ and **91**$^{+}$ are less polarized than the Ge-$O_{triflate}$ bonds in **89**$^{+}$ and **92**$^{+}$. As a result, the germanium atom of the Ge-$O_{triflate}$ systems carries a more positive charge which would shrink the radius of the germanium making it more electrophilic and better able to fit into the cavity of [15]crown-5.

[18]crown-6 complexes of Ge(II) were formed using the same techniques used in the synthesis of the [15]crown-5 compounds.[35] The direct reaction of 2 equivalents of $GeCl_2$·dioxane (**8**) with [18]crown-6 resulted in the formation of **93**[$GeCl_3$] (Scheme 5.14). The structure of **93**[$GeCl_3$] was determined by single crystal X-ray diffraction and

consists of a cationic $(GeCl[18]crown\text{-}6)^+$ moiety with a $[GeCl_3]^-$ anion (Figure 5.16). The Cl-Ge^+ fragment is ligated in a planar fashion with the Ge centre offset from the centroid of the crown ether oxygen atoms. The closest germanium-oxygen distance is 2.195(3) Å for the Ge1–O11 interaction. The remaining Ge–O distances are significantly longer, ranging from 2.359(4) to 3.237(4) Å; this is likely a consequence of the larger cavity size of the [18]crown-6 ring being too large to bind the Ge cation in a symmetrical manner.

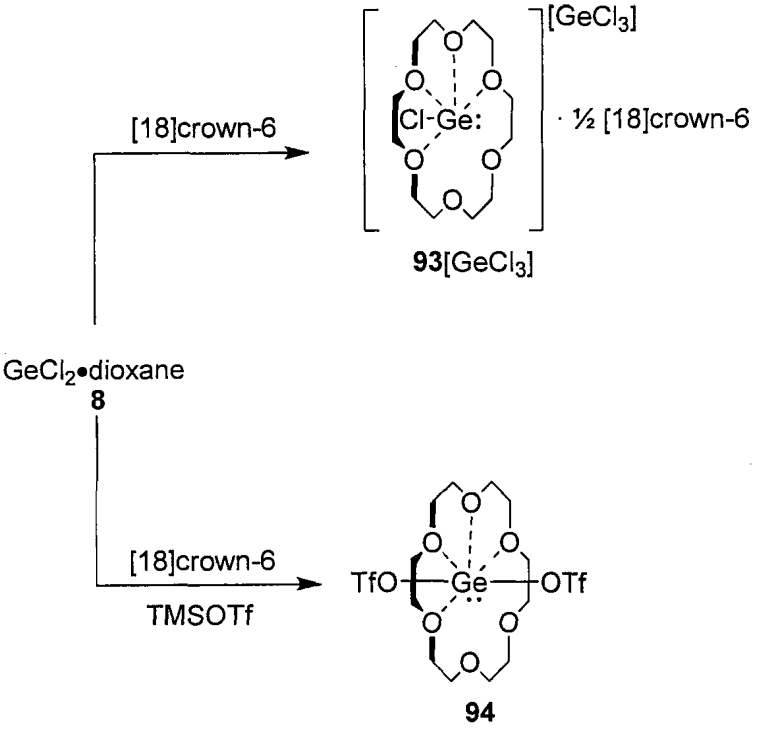

Scheme 5.14[35]

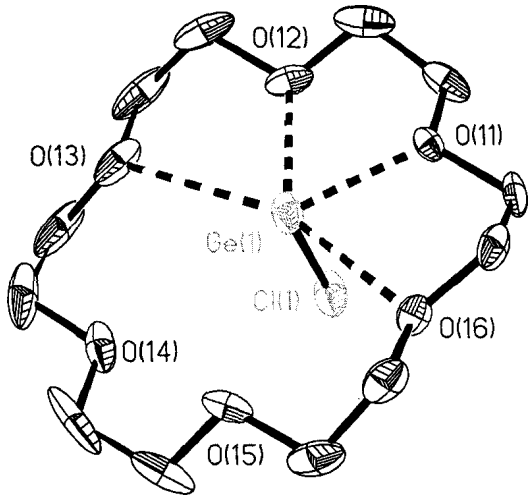

Figure 5.16 Thermal ellipsoid plot (30% probability surface) of $\mathbf{93}^{+}$. Hydrogen atoms, the $^{-}GeCl_3$ counter ion, and the [18]crown-6 solvate molecule are omitted for clarity. Selected distances between atoms (Å): Ge1-Cl1 = 2.201(1), Ge1-O11 = 2.195(3), Ge1-O12 = 2.359(4), Ge1-O13 = 2.869(5), Ge1-O14 = 3.237(4), Ge1-O15 = 3.076(4), Ge1-O16 = 2.640(4).

Finally, to observe the interaction of the larger crown ether with the triflate substituents, $GeCl_2$·dioxane (**8**) was treated with [18]crown-6 and two equivalents of Me_3SiOTf in THF (Scheme 5.14). Suitable single crystals were grown and identified as $Ge(OTf)_2$·[18]crown-6 (**94**), which, surprisingly, consists of a symmetrical $Ge(OTf)_2$ fragment located within the cavity of [18]crown-6 (Figure 5.17). As in $\mathbf{93}^{+}$, the germanium atom is located away from the centroid of the oxygen atoms in the crown ether and is much closer to the O11 and O11A atoms at 2.218(3) Å than the remaining oxygen atoms (two at 2.673(3) Å and two at 3.159(4) Å). The crown ether in **94** is noticeably distorted with the oxygen atoms labelled O13 and O13A being located out of the plane defined by Ge and the other four O atoms in the ligand. The distant O atoms

appear to be oriented in a manner that is not suitable for donation to the Ge center. The triflate-oxygen-germanium bonds are long at 2.204(5) Å and, although they appear incipient towards ionization, **94** is clearly not an ion separated system as observed for the other crown ether germanium salts.

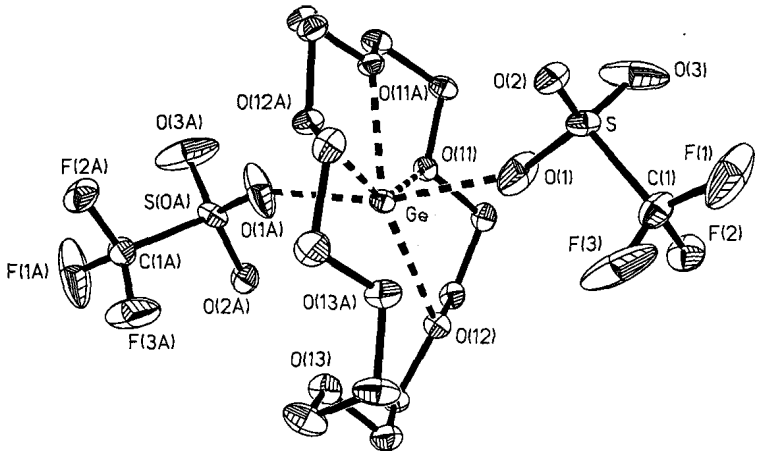

Figure 5.17 Thermal ellipsoid plot (30% probability surface) of **94**. Hydrogen atoms are omitted for clarity. Selected distances between atoms (Å): Ge-O11 = 2.218(3), Ge-O12 = 2.673(3), Ge-O13 = 3.159(4), Ge-O1 = 2.204(5), S-O1 = 1.448(5), S-O2 = 1.422(4), S-O3 = 1.397(6).

5.3 Conclusions

In summary, the synthesis and characterization of mono and dicationic germanium(II) compounds, stabilized by intermolecular donors, was presented. Prior to this work, there were no reported examples of dicationic germanium(II) compounds.

The carbene supported $\mathbf{84}^{2+}$ is the first example of a dicationic germanium(II) complex and was synthesized by the nucleophilic displacement of iodides from the germanium centre by two NHCs. Spectroscopic evidence of the new complex is

consistent with a discrete cation anion pair despite the dicationic charge and the presence of the relatively nucleophilic iodide anions.

The complex $\mathbf{85}^{2+}$ is the first example of a non-metal cation situated within a cryptand. Computational analysis of the germanium centre reveals that its electronic state bares some resemblance to that of a naked Ge^{2+} ion. Crown ethers were also shown to be suitable ligands for the stabilization of cationic germanium(II) systems, the structural properties of which are highly dependent on the size of crown ether used and on the substituents on germanium.

The surprising ease at which the cryptand and crown ethers promote the ionization of Ge(II) demonstrates the effectiveness of these macrocycles in isolating otherwise elusive cationic germanium species. As a result of the simplicity of the synthetic approach and the large number of cryptands and crown ethers available to accommodate cations of different sizes, we anticipate that cationic species of other non-metallic elements will be isolated in the future.[39]

5.4 Experimental

All manipulations were carried out under an anhydrous N_2 atmosphere using standard Schlenk line and glove box techniques at room temperature. Benzene, tetrahydrofuran (THF), CH_2Cl_2, toluene, and CH_3CN were dried by passing through an alumina column[40] and then stored over 4 Å molecular sieves. CD_3CN and CD_2Cl_2 were distilled over CaH_2 and then stored over 4 Å molecular sieves. NMR chemical shifts are reported in ppm. The ^1H NMR spectra were referenced internally to the residual CD_2HCN resonance at 1.94 ppm or the $CDHCl_2$ resonance at 5.32 ppm. The ^{19}F NMR spectra were referenced

externally to $CFCl_3$ (0 ppm) or to C_6H_5F (-113.1 ppm relative to $CFCl_3$). Elemental analysis was performed at Guelph Chemical Laboratories, Guelph, Ontario, Canada. $GeCl_2$·dioxane (**8**)[41] was synthesized according to literature procedures. All other chemicals were purchased from commercial sources and used without further purification. FT-Raman spectra of the bulk material are reported in cm^{-1} and were collected under a N_2 atmosphere in a sealed tube. Melting points were determined under a N_2 atmosphere and are uncorrected. Compounds **88**$[GeCl_3]_2$, **90**$[GeCl_3]$, **93**$[GeCl_3]$, and **94** were synthesized by Rajoshree Bandyopadhyay.[35]

5.4.1 Synthesis of 84$[I]_2$

42 (0.56 g, 1.1 mmol) was dissolved in THF (5 mL) to give a yellow solution. Carbene **25** (0.5 g, 2.75 mmol) was dissolved in THF (3 mL) and then added drop wise to the yellow solution. During addition the yellow colour faded and a white precipitate formed. The reaction mixture was stirred vigorously for 18 hr. The white precipitate was collected by centrifugation, washed with THF (2 x 5 mL) and then dried under high vacuum. Yield: 0.80g (84%). M. P. 158- 162 °C (decomposition). See Figures 5.2 and 5.3 for ^1H NMR spectra. FT-Raman (cm^{-1}): 85 (m), 304 (w), 694 (w), 764 (w), 885 (w), 1277 (s), 1349 (m), 1397 (m), 1442 (m), 1621 (m), 2927 (s), 2970 (s); Anal. Calcd for $C_{33}H_{40}N_4GeI_2$: C, 40.53; H, 6.23; N, 8.65; Found: C, 40.53; H, 6.43; N, 8.91.

5.4.2 The Reaction of 43 with Cryptand [2.2.2]

In a 50 mL round bottom flask, compound **43** (0.20 g, 0.457 mmol) was dissolved in THF (5 mL). Cryptand [2.2.2] (0.06 g, 0.152 mmol) was added to the stirring solution.

The cryptand quickly dissolved, resulting in a clear and colourless solution. After 5 minutes, a white precipitate was observed. The mixture was stirred for 24 hours at room temperature, after which time the precipitate was collected by centrifugation. The supernatant was removed and the precipitate was washed with THF (3 mL). The precipitate was dried under high vacuum to give **85**$[OTf]_2$ (0.10 g, 88%). Crystals suitable for single crystal x–ray diffraction were grown by diffusing diethyl ether into a saturated solution of **85**$[OTf]_2$ in CH_3CN. The supernatant and THF wash were combined in another 50 mL round bottom flask. Removal of solvent yielded a colourless amorphous paste. The paste was triturated with Et_2O (8 mL × 4) to give a white powder identified as **86**[OTf] (0.09 g, 96%) which was confirmed by comparison to the NMR spectral data and ESI-MS spectrograph of an authentic sample (see below). The Et_2O washes were combined in a new 50 mL round bottom flask and the solvent was removed under high vacuum yielding a white powder identified as **39** (0.04 g, 81%) along with trace amounts of unreacted cryptand [2.2.2]. **39** can be purified by washing with hexanes to remove the cryptand. The identity of **39** was confirmed by comparison of the NMR spectral data with those of an authentic sample (See Chapter 3). The purity of both **86**[OTf] and **39** after isolation from the reaction mixture were estimated to be > 90 % by ^1H NMR spectroscopy. Characterization of **85**[OTf]: M. P. 158–160 °C. ^1H NMR (CD_3CN): δ 3.89 (singlet), 3.88 (triplet, $^3J_{HH}$ = 5 Hz) (total 24H), 2.95 (triplet, $^3J_{HH}$ = 5 Hz, 12 H). ^{19}F NMR (CD_3CN): δ -79.36 (singlet). FT-Raman (cm^{-1}): 84 (s), 106 (m), 174 (w), 291 (w), 315 (m), 349 (m), 411 (w), 517 (w), 574 (w), 739 (w), 758 (m), 847 (w), 914 (w), 934 (w), 1033 (s), 1071 (w), 1135 (w), 1170 (w), 1226 (w), 1268 (m), 1286 (m), 1379 (w), 1455 (m), 1488 (m), 2852 (m), 2902 (s), 2939 (s), 3001 (m). Anal. Calcd

for $C_{20}H_{36}F_6GeN_2O_{12}S_2$: Expected: C, 32.15; H, 4.86; N, 3.75. Found: C, 32.44; H, 5.10 N, 3.69. ESI/MS (+ve mode): *m/z* 749 [Cryptand·Ge·OTf_2H^+, <1 %], 599 [Cryptand·Ge·OTf^+, 60%], 225 [Cryptand·Ge^{2+}, 7 %].

5.4.3 Direct Synthesis of 86[OTf]

In a 50 mL round bottom flask, compound **43** (0.20 g, 0.34 mmol) was dissolved in C_6H_6 (5 mL). **25** (0.07 g, 0.39 mmol) was added to the reaction mixture which was stirred for 30 min. The solution turned cloudy and then two distinct liquid layers were observed. Et_2O (10 mL) was added to the reaction mixture which was stirred for an additional 15 min. After this time, a white precipitate was observed. The precipitate was collected, washed with Et_2O, and then dried under vacuum. The precipitate was characterized as **86**[OTf] (0.18 g, 86 %). Repeated attempts to grow crystals of **86**[OTf] suitable for single crystal X-ray diffraction were not successful. M. P. 120–121 °C. ^{1}H NMR (THF-d_8): δ 5.17 (septet, $^3J_{HH}$ = 7.2 Hz, 2 H), 2.38 (singlet, 6H), 1.48 (doublet, $^3J_{HH}$ = 7.8 Hz) 1.47 (doublet, $^3J_{HH}$ = 7.8 Hz). ^{19}F NMR (THF-d_8): δ -77.19 (singlet). FT-Raman (cm^{-1}): 118 (w), 276 (w), 311 (s), 348 (w), 460 (w), 531 (w), 543 (w), 573 (w), 587 (w), 692 (w), 752 (w), 766 (w), 884 (w), 1032 (s), 1136 (w), 1271 (m), 1286 (s), 1353 (m), 1415 (m), 1442 (s), 1630 (s), 2942 (s), 2985 (s). Anal. Calcd for $C_{23}H_{40}ClF_3GeN_4O_3S$: Expected: C, 44.72; H, 6.53; N, 9.07. Found: C, 43.96; H, 6.77, N 8.69. ESI/MS (+ve mode): *m/z* 469 [$(NHC)_2$·Ge·Cl^+, 25%], 289 [NHC·Ge·Cl^+, 100%].

5.4.4 Synthesis of 85[OTf]$_2$ from GeCl$_2$·Dioxane (8)

To a solution of **8** (0.50 g, 2.2 mmol) and cryptand[2.2.2] (0.81 g, 2.2 mmol) in THF (20 mL) was added Me_3SiOTf (0.74 mL, 4.3 mmol). The reaction mixture was stirred vigorously. After about 1 min a white precipitate began to form. The reaction mixture was stirred for an additional 1.5 hr. The white precipitate was collected, washed with THF (10 mL) and dried under vacuum. The white precipitate was identified as **85**[OTf]$_2$.

5.4.5 Synthesis of 88[OTf]$_2$

[12]crown-4 (0.14 mL, 0.86 mmol) was added to a GeCl$_2$·dioxane (**8**) (0.10 g, 0.43 mmol) solution in THF (2 mL). The solution was allowed to stir for 5 min, after which time Me_3SiOTf (0.15 mL, 0.86 mmol) was added. After the reaction mixture was stirred for 1 hr, hexanes (5 mL) was added. A white precipitate formed, which was collected and then washed with Et_2O (4 mL x 2). The precipitate was identified as [Ge·[12]crown-4][OTf]$_2$ (**88**[OTf]$_2$) (0.15 g, 49 %). Crystals suitable for single X-ray diffraction were obtained by slow diffusion of pentane into a saturated THF solution of **88**[OTf]$_2$. M. P.: 156 – 160 °C. ^{1}H NMR (CD_3CN): δ 3.96. ^{19}F NMR (CD_3CN): δ -79.4 FT-Raman (ranked intensities): 313(6), 349(5), 366(12), 494(13), 573(10), 754(7), 853(4), 909(14), 1032(2), 1069(16), 1105(15), 1224(11), 1264(9), 1451(8), 2896(3), 2954(1). ESI/MS(+ mode) m/z: 199 [([12]crown-4)·Na, 100%] 399 [GeOTf·([12]crown-4), 50%], 575 ($GeOTf_2$·([12]crown-4), 5 %]. Anal. Calcd for $C_{18}H_{32}F_6GeO_{14}S_2$: C, 29.89; H, 4.46. Found: C, 30.24; H, 4.29.

5.4.6 Synthesis of 89[OTf]

A solution of [15]crown-5 (0.568 g, 2.59 mmol) and Me_3SiOTf (933 μL, 5.16 mmol) in THF was added to a solution of $GeCl_2$.dioxane (**8**) (0.600 g, 2.59 mmol) in THF. The resultant colorless solution was left to stir for 24 hours. All volatile components were then removed under reduced pressure. The oily residue was washed with pentane (5 mL x 3) to give a white solid which was recrystallized from CH_2Cl_2. The crystalline material was characterized as **89**[OTf] (0.600 g, 39%). Surprisingly, the solution ^{19}F NMR spectrum of **89**[OTf] showed only a single ^{19}F resonance, at both room temperature and -90 °C, rather than the two expected distinct signals. The single ^{19}F resonance at -79 ppm is consistent with anionic triflates and suggests that, in solution, $\mathbf{89}^+$ may exist as a dication rather than as the monocation seen in the solid state structure. The rapid exchange of bound and free triflate fragments is another possible explanation for this observation. ^1H NMR (CD_3CN): 4.02. ^{19}F NMR (CD_3CN): -80.0. M. P.: 128 – 131 °C. FT-Raman (ranked intensities): 313(11), 348(3), 534(15), 572(12), 755(6), 764(7), 857(4), 997(10), 1030(1), 1094(14), 1138(13), 1236(9), 1473(8), 2894(5), 2965(2). ESI/MS(+ mode) m/z: 259 [K·[15]crown-5 , 100%], 443 [GeOTf·[15]crown-5, 10%]. Anal. Calcd for $C_{18}H_{32}F_6GeO_{14}S_2$: C, 24.39; H, 3.41; O, 29.78. Found: C, 23.92; H, 3.12; O, 30.18.

5.4.7 Synthesis of 91[OTf]

To a suspension of $GeCl_2$·dioxane (**8**) (0.10 g, 0.43 mmol) in C_6H_6 (5 mL) was added benzo[15]crown-5 (0.12 g, 0.43 mmol). The mixture was stirred for 5 min after which Me_3SiOTf (157 uL, 0.86 mmol) was added. The reaction mixture was stirred for 18 hr.

Pentane (10 mL) was added to complete the precipitation of a white precipitate. The precipitate was identified as [GeCl·benzo[15]crown-5][OTf] (**91**[OTf]) (0.19 g, 83 %). Crystals suitable for single crystal X-ray diffraction were obtained by slow diffusion of Et_2O into a saturated THF solution of **91**[OTf]. M.P. 128 – 130 °C. ^{1}H NMR (CD_3CN): δ 3.97-3.99 (multiplet, 4H), 4.07-4.10 (multiplet, 4H), 4.26 (singlet, 8H), 7.03 (singlet, 4H). ^{19}F NMR (CD_3CN): δ -79.3 FT-Raman (ranked intensities): 311(1), 465(18), 503(17), 573(9), 756(7), 777(16), 836(3), 1029(2), 1052(6), 1124(15), 1164(14), 1255(12), 1320(13), 1454(10), 1594(8), 2897(11), 2952(4), 3074(5). ESI/MS (+ mode) *m/z:* 269 [(benzo[15]crown-5)·H, 30 %], 377 [(benzo[15]crown-5)·GeCl, 100 %]. Anal. Calcd for $C_{15}H_{20}ClF_3GeO_8S$: C, 34.29; H, 3.84. Found: C, 34.33; H, 4.14.

5.4.8 Synthesis of 92[OTf]

To a solution of **91**[OTf] (0.06 g, 0.11 mmol) in THF (4 mL) was added **43** (0.05 g, 0.11 mmol). The reaction mixture was stirred for 18 hr. A white precipitate was collected by centrifugation and washed with C_6H_6 (4 mL x 2) and then pentane (4 mL x 2). The precipitate was identified as [GeOTf·benzo[15]crown-5][OTf] (**92**[OTf]) (0.06 g, 86%). Crystals suitable for single crystal X-ray diffraction were obtained by slow diffusion of Et_2O into a saturated solution THF solution of **92**[OTf]. M.P.: 128 – 130 °C. ^{1}H NMR (CD_3CN): 4.14-4.16 (multi, 4 H), 4.23-4.25 (multiplet, 4 H), 4.36-4.38 (multiplet, 4 H), 4.42-4.45 (multi, plet 4 H), 7.14 (singlet, 4 H). ^{19}F NMR (CD_3CN): -79.3 FT-Raman (relative intensity): 305(7), 349(6), 575(14), 607(13), 763(5), 830(10), 993(1), 1032(2), 1133(15), 1176(11), 1242(8), 1467(12), 1595(9), 2891(16), 2952(3), 3072(4). ESI/MS (+ mode) *m/z*: 269 [benzo[15]-crown-5·H, 7 %], 291 [benzo[15]crown-

5·Na, 38 %], 491 [benzo[15]crown-5·GeOTf, 100 %]. Anal. Calcd for $C_{16}H_{20}F_6GeO_{11}S_2$: C, 30.07; H, 3.15. Found: C, 29.80; H, 3.37.

5.4.9 Computational Details for 84^{2+}

Calculations were performed at the B3LYP/6-31G(d) level of theory using Gaussian 03.[42] The molecular structure of $\mathbf{84}^{2+}$ as determined by X-ray crystallography, with the iodides and pyridine removed, was used as the import coordinates for the geometry optimization. The symmetry of the molecule (C_3) was maintained during the geometry optimization. Vibrational frequency analysis confirmed that the optimized geometry is an energy minimum. Appendix 1.7 contains the commands issued to Gaussian 03 for the calculations.

5.4.10 Computational Details for 85^{2+}

Calculations were performed at the PBE1PBE/6-311+G(2d,p) level of theory using Gaussian 03.[42] Both the MO visualization and NBO calculations were performed on the unoptimizied coordinates from the solid state structure of $\mathbf{85}^{2+}$. Appendix 1.8 contains the commands issued to Gaussian 03 for the calculations.

5.4.11 X-ray Crystallography Experimental Details

Each crystal was covered in Nujol and placed rapidly into the cold N_2 stream of a Kryo-Flex low temperature device. The data were collected either by employing the SMART[43] software on a Bruker APEX CCD diffractometer or by using the COLLECT[44] software on a Nonius KAPPA CCD diffractometer, each being equipped with a graphite

monochromator with Mo Kα radiation (λ = 0.71073 Å). For each sample, a hemisphere of data was collected using counting times of 10-30 seconds per frame. The data were collected at either -100 or -123 °C. Details of crystal data, data collection and structure refinement are listed in Table 5.1. Data reductions were performed using the SAINT[45] software and the data were corrected for absorption using SADABS[46] or using the DENZO-Scalepack application.[47] The structures were solved by direct methods using either the SHELX[48] suite of programs or SIR97[49] and refined by full-matrix least-squares on F^2 with anisotropic displacement parameters for the non-H atoms using SHELXL-97[48] and the WinGX[50] software package. Details of the final structure solutions were evaluated using PLATON[51] and thermal ellipsoid plots were produced using SHELXTL.[48]

A highly disordered solvent molecule, presumed to be THF, was present in the unit cell of **87**[OTf]. The electron density associated with the disordered solvent was removed using SQUEEZE as implemented in PLATON.[51]

Disorder of the crown ether ring positions (and sometimes in the orientation of the triflate ions) was observed in some instances. When necessary, the disorder was modeled using crown ether fragments in two different orientations and appropriate restraints were employed, including: restraining the thermal parameters for the atoms in each part of the crown ether models to be similar; restraining the geometrical parameters of related crown ethers (or related triflate fragments) to be similar; or restraining related C-O and/or C-C bonds in a crown ether to be similar.

Table 5.1: Crystallographic data for compounds **84**$[I]_2$, **85**$[OTf]_2$, **87**[OTf], **88**$[GeCl_3]_2$, **88**$[OTf]_2$, **89**[OTf], **90**$[GeCl_3]$, **90**[OTf], **92**[OTf], **93**$[GeCl_3]$ and **94**.

Compound	**84**$[I]_2$·pyridine	**85**$[OTf]_2$	**87**[OTf]
CCDC number	N/A	704541	N/A
Empirical formula	$(C_{11}H_{20}N_2)_3Ge$, 2I, C_5H_5N	$C_{20}H_{36}F_6GeN_2O_{12}S_2$	$C_{39}H_{56}ClF_3GeN_4O_3S$
Formula weight	946.36	747.26	825.98
Crystal system	Cubic	Trigonal	Monoclinic
Space group	$P2_13$	P321	C 2/c
a (Å)	16.3681(3)	8.9735(3)	18.6247(4)
b (Å)	16.3681(3)	8.9735(3)	17.5705(4)
c (Å)	16.3681(3)	10.6762(9)	29.4008(6)
α (°)	90	90	90
β (°)	90	90	91.7920(9)
γ (°)	90	120	90
Volume ($Å^3$)	4385.25(14)	744.51(7)	9616.6(4)
Z	4	1	8
Data/restraints/ parameters	3366/0/153	1143 / 0 / 66	11017/0/483
Goodness-of-fit F^2 (all data)	1.199	1.093	1.046
Final R indices [$I>2\sigma(I)$]	0.0632	0.0334	0.0511
wR2 indices (all data)	0.1427	0.0897	0.0801
Largest diff. peak and hole ($eÅ^{-3}$)	1.661 -0.581	0.596, -0.335	0.913, -0.833

Compound	**88**$[GeCl_3]_2$ ·[12]crown-4	**88**$[OTf]_2$	**90**$[GeCl_3]$	**89**[OTf]
CCDC number	722426	N/A	722424	722427
Empirical formula	$C_{24}H_{48}Cl_6Ge_3O_{12}$	$C_{18}H_{32}F_6GeO_{10}S_2$	$C_{10}H_{20}Cl_4Ge_2O_5$	$C_{12}H_{20}F_6GeO_{11}S_2$
Formula weight	959.09	723.17	507.24	590.99
Crystal system	Triclinic	Triclinic	Orthorhombic	Orthorhombic
Space group	P-1	P-1	$Pca2_1$	Pnma
a (Å)	9.942(2)	17.153(3)	30.431(4)	12.690(3)
b (Å)	10.226(2)	19.627(4)	9.9330(13)	11.631(2)
c (Å)	11.402(2)	25.755(5)	24.209(3)	14.340(3)
α (°)	100.663(2)	90.52(3)	90	90
β (°)	109.605(2)	102.43(3)	90	90
γ (°)	110.350(2)	90.32(3)	90	90
Volume ($Å^3$)	962.2(3)	8467(3)	7317.6(16)	2116.5(7)

Z	1	12	16	4
Data/restraints/ parameters	4247/240/314		16511/20/753/	2541/ 0/237
Goodness-of-fit F^2 (all data)	1.149		1.127	1.080
Final R indices [$I>2\sigma(I)$]	0.0418		0.0718	0.0510
wR2 indices (all data)	0.1386		0.1251	0.1211
Largest diff. peak and hole ($eÅ^{-3}$)	0.846 -0.590		1.265 -1.064	0.491 -0.735

Compound	**90**[OTf]	**92**[OTf]	**93**[$GeCl_3$]· ½[18]crown-6
CCDC number	722423	N/A	722425
Empirical formula	$C_{15}H_{20}ClF_3GeO_8S$	$C_{16}H_{20}F_6GeO_{11}S_2$	$C_{18}H_{36}Cl_4Ge_2O_9$
Formula weight	525.41	639.06	683.45
Crystal system	Triclinic	Triclinic	Triclinic
Space group	P-1	P-1	P-1
a (Å)	9.756(2)	13.508(2)	8.5971(15)
b (Å)	9.861(2)	13.784(2)	9.9838(18)
c (Å)	11.836(3)	13.922(2)	17.176(3
α (°)	75.527(3)	101.382(1)	85.803(2)
β (°)	73.229(3)	115.411(1)	76.152(2)
γ (°)	72.522(3)	90.343(2)	88.244(2)
Volume ($Å^3$)	1023.2(4)	2283.3(5)	1427.4(4)
Z	2	4	2
Data/restraints/ parameters	4532/262/0		6319/298/0
Goodness-of-fit F^2 (all data)	1.090		1.051
Final R indices [$I>2\sigma(I)$]	0.0831		0.0625
wR2 indices (all data)	0.1288		0.1551
Largest diff. peak and hole ($eÅ^{-3}$)	0.942 -0.702		0.668 -1.161

Compound	**94**
CCDC number	722428
Empirical formula	$C_{14}H_{24}F_6GeO_{12}S_2$
Formula weight	635.04
Crystal system	Monoclinic
Space group	C2/c
a (Å)	16.197(3)
b (Å)	11.2074(18)
c (Å)	14.163(2)
α (°)	90
β (°)	112.905(2)
γ (°)	90
Volume (Å^3)	2368.3(7)
Z	4
Data/restraints/ parameters	2690//0/159
Goodness-of-fit F^2 (all data)	1.075
Final R indices [$I>2\sigma(I)$]	0.0644
wR2 indices (all data)	0.1586
Largest diff. peak and hole (eÅ^{-3})	0.927 -0.479

5.5 References

1. (a) Lee, V. Y.; Sekiguchi, A. *Acc. Chem. Res.* **2007**, *40*, 410. (b) Lee, V. Y.; Sekiguchi, A. In *Reviews of Reactive Intermediate Chemistry;* Platz, M. S., Moss, R. A, Jones Jr., M., Eds; John Wiley & Sons, Inc., Hoboken, New Jersey, **2002**, pg 47. (c) Müller, T. *Adv. Organomet. Chem.* **2005**, *53*, 155. (d) Zharov, I.; Michl, J. In *The Chemistry of Organic Germanium, Tin and Lead Compounds Vol. 2,* Rappoport, Z; Apeloig, Y., Eds; Wiley & Sons, Chichester, **2002**, pg 633. (e) Reed, C. A. *Acc. Chem. Res.* **1998**, *31*, 325.

2. Kim, K.; Reed, C. A.; Elliott, D. W.; Mueller, L. J.; Tham, F.; Lambert, J. B. *Science* **2002**, *297*, 825.

3. Sekiguchi, A.; Fukawa, T.; Lee, V. Ya.; Nakamoto, M.; Ichinohe, M. *Angew. Chem., Int. Ed.* **2003**, *42*, 1143.

4. Sekiguchi, A.; Tsukamoto, M.; Ichinohe, M. *Science* **1997**, *275*, 60.

5. Schenk, C.; Drost, C.; Schnepf, A. *Dalton Trans.* **2009**, 773.

6. Cosledan, F.; Castel, A.; Rivière, P.; Satgé, J.; Veith, M.; Huch, V. *Organometallics* **1998**, *17*, 2222. (b) Schmidt, H.; Keitemeyer, S.; Neumann, B.; Stammler, H.; Schoeller, W. W.; Jutzi, P. *Organometallics* **1998**, *17*, 2149. (c) Ichinohe, M.; Fukui, H.; Sekiguchi, A. *Chem. Let.* **2000**, 600.

7. Khrustalev, V. N.; Portnyagin, I. A.; Borisova, I. V.; Zemlyansky, N. N.; Ustynyuk, Y. A.; Antipin, M. Y.; Nechaev, M. *Organometallics* **2006**, *25*, 2501.

8. (a) Stender, M.; Phillips, A. D.; Power, P. P. *Inorg. Chem.* **2001**, *40*, 5314. (b) Dias, H. V. R.; Wang, Z. *J. Am. Chem. Soc.* **1997**, *119*, 4650. (c) Probst, T.; Steigelmann, O.; Riede, J.; Schmidbaur, H. *Angew. Chem. Int., Ed. Engl.* **1990**, *29*, 1397.

9. (a) Jutzi, P.; Hampel, B. *Organometallics* **1986**, *5*, 730. (b) Jutzi, P.; Kohl, F.; Hofmann, P.; Kruger, C.; Tsay, Y. H. *Chem. Ber.* **1980**, *113*, 757.

10. The use of neutral ligands to promote the formation of highly charged p-block compounds has strong precedence in inorganic chemistry. Selected examples: (a) Dutton, J. L.; Tuononen, H. M.; Ragogna, P. J. *Angew. Chem., Int. Ed.* **2009**, *48*, 4409. (b) Vidovic, D.; Findlater, M.; Cowley, A. H. *J. Am. Chem. Soc.* **2007**, *129*, 8436. (c) Hensen, K.; Stumpf, T.; Bolte, M.; Näther, C.; Fleischer, H. *J. Am. Chem. Soc.* **1998**, *120*, 10402.

11. Gillespie, R.J.; Popelier, P.L.A. In *Chemical Bonding and Molecular Geometry*, Oxford University Press, Oxford, **2002**.

12. Baines, K. M.; Stibbs, W. G. *Coord. Chem. Rev.* **1995**, *145*, 157.

13. Bondi, A. *J. Phys. Chem.* **1964**, *68*, 441.

14. The IUPAC Compendium of Chemical Terminology (2006) defines a dative bond as "The coordination bond formed upon interaction between molecular species, one of which serves as a donor and the other as an acceptor of the electron pair to be shared in the complex formed. In spite of the analogy of dative bonds with covalent bonds, in that both types imply sharing a common electron pair between two vicinal atoms, the former as distinguished by their significant polarity, lesser strength, and greater length. The distinctive feature of dative bonds is that their minimum-energy rupture in the gas phase or in inert solvent follows the heterolytic bond cleavage path."

15. (a) Reed, A. E.; Weinstock, R. B.; Weinhold, F. *J. Chem. Phys.* **1985**, *83*, 735. (b) NBO Version 3.1, Glendening, E. D.; Reed, A. E.; Carpenter, J. E.; Weinhold, F.

16. Wang, Y.; Xie, Y.; Wei, P.; King, R. B.; Schaefer III, H. F.; Schleyer, P. V. R. Robinson, G. H. *Science* **2008**, *321,* 1069.

17. B. Dietrich In *Comprehensive Supramolecular Chemistry Vol. 1*, J. L. Atwood, J.-M. Lehn, Eds. Pergamon, New York, **1996**, pp. 153–211.

18. There are structurally characterized examples of stable Pb salts complexed by cryptand [2.2.2]. See: (a) Chekhlov, A. N. *J. Struct. Chem.* **2006**, *47*, 351. (b) Chekhlov, A. N., *Russ. J. Coord. Chem.* **2006**, *32*, 552.

19. Krossing, I.; Raabe, I. *Angew. Chem., Int. Ed.* **2004**, *43*, 2066.

20. Ge–N bond lengths in N-heterocyclic Ge(II) cationic compounds are approximately 1.9 Å. For selected examples see Stender, M.; Phillips, A. D.; Power, P. P. *Inorg. Chem.* **2001**, *40*, 5314 and reference 21.

21. Dias, H. V. R; Wang, Z. *J. Am. Chem. Soc.* **1997**, *119*, 4650.

22. Wiberg, K.B. *Tetrahedron* **1968**, *24*, 1083.

23. Rogers, R. D.; Bauer, C. B. In *Comprehensive Supramolecular Chemistry Vol. 1,* J. L Atwood, J.-M. Lehn, Eds; Pergamon, New York , **1996**, pp 315.

24. Bott, S. G.; Alvanipour, A.; Morley, S. D.; Atwood, D. A.; Means, C. M.; Coleman, A. W.; Atwood, J. L. *Angew. Chem., Int. Ed. Engl.* **1987**, *26*, 485.

25. Kloo, L. A.; Taylor, M. J. *J. Chem. Soc., Dalton Trans.* **1997**, 2693.

26. Andrews, C. G.; Macdonald, C. L. B. *Angew. Chem., Int. Ed.* **2005**, *44*, 7453.

27. Cooper, B. F. T.; Macdonald, C. L. B. *J. Organomet. Chem.* **2008**, *693*, 1707.

28. Cooper, B. F. T.; Andrews, C. G.; Macdonald, C. L. B. *J. Organomet. Chem.* **2007**, *692*, 2843.

29. Mudring, A.; Rieger, F. *Inorg. Chem.* **2005**, *44*, 6243.

30. (a) Drew, M. G. B. *J. Chem. Soc., Dalton Trans.* **1986**, 1543. (b) Hough, E.; Nicholson, D. G.; Vasudevan, A. K. *J. Chem. Soc., Dalton Trans.* **1989**, 2155.

31. Willey, G. R.; Aris, D. R. ; Errington, W. *Inorg. Chem. Acta* **2000**, *300-302*, 1004.

32. Thiocrown ether complexes of GeX_2 were reported with the germanium coordinated to the periphery of the macrocycle. See Cheng, F.; Hector, A. L.; Levason, W.; Reid, G.; Webster, M.; Zhang, W. *Chem. Commun.* **2008**, 5508.

33. Schäfer, M.; Frenzen, G.; Neumüller, B.; Dehnicke, K. *Angew. Chem., Int. Ed. Engl.* **1992**, *31*, 334.

34. 1,4-Dioxane is never called "[6]crown-2" but it is the smallest member of the cyclic $(C_2H_4O)_n$ ether family. The solid state structure of $GeCl_2$·dioxane (**8**) consists of $GeCl_2$ moieties linked together by dioxane, forming a 1-D coordination polymer. See Denk, M. K.; Khan, M.; Lough, A. J.; Shuchi, K. *Acta Cryst.* **1998**, *C54*, 1830.

35. The work on crown ether complexes of germanium(II) was a joint project between Prof. Baines' group at the University of Western Ontario and Prof. Macdonald's group at the University of Windsor.

36. The distance between Ge and oxygen in $GeCl_2$·dioxane (**8**) is 2.399 (1) Å. See reference 34.

37. A $^-GeBr_3$ salt of $\mathbf{88}^{2+}$ was recently published by another group. See: Cheng, F.; Hector, A. L.; Levason, W.; Reid, G.; Webster, M.; Zhang, W. *Angew. Chem., Int. Ed.* **2009**, *48*, 5152.

38. The direct reaction of $GeCl_2$·dioxane (**8**), [15]crown-5 and Me_3SiOTf was found to produce **89**[OTf]in a much higher yield. See reference 35.

39. Others have reached the same conclusion. See: (a) Müller, T. *Angew. Chem., Int. Ed.* **2009**, *48*, 3740. (b) Lambert, J. B. *Science* **2008**, *322*, 1333.

40. Pangborn, A. B.; Giardello, M. A.; Grubbs, R. H.; Rosen, R. K.; Timmers, F. J. *Organometallics* **1996**, *15*, 1518.

41. Leigh, W.J.; Harrington, C. R.; Vargas-Baca, I. *J. Am. Chem. Soc.* **2004**, *126*, 16105.

42. Gaussian 03, Revision B.05, Frisch, M. J.; Trucks, G. W.; Schlegel, H. B.; Scuseria, G. E.; Robb, M. A.; Cheeseman, J. R.; Montgomery, Jr., J. A.; Vreven, T.; Kudin, K. N.; Burant, J. C.; Millam, J. M.; Iyengar, S. S.; Tomasi, J.; Barone, V.; Mennucci, B.; Cossi, M.; Scalmani, G.; Rega, N.; Petersson, G. A.; Nakatsuji, H.; Hada, M.; Ehara,

M.; Toyota, K.; Fukuda, R.; Hasegawa, J.; Ishida, M.; Nakajima, T.; Honda, Y.; Kitao, O.; Nakai, H.; Klene, M.; Li, X.; Knox, J. E.; Hratchian, H. P.; Cross, J. B.; Bakken, V.; Adamo, C.; Jaramillo, J.; Gomperts, R.; Stratmann, R. E.; Yazyev, O.; Austin, A. J.; Cammi, R.; Pomelli, C.; Ochterski, J. W.; Ayala, P. Y.; Morokuma, K.; Voth, G. A.; Salvador, P.; Dannenberg, J. J.; Zakrzewski, V. G.; Dapprich, S.; Daniels, A. D.; Strain, M. C.; Farkas, O.; Malick, D. K.; Rabuck, A. D.; Raghavachari, K.; Foresman, J. B.; Ortiz, J. V.; Cui, Q.; Baboul, A. G.; Clifford, S.; Cioslowski, J.; Stefanov, B. B.; Liu, G.; Liashenko, A.; Piskorz, P.; Komaromi, I.; Martin, R. L.; Fox, D. J.; Keith, T.; Al-Laham, M. A.; Peng, C. Y.; Nanayakkara, A.; Challacombe, M.; Gill, P. M. W.; Johnson, B.; Chen, W.; Wong, M. W.; Gonzalez, C.; and Pople, J. A.; Gaussian, Inc., Wallingford CT, **2004**.

43. *SMART*, Bruker AXS Inc.: Madison, WI, **2001**.

44. *COLLECT*, Nonius BV: Delft, The Nëtherlands, **2001**.

45. *SAINTPlus*, Bruker AXS Inc.: Madison, WI, **2001**.

46. *SADABS*, Bruker AXS Inc.: Madison, WI, **2001**.

47. Otwinowski, Z.; Minor, W. In *Methods in Enzymology*, Vol. 276, *Macromolecular Crystallography*, Part A, C. W. Carter Jr & R. M. Sweet, Eds, pp. 307-326. New York: Academic Press **1997**.

48. Sheldrick, G.M. *Acta Crystallogr., Sect. A: Found. Crystallogr.*, **2008**, *64*, 112.

49. Altomare, A.; Burla, M. C.; Camalli, M.; Cascarano, G.; Giacovazzo, C.; Guagliardi, A.; Polidori, G.; Spagna, R. *SIR97*, CNR-IRMEC: Bari, **1997**.

50. Farrugia, L. J., *J. Appl. Crystallogr.* **1999,** *32*, 837.

51. Spek, A. L. *J. Appl. Crystallogr.* **2003**, *36*, 7.

Chapter 6

Summary, Future Work and Conclusions

6.1 Summary

The synthese of two different complexes of $GeMes_2$ (**16**) were reported. Starting from tetramesityldigermene (**15**), the reaction of two equivalents of either the gallium(I) containing **10** or N-heterocyclic carbene (NHC) **25** gave the corresponding dimesitylgermylene complexes **17** and **28**, respectively (Scheme 6.1). Preliminary reactivity studies on both **17** and **28** demonstrated that they react as Lewis bases and nucleophiles: **17** reacted with MeI and Me_3SiCl, while **28** formed an adduct with BH_3. Methyllithium displaced the NHC from **28** and formed germyl anion **33**.

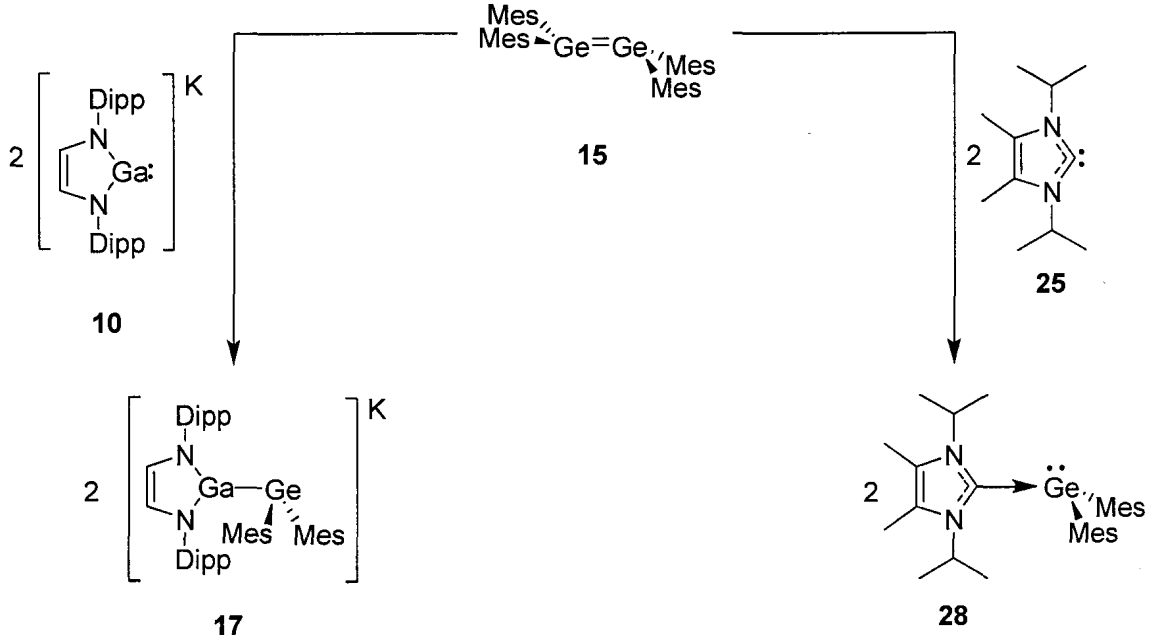

Scheme 6.1

The ease of synthesis of the NHC supported **28** suggested that other reactive GeR_2 may also be readily formed. Using **39** as a starting material, a series of NHC-GeR_2 complexes were synthesized and characterized (Scheme 6.2). The reactions were, for the

most part, simple to perform and produced the desired products in high yield. Attempts to form complexes of highly reactive GeR_2 species, where R = a small alkyl or aryl group, were not successful; evidence of oligomer formation was observed. Thus the stability of **28**, which is a complex of an aryl substituted transient germylene, appears to be in part due to steric protection from the bulky mesityl groups. As such, smaller alkyl or aryl groups on germanium do not provide sufficient steric protection to allow isolation of an NHC-GeR_2 complex.

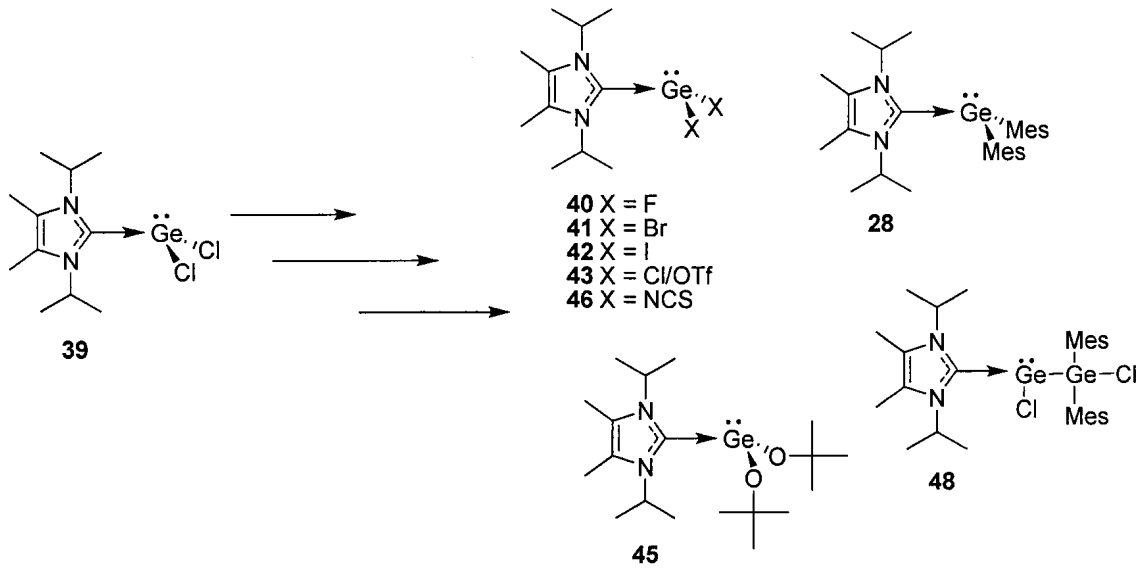

Scheme 6.2

Model NHC-GeR_2 complexes were examined computationally to better understand the effects of substituents on both the carbenic carbon-germanium bond lengths and bond strengths. Although no systematic trend was observed in the carbenic carbon-germanium bond length, the energy of complexation (ΔE_{comp}) between the NHC and the GeR_2 moiety was found decrease versus the Hammett σ_p constants of the substituents on germanium.

The chemistry of compounds **28**, **39**, and **45** towards a variety of reagents was examined; the results were compared to the chemistry of known Ge(II) species (Scheme

6.3). In some cases, the NHC-GeR_2 complexes formed products expected of the corresponding uncoordinated germylenes. However, in other situations, the NHC-GeR_2 complexes reacted quite differently compared to the uncoordinated germylenes. In general, the chloro substituted **39** and ^{t}butoxy substituted **45** were less reactive than the mesityl substituted **28**. The chemistry of **28, 39**, and **45** towards 2,3-dimethylbutadiene (DMB) was noteworthy in that strong substituent effects on the germanium were observed. Specifically, both **28** and **45** reacted with DMB to form a germacyclopentene, while the reaction of **39** with DMB appeared to be thermodynamically unfavoured. The reactivity of **28** with a number other of reagents produced complicated reaction mixtures.

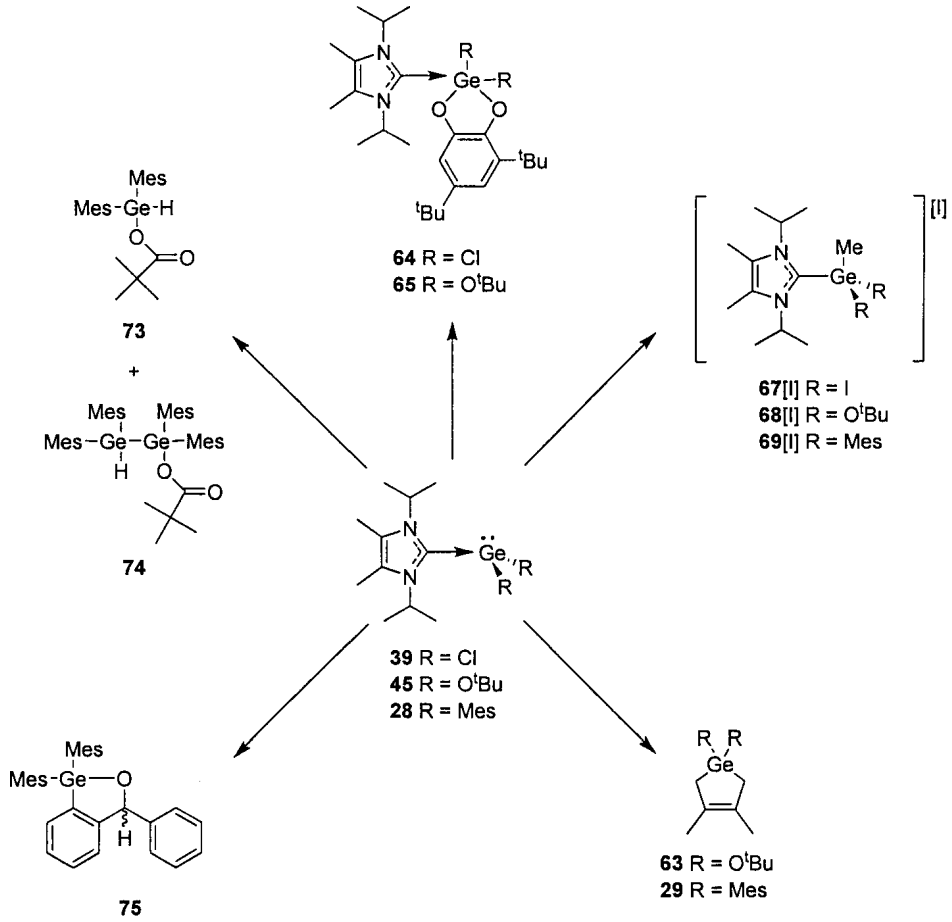

Scheme 6.3

Dicationic Ge(II) was synthesized for the first time by surrounding the germanium with NHCs, cryptand[2.2.2] or crown ethers (Chart 6.1). The NHC supported **84**$[I]_2$ was formed simpley through displacement of two equivalents of I^- by excess NHC **25**. Studies of the chemistry of **84**$[I]_2$ were hampered by its instability and insolubility. The synthesis of **85**$[OTf]_2$ was easily accomplished by the reaction of cryptand[2.2.2] with **43**. Interpretation of the electronic structure of $\mathbf{85}^{2+}$ suggests that it bares some electronic similarity to a naked Ge^{2+} cation. The crown ether complexes of Ge(II) were synthesized from $GeCl_2$·dioxane (**8**) and the corresponding crown ether. Depending on the crown ether employed, neutral, cationic or dicationic germanium(II) species were isolated. The structural properties of the crown ether complexes were highly dependent on the size of crown ether used and on the substituents on germanium.

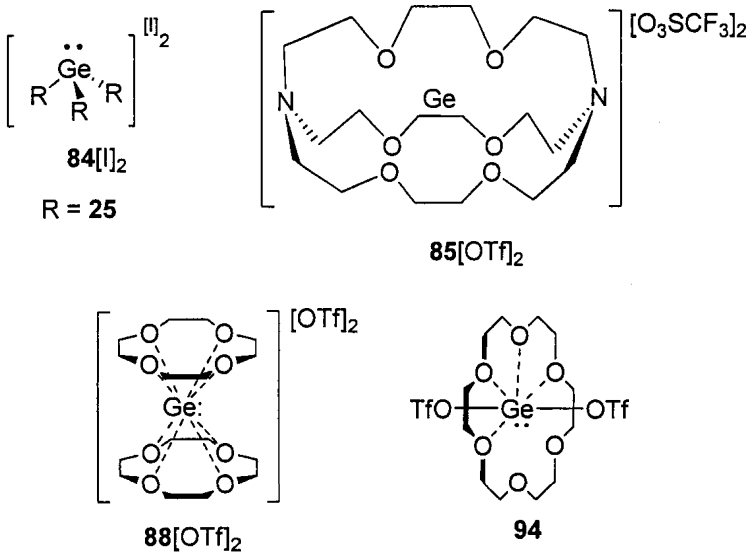

Chart 6.1

6.2 Future work

6.2.1 The Use of Different N-Heterocyclic Carbenes for Ge(II) Stabilization

Although NHC **25** proved to be versatile for the synthesis of numerous Ge(II) complexes, there are a large number of additional N-heterocyclic carbenes available, each

with unique steric and electronic properties.[1] More sterically encumbered NHCs may provide suitable protection allowing for the isolation of germylenes featuring smaller alkyl or aryl groups (Scheme 6.4). Such compounds may be suitable precursors for living polymerizations, providing access to polygermanes with controlled molecular weights (Scheme 6.4).

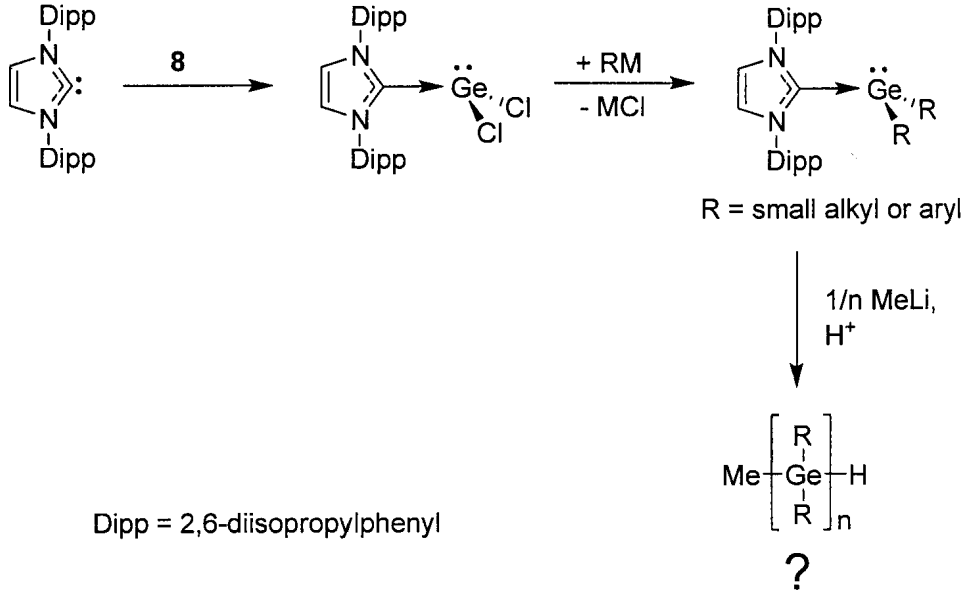

Scheme 6.4

In addition to supporting more reactive Ge(II) centres, bulkier NHCs may also allow for the isolation of Ge(0) complexes by the reduction of a halogenated germanium species (See Chapter 5.2.1).[2]

6.2.2 Complex 43 as a $^{+}$GeCl Synthon

As a consequence of the labile Ge-$O_{triflate}$ bond in **43**, relatively weak neutral donors should easily replace the triflato substituent to form cationic germanium species. Future work could examine the potential of using **43** for the synthesis of novel Ge containing complexes. In preliminary studies, the reaction of **43** with 4,4'-bipyridine produced a

number of interesting products, including a cationic coordination polymer which was identified by single crystal X-ray diffraction (Scheme 6.5).[3]

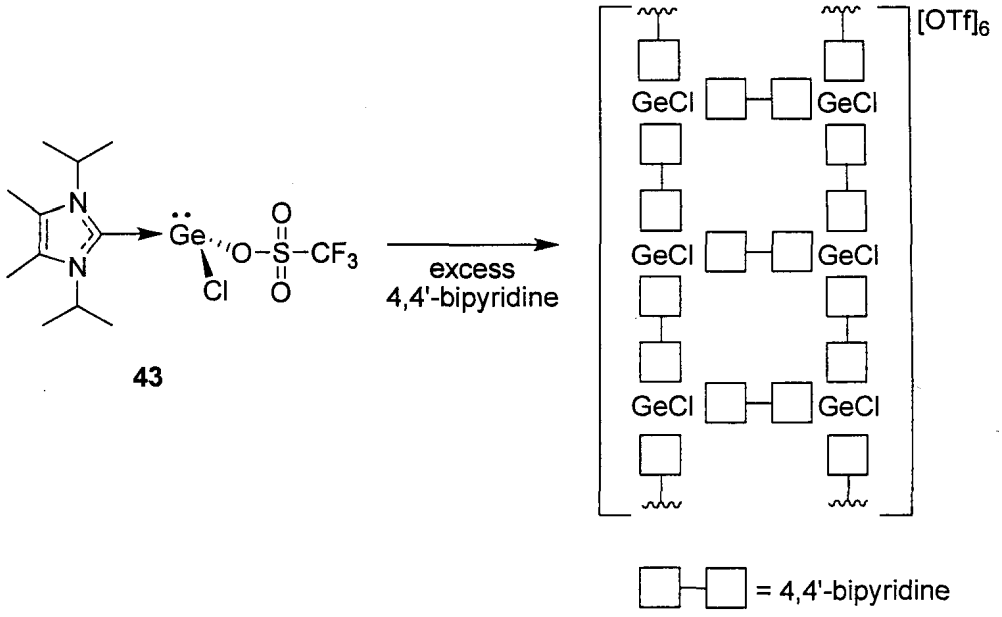

43

Scheme 6.5

6.2.3 The Scope of Cryptands and Crown Ethers for the Encapsulation of Lighter P-block Cations

Future work should explore the possibility of using crown ethers and cryptands to isolate and complex light p-block cations, both metal and non-metal. Potential cations include Ga^{+}, Si^{2+}, P^{+}, P^{3+}, As^{+}, and As^{3+}. A (cryptand[2.2.2]Ga)$^{+}$ complex seems very feasible given gallium's proximity to germanium on the Periodic Table and the fact that Ga^{+} is isoelectronic with Ge^{2+}. A (cryptand[2.2.2]Ga)$^{+}$ cation could prove to be an excellent Ga(I) reagent for more elaborate gallium(I) compounds; there is a notable lack of suitable gallium(I) starting materials available for synthetic exploitation.

The silicon(II) dication is an intriguing target, but will be synthetically challenging because of the increased reactivity of silicon(II) compared to Ge(II). Furthermore, a smaller cryptand may be required.

Cryptands may be unsuitable for cations of the later p-block elements in low oxidation states (eg. P(I), As(I), S(II), Se(II)) because of the extra electron lone pairs located in p-orbitals. The resulting electron-electron repulsion between the electron pairs of the cation with the electron pairs of the donor oxygen and nitrogen atoms may render complexes like $(\text{cryptand[2.2.2]P})^{+}$ unstable. Conversely, crown ethers may be more suitable for cations such as $P(I)^{+}$ and $Se(II)^{2+}$. A crown ether that is oriented in a planar conformation would allow a stereochemically active lone pair of electrons on the cation to be projected orthogonal to the plane of the crown ether. This would alleviate repulsion between the electron pairs on the ligand and the electron pairs on the cation centre.

6.3 Conclusions

This thesis has demonstrated that through judicial selection of ligands, the isolation of stable neutral and cationic germanium(II) complexes is possible. Many of the compounds characterized herein were unprecedented and introduced new bonding motifs to germanium chemistry.

The syntheses of **17** and **28** were important in that they are the first examples of a transient germylene stabilized intermolecularly by Lewis bases. Numerous other NHC complexes were synthesized, including other examples of stabilized transient germylenes. Presumably, under the correct conditions, additional reactive germylenes may be

stabilized.[4] Although it was hoped that the NHC-GeR_2 complexes would be general purpose, easy-to-handle synthons of GeR_2, the chemistry of the NHC-GeR_2 species was often varied and more complicated than anticipated. It is possible that during the course of these reactions, NHC **25** is being released. Since free NHCs are powerful Lewis bases,[1] they may be catalyzing undesired side reactions.

Complex **39** (NHC-$GeCl_2$) proved to be a versatile reagent for further elaboration and we believe that it may find general use as a starting material. Although chemically similar in some respects to $GeCl_2$·dioxane (**8**), coordination of the NHC to the germanium provides additional stabilization relative to 1,4-dioxane. For example, the reaction of **39** with KNCS cleanly produced **46** (Chapter 3.2), while under similar conditions, $GeCl_2$·dioxane (**8**) produced an oligomeric material.[5] Compared to $GeCl_2$·dioxane (**8**), **39** is more soluble in less polar solvents such as benzene or toluene, further enhancing its utility.

This work introduced a new approach for the isolation of cationic germanium compounds by encasing them within either cryptands or crown ethers. Complex $\mathbf{85}^{2+}$ was the first example of non-metal cation entombed within the cavity of a cyptand and represented a new paradigm for the isolation of non-metal cationic species. Prior to this work, Ge(II)-crown ether complexes were unprecedented in germanium chemistry;[6] in general, cationic crown ether complexes of non-metals are rare. The surprising ease with which cryptand[2.2.2] and the crown ethers promoted the ionization of Ge(II) demonstrated the effectiveness of these macrocycles in isolating otherwise elusive cationic germanium species. The simplicity of the synthetic approach should render it applicable to the preparation of other novel non-metal cations.

Throughout the course of this project, a number of significant observations were made. Hopefully this work will have a lasting impact not only on the chemistry of germanium, but in the chemistry of the p-block elements as well. It has sure been a fun ride.

6.4 References

1. (a) Hahn, F. E.; Jahnke, M. C. *Angew. Chem., Int. Ed.* **2008**, *47*, 3122. (b) de Fremont, P.; Marion, N.; Nolan, S. P. *Coord. Chem. Rev.* **2009**, *253*, 862. (c) Kuhl, O. *Chem. Soc. Rev.* **2007**, *36*, 592. (d) Cavallo, L.; Correa, A.; Costabile, C.; Jacobsen, H. *J. Organomet. Chem.* **2005**, *690*, 5407.
2. Wang, Y.; Xie, Y.; Wei, P.; King, R. B.; Schaefer III, H. F.; Schleyer, P. V. R.; Robinson, G. H. *Science* **2008**, *321*, 1069.
3. Although there is no ambiguity that coordination polymers are forming, the reproducibility of the reaction is poor. Optimization of the reaction conditions is still needed. Rupar, P. A.; Baines, K. M. *Unpublished Work.*
4. Recently, other researchers have applied this chemistry to silicon and have shown that bulky NHCs are capable of stabilizing $SiCl_2$ and $SiBr_2$. These results may revolutionize silicon chemistry since simple Si(II) starting materials are not otherwise known. See (a) Fillippou, A. C.; Chernov, O.; Schnakenburg, G. *Angew. Chem., Int. Ed.* **2009**, DOI: 10.1002/anie.200902431. (b) Ghadwai, R. S.; Roesky, H. W.; Merkel, S.; Henn, J.; Stalke, D. *Angew. Chem., Int. Ed.* **2009**, DOI: 10.1002/anie.200901766.
5. Onyszchuk, M.; Castel, A.; Rivière, P.; Satgé, J. *J. Organomet. Chem.* **1986**, *317*, C35.

6. Others have also recently published crown ether and aza crown ether complexes of Ge(II). See Cheng, F.; Hector, A. L.; Levason, W.; Reid, G.; Webster, M.; Zhang, W. *Angew. Chem. Int. Ed.,* **2009**, *48*, 5152.

Appendix 1

Gaussian03 Input Files

A1.1 Input Files for the Geometry Optimization of Compounds 54-60

The following are the input files used for the geometry optimization of compounds **54 – 60**. Only the DFT optimizations input files are shown. The MP2 geometry optimizations were performed on identical geometries but with MP2 keyword in place of PBE1PBE in the input file.

A1.1.1 Compound 54 (R=H)

```
# opt freq rpbe1pbe/6-311+g(d,p) geom=connectivity scf=tight
int=grid=ultrafine symm=loose

Title Card Required

0 1
 Ge
 C                  1             B1
 N                  2             B2     1             A1
 N                  2             B3     1             A2     3
D1
 C                  3             B4     2             A3     1
D2
 C                  5             B5     3             A4     2
D3
 H                  5             B6     3             A5     2
D4
 H                  6             B7     5             A6     3
D5
 C                  3             B8     2             A7     1
D6
 H                  9             B9     3             A8     2
D7
 H                  9            B10     3             A9     2
D8
 H                  9            B11     3            A10     2
D9
 C                  4            B12     2            A11     1
D10
 H                 13            B13     4            A12     2
D11
```

```
 H                13           B14     4              A13     2
D12
 H                13           B15     4              A14     2
D13
 H                 1           B16     2              A15     4
D14
 H                 1           B17     2              A16     4
D15
```

B1	2.04701656
B2	1.35872697
B3	1.35872697
B4	1.37802600
B5	1.35224340
B6	1.07751429
B7	1.07751429
B8	1.44792230
B9	1.09006147
B10	1.08951610
B11	1.09340687
B12	1.44792230
B13	1.09340687
B14	1.08951610
B15	1.09006147
B16	1.51989300
B17	1.51989300
A1	126.42565675
A2	126.42565675
A3	111.18167017
A4	106.70758172
A5	122.43325826
A6	130.85617294
A7	124.24080156
A8	108.67404997
A9	110.71370138
A10	109.59558683
A11	124.24080156
A12	109.59558683
A13	110.71370138
A14	108.67404997
A15	99.81426146
A16	99.81426146
D1	157.51276049
D2	160.97956830
D3	0.32698743
D4	179.76107477
D5	179.36849462
D6	-13.94961957
D7	173.49645588
D8	-66.13775776
D9	54.08336363
D10	13.94961957
D11	-54.08336363
D12	66.13775776
D13	-173.49645588
D14	-149.82010658
D15	-52.66713293

```
 1 2 1.0 17 1.0 18 1.0
 2 3 1.5 4 1.5
 3 5 1.5 9 1.0
 4 6 1.5 13 1.0
 5 6 2.0 7 1.0
 6 8 1.0
 7
 8
 9 10 1.0 11 1.0 12 1.0
 10
 11
 12
 13 14 1.0 15 1.0 16 1.0
 14
 15
 16
 17
 18
```

A1.1.2 Compound 55 (R=OH)

```
# opt freq pbe1pbe/6-311+g(d,p) geom=connectivity scf=tight
integral(grid=ultrafine) pop=nboread

Title Card Required

0 1
 Ge
 C                  1             B1
 N                  2             B2    1             A1
 N                  2             B3    1             A2    3
D1
 C                  3             B4    2             A3    1
D2
 C                  5             B5    3             A4    2
D3
 H                  5             B6    3             A5    2
D4
 H                  6             B7    5             A6    3
D5
 C                  3             B8    2             A7    1
D6
 H                  9             B9    3             A8    2
D7
 H                  9            B10    3             A9    2
D8
 H                  9            B11    3            A10    2
D9
 C                  4            B12    2            A11    1
D10
 H                 13            B13    4            A12    2
D11
```

```
 H                13              B14     4               A13     2
D12
 H                13              B15     4               A14     2
D13
 O                 1              B16     2               A15     3
D14
 H                17              B17     1               A16     2
D15
 O                 1              B18    17               A17     2
D16
 H                19              B19     1               A18    17
D17

   B1              2.11490064
   B2              1.34986478
   B3              1.35103073
   B4              1.37625205
   B5              1.35318110
   B6              1.07772729
   B7              1.07768031
   B8              1.45546804
   B9              1.09157849
   B10             1.09151644
   B11             1.09293242
   B12             1.45520840
   B13             1.09086863
   B14             1.09321638
   B15             1.09061393
   B16             1.87589628
   B17             0.95896385
   B18             1.87699409
   B19             0.95905201
   A1            129.96673865
   A2            123.94967943
   A3            110.81185689
   A4            106.69223066
   A5            122.30144594
   A6            130.98054502
   A7            125.79442032
   A8            108.03891358
   A9            109.03181507
   A10           109.77437553
   A11           125.16527828
   A12           108.10828833
   A13           110.12614013
   A14           108.71004622
   A15            91.55416075
   A16           108.76979400
   A17           100.06233460
   A18           109.38328585
   D1           -166.10514680
   D2           -168.14226256
   D3              0.07108488
   D4           -178.76380913
   D5           -178.92165557
   D6             12.05481710
   D7             12.07870227
```

```
   D8           131.35278120
   D9          -108.69974589
   D10           -9.44727407
   D11          -30.15613096
   D12           90.44981769
   D13         -149.60802371
   D14          -37.50116775
   D15          159.28737451
   D16           88.44233849
   D17           98.97594925

 1 17 1.0 19 1.0
 2 3 1.5 4 1.5
 3 5 1.5 9 1.0
 4 6 1.5 13 1.0
 5 6 2.0 7 1.0
 6 8 1.0
 7
 8
 9 10 1.0 11 1.0 12 1.0
 10
 11
 12
 13 14 1.0 15 1.0 16 1.0
 14
 15
 16
 17 18 1.0
 18
 19 20 1.0
 20

 $nbo bndidx $end
```

A1.1.3 Compound 56 (R=NH_2)

```
# opt freq pbe1pbe/6-311+g(d,p) geom=connectivity scf=tight
integral(grid=ultrafine) pop=nboread

Title Card Required

0 1
 Ge
 C                  1             B1
 N                  2             B2    1             A1
 N                  2             B3    1             A2    3
D1
 C                  3             B4    2             A3    1
D2
 C                  5             B5    3             A4    2
D3
 H                  5             B6    3             A5    2
D4
```

H	6	B7	5	A6	3
D5					
N	1	B8	2	A7	3
D6					
H	9	B9	1	A8	2
D7					
H	9	B10	1	A9	2
D8					
N	1	B11	9	A10	2
D9					
H	12	B12	1	A11	9
D10					
H	12	B13	1	A12	9
D11					
C	3	B14	2	A13	1
D12					
H	15	B15	3	A14	2
D13					
H	15	B16	3	A15	2
D14					
H	15	B17	3	A16	2
D15					
C	4	B18	2	A17	1
D16					
H	19	B19	4	A18	2
D17					
H	19	B20	4	A19	2
D18					
H	19	B21	4	A20	2
D19					

B1	2.11376578
B2	1.35533718
B3	1.35535153
B4	1.37607988
B5	1.35226900
B6	1.07779724
B7	1.07779809
B8	1.92854819
B9	1.01567374
B10	1.01376892
B11	1.92858646
B12	1.01377322
B13	1.01567734
B14	1.45430085
B15	1.09440837
B16	1.09179669
B17	1.09350568
B18	1.45429714
B19	1.09440656
B20	1.09350561
B21	1.09179680
A1	126.46724804
A2	126.45454682
A3	111.01648105
A4	106.71530063
A5	122.27535018

```
  A6            131.00190962
  A7             93.63841098
  A8            115.08509487
  A9            110.14680045
  A10           102.22155295
  A11           110.14485793
  A12           115.06763902
  A13           125.58800639
  A14           108.04340048
  A15           109.10994773
  A16           109.76560382
  A17           125.58721310
  A18           108.04417518
  A19           109.76614453
  A20           109.10900855
  D1           -159.06917934
  D2           -162.58246367
  D3             -0.09519799
  D4           -179.21661163
  D5           -179.01500251
  D6           -151.70562090
  D7             79.29427310
  D8           -159.76727733
  D9            -94.52525836
  D10          -105.72658001
  D11            15.19399679
  D12            13.99685880
  D13            18.28641095
  D14           138.08758566
  D15          -101.97435517
  D16           -13.98031215
  D17           -18.32725121
  D18           101.93447115
  D19          -138.12734445

1 9 1.0 12 1.0
2 3 1.5 4 1.5
3 5 1.5 15 1.0
4 6 1.5 19 1.0
5 6 2.0 7 1.0
6 8 1.0
7
8
9 10 1.0 11 1.0
10
11
12 13 1.0 14 1.0
13
14
15 16 1.0 17 1.0 18 1.0
16
17
18
19 20 1.0 21 1.0 22 1.0
20
21
22
```

```
 $nbo bndidx $end
```

A1.1.4 Compound 57 (R=CH_3)

```
# opt freq pbe1pbe/6-311+g(d,p) geom=connectivity scf=tight
integral(grid=ultrafine) pop=nboread

Title Card Required

0 1
 Ge
 C                  1             B1
 N                  2             B2     1             A1
 N                  2             B3     1             A2     3
D1
 C                  3             B4     2             A3     1
D2
 C                  5             B5     3             A4     2
D3
 H                  5             B6     3             A5     2
D4
 H                  6             B7     5             A6     3
D5
 C                  1             B8     2             A7     4
D6
 H                  9             B9     1             A8     2
D7
 H                  9            B10     1             A9     2
D8
 H                  9            B11     1            A10     2
D9
 C                  1            B12     9            A11     2
D10
 H                 13            B13     1            A12     9
D11
 H                 13            B14     1            A13     9
D12
 H                 13            B15     1            A14     9
D13
 C                  3            B16     2            A15     1
D14
 H                 17            B17     3            A16     2
D15
 H                 17            B18     3            A17     2
D16
 H                 17            B19     3            A18     2
D17
 C                  4            B20     2            A19     1
D18
 H                 21            B21     4            A20     2
D19
```

```
 H                21            B22     4             A21     2
D20
 H                21            B23     4             A22     2
D21

   B1           2.04701657
   B2           1.35875670
   B3           1.35875188
   B4           1.37802600
   B5           1.35170801
   B6           1.07751429
   B7           1.07751395
   B8           2.02507052
   B9           1.09299446
   B10          1.09510052
   B11          1.09514138
   B12          2.02505480
   B13          1.09299226
   B14          1.09514251
   B15          1.09510106
   B16          1.44792230
   B17          1.09006147
   B18          1.08951610
   B19          1.09340687
   B20          1.44792038
   B21          1.09339647
   B22          1.08952411
   B23          1.09006225
   A1         126.42767263
   A2         126.43646474
   A3         111.18069455
   A4         106.71564773
   A5         122.43325826
   A6         130.84827547
   A7          99.81130435
   A8         113.41630684
   A9         113.93849629
   A10        105.30233570
   A11         95.28119494
   A12        113.41963269
   A13        105.30243252
   A14        113.93595868
   A15        124.24177413
   A16        108.67404997
   A17        110.71370138
   A18        109.59558683
   A19        124.24292029
   A20        109.59419025
   A21        110.71603635
   A22        108.67367039
   D1         157.50490482
   D2         160.97907361
   D3           0.32344992
   D4         179.76106546
   D5         179.37083949
   D6        -149.83190317
   D7         -82.87499741
```

```
   D8             43.15251858
   D9            160.61828255
   D10          -100.93578129
   D11          -176.24558900
   D12           -59.73898437
   D13            57.72705800
   D14           -13.95006482
   D15           173.49636204
   D16           -66.13785161
   D17            54.08326978
   D18            13.96348672
   D19           -54.04054917
   D20            66.18264136
   D21          -173.45075399

 1 2 1.0 9 1.0 13 1.0
 2 3 1.5 4 1.5
 3 5 1.5 17 1.0
 4 6 1.5 21 1.0
 5 6 2.0 7 1.0
 6 8 1.0
 7
 8
 9 10 1.0 11 1.0 12 1.0
 10
 11
 12
 13 14 1.0 15 1.0 16 1.0
 14
 15
 16
 17 18 1.0 19 1.0 20 1.0
 18
 19
 20
 21 22 1.0 23 1.0 24 1.0
 22
 23
 24

 $nbo bndidx $end
```

A1.1.5 Compound 58 (R=F)

```
%chk=MeNHCGeF2_6311_scftight.chk
%mem=6MW
%nproc=1
# opt freq pbe1pbe/6-311+g(d,p) geom=connectivity pop=nboread scf=tight
integral(grid=ultrafine)

Title Card Required

0 1
 Ge
```

```
 C                1              B1
 N                2              B2     1              A1
 N                2              B3     1              A2     3
D1
 C                3              B4     2              A3     1
D2
 C                5              B5     3              A4     2
D3
 H                5              B6     3              A5     2
D4
 H                6              B7     5              A6     3
D5
 C                3              B8     2              A7     1
D6
 H                9              B9     3              A8     2
D7
 H                9             B10     3              A9     2
D8
 H                9             B11     3             A10     2
D9
 C                4             B12     2             A11     1
D10
 H               13             B13     4             A12     2
D11
 H               13             B14     4             A13     2
D12
 H               13             B15     4             A14     2
D13
 F                1             B16     2             A15     3
D14
 F                1             B17     2             A16     3
D15

   B1          2.15020622
   B2          1.34413991
   B3          1.34739512
   B4          1.37427060
   B5          1.35551735
   B6          1.07788491
   B7          1.07773631
   B8          1.45890676
   B9          1.08887123
   B10         1.08999791
   B11         1.09022188
   B12         1.45154325
   B13         1.08951637
   B14         1.09187039
   B15         1.09169311
   B16         1.83171029
   B17         1.82804175
   A1        126.81452875
   A2        127.72568156
   A3        110.63162252
   A4        106.91560404
   A5        122.40170712
   A6        131.00735213
   A7        124.52552684
```

```
   A8            108.63995297
   A9            109.74024404
   A10           108.34162478
   A11           124.70164432
   A12           108.63531313
   A13           110.17598046
   A14           110.05822056
   A15            88.64181358
   A16            87.63892933
   D1            176.68986307
   D2            177.08885115
   D3              0.23587098
   D4            179.98178407
   D5            179.41779258
   D6             -1.08234165
   D7            -39.67697511
   D8             79.32585909
   D9           -159.73026309
   D10             3.48119975
   D11            -2.56580662
   D12           116.95768954
   D13          -122.02709763
   D14            49.59166055
   D15           -45.68748716

 1 17 1.0 18 1.0
 2 3 1.5 4 1.5
 3 5 1.5 9 1.0
 4 6 1.5 13 1.0
 5 6 2.0 7 1.0
 6 8 1.0
 7
 8
 9 10 1.0 11 1.0 12 1.0
 10
 11
 12
 13 14 1.0 15 1.0 16 1.0
 14
 15
 16
 17
 18

 $nbo bndidx $end
```

A1.1.6 Compound 59 (R=Cl)

```
# opt freq rpbe1pbe/6-311+g(d,p) geom=connectivity symm=loose scf=tight
int=grid=ultrafine

Title Card Required
```

```
0 1
 C
 N                  1             B1
 N                  1             B2     2             A1
 C                  2             B3     1             A2     3
D1
 C                  4             B4     2             A3     1
D2
 H                  4             B5     2             A4     1
D3
 H                  5             B6     4             A5     2
D4
 C                  3             B7     1             A6     2
D5
 H                  8             B8     3             A7     1
D6
 H                  8             B9     3             A8     1
D7
 H                  8            B10     3             A9     1
D8
 C                  2            B11     1            A10     3
D9
 H                 12            B12     2            A11     1
D10
 H                 12            B13     2            A12     1
D11
 H                 12            B14     2            A13     1
D12

   B1            1.36101979
   B2            1.36101979
   B3            1.38199182
   B4            1.35288200
   B5            1.07882651
   B6            1.07882651
   B7            1.44482576
   B8            1.08870427
   B9            1.09375790
   B10           1.09375790
   B11           1.44482576
   B12           1.09375790
   B13           1.08870427
   B14           1.09375790
   A1          102.10521284
   A2          112.89876211
   A3          106.04863147
   A4          123.37503997
   A5          130.57632856
   A6          122.88627133
   A7          107.44921411
   A8          110.85938256
   A9          110.85938256
   A10         122.88627133
   A11         110.85938256
   A12         107.44921411
   A13         110.85938256
   D1            0.00000000
```

```
   D2              0.00000000
   D3            180.00000000
   D4           -180.00000000
   D5           -180.00000000
   D6              0.00000000
   D7            119.33248504
   D8           -119.33248504
   D9            180.00000000
   D10          -119.33248504
   D11             0.00000000
   D12           119.33248504

 1 2 1.5 3 1.5
 2 4 1.0 12 1.0
 3 5 1.0 8 1.0
 4 5 2.0 6 1.0
 5 7 1.0
 6
 7
 8 9 1.0 10 1.0 11 1.0
 9
 10
 11
 12 13 1.0 14 1.0 15 1.0
 13
 14
 15
```

A1.1.7 Compound 60

```
%mem=300MB
# opt freq rpbe1pbe/6-311+g(d,p) geom=connectivity int=grid=ultrafine
scf=tight

Title Card Required

0 1
 C
 N                  1             B1
 N                  1             B2    2             A1
 C                  2             B3    1             A2    3
D1
 C                  4             B4    2             A3    1
D2
 H                  4             B5    2             A4    1
D3
 H                  5             B6    4             A5    2
D4
 C                  3             B7    1             A6    2
D5
 H                  8             B8    3             A7    1
D6
```

```
 H                8             B9    3             A8    1
D7
 H                8             B10   3             A9    1
D8
 C                2             B11   1             A10   3
D9
 H               12             B12   2             A11   1
D10
 H               12             B13   2             A12   1
D11
 H               12             B14   2             A13   1
D12

   B1          1.36100436
   B2          1.36100436
   B3          1.38161964
   B4          1.35237800
   B5          1.07866046
   B6          1.07866046
   B7          1.44461996
   B8          1.08856374
   B9          1.09362527
   B10         1.09362527
   B11         1.44461996
   B12         1.09362527
   B13         1.08856374
   B14         1.09362527
   A1        102.06410119
   A2        112.91776920
   A3        106.05018020
   A4        123.35341658
   A5        130.59640321
   A6        122.85815320
   A7        107.49800480
   A8        110.84424534
   A9        110.84424534
   A10       122.85815320
   A11       110.84424534
   A12       107.49800480
   A13       110.84424534
   D1          0.00000000
   D2          0.00000000
   D3        180.00000000
   D4       -180.00000000
   D5       -180.00000000
   D6          0.00000000
   D7        119.35348982
   D8       -119.35348982
   D9        180.00000000
   D10      -119.35348982
   D11         0.00000000
   D12       119.35348982

 1 2 1.5 3 1.5
 2 4 1.5 12 1.0
 3 5 1.5 8 1.0
 4 5 2.0 6 1.0
```

```
 5 7 1.0
 6
 7
 8 9 1.0 10 1.0 11 1.0
 9
 10
 11
 12 13 1.0 14 1.0 15 1.0
 13
 14
 15
```

A1.2 Input File for the Geometry Optimization of Germylenes GeR_2 (R= H, NH_2, CH_3, OH, F, Cl)

A1.2.1 GeH_2

```
%mem=300MB
# opt freq rpbe1pbe/6-311+g(d,p) geom=connectivity symm=loose scf=tight
int=grid=ultrafine

Title Card Required

0 1
 Ge
 H                    1              B1
 H                    1              B2     2               A1

   B1              1.52000000
   B2              1.52000000
   A1            120.00000011

 1 2 1.0 3 1.0
 2
 3
```

A1.2.2 $Ge(NH_2)_2$

```
%mem=1000MB
# opt freq rpbe1pbe/6-311+g(d,p) geom=connectivity scf=tight
int=grid=ultrafine symm=loose

Title Card Required

0 1
 Ge
 N                    1              B1
```

```
 H                     2              B2     1              A1
 H                     2              B3     1              A2     3
D1
 N                     1              B4     2              A3     4
D2
 H                     5              B5     1              A4     2
D3
 H                     5              B6     1              A5     2
D4

   B1              1.83232120
   B2              1.01000286
   B3              1.00784142
   B4              1.83232120
   B5              1.01000286
   B6              1.00784142
   A1            126.75035432
   A2            120.97496698
   A3             97.03771745
   A4            126.75035432
   A5            120.97496698
   D1            180.00000000
   D2            180.00000000
   D3              0.00000000
   D4            180.00000000

 1 2 1.0 5 1.0
 2 3 1.0 4 1.0
 3
 4
 5 6 1.0 7 1.0
 6
 7
```

A1.2.3 $Ge(CH_3)_2$

```
%mem=500MB
# opt freq rpbe1pbe/6-311+g(d,p) geom=connectivity symm=loose scf=tight
int=grid=ultrafine

Title Card Required

0 1
 Ge
 C                     1              B1
 H                     2              B2     1              A1
 H                     2              B3     1              A2     3
D1
 H                     2              B4     1              A3     4
D2
 C                     1              B5     2              A4     3
D3
 H                     6              B6     1              A5     2
D4
```

```
 H                     6              B7     1              A6     2
D5
 H                     6              B8     1              A7     2
D6

   B1              1.99592074
   B2              1.09181690
   B3              1.09979500
   B4              1.09542168
   B5              1.99593310
   B6              1.09181754
   B7              1.09976539
   B8              1.09544026
   A1            112.99740532
   A2            106.78941992
   A3            112.20251075
   A4             95.58323625
   A5            112.99479466
   A6            106.82216947
   A7            112.17426947
   D1            118.46168953
   D2            116.74482380
   D3            166.43079093
   D4            166.48083285
   D5            -75.02747395
   D6             41.72026486

 1 2 1.0 6 1.0
 2 3 1.0 4 1.0 5 1.0
 3
 4
 5
 6 7 1.0 8 1.0 9 1.0
 7
 8
 9
```

A1.2.4 $Ge(OH)_2$

```
%mem=1000MB
# opt freq rpbe1pbe/6-311+g(d,p) geom=connectivity symm=loose scf=tight
int=grid=ultrafine

Title Card Required

0 1
 Ge
 O                     1              B1
 H                     2              B2     1              A1
 O                     1              B3     2              A2     3
D1
 H                     4              B4     1              A3     2
D2

   B1              1.79354851
```

```
   B2              0.96025887
   B3              1.79237708
   B4              0.96031894
   A1            113.40526636
   A2             93.19524255
   A3            113.47928602
   D1            180.00000000
   D2            180.00000000

 1 2 1.0 4 1.0
 2 3 1.0
 3
 4 5 1.0
 5
```

A1.2.5 GeF_2

```
%mem=1000MB
# opt freq rpbe1pbe/6-311+g(d,p) geom=connectivity symm=loose scf=tight
int=grid=ultrafine

Title Card Required

0 1
 Ge
 F                  1             B1
 F                  1             B2    2              A1

   B1             1.75594879
   B2             1.75594879
   A1            97.37742430

 1 2 1.0 3 1.0
 2
 3
```

A1.2.6 $GeCl_2$

```
%mem=1000MB
%nproc=1
# opt freq rpbe1pbe/6-311+g(d,p) geom=connectivity symm=loose scf=tight
int=grid=ultrafine

Title Card Required

0 1
 Ge
 Cl                 1             B1
 Cl                 1             B2    2              A1

   B1             2.19508970
   B2             2.19508970
   A1            99.88058591
```

```
 1 2 1.0 3 1.0
 2
 3
```

A1.3 Input Files for the Dihedral Angle Scan about the Carbenic Carbon-Germanium Bond in Compounds 54-59

A1.3.1 Compound 54 (R = H)

```
# opt=modredundant pbe1pbe/6-311+g(d,p) geom=connectivity nosymm
scf=tight int=grid=ultrafine

Title Card Required

0 1
 Ge
 C                  1               B1
 N                  2               B2     1               A1
 N                  2               B3     1               A2     3
D1
 C                  3               B4     2               A3     1
D2
 C                  5               B5     3               A4     2
D3
 H                  5               B6     3               A5     2
D4
 H                  6               B7     5               A6     3
D5
 C                  3               B8     2               A7     1
D6
 H                  9               B9     3               A8     2
D7
 H                  9              B10     3               A9     2
D8
 H                  9              B11     3              A10     2
D9
 C                  4              B12     2              A11     1
D10
 H                 13              B13     4              A12     2
D11
 H                 13              B14     4              A13     2
D12
 H                 13              B15     4              A14     2
D13
 H                  1              B16     2              A15     3
D14
 H                  1              B17     2              A16     3
D15
```

```
  B1              2.02087291
  B2              1.35483158
  B3              1.35483158
  B4              1.37853784
  B5              1.35308200
  B6              1.07744622
  B7              1.07744622
  B8              1.44673058
  B9              1.08990362
  B10             1.09156097
  B11             1.09306709
  B12             1.44673058
  B13             1.09306709
  B14             1.09156097
  B15             1.08990362
  B16             1.58373897
  B17             1.58373897
  A1            126.96042978
  A2            126.96042978
  A3            110.88416222
  A4            106.72580538
  A5            122.48744051
  A6            130.78577189
  A7            123.53611915
  A8            108.96467163
  A9            109.87821648
  A10           109.98630898
  A11           123.53611915
  A12           109.98630898
  A13           109.87821648
  A14           108.96467163
  A15            92.24916501
  A16            92.24916501
  D1            164.96367864
  D2            167.79144660
  D3             -0.10917599
  D4            179.56602449
  D5            179.63815743
  D6            -11.10086165
  D7           -178.09389364
  D8            -57.55089404
  D9             61.82002673
  D10            11.10086165
  D11           -61.82002673
  D12            57.55089404
  D13           178.09389364
  D14            49.26940450
  D15           145.76691686

1 2 1.0 17 1.0 18 1.0
2 3 1.5 4 1.5
3 5 1.5 9 1.0
4 6 1.5 13 1.0
5 6 2.0 7 1.0
6 8 1.0
7
8
```

```
 9 10 1.0 11 1.0 12 1.0
 10
 11
 12
 13 14 1.0 15 1.0 16 1.0
 14
 15
 16
 17
 18

D 18 1 2 4 S 18 10.000000
```

A1.3.2 Compound 55 (R = OH)

```
# opt=modredundant pbe1pbe/6-311+g(d,p) nosymm geom=connectivity
scf=tight int=grid=ultrafine

Title Card Required

0 1
 Ge
 C                  1             B1
 N                  2             B2    1             A1
 N                  2             B3    1             A2    3
D1
 C                  3             B4    2             A3    1
D2
 C                  5             B5    3             A4    2
D3
 H                  5             B6    3             A5    2
D4
 H                  6             B7    5             A6    3
D5
 C                  3             B8    2             A7    1
D6
 H                  9             B9    3             A8    2
D7
 H                  9            B10    3             A9    2
D8
 H                  9            B11    3            A10    2
D9
 C                  4            B12    2            A11    1
D10
 H                 13            B13    4            A12    2
D11
 H                 13            B14    4            A13    2
D12
 H                 13            B15    4            A14    2
D13
 O                  1            B16    2            A15    3
D14
 H                 17            B17    1            A16    2
D15
```

O	1	B18	17	A17	2
D16					
H	19	B19	1	A18	17
D17					

B1	2.11468785
B2	1.35048427
B3	1.35106221
B4	1.37586971
B5	1.35313833
B6	1.07771203
B7	1.07769030
B8	1.45551442
B9	1.09138140
B10	1.09127656
B11	1.09309440
B12	1.45536618
B13	1.09103119
B14	1.09321059
B15	1.09084143
B16	1.87549255
B17	0.95895411
B18	1.87622566
B19	0.95899883
A1	128.44650089
A2	125.31997616
A3	110.83095621
A4	106.68804700
A5	122.30511163
A6	130.98620939
A7	125.74195566
A8	108.05618237
A9	108.92575451
A10	109.87136093
A11	125.41221541
A12	108.08363067
A13	110.04671515
A14	108.77003177
A15	90.95100882
A16	108.83160405
A17	99.87296952
A18	109.19997245
D1	-165.08969441
D2	-167.43846612
D3	0.01571122
D4	-178.80966691
D5	-178.80599448
D6	12.07788796
D7	16.80452561
D8	136.15386043
D9	-103.92202836
D10	-10.61674222
D11	-25.64990299
D12	95.03001269
D13	-145.04519900
D14	-42.69276457
D15	161.57847493

```
   D16            89.29487290
   D17           101.40815355

 1 17 1.0 19 1.0
 2 3 1.5 4 1.5
 3 5 1.5 9 1.0
 4 6 1.5 13 1.0
 5 6 2.0 7 1.0
 6 8 1.0
 7
 8
 9 10 1.0 11 1.0 12 1.0
 10
 11
 12
 13 14 1.0 15 1.0 16 1.0
 14
 15
 16
 17 18 1.0
 18
 19 20 1.0
 20

D 17 1 2 3 S 18 10.000000
```

A1.3.3 Compound 56 (R = NH_2)

```
# opt=modredundant pbe1pbe/6-311+g(d,p) geom=connectivity scf=tight
nosymm int=grid=ultrafine

Title Card Required

0 1
 Ge
 C                  1             B1
 N                  2             B2    1             A1
 N                  2             B3    1             A2    3
D1
 C                  3             B4    2             A3    1
D2
 C                  5             B5    3             A4    2
D3
 H                  5             B6    3             A5    2
D4
 H                  6             B7    5             A6    3
D5
 N                  1             B8    2             A7    4
D6
 H                  9             B9    1             A8    2
D7
 H                  9            B10    1             A9    2
D8
 N                  1            B11    9            A10    2
D9
```

H	12	B12	1	A11	9
D10					
H	12	B13	1	A12	9
D11					
C	3	B14	2	A13	1
D12					
H	15	B15	3	A14	2
D13					
H	15	B16	3	A15	2
D14					
H	15	B17	3	A16	2
D15					
C	4	B18	2	A17	1
D16					
H	19	B19	4	A18	2
D17					
H	19	B20	4	A19	2
D18					
H	19	B21	4	A20	2
D19					

B1	2.11362818
B2	1.35535527
B3	1.35535437
B4	1.37603462
B5	1.35233800
B6	1.07779047
B7	1.07778917
B8	1.92848552
B9	1.01574232
B10	1.01379225
B11	1.92848119
B12	1.01379211
B13	1.01574261
B14	1.45430420
B15	1.09434710
B16	1.09181484
B17	1.09353979
B18	1.45430527
B19	1.09434464
B20	1.09354102
B21	1.09181330
A1	126.44738469
A2	126.43629760
A3	111.02216888
A4	106.71280833
A5	122.27932612
A6	131.00097721
A7	93.71399567
A8	115.02445630
A9	110.07509828
A10	102.22135530
A11	110.07335960
A12	115.02467490
A13	125.59235022
A14	108.04513441
A15	109.10714170

```
   A16           109.79324354
   A17           125.59113175
   A18           108.04523099
   A19           109.79386340
   A20           109.10608145
   D1           -158.88990865
   D2           -162.41562868
   D3             -0.10672378
   D4           -179.24364955
   D5           -179.03427682
   D6             49.31669639
   D7             79.50626443
   D8           -159.67830009
   D9            -94.62333387
   D10          -105.73068980
   D11            15.08334783
   D12            14.32910449
   D13            18.05034530
   D14           137.85382863
   D15          -102.21803251
   D16           -14.32313384
   D17           -18.08694198
   D18           102.18074893
   D19          -137.89111562

 1 9 1.0 12 1.0
 2 3 1.5 4 1.5
 3 5 1.5 15 1.0
 4 6 1.5 19 1.0
 5 6 2.0 7 1.0
 6 8 1.0
 7
 8
 9 10 1.0 11 1.0
 10
 11
 12 13 1.0 14 1.0
 13
 14
 15 16 1.0 17 1.0 18 1.0
 16
 17
 18
 19 20 1.0 21 1.0 22 1.0
 20
 21
 22

D 12 1 2 3 S 18 10.000000
```

A1.3.4 Compound 57 (R = CH_3)

```
# opt=modredundant pbe1pbe/6-311+g(d,p) nosymm geom=connectivity
scf=tight int=grid=ultrafine
```

```
Title Card Required

0 1
 Ge
 C                    1              B1
 N                    2              B2     1              A1
 N                    2              B3     1              A2     3
D1
 C                    3              B4     2              A3     1
D2
 C                    5              B5     3              A4     2
D3
 H                    5              B6     3              A5     2
D4
 H                    6              B7     5              A6     3
D5
 C                    1              B8     2              A7     3
D6
 H                    9              B9     1              A8     2
D7
 H                    9             B10     1              A9     2
D8
 H                    9             B11     1             A10     2
D9
 C                    1             B12     9             A11     2
D10
 H                   13             B13     1             A12     9
D11
 H                   13             B14     1             A13     9
D12
 H                   13             B15     1             A14     9
D13
 C                    3             B16     2             A15     1
D14
 H                   17             B17     3             A16     2
D15
 H                   17             B18     3             A17     2
D16
 H                   17             B19     3             A18     2
D17
 C                    4             B20     2             A19     1
D18
 H                   21             B21     4             A20     2
D19
 H                   21             B22     4             A21     2
D20
 H                   21             B23     4             A22     2
D21

   B1              2.04705183
   B2              1.35872445
   B3              1.35872547
   B4              1.37803534
   B5              1.35179900
   B6              1.07751504
   B7              1.07751485
   B8              2.02489367
```

B9	1.09297735
B10	1.09511457
B11	1.09516390
B12	2.02490181
B13	1.09297748
B14	1.09516271
B15	1.09511373
B16	1.44781966
B17	1.09005055
B18	1.08960004
B19	1.09331637
B20	1.44781886
B21	1.09332027
B22	1.08959948
B23	1.09005108
A1	126.41781649
A2	126.41014373
A3	111.17589623
A4	106.71569988
A5	122.43886442
A6	130.84285033
A7	99.95000946
A8	113.47511316
A9	113.96230590
A10	105.26117454
A11	95.28828212
A12	113.47405706
A13	105.26196776
A14	113.96227530
A15	124.21533406
A16	108.67820104
A17	110.75346662
A18	109.53975553
A19	124.21432058
A20	109.53865802
A21	110.75397002
A22	108.67838685
D1	157.40964930
D2	160.93881248
D3	0.29407266
D4	179.77049479
D5	179.41468604
D6	52.67586547
D7	-82.23061725
D8	43.82759023
D9	161.27373069
D10	-101.09067451
D11	-176.65787922
D12	-60.16161417
D13	57.28494284
D14	-13.96571002
D15	172.64933095
D16	-66.96120836
D17	53.25000614
D18	13.96058332
D19	-53.24215131
D20	66.96839442

```
   D21          -172.64163290

 1 2 1.0 9 1.0 13 1.0
 2 3 1.5 4 1.5
 3 5 1.5 17 1.0
 4 6 1.5 21 1.0
 5 6 2.0 7 1.0
 6 8 1.0
 7
 8
 9 10 1.0 11 1.0 12 1.0
 10
 11
 12
 13 14 1.0 15 1.0 16 1.0
 14
 15
 16
 17 18 1.0 19 1.0 20 1.0
 18
 19
 20
 21 22 1.0 23 1.0 24 1.0
 22
 23
 24

D 13 1 2 4 S 18 10.000000
```

A1.3.5 Compound 58 (R = F)

```
# opt=modredundant pbe1pbe/6-311+g(d,p) nosymm geom=connectivity
scf=tight int=grid=ultrafine

Title Card Required

0 1
 Ge
 C                  1             B1
 N                  2             B2    1             A1
 N                  2             B3    1             A2    3
D1
 C                  3             B4    2             A3    1
D2
 C                  5             B5    3             A4    2
D3
 H                  5             B6    3             A5    2
D4
 H                  6             B7    5             A6    3
D5
 C                  3             B8    2             A7    1
D6
 H                  9             B9    3             A8    2
D7
```

H	9	B10	3	A9	2
D8					
H	9	B11	3	A10	2
D9					
C	4	B12	2	A11	1
D10					
H	13	B13	4	A12	2
D11					
H	13	B14	4	A13	2
D12					
H	13	B15	4	A14	2
D13					
F	1	B16	2	A15	3
D14					
F	1	B17	2	A16	3
D15					

B1	2.15094735
B2	1.34420566
B3	1.34744250
B4	1.37426165
B5	1.35546969
B6	1.07786379
B7	1.07773711
B8	1.45890511
B9	1.08886024
B10	1.09001168
B11	1.09021114
B12	1.45151144
B13	1.08951920
B14	1.09187590
B15	1.09170991
B16	1.83130395
B17	1.82853845
A1	126.79097132
A2	127.74291147
A3	110.63848469
A4	106.91323818
A5	122.39828575
A6	131.00641911
A7	124.54746704
A8	108.64807994
A9	109.72775225
A10	108.33488196
A11	124.73434212
A12	108.66628941
A13	110.17093561
A14	110.05036290
A15	88.74904846
A16	87.52555748
D1	176.29165857
D2	176.76323450
D3	0.23429910
D4	179.98791694
D5	179.43180617
D6	-1.36826224
D7	-39.95504642

```
   D8            79.03506073
   D9          -160.02806783
   D10            3.75782268
   D11           -2.44931132
   D12          117.08504800
   D13         -121.91042627
   D14           49.26764870
   D15          -45.92803357

 1 17 1.0 18 1.0
 2 3 1.5 4 1.5
 3 5 1.5 9 1.0
 4 6 1.5 13 1.0
 5 6 2.0 7 1.0
 6 8 1.0
 7
 8
 9 10 1.0 11 1.0 12 1.0
 10
 11
 12
 13 14 1.0 15 1.0 16 1.0
 14
 15
 16
 17
 18

D 17 1 2 3 S 18 10.000000
```

A1.3.6 Compound 59 (R = Cl)

```
# opt=modredundant pbe1pbe/6-311+g(d,p) nosymm geom=connectivity scf
int=grid=ultrafine

Title Card Required

0 1
 Ge
 Cl                  1             B1
 Cl                  1             B2     2             A1
 C                   1             B3     3             A2     2
D1
 N                   4             B4     1             A3     3
D2
 N                   4             B5     1             A4     5
D3
 C                   5             B6     4             A5     1
D4
 C                   7             B7     5             A6     4
D5
 H                   7             B8     5             A7     4
D6
```

H	8	B9	7	A8	5
D7					
C	5	B10	4	A9	1
D8					
H	11	B11	5	A10	4
D9					
H	11	B12	5	A11	4
D10					
H	11	B13	5	A12	4
D11					
C	6	B14	4	A13	1
D12					
H	15	B15	6	A14	4
D13					
H	15	B16	6	A15	4
D14					
H	15	B17	6	A16	4
D15					

B1	2.28771404
B2	2.28256465
B3	2.12958724
B4	1.34687090
B5	1.35020921
B6	1.37415023
B7	1.35396871
B8	1.07773376
B9	1.07763282
B10	1.45683907
B11	1.08821551
B12	1.09030430
B13	1.09038739
B14	1.45278647
B15	1.08982795
B16	1.09174338
B17	1.09146193
A1	99.84986870
A2	91.56448536
A3	132.19335646
A4	122.53694314
A5	110.58761688
A6	106.99632003
A7	122.23537405
A8	131.05102222
A9	125.75864859
A10	109.13993745
A11	110.00032965
A12	108.24120124
A13	125.50565039
A14	108.87042121
A15	110.04397908
A16	109.81606131
D1	91.94305991
D2	-46.44960622
D3	178.25314797
D4	178.31434506
D5	0.19096653

```
   D6           -179.96426569
   D7            179.44562595
   D8              0.20421750
   D9            -34.97066735
   D10            84.89950570
   D11          -154.32951978
   D12             2.46038419
   D13            -4.48912256
   D14           115.08367368
   D15          -123.99055851

 1 2 1.0 3 1.0
 2
 3
 4 5 1.5 6 1.5
 5 7 1.5 11 1.0
 6 8 1.5 15 1.0
 7 8 2.0 9 1.0
 8 10 1.0
 9
 10
 11 12 1.0 13 1.0 14 1.0
 12
 13
 14
 15 16 1.0 17 1.0 18 1.0
 16
 17
 18

D 2 1 4 5 S 18 10.000000
```

A1.4 Input Files for the Geometry Optimization of GeR_2 Adducts of Butadiene

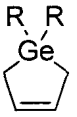

The following is a representative input file used for the geometry optimization of the GeR_2 adducts of butadiene. In the example below, R = F. The input file for the other complexes, where R = H, OH, NH_2, Me or Cl, are identical, except in the identity of the 'R' atom.

```
%mem=700MB
# opt freq rpbe1pbe/6-311+g(d,p) geom=connectivity symm=loose scf=tight
int=grid=ultrafine

Title Card Required

0 1
 C
 C                    1              B1
 C                    2              B2     1              A1
 C                    3              B3     2              A2     1
D1
 H                    1              B4     2              A3     3
D2
 H                    1              B5     2              A4     3
D3
 H                    2              B6     1              A5     3
D4
 H                    3              B7     2              A6     1
D5
 H                    4              B8     3              A7     2
D6
 H                    4              B9     3              A8     2
D7
 Ge                   4             B10     3              A9     2
D8
 F                   11             B11     4             A10     3
D9
 F                   11             B12     4             A11     3
D10

   B1             1.50414213
   B2             1.33645400
   B3             1.50414213
   B4             1.09492053
   B5             1.09492053
   B6             1.08859184
   B7             1.08859184
   B8             1.09492053
   B9             1.09492053
   B10            1.97257427
   B11            1.80000000
```

```
   B12              1.80000000
   A1             120.76194721
   A2             120.76194721
   A3             111.66113850
   A4             111.66113850
   A5             119.01237528
   A6             120.22567751
   A7             111.66113850
   A8             111.66113850
   A9             102.45463055
   A10            113.49266419
   A11            113.49266419
   D1               0.00000000
   D2             120.26302934
   D3            -120.26302934
   D4            -180.00000000
   D5            -180.00000000
   D6            -120.26302934
   D7             120.26302934
   D8               0.00000000
   D9             117.55486268
   D10           -117.55486268

 1 2 1.0 5 1.0 6 1.0 11 1.0
 2 3 2.0 7 1.0
 3 4 1.0 8 1.0
 4 9 1.0 10 1.0 11 1.0
 5
 6
 7
 8
 9
 10
 11 12 1.0 13 1.0
 12
 13
```

A1.5 Input File for the Geometry Optimization of Butadiene

```
# freq pbe1pbe/6-311+g(d,p) geom=connectivity symm=loose scf=tight
int=grid=ultrafine

Title Card Required

0 1
 C
 H                  1             B1
 H                  1             B2    2             A1
 C                  1             B3    2             A2    3
D1
 H                  4             B4    1             A3    2
D2
 C                  4             B5    1             A4    2
D3
```

```
 H                     6              B6     4              A5     1
D4
 C                     6              B7     4              A6     1
D5
 H                     8              B8     6              A7     4
D6
 H                     8              B9     6              A8     4
D7

   B1              1.08422553
   B2              1.08662706
   B3              1.33588100
   B4              1.08919695
   B5              1.45199192
   B6              1.08919695
   B7              1.33588100
   B8              1.08422553
   B9              1.08662706
   A1            117.06574414
   A2            121.63891629
   A3            119.44469875
   A4            124.13425607
   A5            116.42104518
   A6            124.13425607
   A7            121.63891629
   A8            121.29533957
   D1            180.00000000
   D2              0.00000000
   D3            180.00000000
   D4              0.00000000
   D5            180.00000000
   D6            180.00000000
   D7              0.00000000

1 2 1.0 3 1.0 4 2.0
2
3
4 5 1.0 6 1.0
5
6 7 1.0 8 2.0
7
8 9 1.0 10 1.0
9
10
```

A1.6 Input Files for the Geometry Optimization of NHC-GeR_2-Butadiene Adducts (R = H, Me, OH, NH_2, F, Cl)

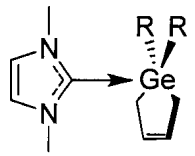

A1.6.1 Input Files for the Geometry Optimization, R = H

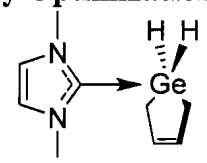


```
# opt freq rpbe1pbe/6-311+g(d,p) geom=connectivity scf=tight
int=grid=ultrafine nosymm

Title Card Required

0 1
 Ge                   0.00000000    0.00000000    0.00000000
 C                    3.27169902    0.00000000    0.00000000
 H                    2.57435390    0.71744072    0.00000000
 N                    2.61909721   -1.22907964   -0.52045961
 N                    1.01847081   -2.48926884   -1.26516584
 C                   -0.34454702   -2.85289433   -1.71383364
 H                   -0.96468036   -2.15957326   -1.34683816
 C                    1.29296699   -1.31110930   -0.68440834
 C                    3.21365119   -2.40001386   -0.97637544
 C                    2.21594326   -3.18483643   -1.45282412
 C                    0.24758242    1.41483222    1.30690348
 H                    0.58927752    1.06256703    2.16600654
 H                    0.85868558    2.11886152    0.97244192
 C                   -1.17333488    1.92250903    1.43582181
 C                   -2.18210262    1.35304184    0.75501651
 C                   -1.92530246    0.18696768   -0.18321480
 H                   -2.18447488    0.40246198   -1.11398527
 H                   -2.40178419   -0.63028108    0.11085729
 H                    3.58190125   -0.12571958    1.01630171
 H                    4.04891659    0.32709229   -0.65866796
 H                    4.25745133   -2.62998737   -0.92644099
 H                    2.31022230   -4.15471431   -1.89480644
 H                   -0.66690758   -3.79588359   -1.32427631
 H                   -0.40779389   -2.79268839   -2.78026464
 H                   -3.20236310    1.66316780    0.84327998
 H                   -1.30961637    2.74505988    2.10644648
 H                    0.33682030    0.85230719   -1.21265186
 H                   -0.17919803   -1.05484119    1.07962870

 1 8 1.0 11 1.0 16 1.0 27 1.0 28 1.0
 2 3 1.0 4 1.0 19 1.0 20 1.0
 3
 4 8 1.0 9 1.0
 5 6 1.0 8 1.0 10 1.0
 6 7 1.0 23 1.0 24 1.0
 7
 8
 9 10 1.0 21 1.0
 10 22 1.0
 11 12 1.0 13 1.0 14 1.0
 12
 13
 14 15 1.0 26 1.0
```

```
 15 16 1.0 25 1.0
 16 17 1.0 18 1.0
 17
 18
 19
 20
 21
 22
 23
 24
 25
 26
 27
 28
```

A1.6.2 Input Files for the Geometry Optimization, R = Me

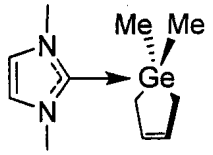


```
# opt freq rpbe1pbe/6-311+g(d,p) geom=connectivity scf=tight
int=grid=ultrafine nosymm

Title Card Required

0 1
 Ge                  0.00000000    0.00000000    0.00000000
 C                   3.27169902    0.00000000    0.00000000
 H                   2.57435390    0.71744072    0.00000000
 N                   2.61909721   -1.22907964   -0.52045961
 N                   1.01847081   -2.48926884   -1.26516584
 C                  -0.34454702   -2.85289433   -1.71383364
 H                  -0.96468036   -2.15957326   -1.34683816
 C                   1.29296699   -1.31110930   -0.68440834
 C                   3.21365119   -2.40001386   -0.97637544
 C                   2.21594326   -3.18483643   -1.45282412
 C                   0.24758242    1.41483222    1.30690348
 H                   0.58927752    1.06256703    2.16600654
 H                   0.85868558    2.11886152    0.97244192
 C                  -1.17333488    1.92250903    1.43582181
 C                  -2.18210262    1.35304184    0.75501651
 C                  -1.92530246    0.18696768   -0.18321480
 H                  -2.18447488    0.40246198   -1.11398527
 H                  -2.40178419   -0.63028108    0.11085729
 H                   3.58190125   -0.12571958    1.01630171
 H                   4.04891659    0.32709229   -0.65866796
 H                   4.25745133   -2.62998737   -0.92644099
 H                   2.31022230   -4.15471431   -1.89480644
 H                  -0.66690758   -3.79588359   -1.32427631
 H                  -0.40779389   -2.79268839   -2.78026464
 H                  -3.20236310    1.66316780    0.84327998
```

```
H                  -1.30961637    2.74505988    2.10644648
H                   0.33682030    0.85230719   -1.21265186
H                  -0.17919803   -1.05484119    1.07962870

1 8 1.0 11 1.0 16 1.0 27 1.0 28 1.0
2 3 1.0 4 1.0 19 1.0 20 1.0
3
4 8 1.0 9 1.0
5 6 1.0 8 1.0 10 1.0
6 7 1.0 23 1.0 24 1.0
7
8
9 10 1.0 21 1.0
10 22 1.0
11 12 1.0 13 1.0 14 1.0
12
13
14 15 1.0 26 1.0
15 16 1.0 25 1.0
16 17 1.0 18 1.0
17
18
19
20
21
22
23
24
25
26
27
28
```

A1.6.3 Input Files for the Geometry Optimization, R = OH

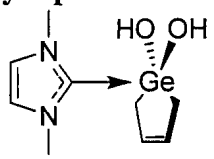


```
# pbe1pbe/6-311+g(d,p) geom=connectivity symm=loose scf=tight
int=grid=ultrafine

Title Card Required

0 1
 Ge
 C                    1              B1
 H                    2              B2     1              A1
 N                    2              B3     1              A2     3
D1
 N                    4              B4     2              A3     1
D2
 C                    5              B5     4              A4     2
D3
 H                    6              B6     5              A5     4
D4
```

C	5	B7	4	A6	2
D5					
C	4	B8	2	A7	1
D6					
C	9	B9	4	A8	2
D7					
C	1	B10	8	A9	5
D8					
H	11	B11	1	A10	8
D9					
H	11	B12	1	A11	8
D10					
C	11	B13	1	A12	8
D11					
C	14	B14	11	A13	1
D12					
C	15	B15	14	A14	11
D13					
H	16	B16	15	A15	14
D14					
H	16	B17	15	A16	14
D15					
H	2	B18	1	A17	11
D16					
H	2	B19	1	A18	11
D17					
H	9	B20	4	A19	2
D18					
H	10	B21	9	A20	4
D19					
H	6	B22	5	A21	4
D20					
H	6	B23	5	A22	4
D21					
H	15	B24	14	A23	11
D22					
H	14	B25	11	A24	1
D23					
O	1	B26	11	A25	14
D24					
H	27	B27	1	A26	11
D25					
O	1	B28	27	A27	8
D26					
H	29	B29	1	A28	27
D27					

B1	3.50898034
B2	1.08936496
B3	1.45335064
B4	2.13562852
B5	1.45448840
B6	1.08894101
B7	1.35437039
B8	1.37626488
B9	1.35047338
B10	1.99417330

B11	1.09531066
B12	1.09787320
B13	1.49524093
B14	1.33954901
B15	1.49527310
B16	1.09963098
B17	1.09709173
B18	1.09308123
B19	1.09121417
B20	1.07782752
B21	1.07781881
B22	1.09282338
B23	1.09259217
B24	1.08948844
B25	1.08863609
B26	1.82804224
B27	0.95935256
B28	1.83677970
B29	0.96004409
A1	52.89214505
A2	65.92023219
A3	163.97168315
A4	164.98828662
A5	108.37707457
A6	38.05536483
A7	122.45563482
A8	106.50009630
A9	89.72175653
A10	111.96030535
A11	108.79304175
A12	104.45168101
A13	119.75358588
A14	119.65928502
A15	110.40397165
A16	112.07213961
A17	97.47577352
A18	152.66215148
A19	122.45035732
A20	131.05439396
A21	109.40940073
A22	109.30416520
A23	119.85422938
A24	119.72933154
A25	116.91418620
A26	108.69493982
A27	117.38205147
A28	108.77427710
D1	-140.40234072
D2	-0.28353568
D3	6.32738700
D4	-1.04833328
D5	4.39493335
D6	-175.28306536
D7	178.68057330
D8	101.97874910
D9	-42.58705734
D10	75.39145550

```
  D11          -164.85147893
  D12           -14.53867378
  D13            -0.77653051
  D14          -101.95011750
  D15           140.32689279
  D16            -8.22031880
  D17          -174.94551528
  D18            -1.84450195
  D19           179.11874205
  D20          -121.47171620
  D21           118.84553441
  D22           178.70448228
  D23           164.05065954
  D24           -79.26763898
  D25            91.42610912
  D26            78.12981926
  D27            95.41801787

1 11 1.0 16 1.0 27 1.0 29 1.0
2 3 1.0 4 1.0 19 1.0 20 1.0
3
4 8 1.5 9 1.5
5 6 1.0 8 1.5 10 1.5
6 7 1.0 23 1.0 24 1.0
7
8
9 10 2.0 21 1.0
10 22 1.0
11 12 1.0 13 1.0 14 1.0
12
13
14 15 2.0 26 1.0
15 16 1.0 25 1.0
16 17 1.0 18 1.0
17
18
19
20
21
22
23
24
25
26
27 28 1.0
28
29 30 1.0
30
```

A1.6.4 Input Files for the Geometry Optimization, R = NH_2

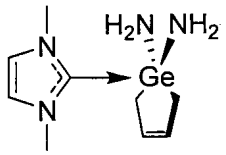


```
# opt freq pbe1pbe/6-311+g(d,p) geom=connectivity nosymm scf=tight
int=grid=ultrafine

Title Card Required

0 1
 Ge                   0.00000000    0.00000000    0.78858200
 C                    2.07009300    1.31863800   -1.70496500
 H                    1.77110900    1.86883900   -0.80567200
 N                    0.89924800    0.58255400   -2.15697500
 N                   -0.89924800   -0.58255400   -2.15697500
 C                   -2.07009300   -1.31863800   -1.70496500
 H                   -1.77110900   -1.86883900   -0.80567200
 C                    0.00000000    0.00000000   -1.33856100
 C                    0.57089800    0.36443900   -3.47478800
 C                   -0.57089800   -0.36443900   -3.47478800
 C                    1.46046600    0.11147000    2.13789500
 H                    2.17259200   -0.71847700    2.07460000
 H                    2.03142000    1.04482700    2.07214500
 C                    0.66809800    0.04843100    3.41660000
 C                   -0.66809800   -0.04843100    3.41660000
 C                   -1.46046600   -0.11147000    2.13789500
 H                   -2.17259200    0.71847700    2.07460000
 H                   -2.03142000   -1.04482700    2.07214500
 H                    2.89319900    0.63137500   -1.49536800
 H                    2.36987800    2.01398500   -2.48982900
 H                    1.17019500    0.73789700   -4.28876300
 H                   -1.17019500   -0.73789700   -4.28876300
 H                   -2.36987800   -2.01398500   -2.48982900
 H                   -2.89319900   -0.63137500   -1.49536800
 H                   -1.19946200   -0.08398700    4.36838300
 H                    1.19946200    0.08398700    4.36838300
 N                    0.00000000    1.96244500    0.48613200
 H                   -0.85071700    2.28539900    0.03029000
 H                    0.03070500    2.44847000    1.38003300
 N                    0.00000000   -1.96244500    0.48613200
 H                    0.85071700   -2.28539900    0.03029000
 H                   -0.03070500   -2.44847000    1.38003300

 1 11 1.0 16 1.0 27 1.0 30 1.0
 2 3 1.0 4 1.0 19 1.0 20 1.0
 3
 4 8 1.5 9 1.5
 5 6 1.0 8 1.5 10 1.5
 6 7 1.0 23 1.0 24 1.0
 7
 8
 9 10 2.0 21 1.0
 10 22 1.0
 11 12 1.0 13 1.0 14 1.0
 12
 13
```

```
 14 15 2.0 26 1.0
 15 16 1.0 25 1.0
 16 17 1.0 18 1.0
 17
 18
 19
 20
 21
 22
 23
 24
 25
 26
 27 28 1.0 29 1.0
 28
 29
 30 31 1.0 32 1.0
 31
 32
```

A1.6.5 Input Files for the Geometry Optimization, R = F

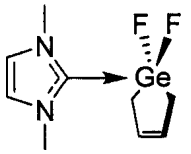


```
# opt freq rpbe1pbe/6-311+g(d,p) geom=connectivity symm=loose
int=grid=ultrafine scf=tight

Title Card Required

0 1
 Ge                  0.00000000   -0.00000000   -0.75823403
 C                  -0.14257827    2.45874425    1.63440036
 H                   0.45954618    2.56835316    0.73173191
 N                  -0.04436867    1.07325450    2.07332598
 N                   0.04436867   -1.07325450    2.07332598
 C                   0.14257827   -2.45874425    1.63440036
 H                  -0.45954618   -2.56835316    0.73173191
 C                   0.00000000   -0.00000000    1.26370707
 C                  -0.03415006    0.67701891    3.38866045
 C                   0.03415006   -0.67701891    3.38866045
 C                  -0.99931915    1.07457662   -2.04415029
 H                  -2.07864568    0.92263521   -1.95878281
 H                  -0.77843149    2.14309347   -1.96872315
 C                  -0.45706806    0.49099287   -3.32450191
 C                   0.45706806   -0.49099287   -3.32450191
 C                   0.99931915   -1.07457662   -2.04415029
 H                   2.07864568   -0.92263521   -1.95878281
 H                   0.77843149   -2.14309347   -1.96872315
 H                  -1.18598037    2.71722555    1.44098161
 H                   0.24953978    3.09894903    2.42457409
 H                  -0.07798996    1.38255921    4.20164319
 H                   0.07798996   -1.38255921    4.20164319
```

```
 H                  -0.24953978   -3.09894903    2.42457409
 H                   1.18598037   -2.71722555    1.44098161
 H                   0.81894519   -0.88393011   -4.27260838
 H                  -0.81894519    0.88393011   -4.27260838
 F                   1.39325090    1.27951735   -0.52148106
 F                  -1.39325090   -1.27951735   -0.52148106

 1 8 1.0 11 1.0 16 1.0 27 1.0 28 1.0
 2 3 1.0 4 1.0 19 1.0 20 1.0
 3
 4 8 1.5 9 1.5
 5 6 1.0 8 1.5 10 1.5
 6 7 1.0 23 1.0 24 1.0
 7
 8
 9 10 2.0 21 1.0
 10 22 1.0
 11 12 1.0 13 1.0 14 1.0
 12
 13
 14 15 2.0 26 1.0
 15 16 1.0 25 1.0
 16 17 1.0 18 1.0
 17
 18
 19
 20
 21
 22
 23
 24
 25
 26
 27
 28
```

A1.6.6 Input Files for the Geometry Optimization, R = Cl

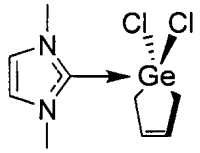


```
# pbe1pbe/6-311+g(d,p) geom=connectivity symm=loose scf=tight
int=grid=ultrafine

Title Card Required

0 1
 Ge
 Cl                  1             B1
 Cl                  1             B2     2              A1
 C                   1             B3     3              A2     2
D1
```

H	4	B4	1	A3	3
D2					
N	4	B5	1	A4	3
D3					
N	6	B6	4	A5	1
D4					
C	7	B7	6	A6	4
D5					
H	8	B8	7	A7	6
D6					
C	7	B9	6	A8	4
D7					
C	6	B10	4	A9	1
D8					
C	11	B11	6	A10	4
D9					
C	1	B12	10	A11	7
D10					
H	13	B13	1	A12	10
D11					
H	13	B14	1	A13	10
D12					
C	13	B15	1	A14	10
D13					
C	16	B16	13	A15	1
D14					
C	17	B17	16	A16	13
D15					
H	18	B18	17	A17	16
D16					
H	18	B19	17	A18	16
D17					
H	4	B20	1	A19	13
D18					
H	4	B21	1	A20	13
D19					
H	11	B22	6	A21	4
D20					
H	12	B23	11	A22	6
D21					
H	8	B24	7	A23	6
D22					
H	8	B25	7	A24	6
D23					
H	17	B26	16	A25	13
D24					
H	16	B27	13	A26	1
D25					

B1	2.41896543
B2	2.41896543
B3	3.36444616
B4	1.09204977
B5	1.45315771
B6	2.15115573
B7	1.45315771
B8	1.09204977

B9	1.33994546
B10	1.37569292
B11	1.35595644
B12	1.95365788
B13	1.09281593
B14	1.09291968
B15	1.50621330
B16	1.33697135
B17	1.50621330
B18	1.09281593
B19	1.09291968
B20	1.09150059
B21	1.08911688
B22	1.07708624
B23	1.07708624
B24	1.08911688
B25	1.09150059
B26	1.08808236
B27	1.08808236
A1	165.99356427
A2	95.89260396
A3	71.06582323
A4	62.29222501
A5	160.95575749
A6	160.95575749
A7	108.83978103
A8	36.61102646
A9	125.80575054
A10	106.79915785
A11	131.14660109
A12	112.04944875
A13	112.17341836
A14	98.94430045
A15	122.20203575
A16	122.20203575
A17	111.78658260
A18	111.64209516
A19	79.25093602
A20	169.74664312
A21	122.22696696
A22	130.97380810
A23	108.59838658
A24	109.93563205
A25	119.78373971
A26	118.01190593
D1	-45.00335712
D2	-161.48591940
D3	74.05801137
D4	3.12614612
D5	-6.69979378
D6	-52.37075935
D7	-3.34989689
D8	179.17450148
D9	-178.64800798
D10	165.55057342
D11	-62.08096233
D12	62.08257943

```
  D13          179.94219692
  D14            0.19699302
  D15           -0.29701334
  D16         -117.97813286
  D17          118.45746038
  D18           48.65908093
  D19         -163.47329726
  D20            1.43665500
  D21          179.89569407
  D22         -171.74651978
  D23           68.63346073
  D24         -179.73185963
  D25          179.64140568

1 10 1.0 13 1.0 18 1.0
2
3
4 5 1.0 6 1.0 21 1.0 22 1.0
5
6 10 1.5 11 1.5
7 8 1.0 10 1.5 12 1.5
8 9 1.0 25 1.0 26 1.0
9
10
11 12 2.0 23 1.0
12 24 1.0
13 14 1.0 15 1.0 16 1.0
14
15
16 17 2.0 28 1.0
17 18 1.0 27 1.0
18 19 1.0 20 1.0
19
20
21
22
23
24
25
26
27
28
```

A1.7 Input Files for the Geometry Optimization of 84^{2+}

```
# opt freq rpbe1pbe/6-311+g(d,p) pop=npa geom=connectivity scf=tight
int=grid=ultrafine

Title Card Required

2 1
 Ge
 N                  1             B1
 N                  2             B2    1             A1
```

C	2	B3	1	A2	3
D1					
C	2	B4	1	A3	4
D2					
C	5	B5	2	A4	1
D3					
C	3	B6	2	A5	1
D4					
C	2	B7	1	A6	4
D5					
N	1	B8	4	A7	2
D6					
N	9	B9	1	A8	4
D7					
C	9	B10	1	A9	4
D8					
C	9	B11	1	A10	4
D9					
C	12	B12	9	A11	1
D10					
C	10	B13	9	A12	1
D11					
C	9	B14	1	A13	4
D12					
N	1	B15	4	A14	2
D13					
N	16	B16	1	A15	4
D14					
C	16	B17	1	A16	4
D15					
C	16	B18	1	A17	4
D16					
C	19	B19	16	A18	1
D17					
C	17	B20	16	A19	1
D18					
C	16	B21	1	A20	4
D19					
H	7	B22	3	A21	2
D20					
H	8	B23	2	A22	1
D21					
H	14	B24	10	A23	9
D22					
H	15	B25	9	A24	1
D23					
H	21	B26	17	A25	16
D24					
H	22	B27	16	A26	1
D25					
H	7	B28	3	A27	2
D26					
H	7	B29	3	A28	2
D27					
H	6	B30	5	A29	2
D28					

```
 H                5          B31    2          A30    1
D29
 H                8          B32    2          A31    1
D30
 H                8          B33    2          A32    1
D31
 H               14          B34   10          A33    9
D32
 H               14          B35   10          A34    9
D33
 H               13          B36   12          A35    9
D34
 H               12          B37    9          A36    1
D35
 H               15          B38    9          A37    1
D36
 H               15          B39    9          A38    1
D37
 H               21          B40   17          A39   16
D38
 H               21          B41   17          A40   16
D39
 H               22          B42   16          A41    1
D40
 H               22          B43   16          A42    1
D41
 H               19          B44   16          A43    1
D42
 H               20          B45   19          A44   16
D43
```

B1	3.12250482
B2	2.15351613
B3	1.35203954
B4	1.37491205
B5	1.35878672
B6	1.45966413
B7	1.45468744
B8	3.12250482
B9	2.15351613
B10	1.35203954
B11	1.37491205
B12	1.35878672
B13	1.45966413
B14	1.45468744
B15	3.12250482
B16	2.15351613
B17	1.35203954
B18	1.37491205
B19	1.35878672
B20	1.45966413
B21	1.45468744
B22	1.09173148
B23	1.09030171
B24	1.09173148
B25	1.09030171
B26	1.09173148

B27	1.09030171
B28	1.09030154
B29	1.09307932
B30	1.07995757
B31	1.08004677
B32	1.09294562
B33	1.09070119
B34	1.09030154
B35	1.09307932
B36	1.07995757
B37	1.08004677
B38	1.09294562
B39	1.09070119
B40	1.09030154
B41	1.09307932
B42	1.09294562
B43	1.09070119
B44	1.08004677
B45	1.07995757
A1	63.09877015
A2	26.20546154
A3	135.76653880
A4	106.88373229
A5	161.75312729
A6	100.30287823
A7	106.00481255
A8	63.09877015
A9	26.20546154
A10	135.76653880
A11	106.88373229
A12	161.75312729
A13	100.30287823
A14	85.77801458
A15	63.09877015
A16	26.20546154
A17	135.76653880
A18	106.88373229
A19	161.75312729
A20	100.30287823
A21	110.31358276
A22	109.54579299
A23	110.31358276
A24	109.54579299
A25	110.31358276
A26	109.54579299
A27	108.76707344
A28	109.64353187
A29	130.76838358
A30	122.36257999
A31	110.73600594
A32	108.88198314
A33	108.76707344
A34	109.64353187
A35	130.76838358
A36	122.36257999
A37	110.73600594
A38	108.88198314

```
  A39          108.76707344
  A40          109.64353187
  A41          110.73600594
  A42          108.88198314
  A43          122.36257999
  A44          130.76838358
  D1            -8.18524890
  D2            16.33671860
  D3            -7.88913319
  D4             2.04607727
  D5          -170.91516487
  D6           -12.56023915
  D7            90.78859456
  D8            82.60334566
  D9            98.94006426
  D10           -7.88913319
  D11            2.04607727
  D12          -88.31181920
  D13         -100.33947781
  D14         -166.80695876
  D15         -174.99220766
  D16         -158.65548906
  D17           -7.88913319
  D18            2.04607727
  D19           14.09262747
  D20          -63.27775928
  D21           43.09102552
  D22          -63.27775928
  D23           43.09102552
  D24          -63.27775928
  D25           43.09102552
  D26          176.98738206
  D27           56.84461862
  D28         -179.50918959
  D29          172.16455096
  D30          -77.87018207
  D31          162.30247132
  D32          176.98738206
  D33           56.84461862
  D34         -179.50918959
  D35          172.16455096
  D36          -77.87018207
  D37          162.30247132
  D38          176.98738206
  D39           56.84461862
  D40          -77.87018207
  D41          162.30247132
  D42          172.16455096
  D43         -179.50918959

1 4 1.0 11 1.0 18 1.0
2 4 1.5 5 1.5 8 1.0
3 4 1.5 6 1.5 7 1.0
4
5 6 2.0 32 1.0
6 31 1.0
7 23 1.0 29 1.0 30 1.0
```

```
 8 24 1.0 33 1.0 34 1.0
 9 11 1.5 12 1.5 15 1.0
 10 11 1.5 13 1.5 14 1.0
 11
 12 13 2.0 38 1.0
 13 37 1.0
 14 25 1.0 35 1.0 36 1.0
 15 26 1.0 39 1.0 40 1.0
 16 18 1.5 19 1.5 22 1.0
 17 18 1.5 20 1.5 21 1.0
 18
 19 20 2.0 45 1.0
 20 46 1.0
 21 27 1.0 41 1.0 42 1.0
 22 28 1.0 43 1.0 44 1.0
 23
 24
 25
 26
 27
 28
 29
 30
 31
 32
 33
 34
 35
 36
 37
 38
 39
 40
 41
 42
 43
 44
 45
 46
```

A1.8 Input Files for the MO visualization and NBO calculations of 85^{2+}

```
%chk=crypto-ge-D3-xray-NBO
# PBE1PBE/6-311+G(2d,p) SCF=Tight Int(Grid=UltraFine)
  Pop=(NBORead,SaveNBOs)

[cryptand*Ge]2+ / Experimental X-ray D3 geometry

2,1
Ge     0.000000    0.000000     0.000000
O      1.067743    2.050487    -0.912711
N      0.000000    0.000000    -2.523900
C      1.088007    0.884821    -2.986102
H      1.017250    0.995571    -3.967303
H      1.957568    0.452722    -2.792895
```

C	1.060738	2.245615	-2.334913
H	1.853385	2.771507	-2.611413
H	0.247055	2.738728	-2.608220
C	0.735119	3.225971	-0.169822
H	0.952746	4.030010	-0.704627
H	1.269751	3.255568	0.662980
O	-2.309645	-0.100551	-0.912711
C	-1.310281	0.499831	-2.986102
H	-1.370815	0.383178	-3.967303
H	-1.370853	1.468943	-2.792895
C	-2.475128	-0.204182	-2.334913
H	-3.326888	0.219325	-2.611413
H	-2.495336	-1.155408	-2.608220
C	-3.161332	-0.976354	-0.169822
H	-3.966464	-1.189903	-0.704627
H	-3.454280	-0.528147	0.662980
O	1.241902	-1.949936	-0.912711
C	0.222274	-1.384652	-2.986102
H	0.353565	-1.378750	-3.967303
H	-0.586715	-1.921665	-2.792895
C	1.414391	-2.041433	-2.334913
H	1.473503	-2.990832	-2.611413
H	2.248281	-1.583320	-2.608220
C	2.426214	-2.249617	-0.169822
H	3.013718	-2.840108	-0.704627
H	2.184529	-2.727421	0.662980
O	-1.067743	2.050487	0.912711
N	0.000000	0.000000	2.523900
C	-1.088007	0.884821	2.986102
H	-1.017250	0.995571	3.967303
H	-1.957568	0.452722	2.792895
C	-1.060738	2.245615	2.334913
H	-1.853385	2.771507	2.611413
H	-0.247055	2.738728	2.608220
C	-0.735119	3.225971	0.169822
H	-0.952746	4.030010	0.704627
H	-1.269751	3.255568	-0.662980
O	2.309645	-0.100551	0.912711
C	1.310281	0.499831	2.986102
H	1.370815	0.383178	3.967303
H	1.370853	1.468943	2.792895
C	2.475128	-0.204182	2.334913
H	3.326888	0.219325	2.611413
H	2.495336	-1.155408	2.608220
C	3.161332	-0.976354	0.169822
H	3.966464	-1.189903	0.704627
H	3.454280	-0.528147	-0.662980
O	-1.241902	-1.949936	0.912711
C	-0.222274	-1.384652	2.986102
H	-0.353565	-1.378750	3.967303
H	0.586715	-1.921665	2.792895
C	-1.414391	-2.041433	2.334913
H	-1.473503	-2.990832	2.611413
H	-2.248281	-1.583320	2.608220
C	-2.426214	-2.249617	0.169822
H	-3.013718	-2.840108	0.704627
H	-2.184529	-2.727421	-0.662980

Appendix 2

Copyrighted Material and Permissions

A2.1 National Research Council Research Free Policy on Authors' Rights*

All articles in NRC Research Press journals are copyright NRC Research Press or its licensors (see Copyright).

However, NRC Research Press recognizes the importance of sharing significant research among the scholarly community. With this in mind, we grant authors who have transferred copyright or granted a license to the NRC Research Press the following privileges to support this effort.

Authors will retain the right to

- Place a draft of a submitted article(s) (pre-acceptance) on their web site or their organization's server, provided that it is not amended once accepted for publication by NRC Research Press. We encourage authors to insert hypertext links from their preprints to the NRC Research Press web site, http://pubs.nrc-cnrc.gc.ca
- Post a published article on their web site or their organization's server six months after the NRC Research Press' original electronic publication date. The author must include NRC Research Press' copyright notice and acknowledge the article's source.
- Make copies of their article(s) in electronic or paper format, for personal or educational use within the home institution provided no financial gain is realized.

---

* This Material is available at http://pubs.nrc-cnrc.gc.ca/cgi-bin/rp/rp2_prog_e?arights_e.html

- Reproduce their article(s) in paper format for placement in the home institution's reserve collection.
- Re-use all or part of their article(s) in subsequent publications provided the source is acknowledged and no financial gain is realized.

NRC Research Press must retain certain rights in order to conduct day-to-day business for the benefit of the authors, the scholarly community and NRC.

NRC Research Press will retain the right to

- Negotiate agreements with secondary publishers and other third parties to further the dissemination of the published information.
- Administer copyright for all published materials to permit the above negotiations and to facilitate the process of granting permission to reproduce.
- Republish articles in alternative formats and editions.

A2.2 American Chemical Society's Policy on Theses and Dissertations[♦]

Thank you for your request for permission to include your paper(s) or portions of text from your paper(s) in your thesis. Permission is now automatically granted; please pay special attention to the implications paragraph below. The Copyright Subcommittee of the Joint Board/Council Committees on Publications approved the following:

Copyright permission for published and submitted material from theses and dissertations ACS extends blanket permission to students to include in their theses and dissertations their own articles, or portions thereof, that have been published in ACS journals or submitted to ACS journals for publication, provided that the ACS copyright credit line is noted on the appropriate page(s).

Publishing implications of electronic publication of theses and dissertation material: Students and their mentors should be aware that posting of theses and dissertation material on the Web prior to submission of material from that thesis or dissertation to an ACS journal may affect publication in that journal. Whether Web posting is considered prior publication may be evaluated on a case-by-case basis by the journal's editor. If an ACS journal editor considers Web posting to be "prior publication", the paper will not be accepted for publication in that journal. If you intend to submit your unpublished paper to ACS for publication, check with the appropriate editor prior to posting your manuscript electronically.

If your paper has not yet been published by ACS, we have no objection to your including the text or portions of the text in your thesis/dissertation in print and microfilm formats; please note, however, that electronic distribution or Web posting of the

---

[♦] This material is available at http://pubs.acs.org/copyright/forms/dissertation.pdf

unpublished paper as part of your thesis in electronic formats might jeopardize publication of your paper by ACS. Please print the following credit line on the first page of your article: "Reproduced (or 'Reproduced in part') with permission from [JOURNAL NAME], in press (or 'submitted for publication'). Unpublished work copyright [CURRENT YEAR] American Chemical Society." Include appropriate information.

If your paper has already been published by ACS and you want to include the text or portions of the text in your thesis/dissertation in print or microfilm formats, please print the ACS copyright credit line on the first page of your article: "Reproduced (or 'Reproduced in part') with permission from [FULL REFERENCE CITATION.] Copyright [YEAR] American Chemical Society." Include appropriate information.

Submission to a Dissertation Distributor: If you plan to submit your thesis to UMI or to another dissertation distributor, you should not include the unpublished ACS paper in your thesis if the thesis will be disseminated electronically, until ACS has published your paper. After publication of the paper by ACS, you may release the entire thesis (not the individual ACS article by itself) for electronic dissemination through the distributor; ACS's copyright credit line should be printed on the first page of the ACS paper.

Use on an Intranet: The inclusion of your ACS unpublished or published manuscript is permitted in your thesis in print and microfilm formats. If ACS has published your paper you may include the manuscript in your thesis on an intranet that is not publicly available. Your ACS article cannot be posted electronically on a publicly available medium (i.e. one that is not password protected), such as but not limited to, electronic archives, Internet, library server, etc. The only material from your paper that

can be posted on a public electronic medium is the article abstract, figures, and tables, and you may link to the article's DOI or post the article's author-directed URL link provided by ACS. This paragraph does not pertain to the dissertation distributor paragraph above.

A2.3 American Association for the Advancement of Science's Copyright release

American Association for the Advancement of Science TERMS AND CONDITIONS

Regarding your request, we are pleased to grant you non-exclusive, non-transferable permission, to republish the AAAS material identified above in your work identified above, subject to the terms and conditions herein. We must be contacted for permission for any uses other than those specifically identified in your request above.

The following credit line must be printed along with the AAAS material: "From [Full Reference Citation]. Reprinted with permission from AAAS."

All required credit lines and notices must be visible any time a user accesses any part of the AAAS material and must appear on any printed copies and authorized user might make.

This permission does not apply to figures / photos / artwork or any other content or materials included in your work that are credited to non-AAAS sources. If the requested material is sourced to or references non-AAAS sources, you must obtain authorization from that source as well before using that material. You agree to hold harmless and indemnify AAAS against any claims arising from your use of any content in your work that is credited to non-AAAS sources.

If the AAAS material covered by this permission was published in Science during the years 1974 - 1994, you must also obtain permission from the author, who may grant or withhold permission, and who may or may not charge a fee if permission is granted. See original article for author's address. This condition does not apply to news articles.

The AAAS material may not be modified or altered except that figures and tables may be modified with permission from the author. Author permission for any such changes must be secured prior to your use.

Whenever possible, we ask that electronic uses of the AAAS material permitted herein include a hyperlink to the original work on AAAS's website (hyperlink may be embedded in the reference citation).

AAAS material reproduced in your work identified herein must not account for more than 30% of the total contents of that work.

AAAS must publish the full paper prior to use of any text.

AAAS material must not be used in a derogatory manner and must not imply any endorsement by the American Association for the Advancement of Science.

This permission is not valid for the use of the AAAS and/or Science logos.

AAAS makes no representations or warranties as to the accuracy of any information contained in the AAAS material covered by this permission, including any warranties of merchantability or fitness for a particular purpose.

If permission fees for this use are waived, please note that AAAS reserves the right to charge for reproduction of this material in the future.

Permission is not valid unless payment is received within sixty (60) days of the issuance of this permission. If payment is not received within this time period then all rights granted herein shall be revoked and this permission will be considered null and void.

In the event of breach of any of the terms and conditions herein or any of CCC's Billing and Payment terms and conditions, all rights granted herein shall be revoked and this permission will be considered null and void.

AAAS reserves the right to terminate this permission and all rights granted herein at its discretion, for any purpose, at any time. In the event that AAAS elects to terminate this permission, you will have no further right to publish, publicly perform, publicly display, distribute or otherwise use any matter in which the AAAS content had been included, and all fees paid hereunder shall be fully refunded to you. Notification of termination will be sent to the contact information as supplied by you during the request process and termination shall be immediate upon sending the notice. Neither AAAS nor CCC shall be liable for any costs, expenses, or damages you may incur as a result of the termination of this permission, beyond the refund noted above.

This Permission may not be amended except by written document signed by both parties. The terms above are applicable to all permissions granted for the use of AAAS material. Below you will find additional conditions that apply to your particular type of use.

FOR A THESIS OR DISSERTATION

Permission covers figure/table and text excerpt use in print and electronic versions of a dissertation or thesis. A full text article may be used in print versions only of a dissertation or thesis (except in the case of original authors who may include the accepted version of their papers in both print and electronic dissertations).

Permission covers the distribution of your dissertation or thesis on demand by ProQuest / UMI, provided the AAAS material covered by this permission remains in situ.

By using the AAAS Material identified in your request, you agree to abide by all the terms and conditions herein.

Questions about these terms can be directed to the AAAS Permissions department. Email us at permissions@aaas.org.

v1.2

A2.4 Wiley-VCH Verlag GmbH & Co. KGaA's Copyright release

We hereby grant permission for the requested use expected that due credit is given to the original source.

For material published before 2007 additionally: Please note that the author's permission is also required.

. Please note that we only grant rights for a printed version, but not the rights for an electronic/ online/ web/ microfiche publication, but you are free to create a link to the article in question which is posted on our website (http://www3.interscience.wiley.com)

If material appears within our work with credit to another source, authorisation from that source must be obtained.

Journal: Angewandte Chemie, International Edition

Authors: Paul A. Rupar, Rajoshree Bandyopadhyay, Benjamin F. T. Cooper, Michael R. Stinchcombe, Paul J. Ragogna, Charles L. B. Macdonald, Kim M. Baines

Pages: 5155-5158

Year: 2009

Volume: 48